Development of analytical techniques for detection and remediation of polychlorinated biphenyls in soil and water samples

Ofure Ruth Idialu

August 2016

Development of analytical techniques for detection and remediation of polychlorinated biphenyls in soil and water samples

Ofure Ruth Idialu

Supervisor: Dr Lorraine T. Gibson

Department of Pure and Applied Chemistry
University of Strathclyde

A thesis submitted to the Department of Pure and Applied Chemistry, University of Strathclyde, in part fulfilment of the regulations for the degree of Doctor of Philosophy (Ph.D)

August 2016

This thesis is the result of the author's original research. It has been composed by the author and has not been previously submitted for examination which has led to the award of a degree.

The copyright of this thesis belongs to the author under the terms of the United Kingdom Copyrights Acts as qualified by University of Strathclyde Regulation 3.5.0. Due acknowledgement must always be made of the use of any material contained in, or derived from, this thesis.

Abstract

In this study, GC-MS methods were developed for identifying and quantifying nineteen and five pre-selected PCB congeners in solution. The developed methods were repeatable ($\leq$ 4.9 %) and reproducible ($\leq$ 7.7 %) with detection limits of 1.25 - 15 ng μL^{-1}. The extraction of PCBs from soil and water samples was achieved using the ASE and C18 (EC) SPE methods with recoveries of 81 - 94 % and 41 - 49 % respectively. Although none of the target PCB congeners were detected in soil and water samples collected from Lagos, Nigeria, similar recoveries were obtained from spiked samples; indicating that the developed methods could be satisfactorily used to extract PCBs from environmental samples.

The adsorption of PCBs from aqueous solutions onto activated carbons - PAC, GAC and EAC was examined using batch experiments. The removal efficiencies obtained for PAC (75 - 90 %), GAC (79 - 99 %) and EAC (60 - 74 %) indicated that each AC could be successfully used to remove PCBs from water. In contrast to EAC, which had a slight decrease in performance as the concentration of aqueous solution increased, a significant decrease in performance was observed for PAC and GAC. The equilibrium data obtained for each AC was well described by the Langmuir isotherm model corresponding to the presence of a homogeneous surface. Amongst the three ACs, EAC had the highest maximum adsorption capacity (35 mg g^{-1}) compared to PAC (29.4 mg g^{-1}) and GAC (30.4 mg g^{-1}). The adsorption kinetic data obtained for each AC had a better fit to the pseudo second-order kinetic model indicating that chemisorption was responsible for the sorption of PCBs onto each AC. The optimum performance of the three ACs was achieved at solution pH 3.

Acknowledgements

Table of Contents

List of abbreviations

AC   Activated carbon

ANOVA   Analysis of variance

ASE   Accelerated solvent extraction

As-syn MCM-41   As-synthesised MCM-41

As-syn Fe-GN   As-synthesised iron green nanomaterial

BET   Brunauer Emmett Teller

BJH   Barett Joyner Halenda

BZ   Ballschmiter and Zell

Calc Fe-GN   Calcined iron green nanomaterial

Calc MCM-41   Calcined MCM-41

CAS   Chemical abstracts service

CB   Chlorobiphenyl

DE   Diatomaceous earth

DiCB   Dichlorobiphenyl

EAC   Extruded activated carbon

Fe-GN   Iron green nanomaterial

GAC   Granular activated carbon

GC-MS   Gas chromatography-mass spectrometry

M.A   Micropore area

MAE   Microwave assisted extraction

MCM   Mobile composition of matter

MonoCB   Monochlorobiphenyl

M.P.V   Micropore volume

NP SPE   Normal phase solid phase extraction

PAC   Powdered activated carbon

PCBs   Polychlorinated biphenyls

RP SPE   Reverse phase solid phase extraction

SOM   Soil organic matter

SPE   Solid phase extraction

T.P.V   Total pore volume

1. Introduction to polychlorinated biphenyls

1.1 Definition and Nomenclature of Polychlorinated biphenyls

Polychlorinated biphenyls (PCBs) are a class of man-made organic chemicals consisting of a biphenyl with varying numbers of chlorine atoms ranging from 1 – 10 and a general chemical formula $C_{12}H_{10-n} Cl_n$ where n= 1-10 (Figure 1.1).[1-8]
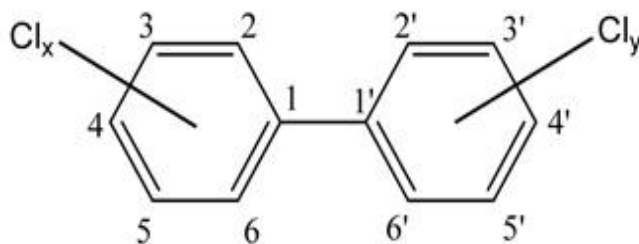
Figure 1.1: Chemical structure of PCBs showing possible sites available for chlorine substitution.[1, 8]

The entire set of PCBs consists of 209 congeners which are further subdivided into 10 groups of congeners termed homologues depending on their degree of chlorination; congeners which have the same number of chlorine atoms are grouped into the same homologue (Table 1.1).[1, 8-10] Only 130 out of the entire set of PCB congeners have been detected in commercial products.[1, 3, 9]

Table 1.1: Composition of Polychlorinated biphenyls by homologue.[8]

Homologue	Empirical formula	Chlorine (%)	No of Isomers
Monochlorobiphenyl	$C_{12}H_9Cl$	19	3
Dichlorobiphenyl	$C_{12}H_8Cl_2$	32	12
Trichlorobiphenyl	$C_{12}H_7Cl_3$	41	24
Tetrachlorobiphenyl	$C_{12}H_6Cl_4$	49	42
Pentachlorobiphenyl	$C_{12}H_5Cl_5$	54	46
Hexachlorobiphenyl	$C_{12}H_4Cl_6$	59	42
Heptachlorobiphenyl	$C_{12}H_3Cl_7$	63	24
Octachlorobiphenyl	$C_{12}H_2Cl_8$	66	12
Nonachlorobiphenyl	$C_{12}HCl_9$	69	3
Decachlorobiphenyl	$C_{12}Cl_{10}$	71	1

PCBs within the same homologue could also have different patterns of chlorine substitution known as isomers. For example, two isomers of tetrachlorobiphenyl are 2,2',5,5'-tetrachlorobiphenyl and 3,3',4,4'-tetrachlorobiphenyl as illustrated in Figure 1.2.[8, 9]
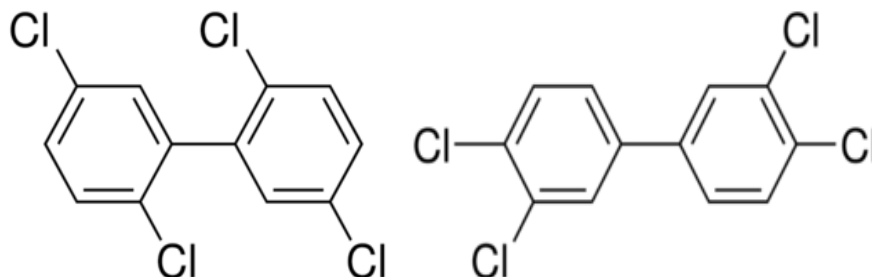
Figure 1.2: Chemical structure of two isomers of tetrachlorobiphenyl.

PCB nomenclature follows one of three systems.[8, 10] The first system is the International Union of Pure and Applied Chemistry (IUPAC) system of nomenclature which lists PCB numbers in a sequential order by identifying the point of substitution of the chlorine atom on the biphenyl ring.[9] IUPAC names of some individual congeners may be very long making it quite difficult to differentiate one congener from another; consequently resulting in wrong identification of congeners. A typical example of this is 2,2',3,3',4,5-hexachlorobiphenyl and 2,2',3,3',4,5'-hexachlorobiphenyl. The second system used is the Ballschmiter and Zell (BZ) numbering system which arranges the number of PCB congeners in an ascending order from PCB-1 to PCB-209 for each consecutive homologue.[11] The BZ system, developed in 1980, eliminates the difficulties associated with the use of the IUPAC naming system in identifying congeners with lengthy substituents. A primed number is generally considered higher than a number that's unprimed. The systematic numbering of PCB congeners using the BZ numbering system is displayed in Table 1.2. The Chemical Abstracts Service (CAS) registry number is the third system used for classification of PCBs. These numbers are assigned by the CAS and held in the CAS registry database.[8]

Table 1.2: Systematic numbering of PCB compounds.[11]

No	Structure	No	Structure	No	Structure	No	Structure
	MonoCBs*		**TetraCBs**		**PentaCBs**		**HexaCBs**
1	2	52	2,2',5,5'	105	2,3,3',4,4'	161	2,3,3',4,5',6
2	3	53	2,2',5,6'	106	2,3,3',4,5	162	2,3,3',4',5,5'
3	4	54	2,2',6,6'	107	2,3,3',4',5	163	2,3,3',4',5,6
	DiCBs	55	2,3,3'4	108	2,3,3',4,5'	164	2,3,3',4',5',6
4	2,2'	56	2,3,3',4'	109	2,3,3',4,6	165	2,3,3',5,5',6
5	2,3	57	2,3,3',5	110	2,3,3',4',6	166	2,3,4,4',5,6
6	2,3'	58	2,3,3',5'	111	2,3,3',5,5'	167	2,3,4,4',5,5'
7	2,4	59	2,3,3',6	112	2,3,3',5,6	168	2,3',4,4',5',6
8	2,4'	60	2,3,4,4'	113	2,3,3',5',6	169	3,3',4,4',5,5'
9	2,5	61	2,3,4,5	114	2,3,4,4',5		**HeptaCBs**
10	2,6	62	2,3,4,6	115	2,3,4,4',6	170	2,2',3,3',4,4',5
11	3,3'	63	2,3,4',5	116	2,3,4,5,6	171	2,2',3,3',4,4',6
12	3,4	64	2,3,4',6	117	2,3,4',5,6	172	2,2',3,3',4,5,5'
13	3,4'	65	2,3,5,6	118	2,3',4,4',5	173	2,2',3,3',4,5,6
14	3,5	66	2,3',4,4'	119	2,3',4,4',5	174	2,2',3,3',4,5,6
15	4,4'	67	2,3',4,5	120	2,3',4,5,5'	175	2,2',3,3',4,5',6
	TriCBs	68	2,3',4,5'	121	2,3',4,5',6	176	2,2',3,3',4,6,6
16	2,2',3	69	2,3',4,6	123	2',3,3',4,5	177	2,2',3,3',4',5,6
17	2,2',4	70	2,3',4',5	124	2',3,4,5,5'	178	2,2',3,3',5,5',6
18	2,2'5	71	2,3',4',6	125	2',3,4,5,6'	179	2,2',3,3',5,6,6'
19	2,2',6	72	2,3',5,5'	126	3,3',4,4',5	180	2,2',3,4,4',5,5'
20	2,3,3'	73	2,3',5',6	127	3,3',4,5,5'	181	2,2',3,4,4',5,6
21	2,3,4	74	2,4,4',5		**HexaCBs**	182	2,2',3,4,4',5,6'
22	2,3,4'	75	2,4,4',6	128	2,2',3,3',4,4'	183	2,2',3,4,4',5',6
23	2,3,5	76	2',3,4,5	129	2,2',3,3',4,5	184	2,2',3,4,4',6,6'
24	2,3,6	77	3,3',4,4'	130	2,2',3,3',4,5'	185	2,2',3,4,5,5',6
25	2,3',4	78	3,3',4,5'	131	2,2',3,3',4,6	186	2,2',3,4,5,6,6'
26	2,3',5	79	3,3',4,5'	132	2,2',3,3',4,6	187	2,2',3,4',5,5',6
27	2,3',6	80	3,3',5,5'	133	2,2',3,3',5,5'	188	2,2',3,4',5,6,6'
28	2,4,4'	81	3,4,4',5	134	2,2',3,3',5,6	189	2,3,3',4,4',5,5'
29	2,4,5		**PentaCBs**	135	2,2',3,3',5,6'	190	2,3,3',4,4',5,6
30	2,4,6	82	2,2',3,3',4	136	2,2',3,3',6,6'	191	2,3,3',4,4',5',6
31	2,4',5	83	2,2',3,3',5	137	2,2',3,4,4',5	192	2,3,3',4,5,5',6
32	2,4',6	84	2,2',3,3',6	138	2,2',3,4,4',5'	193	2,3,3',4',5,5',6
33	2',3,4	85	2,2',3,4,4'	139	2,2',3,4,4',6		**OctaCBs**
34	2',3,5	86	2,2',3,4,5	140	2,2',3,4,4',6'	194	2,2',3,3',4,4',5,5'
35	3,3',4	87	2,2',3,4,5'	141	2,2',3,4,5,5'	195	2,2',3,3',4,4',5,6
36	3,3',5	88	2,2',3,4,6	142	2,2',3,4,5,6	196	2,2',3,3',4,4',5',6
37	3,4,4'	89	2,2',3,4,6'	143	2,2',3,4,5,6'	197	2,2',3,3',4,4',6,6'
38	3,4,5	90	2,2',3,4',5	144	2,2',3,4,5',6	198	2,2',3,3',4,5,5',6
39	3,4',5	91	2,2',3,4',6	145	2,2',3,4,6,6'	199	2,2',3,3',4,5,6,6'
	TetraCBs	92	2,2',3,5,5'	146	2,2',3,4',5,5'	200	2,2',3,3',4,5',6,6'
40	2,2',3,3'	93	2,2',3,5,6	147	2,2',3,4',5,6	201	2,2',3,3',4',5,5',6
41	2,2',3,4	94	2,2',3,5,6'	148	2,2',3,4',5,6'	202	2,2',3,3',5,5',6,6'
42	2,2',3,4'	95	2,2',3,5',6	149	2,2',3,4',5',6	203	2,2',3,4,4',5,5',6
43	2,2',3,5	96	2,2',3,6,6'	150	2,2',3,4',6,6'	204	2,2',3,4,4',5,6,6'
44	2,2',3,5'	97	2,2',3',4,5	151	2,2',3,5,5',6	205	2,3,3',4,4',5,5',6
45	2,2',3,6	98	2,2',3',4,6	152	2,2',3,5,6,6'		**NonaCBs**
46	2,2',3,6'	99	2,2',4,4',5	153	2,2',4,4',5,5'	206	2,2',3,3',4,4',5,5',6
47	2,2',4,4'	100	2,2',4,4',6	154	2,2',4,4',5,6'	207	2,2',3,3',4,4',5,6,6'
48	2,2',4,5	101	2,2',4,5,5'	155	2,2',4,4',6,6'	208	2,2',3,3',4,5,5',6,6'
49	2,2',4,5'	102	2,2',4,5,5'	156	2,3,3',4,4',5		**DecaCB**
50	2,2'4,6	103	2,2',4,5',6	157	2,3,3',4,4',5'	209	2,2',3,3',4,4',5,5',6,6'
51	2,2',4,6'	104	2,2',4,6,6'	158	2,3,3',4,4',6		
				159	2,3,3',4,5,5		
				160	2,3,3',4,5,6		

*CBs denotes chlorobiphenyls

1.2 Properties and Classification of PCBs

PCBs are oily liquids, or solids, with colour ranging from colourless to light yellow.[8] They are characterised by low electrical conductivity, high physical and chemical stability and resistance to attack by acids.[6] They have high boiling points, good fire resistance, low water solubility and high solubility in organic compounds.[1, 2, 6, 12] Hence, they have been identified as one of the most stable organic compounds.[6, 8] The classification and properties of PCB congeners is highly influenced by the number and substitution pattern of chlorine atoms attached to the biphenyl molecule.[6] PCB congeners with a high number of chlorine atoms tend to be more viscous and have a low volatility than lowly chlorinated PCB congeners which flow easily.[6] Some physical properties of PCB homologues are given in Table 1.3.

Table 1.3: Physical properties of PCB Homologues.[8]

PCB Isomer group	Melting point / °C	Boiling point / °C	Vapour pressure / Pa at 25 °C	Water solubility / g/m^3 at 25 °C	Log octanol - water partition coefficient
MonoCB*	25 - 77.9	285	1.1	4	4.7
DiCB	24.4 - 149	312	0.24	1.6	5.1
TriCB	28 - 87	337	0.054	0.65	5.5
TetaCB	47 - 180	360	0.012	0.26	5.9
PentaCB	76.5 - 124	381	2.6×10^{-3}	0.099	6.3
HeptaCB	77 - 150	400	5.8×10^{-4}	0.038	6.7
HexaCB	122.4 - 149	417	1.3×10^{-4}	0.014	7.1
OctaCB	159 - 162	432	2.8×10^{-5}	5.5×10^{-3}	7.5
NonaCB	182.8 - 206	445	6.3×10^{-6}	2.0×10^{-3}	7.9
DecaCB	305.9	456	1.4×10^{-6}	7.6×10^{-4}	8.3

*CB denotes chlorobiphenyl

Due to the complex nature of the 209 congeners, the representative congeners of PCBs are generally classified into two groups: indicator PCBs and dioxin-like PCBs.[13] The indicator PCBs comprises 7 compounds (PCB-28, 52, 101, 118, 138, 153 and 180) which have been selected based on their prevalence in commercial mixtures of PCBs, persistence in the food chain and likelihood of biomagnification.[13-15] The dioxin-like PCBs consists of 12 compounds which are further subdivided into two groups termed

the non-ortho PCBs (PCB 77, 81, 126 and 169) and the mono-ortho PCBs (PCB 105, 114, 118, 123, 156, 157, 167 and 189).[13, 16] The dioxin-like group was selected based on the similarity of their toxicity with polychlorinated dibenzo-p-dioxins (PCDDs) known as dioxins and polychlorinated dibenzofurans (PCDFs) termed furans.[17-19] Dioxin-like PCB congeners are generally termed planar or coplanar congeners because of their flat molecular structure usually with a single chlorine atom or none at all substituted at the ortho position (positions 2, 2' or 6, 6').[12, 20]

PCDDs and PCDFs are tricyclic aromatic compounds with identical chemical properties; two benzene rings linked by two oxygen atoms for PCDDs and a single oxygen atom and carbon − carbon bond for PCDFs as shown in Figure 1.3.[21, 22] The chlorine atom substitution on the two benzene rings could vary from 1 to 8 giving rise to 75 PCDD or 135 PCDF congeners. However, only 17 congeners (7 PCDDs and 10 PCDFs) with chlorine atoms substituted on the 2, 3, 7 and 8 positions exhibit the dioxin-like toxicity.[17, 22, 23]
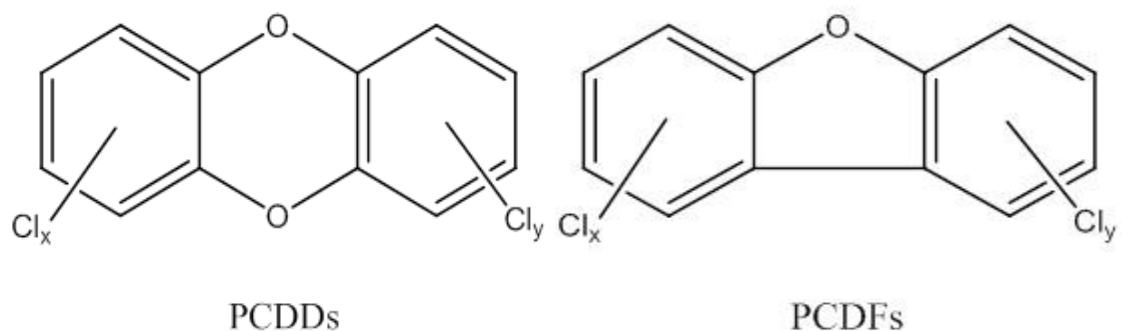
PCDDs   PCDFs

Figure 1.3: Generalised structure of dioxins (PCDDs) and furans (PCDFs).[20]

PCDDs and PCDFs are persistent, bioaccumulative and toxic compounds that are not produced commercially but are formed as by-products of several industrial processes such as metal processing, drying and baking operations.[5, 22, 24] In addition, thermal combustion processes involving chlorine in any form also results in their formation.[12, 22] 2,3,7,8-tetrachlorodibenzo-para-dioxin (2,3,7,8-TCDD) is classified as the most toxic of the PCDD/PCDF congeners and is a human carcinogen.[22, 25] Thus, it is used a reference point to assess the toxicity of other PCDDs, PCDFs and PCBs related to it through a system of toxic equivalent factors (TEFs).[21, 23]

6

1.3 Production and Uses of PCBs

The first synthesis of PCBs was carried out by Schmidt and Schulz in 1881 and production on a commercial scale commenced in the United States in 1929 by the Mosanto Chemical Company.[26, 27] Commercial formulations of PCBs originally manufactured by Mosanto in the U.S.A include Aroclor 1221, 1232, 1242, 1248, 1254, 1260, 1262 and 1268.[12, 28] This was later reduced to Aroclor 1016, 1242, 1254 and small amounts of 1221.[11, 12] Aroclors are generally distinguished by a four-digit number such that the first two numbers represent the number of carbon atoms present in the biphenyl ring and the last two numbers indicate the degree of chlorination (% of chlorine by weight).[12, 28]

Countries such as the United Kingdom, the Russian federation, Japan, Italy, Germany, France, China and Australia were also involved in the commercial production of PCBs.[6, 10] The different trade names under which PCBs have been sold in various countries include Aroclor, Askarel (U.K., U.S.A), Apirolio, DK, Fenclor (Italy), Pyroclor (U.K), Bakola 131, Chlorextol, Asbestol, Diaclor, Pykanol, Elemex, Hydol, Interteen, Noflamol, Pyranol (U.S.A), Clophen, Elaol (Germany), Delor (Czechoslovakia), Phenoclor, Pyralene (France), Saft-kuhl (U.S.A), Sovol, Sovtol (U.S.S.R), kanechlor, Santotherm (Japan).[1, 9, 10, 28]

PCBs have been used in several industrial applications due to their high degree of chemical and thermal stability.[1, 3, 6, 8, 12, 29, 30] These applications are generally grouped into three major types: closed, partially closed and open applications.[1, 8] In closed applications, there is no tendency for exposure to the user or environment as PCBs are completely held within the system.[1, 8] Nevertheless, PCBs may be released during maintenance or decommissioning of equipment. The most commonly used closed applications are electrical capacitors and transformers.[1] In partially closed applications, direct emissions of PCBs to the environment are unlikely but may occur periodically from typical use such as air and water discharges.[1, 8] Heat transfer fluids, hydraulic fluids, vacuum pumps and switches are typical examples of partially closed applications of PCBs. Open application systems are of greatest concern as PCBs are in direct contact with the environment.[1] These include plasticisers used in PVC (polyvinyl chloride),

neoprene, adhesives and other chlorinated rubber formulations. Other applications include their use as flame- retardants in paints and surface coatings.

About 1 million tonnes of PCBs have been manufactured globally since 1930 and a substantial amount of this released into the environment.[28, 31] In 1976, the production, distribution and use of PCBs was banned in the United States under the Toxic Substances Control Act (TSCA) and the Resource Conservation and Recovery Act (RCRA) based on evidence that they had a high tendency of accumulating in the environment which could result in serious deleterious effects to the environment.[12]

1.4 Sources of PCBs in the Environment

PCBs have been released from several sources into the environment despite the fact their manufacture and use has been banned since the 1970s.[1, 12, 23, 28, 32, 33] These sources include poorly managed hazardous waste sites containing PCBs, unlawful disposal of PCB wastes (used transformer fluids), paints and PCB containing equipment, waste incineration processes and leaks from sites containing electrical transformers, capacitors or other products containing PCBs.[12]

The release of PCBs into the atmosphere stems mainly from their redistribution in soil and water although smaller amounts may be released from hazardous waste sites. Smaller quantities of PCBs may be discharged into surface water via runoffs or accidental spills from fluids containing PCBs. However, the environmental cycling process serves as a predominant source of PCB release to surface water. Accidental spills and leaks from PCB containing equipment and discharges from hazardous waste sites contribute significantly to the release of PCBs into soil. A summary of the different persistent cycles and pathways that resulted in the widespread distribution of PCBs in the environment is illustrated in Figure 1.4.[1]

Closed Applications

Dielectric fluids
Transformers
Capacitors
Electrical light
Ballasts
Electric motors

Partially Closed Applications

Hydraulic fluids
Heat Transfer fluids
Capacitors
Voltage Regulators
Vacuum pumps

Open Applications

Inks
Lubricants
Waxes
Flame Retardants
Paints
Dyes
Adhesives
Insulating Materials

Waste

Fluff
Inadvertent Production
Spills
Decommissioned
Equipment
Building Demolition

Recycling Operations

Oil
Carbonless Copy
Paper

Interim Storage/ Permanent Disposal

Temporary Storage Facilities
High Temperature Incineration
Underground Storage Facilities

Industrial Dumpsite

Landfills

Products made with Recycled Material

Soil

Air

Water

Food

Figure 1.4: PCB Movement in the Environment.[1]

_____ Movement of PCBs via manufacturing, use and disposal

— _ — Inadvertent and intentional recycling of PCBs

9

1.5 Soil and Water

Soil is an important feature of the terrestrial environment consisting of a mixture of minerals (clay, quartz), organic matter and water which provide a means of physical support for all terrestrial organisms, plants and animals on the earth's surface.[34] In general, it has a loose structure which contains air pockets. Soil is formed by the weathering of parent rock and decomposition of organic matter such as dead leaves and twigs.[34] The solid fraction of a productive soil typically consists of 5 % organic matter and 95 % inorganic matter.[34, 35]

Typical soils exhibit distinctive layers referred to as horizons which form due to complex interactions and processes that occur during weathering.[34] Five basic horizons denoted O, A, B, C or R are generally found within a soil profile (Figure 1.5).[35] These horizons have different physical and chemical properties which make it possible to distinguish them within the soil profile.
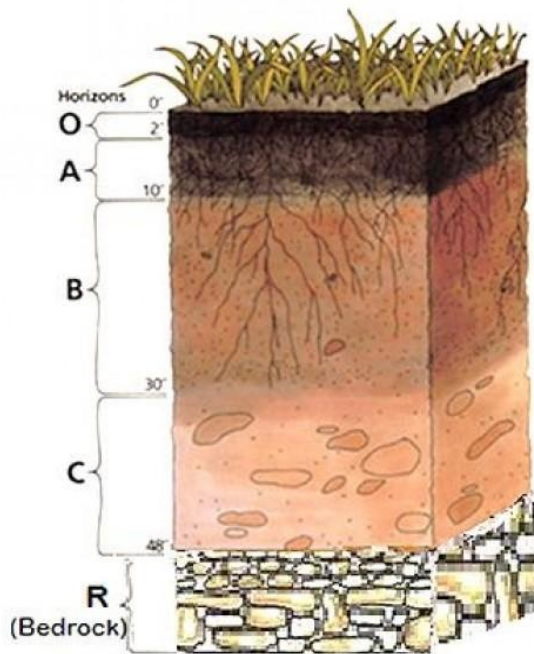
Figure 1.5: A Generalised soil profile [35]

Horizon O is a surface layer formed mainly from decomposed leaf litter (decayed or decaying plant biomass). Horizon A, also known as the top soil, is rich in partially decayed organic matter (humus), plant roots and characterised by high biological

activity.[34, 35] In this layer, the accumulated organic matter and mineral fraction are mixed to form an uppermost part rich in nutrients and living organisms and a lower part consisting of lower nutrient levels.[34, 35] Horizon B (the subsoil) is essentially a layer which consists of minerals such as silicate clay, iron, aluminium, humus, gypsum and silica.[34, 35] This layer predominantly receives materials (organic matter and living organisms) leached out of Horizon A. Horizon C is composed mainly of weathered rock which serves as parent material or the mineral fraction of the soil and is virtually deficient in organic materials.[34, 35] Horizon R is the bedrock (solid rock) comprising of unweathered rock such as granite, basalt, limestone or sand stone which may or may not have been derived from soil.[35]

Water covers 70 % of the earth surface and is essential for all known forms of life.[34] 97 % of the earth's crust water is found in seas and oceans while 2.5 % is found in ground waters with the remaining small fraction being found in polar ice caps, rivers and lakes. The introduction of toxic pollutants such as PCBs, volatile organic compounds (VOCs), polynuclear aromatic hydrocarbons (PAHs) into water via anthropogenic activities is of particular concern due to their aforementioned toxicity. Primary sources of water pollution include oil spills, sewage, industrial waste waters and land drainage.

1.6 Environmental fate and Transport of PCBs

PCBs present a serious worldwide problem due to their ability to undergo long-range transport in different environmental media such as air, water and soil.[12] Although they are cycled between air, water and soil, atmospheric transport remains the major pathway for their movement globally.[8, 12, 25, 27] PCBs are usually present in either the vapour or particle-bound phase in the atmosphere with more tendencies to be transported further in the vapour phase than the particle - bound phase.[12] They leave the atmosphere by wet (in form of rain or snow) and dry deposition (in form of aerosols).[12, 36] The main mode by which PCBs are released into water is via atmospheric deposition.[8, 12] They may be conveyed by currents and subsequently adhere to sediments at the bottom of water. Similarly, PCBs are usually deposited onto land from the atmosphere and volatilisation

from soil and water is the predominant source of their release back into the atmosphere.[37]

Soil properties such as organic matter content, porosity, moisture content, texture and structure have been shown to strongly influence the partitioning of PCBs between soil and air as well as their subsequent volatilisation from soil.[12, 38-40] In soils, PCBs rarely migrate to ground water as they bind strongly to soil organic matter due to their liphophilicity and high propensity for accumulating in surface soils.[27, 41] Their behaviour in soil is greatly determined by the degree of chlorination and ortho substitution on the biphenyl molecule; PCBs with high chlorine content and few ortho substitution are highly persistent and strongly retained by soil and sediments as their low water solubility and high octanol/water partition co-efficient (K_{ow}) values make it possible for them to adhere strongly to soil organic matter.[5, 41, 42]

The concentration of PCBs in living organisms serves as an important mechanism for their removal in water.[12] This occurs via the consumption of food containing PCBs and subsequent accumulation in the higher trophic level in a process termed biomagnification.[12] Bioaccumulation factors tend to increase for highly chlorinated PCBs with low water solubility. A significant level of bioaccumulation does not occur in highly chlorinated PCBs (chlorines 7-10) because they are tightly bound to organic matter in soil and sediment.[12] Similarly, PCBs containing a low number of chlorine atoms (1- 4 chlorines) which are easily taken up by organisms are not bioaccumulated to a great extent as they are readily eliminated.[12] On the contrary, penta- hexa- and hepta-CBs are bioaccumulated greatly in organisms due to their high resistance to degradation.[19, 43] Three possible mechanisms exist for the accumulation of PCBs in terrestrial vegetation.[12] These include: uptake from soil via roots, dry deposition (in form of particles or gas) and wet deposition (in form of particles or solute) on aerial parts. Vapour-to-plant transfer represents the major pathway for the uptake of total PCBs in terrestrial vegetation. The diagram in Figure 1.6 illustrates the environmental transport pathways of PCBs in the environment.[2]
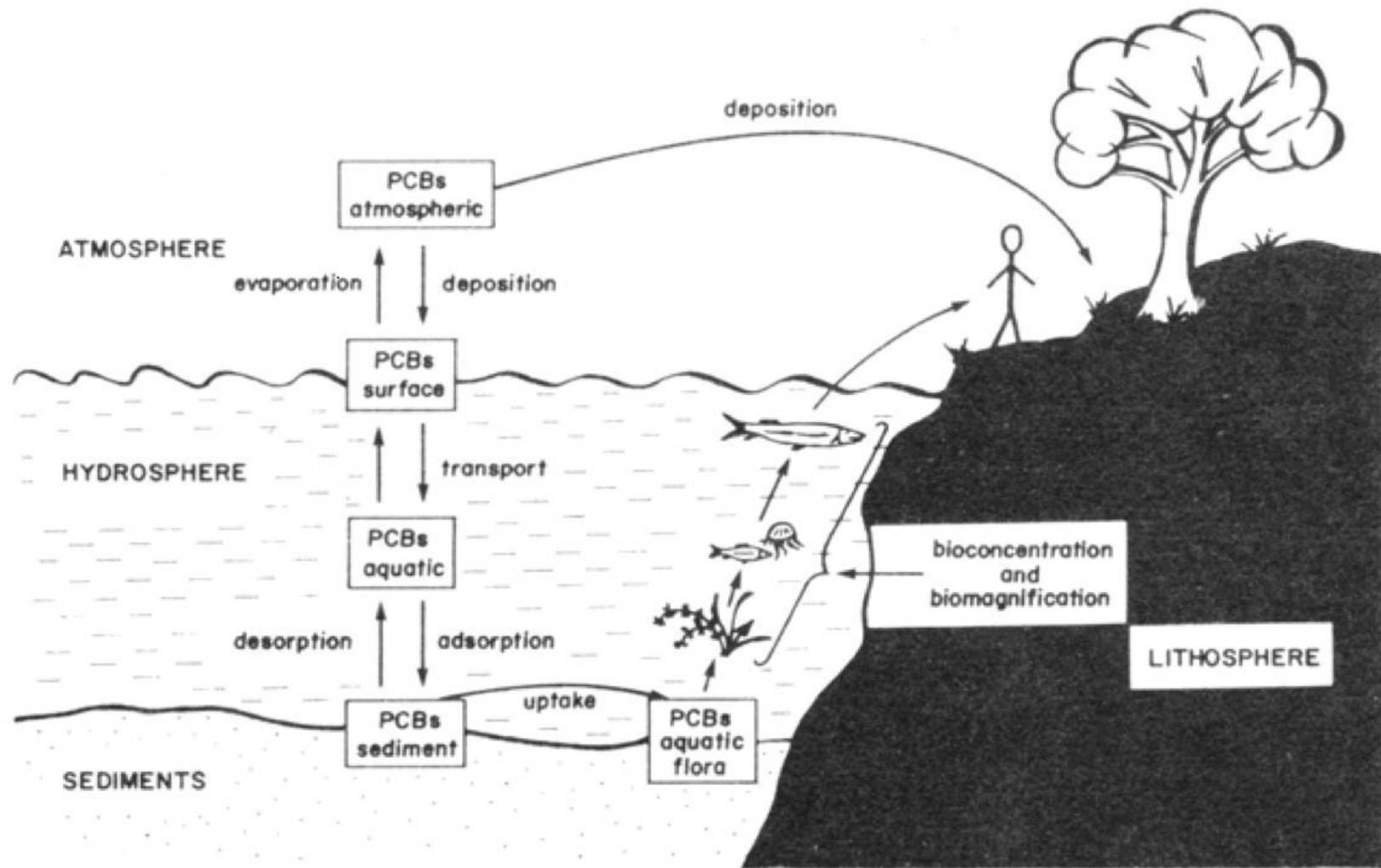
Figure 1.6: Environmental Fate and Transport of PCBs [2]

1.7 Toxicity of PCBs

PCBs are ubiquitous environmental pollutants which have been detected in various environmental matrices such as wild life, fish, domestic animals, water bodies (oceans, lakes and rivers), air and soil.[25, 31, 44-48] Their high degree of stability and tendency for bioaccumulation in the food chain resulted in their classification as persistent organic pollutants (POPs) by the United Nations Environment Programme (UNEP) Governing Council in 1997.[14, 46, 47, 49-51]

POPs are toxic organic chemicals which persist in the environment for long periods of time, accumulate in the fatty tissues of living organisms and can be transported globally far from their point of release.[22, 46] They are twelve in number and referred to as the "dirty dozen": aldrin, chlordane, dichlorodiphenyltrichloroethane (DDT), hexachlorobenzene, toxaphene, mirex, dieldrin, endrin, heptachlor, polychlorinated biphenyls (PCBs), polychlorinated dibenzo-p-dioxins (PCDDs) and polychlorinated dibenzofurans (PCDFs).[22] The adverse human health and environmental effects associated with POPs particularly PCBs, PCDDs and PCDFs have gained concern globally. Thus, the need to eliminate or reduce their use led to the implementation of the Stockholm Convention on POPs; a global treaty ratified in 2004.[52]

In 2009, nine new compounds were added to the POPs list in the Stockholm Convention based on their potential toxicity to human health and the environment similar to that of the dirty dozen; giving a total of 21 compounds.[53] The nine new compounds included alpha hexachlorocyclohexane (α-HCH), beta hexachlorocyclohexane (β-HCH), chlordecone, hexabromobiphenyl (HBB), hexabromodiphenyl ether and heptabromodiphenyl ether (PBDE), lindane (gamma hexachlorocyclohexane γHCH), tetrabromodiphenyl ether and pentabromodiphenyl ether (PBDE), pentachlorobenzene (PeCBz) and perfluorooctane sulfonic acid (PFOS).[53]

PCBs cause a wide variety of adverse health effects such as endocrine disruption, birth defects, damage to the reproductive, neurological, immune and gastrointestinal system.[54, 55] They have been reported to cause cancer in animals and classified as "probable human carcinogens".[55] Ocular effects (conjunctiva) and dermal lesions such as chloracne and hyperpigmentation have also been observed in humans.[10, 12, 18, 29, 32, 33,]

14

[50, 54] The exposure of humans to PCBs stems mainly from the consumption of contaminated water or food and by inhalation of contaminated air.[12, 50]

Two significant episodes of PCB poisoning that provoked international concern were the Yusho and Yucheng incidents.[10, 12, 56] The Yusho incident occurred in Japan in 1968 from the contamination of rice cooking oil with fluids containing polychlorinated biphenyls (PCBs), polychlorinated dibenzofurans (PCDFs) and small amounts of polychlorinated quaterphenyls (PCQ) which had leaked from the heat exchange equipment used in food processing.[1, 57] Kanechlor 400 was the commercial PCB mixture used in this equipment.[10] People who consumed the oil suffered some clinical manifestations like conjunctiva, chloracne, nail and skin pigmentation.[56] Low birth weights were also recorded in babies delivered by women who consumed the contaminated oil. The Yucheng incident was a similar outbreak,[56, 58] which occurred in Taiwan in 1979 and resulted in symptoms similar to that found in patients with the Yusho disease.[58]

Another unprecedented accidental contamination of PCB poisoning, which occurred in Belgium in 1999, was due to the use of PCB and dioxin (PCDDs and PCDFs) contaminated recycled fat in the production of animal feed.[59-62] The contaminated animal feed was supplied to poultry and pig farms resulting in severe symptoms in poultry and pigs and consequently a major food crisis globally known as the Belgian PCB/Dioxin Crisis.[59, 61] The symptoms of poultry poisoning observed include increased mortality of chicks, neurological disturbances and manifestations similar to chick-edema disease.[59] Pigs were affected to a lesser extent compared to poultry as hens and chicks were reported to have the highest concentrations of PCBs.[59, 60] Congener patterns identical to the commercial mixture Aroclor 1260/1254 were found for the PCB oil examined.[60]

The toxicity and prevalence of PCBs in the environment requires accurate methods of detection and mitigation processes. These details will be discussed in Parts A and B respectively. As the mitigation methods investigated during this research were based on adsorption processes, the general theory associated with adsorption is given below.

1.8 Adsorption

Adsorption is a process that occurs when molecules, ions or atoms of a gas, liquid adhere to the surface of the adsorbent.[63] It occurs as a result of interactions between molecules in the fluid phase and the solid.[64] The solid material which provides the surface for adsorption is referred to as the adsorbent and the species for adsorption is adsorbate.[63, 65, 66] It involves the enrichment of chemical species from a fluid phase onto the surface of a liquid or solid. Adsorption is a widely used process for the removal of contaminants from water systems.[63, 67]

Adsorption is generally classified into two types: physical adsorption (physisorption) and chemical adsorption (chemisorption) depending on the forces of interaction responsible for the process.[64, 65, 67] Physisorption is a reversible process in which molecules are attached to the surface of the adsorbent by weak van der Waals forces. In this process, the adsorbed molecules are not fixed to a site at the surface but move freely within the interface.[64, 66, 67] Chemisorption is brought about by chemical interactions between the solute molecules and the adsorbent.[67] Functional groups present on the surface of the adsorbent participate in adsorption via electron sharing.[67] In chemisorption, the chemically adsorbed molecules do not move freely on the surface or within the interface. In contrast to physisorption which occurs primarily at temperatures below 150 $^\circ$C and requires a relatively low energy of adsorption and low activation energies (5-10 kJ mol^{-1}), chemisorption is predominant at higher temperatures and requires higher activation energies (15 - 30 kJ).[67]

Porous materials are solids with pores which are of two types: open pores which are connected to the surface of the material and closed pores which are isolated from the surface of the material (see Figure 1.7).[68] Open pores (regions b, c, d, e and f) are further subdivided into through pores and blind pores.[68] Through pores have at least two openings on two sides of a porous material with a pore channel beginning at one end of the surface, extending into the pores and re-emerging on another end of the surface (regions c,e,c or c,e,d).[68] Blind pores (regions b and f) are connected to the surface of the material only at one end.[68]

Although closed pores (region a) do not permit the entry of external fluids, they have an influence on the elasticity, bulk density, thermal conductivity and mechanical strength of

the materials. However, the introduction of open pores in materials results in decreased density and increased surface area thereby generating useful properties such as fluid permeability and filtration capability.[68] Open porous materials are used as filters in a wide variety of industrial applications.[68] Closed porous materials are mainly applied in sonic and thermal insulation.[68]
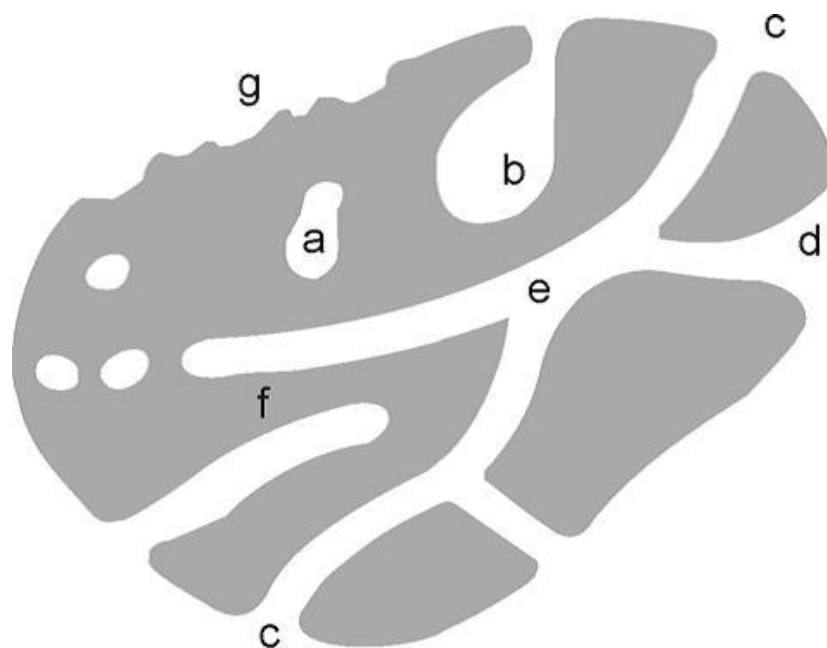
Figure 1.7: Cross-section of a porous solid showing the different types of pores. [64]

The classification of porous materials is based on properties such as pore size, pore shape and methods used for production (see Figure 1.8).[65] According to the International Union of Pure and Applied Chemistry (IUPAC), porous materials are classified into microporous (< 2 nm), mesoporous (2 - 50 nm) and macroporous (> 50 nm) materials based on their pore sizes.[65] Porous materials such as zeolites, clays, silica gels, activated carbon and polymeric sorbents have been used for sequestration of organic pollutants from water bodies.[63, 69, 70] Zeolites are a well-defined class of crystalline aluminosilicates which are interlinked in various ways by sharing oxygen atoms.[70] They contain an extensive framework of SiO_4 and AlO_4 tetahedra and framework cations that are exchangeable.[70, 71] Zeolites were first discovered by a Swedish mineralogist, Baron von Cronstedt who observed that the minerals released large amounts of water upon rapid heating.[72] As a result of this observation, the materials were named zeolites from the Greek words zeo "to boil" and lithos "stone".[72]
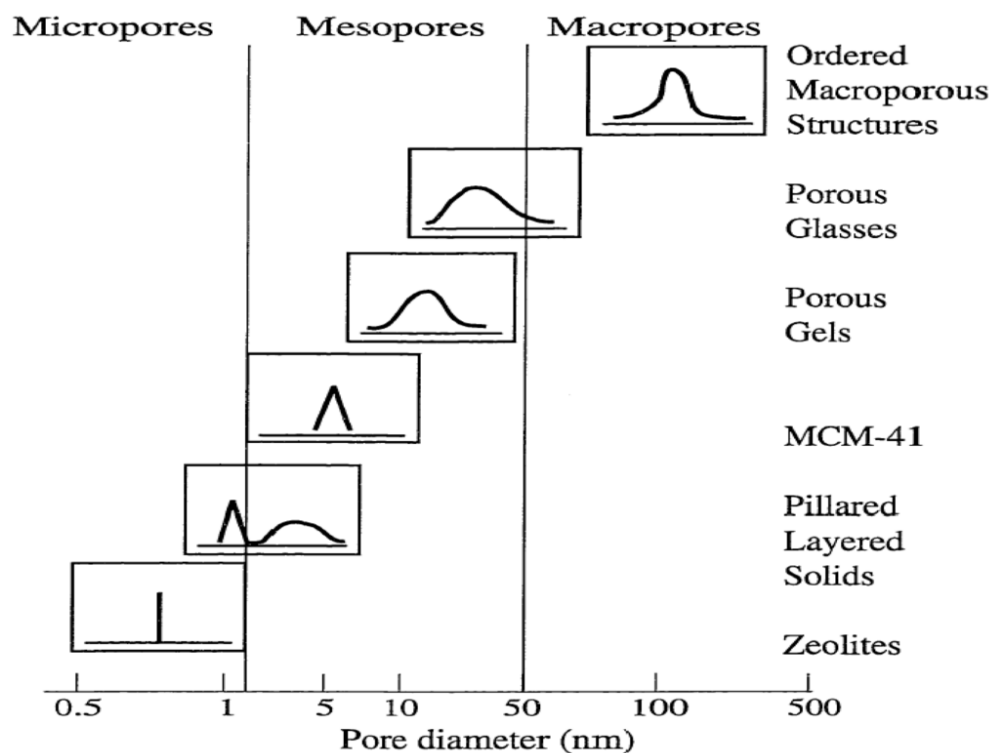
Figure 1.8: Schematic diagram of porous materials and their pore size distribution.[73, 74]

The natural form of zeolites occurs in small cavities of rocks which originate from volcanoes while the synthetic form can be manufactured from a known naturally occurring material under mild conditions.[75] Zeolites were first synthesised on a large scale in 1938 by Barrer [75] after which three new zeolites (types A, X and Y) were produced by Milton and colleagues in the 1950s.[73, 76] In 1954, the three synthetic zeolites were commercialised by Union Carbide Corporation which have been used in several industrial applications such as ion exchange, separation and catalysis.[72] Although they were previously considered as rare minerals, they have been considered as some of the most abundant species on earth. Hence the name "molecular sieves" was given to them by Mc Bain in 1932.[77] The tendency for zeolites to act as molecular sieves (selectively adsorb or reject molecules) is based on their uniform pore size (0.3 − 1.5 nm); although their use in processes involving large molecules (> 1.5 nm) is limited as a result of this. In the late 1940s, Barrer reported that the separation of nitrogen and oxygen could be achieved by using zeolites with a specific shape.[78] The synthesis of zeolites typically involves the crystallisation of a silicate around a single molecule.[79] Their outstanding

18

properties have made them very useful materials in several applications such as adsorbents, soil modifiers, ion exchangers and molecular sieves.[80] However, the major drawback of their use is associated with their narrow pore size which excludes larger molecules from the size-specific processes occurring in the pores of the materials.[73, 77] Hence, pillared clays which are a class of two-dimensional microporous materials with high surface areas and tunable pore sizes have proven to be very attractive solids for adsorption and catalysis compared to zeolites.[81] Porous gels and porous glasses which are basically a special form of silica gel are characterised by larger pores.[82] Silica gel is an amorphous solid which consists of a coherent, rigid, three dimensional network of colloidal silica particles in the mesopore range.[70, 82] However, they exhibit a broad pore size distribution with pore sizes greater than 2 nm which could get to the macroporous range.

1.9 Aims and Objectives

The overall aims of this work were:

1. To develop innovative analytical techniques for detecting and assessing the level of polychlorinated biphenyls (PCBs) in soils and water.

2. To explore different remediation techniques for removing PCBs from the aquatic environment using sustainable materials.

Herein, the key objectives of this research were:

I. To develop a simplified and efficient analytical method for extracting PCBs from soil using accelerated solvent extraction (ASE) and microwave-assisted extraction (MAE).

II. To develop a simplified and efficient analytical method for extracting PCBs from water using solid phase extraction (SPE).

III. To develop an analytical method for quantifying the extracted PCBs from soil and water using gas chromatography-mass spectrometry (GC-MS).

IV. To explore the feasibility of removing PCBs from water (remediation) using low-cost adsorbents; silica based platforms and carbonaceous materials.

V. To characterise the adsorbents used with analytical tools such as the Brunauer-Emmett-Teller (BET) method, Fourier Transform Infrared (FTIR) Spectroscopy, thermogravimetric analysis (TGA) and CHN microanalysis.

VI. To assess the viability of the adsorbent materials under a range of conditions for sequestration of PCBs from water using spiked solutions and real samples.

Therefore, this thesis consists of three chapters and two parts: Part A and Part B which underpin the overall research objectives mentioned earlier. In Chapter 1, a general study of the properties, classifications, production, uses, sources, toxicity, environmental fate and transport of PCBs is provided. In Chapters 2 and 3, an overview of the theory of extraction and instrumental techniques as well as the experimental methods employed in this research is given.

Part A is subdivided into three chapters; 4, 5 and 6 while Part B is subdivided into two chapters; 7 and 8. In Part A, Chapter 4 provides full details of the method development for determination of PCBs in solution as well as validation of the developed method. Chapters 5 and 6 will provide an assessment of the efficiency of different extraction techniques applied for extracting PCBs from soil and water respectively.

In Part B, Chapter 7 presents an investigation of the feasibility of removing PCBs from aqueous solutions using mesoporous silica (MCM-41) and iron bioinspired silica (Fe-GN) as adsorbents. In Chapter 8, a study of the feasibility and efficiency of activated carbons with different surface and/ or textural properties to sequester PCBs from aqueous solutions will be reported. Parameters such as contact time, concentration of PCB ions and pH which influence the sorption process in aqueous solutions were examined. The equilibrium data obtained were fitted into the linear form of the Langmuir and Freundlich equations and kinetic data obtained analysed using the pseudo-first and pseudo-second order kinetic models. The final conclusions of thesis and future work will be presented in Chapter 9.

2: Theory of instrumental techniques

2.1 Material Characterisation

2.1.1 Nitrogen sorption isotherms

The physical adsorption-desorption of gaseous molecules on the surface of solid materials is a widely used technique for the characterisation of surface and textural properties of porous materials.[65, 83] Physical adsorption involves the attraction of adsorbate molecules to an adsorbent surface which is caused by weak Van der Waal's forces. When a gaseous molecule approaches a solid surface, equilibrium is established between molecules in the gas phase and the adsorbed species (molecules attached to the solid surface). The adsorption process typically involves four stages which can occur on the surface of solid materials as shown in Figure 2.1.[84]
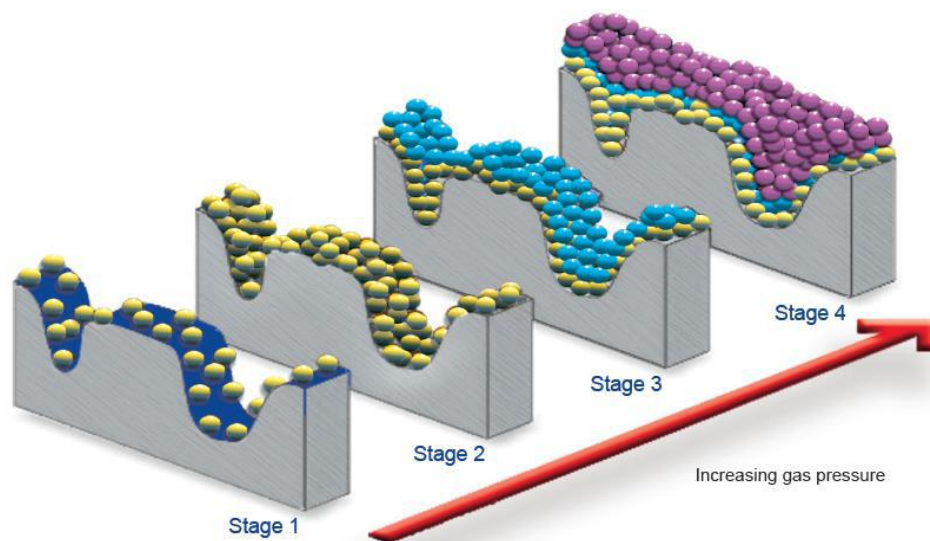
Figure 2.1: Stages of adsorption on porous materials.[84]

In the first stage, gaseous molecules are adsorbed by the isolated sites present on the surface of the sample at low pressures. As the gas pressure increases in stage 2, a monolayer is produced as all the isolated sites become covered with gaseous molecules. In stage 3, as the gas pressure increases further, multilayer coverage begins with the smaller pores in the sample filling first. The surface area can be calculated at this stage using the Branauer-Emmett-Teller (BET) equation. In the last stage, complete coverage of the sample is achieved as the gas pressure increases; all the pores are filled. Pore diameter, volume and distribution can be determined at this stage using the Barrett-Joyner-Halenda (BJH) equation.

Adsorption isotherms provide information on the amount of gas adsorbed by a porous solid across a wide range of relative pressures at a fixed temperature (typically liquid nitrogen at a temperature of 77 K; nitrogen is commonly used as an adsorbate due to its inertness.[65, 83] In 1985, adsorption isotherms and hysteresis loops were classified into six types by the International Union of Pure and Applied Chemistry (IUPAC). [65, 85-87] However, this classification and the associated hysteresis loops have been refined and updated based on identification of new isotherm types which are closely related to specific types of pore structures.[88] Going by the recent classifications, adsorption isotherms are classified into eight types as depicted in Figure 2.2.[88]
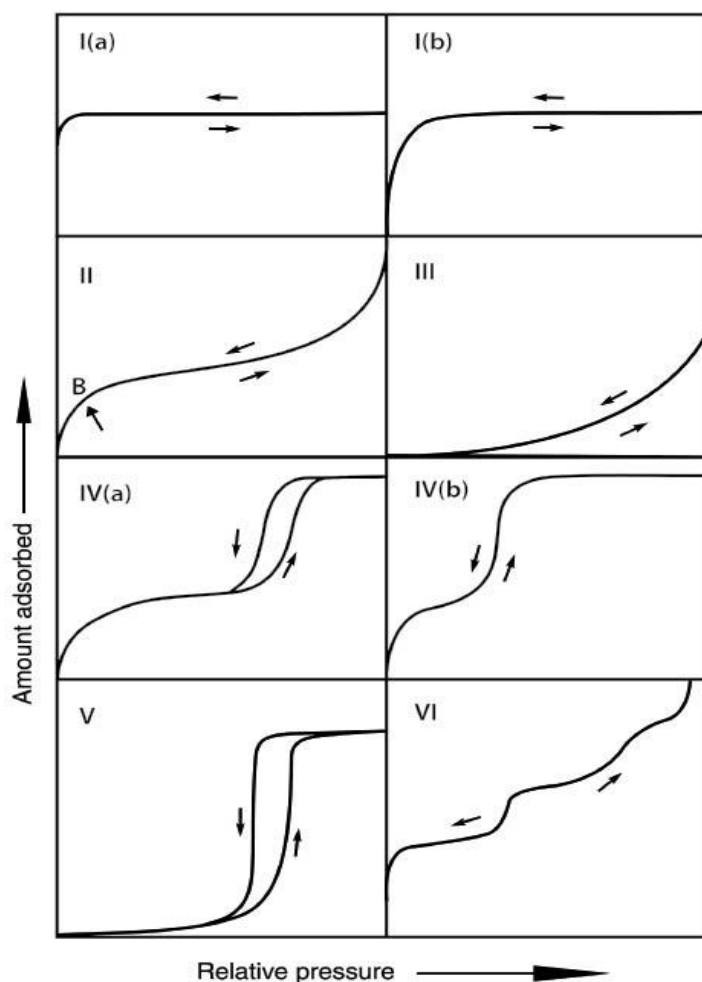
Figure 2.2: Adsorption isotherms.[88]

Type I isotherms are concave to the relative pressure axis and exhibited by microporous solids such as activated carbons, molecular sieve zeolites and porous oxides characterised by relatively small external surfaces.[88] They rise sharply at low relative pressures and reach a horizontal plateau which intersects the relative pressure axis without exhibiting any hysteresis in the desorption curve.[88] The horizontal plateau on the adsorption isotherm can be ascribed to the narrow nature of the pores in the solid (micropores) which are filled at relatively low pressures (below 0.01); indicating a very small external surface area. Type I(a) isotherms are associated with microporous solids which have narrow micropores < 1 nm. Type I(b) isotherms are exhibited by materials which have a broader range of pore size distribution (<2.5 nm); wider micropores and narrow mesopores.[65, 88]

Type II isotherms describe adsorption typically encountered in mesoporous materials which exhibit monolayer adsorption at lower relative pressures, multilayer adsorption and pore condensation with no hysteresis at higher relative pressures (saturation point).[65, 88] These isotherms are sigmoidal in shape. The knee-point (B) of the isotherm corresponds to the stage at which monolayer adsorption is complete and multilayer adsorption begins.[65, 88] Type II isotherms can also be observed in non-porous or macroporous solids.[88]

Type III isotherms are convex over the entire range of relative pressure with no knee-point at B.[65, 88] These isotherms are rare and obtained for materials with very weak adsorbate-adsorbent interactions.[65]

Type IV isotherms are characteristic of mesoporous materials such as oxide gels and mesoporous molecular sieves.[88] The initial region of the isotherm is closely related to type II isotherms indicating monolayer adsorption with the knee point corresponding to multilayer adsorption.[65, 88] At higher relative pressures, a sharp increase in adsorption is observed in the next region of the isotherm which is due to the occurrence of capillary condensation in the pores of the material.[65] A typical feature of Type IV isotherms is the final plateau which they exhibit at saturation pressure.[65, 88] In Type IV(a) isotherms, the hysteresis loop exhibited is associated with the mechanism of pore filling and emptying by capillary condensation.[87, 88] This is usually observed in materials with pore widths above 4 nm. Different types of hysteresis loops are possible for these isotherms.

However, Type IV(b) isotherms are usually observed in adsorbents with smaller pore widths.[88]

Type V isotherms are typical for materials which have weak adsorbate-adsorbent interactions.[65, 88] These isotherms are closely related to type III isotherms.[65] However, the difference occurs at higher relative pressures where type IV isotherms exhibit hysteresis loops due to pore condensation.[65]

Type VI isotherms are associated with step-wise multilayer adsorption on a homogeneous, non-porous surface.[65] These isotherms are not common.[88]

As mentioned previously, hysteresis loops which appear in the multilayer range of adsorption isotherms are generally due to capillary condensation in mesoporous or macroporous materials.[88] A hysteresis loop is obtained in porous materials when the adsorption and desorption branches of the isotherm do not coincide.[83] This occurs when the pore desorption via evaporation occurs at a lower relative pressure than adsorption via condensation. As mentioned earlier, hysteresis loops have been classified into six major types by the IUPAC [88]as shown in Figures 2.3. Some of these loops have a well defined pore structure. Type H1 hysteresis loops are exhibited by mesoporous materials which have a narrow and uniform pore size distribution.[88] They have very steep parallel adsorption and desorption branches in a fairly narrow range.[65, 88]

Type H2 hysteresis loops are typical for inorganic oxide gels associated with a complex pore structure that is made up of interconnected networks with pores of different shapes and sizes.[88] Type H2(a) loops have a very steep desorption branch which could either be due to the presence of blocked pores or occurrence of percolation in pore necks.[88] Type H2(b) loops are usually found in mesosilica material.

Type H3 hysteresis loops are exhibited by materials with slit-shaped pores (aggregates of plate-like particles such as clays). They do not terminate in a plateau at higher relative pressures.[65, 88]

Type H4 hysteresis loops are closely related to H3 as they are obtained in materials with slit-shaped pores but mainly in the micropore range.[88] Like H3 loops, they do not terminate in a plateau at higher relative pressure; the loops do not close until the

equilibrium pressure is equal to or near saturation pressure.[65] H4 loops are typically exhibited by mesoporous or aggregated crystals of zeolites and micro-mesoporous carbon materials.[88]

Type H5 loop is unusual, it is associated with materials which have pore structures that are open and partially blocked.[88]
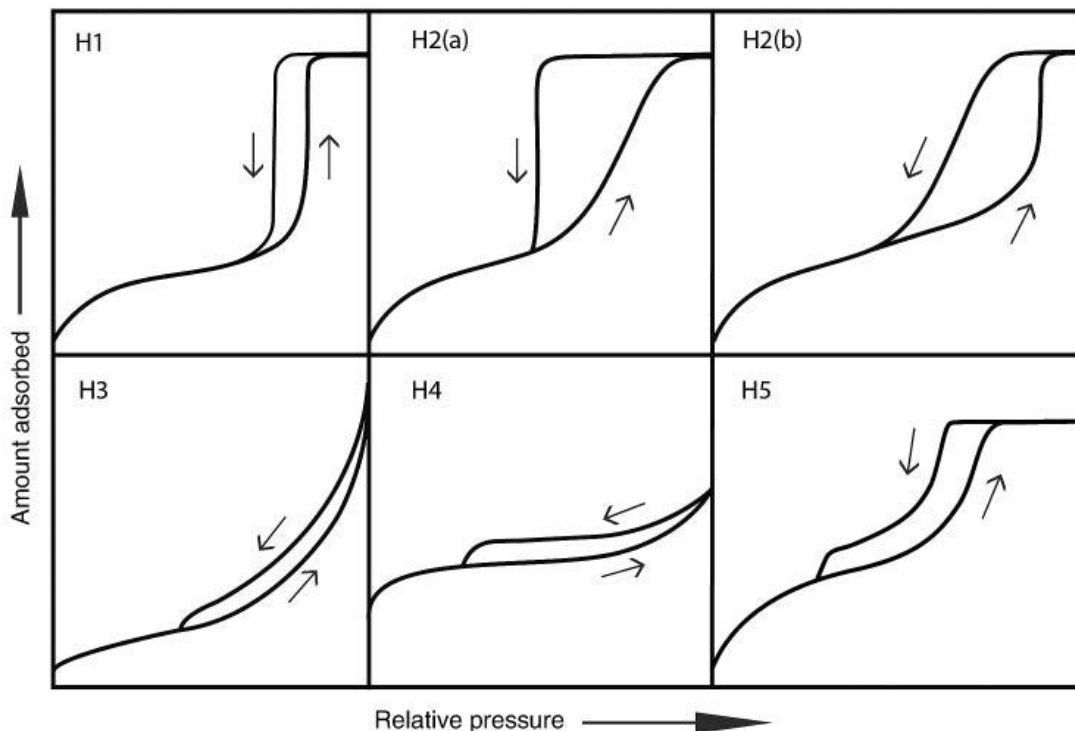
Figure 2.3: The IUPAC classification of hysteresis loops.[88]

2.1.2 BET Surface area

The concept of adsorption originally developed by Langmuir was based upon the assumption that a dynamic equilibrium exists between gaseous molecules and a solid surface resulting in the formation of a monolayer at maximum adsorption.[89] Brunauer, Emmett and Teller (BET) extended this theory stating that multilayer formation was the basis of physical adsorption. [89] The BET equation is widely used for determining the specific surface area of porous materials.[83, 90]

The BET equation is expressed in the linear form as[65]:

$$\frac{1}{V[(P_0/P)-1]} = \frac{1}{V_m C} + \frac{P(C-1)}{P_0 V_m C}$$

Eq.2.1

Where V is the volume of gas adsorbed at standard temperature and pressure (S.T.P) gram of adsorbent, P_0 is the saturated pressure of the adsorbate gas, P is the equilibrium pressure of the adsorbate gas, V_m is the monolayer capacity (volume of gas adsorbed at STP to produce an apparent monolayer) and C is the BET constant.[65, 83] A BET plot of $\frac{1}{V[(P_0/P)-1]}$ versus $\frac{P}{P_0}$ will give a straight line with slope $= \frac{C-1}{V_m C}$ and intercept $= \frac{1}{V_m C}$

The linear form of the BET equation is restricted to the section of the isotherm in the relative pressure range of 0.05 - 0.25 where complete monolayer adsorption occurs.[65, 83] V_m and C can thus be obtained from the slope and intercept of the plot. The specific surface area (S_{BET}) of the adsorbent can be calculated from the monolayer capacity using equation 2.2.[83, 88]

$$S_{BET} = \frac{V_m N_a \sigma}{m \times 22400}$$

Eq.2.2

Where N_a is Avogadro's constant (6.022×10^{23} mol), σ is the effective cross-sectional area of one adsorbate molecule in m^2 (0.162 nm for nitrogen at 77 K), m is the mass of test sample used in grams and 22400 corresponds to the volume occupied by 1 mole of the adsorbate gas at STP.[83]

2.1.3 Determination of pore size distribution

The Barrett-Joyner-Halenda (BJH) method is the most commonly used algorithm for calculating pore size distribution from sorption isotherm data based on the cylindrical pore model.[91] In addition to multilayer adsorption, capillary condensation also occurs as the pressure of the gas in contact with the porous solid increases.[65]

The BJH method accounts for these phenomena in the pores using the classical Kelvin equation (Equation 2.3). [65, 92, 93]

$$\ln\left(\frac{P}{P_0}\right) = \frac{2\gamma V_1}{RTr_k}$$

Eq. 2.3

Where P is the actual vapour pressure, P_0 is the saturated vapour pressure, γ is the surface tension of the liquid, v is the molar volume of the liquid, r_k is the Kelvin radius (the radius of the hemispherical meniscus of the liquid condensate in the filled pore), R is the universal gas constant and T is temperature.[65]

2.2 Fourier Transform Infrared Spectroscopy (FTIR)

Infrared (IR) spectroscopy is a widely used technique for structural elucidation of organic molecules which is based upon vibrations of atoms within the molecule once infrared radiation is absorbed.[94, 95] Thus, it's very useful for qualitative and quantitative analysis of samples.[94] The process is initiated by the passage of a beam of infrared radiation from an IR source through the sample under investigation such that a fraction of the radiation is absorbed by the sample and some transmitted.[95] This results in an IR spectrum which corresponds to the amount of light absorbed by the sample at a particular wavelength; thereby creating a molecular fingerprint of the sample being studied.[94]

The sample molecules absorb IR radiation if the vibrational frequency of the molecule is similar to that of the incident radiation.[96] However, if the vibrational frequency of the molecule is different from the frequency of the incident radiation, the radiation is reflected or undiminished in some cases.[96] The vibrational frequency of a diatomic molecule is usually derived using Hooke's law (see Equation 2.4). [96]

$$v = \frac{1}{2\pi}\sqrt{\frac{k}{\mu}}$$

Eq. 2.4

where v is the vibrational frequency, k is the force constant of the bond joining the atoms and μ is the reduced mass of the atoms in the bond which is calculated as[96]:

$$\mu = \frac{m_1 \times m_2}{m_1 + m_2}$$

In order for a pair or group of atoms to absorb IR, it must be capable of undergoing a change in dipole moment during vibration.[94, 96] Molecular vibrations are basically the most useful vibrational frequencies in IR. They are classified based on their mode of vibration; stretching vibrations which could be symmetric or asymmetric and bending vibrations which could be due to scissoring, twisting, wagging, rocking and torsion.[96]

Infrared spectrometers used for analysis are generally categorised into dispersive and interferometric spectrometers.[97] In dispersive spectrometers, the separation of energy emitted from the infrared source is achieved using a prism or grating and the amount of energy absorbed by the sample at each frequency is subsequently measured by the detector.[94, 96] This results in a spectrum which is a plot of intensity against frequency.[96]

Fourier transform (FT) infrared spectrometers which involve the use of interferometers were developed to overcome several limitations such as slow scanning and reduced sensitivity inherent in dispersive spectrometers. In principle, the interferometer is a simple optical device which produces a specific type of signal that consists of all infrared frequencies encoded into it.[96] A beamsplitter which is capable of splitting the incident infrared beam into two optical beams is often employed in most interferometers.[94, 96] As a consequence, one beam is reflected off the flat mirror which is fixed and the other beam is reflected off the flat mirror which moves a short distance from the beam splitter.[94] Finally, the two beams recombine at the beam splitter producing a signal referred to as an interferogram which is subsequently decoded by a Fourier transform algorithm. The Michelson interferometer shown in Figure 2.4 is one of the most commonly used interferometers in FTIR.

In this study, Attenuated Total Reflectance (ATR) – FTIR was employed to examine the samples being studied. ATR measures the change that occurs in a totally internally reflected infrared beam when it comes in contact with the sample.[98] In this process, the incident IR beam passes through the high refractive index ATR crystal such that it is reflected off the internal surface of the crystal which is in close contact with the sample at least once.[98] This total internal reflection produces an evanescent wave which penetrates into the sample usually between 0.5 – 5 μm.[94, 99] The sample absorbs a

fraction of the energy of the evanescent wave and the reflected radiation is subsequently transmitted to the detector.[94] The beam is finally collected off the detector and transformed into an electrical signal as it leaves the crystal.[100] A schematic representation of the ATR process is given in Figure 2.5.[101]

The depth of penetration (d_p) of light into the sample is usually determined by the wavelength of the light, angle of incidence of the light and refractive index of the ATR crystal.[101] Therefore, it is highly critical for the ATR crystal to be made of an optical material with a refractive index higher than that of the sample to prevent the entire incident beam from being absorbed by the sample; to permit the evanescent effect.[98] In addition, it is important for a good contact to be established between the samples and the surface of the crystal for good results to be obtained. Hence, solid samples usually require the application of moderate pressure compared to liquid samples where an intimate contact is usually achieved by pouring a small amount over the surface of the crystal.[96] The most commonly used materials for making ATR crystals are diamond, germanium and zinc selenide.[96]
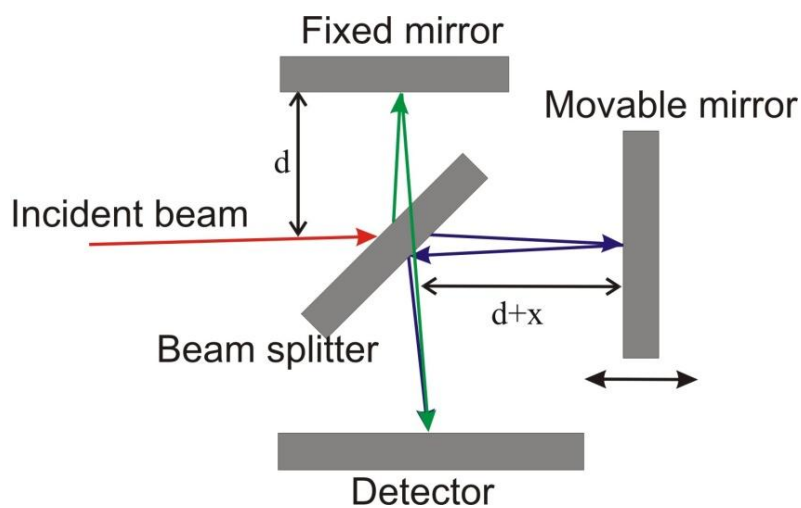
Figure 2.4: Schematic diagram of a Michelson Interferometer.[97]
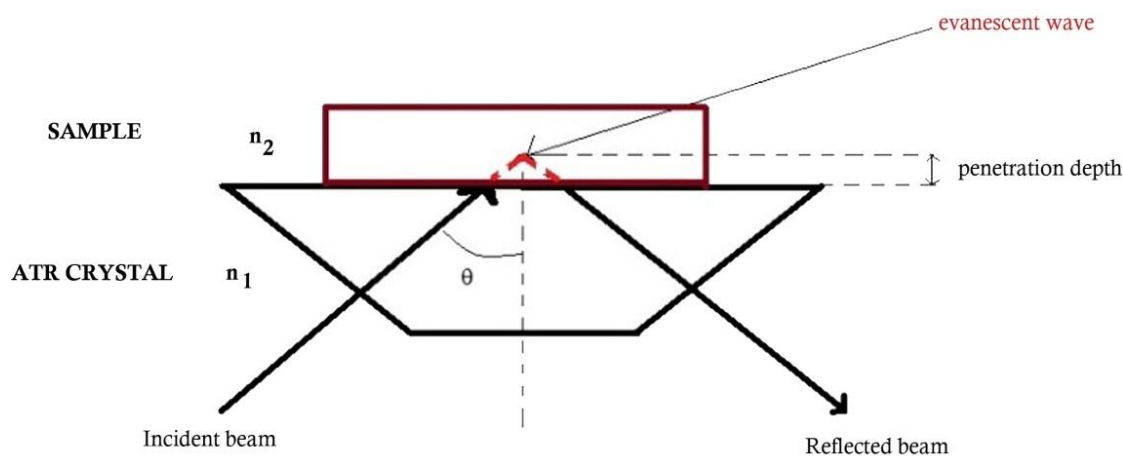
Figure 2.5: Schematic representation of a single reflection ATR.[101]

2.3 CHN Microanalysis

CHN microanalysis is essentially a technique that is widely used for rapid determination of elements such as carbon (C), hydrogen (H), nitrogen (N) and sulfur (S) in organic matrices.[102, 103] It can be employed for analysis of various sample types such as solids and liquids which are volatile and viscous in nature. Thus, it is used for measuring these elements for industrial (environment, food, energy, chemicals and pharmaceuticals) and research applications.

In CHN analysis, the sample is accurately weighed into a tin or silver capsule and sealed. The sample introduction system is selected based on the application or sample type.[103, 104] The materials used for introduction of the solid and liquid samples are tin capsules and aluminium vials/autosamplers respectively.[103] At the start of the run, helium gas is swept through the analyser and a measured excess of oxygen is added to the stream. The sample is then combusted at a temperature of 1000 °C in the combustion chamber resulting in the conversion of carbon to carbon dioxide, hydrogen to water, nitrogen to nitrogen gas or oxides of nitrogen and sulfur to sulfur dioxide as shown in Equation 2.5.[102, 103]

$$C, H, N, S \xrightarrow{\sim 1000°C/O_2} CO_{2\,(g)} + H_2O_{(g)} + N_{2\,(g)} + SO_{2\,(g)} + SO_{3\,(g)} \qquad \text{Eq.2.5}$$
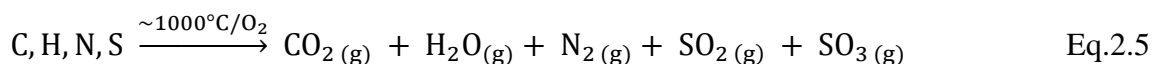
The combustion products are swept by helium through a hot tungsten trioxide catalyst to complete the conversion of carbon to carbon dioxide. The mixture is subsequently passed through metallic copper heated at 850 ℃ to convert sulfur trioxide gas to sulfur dioxide gas and remove any form of excess oxygen remaining from the initial combustion process. A schematic diagram of a CHN analyser is shown in Figure 2.6.[103]

$$Cu \ + \ SO_3 \xrightarrow{850℃} SO_2 \ + CuO_{(s)} \hspace{3cm} \text{Eq.2.6}$$

$$Cu \ + \frac{1}{2} \ O_2 \xrightarrow{850℃} CuO_{(S)} \hspace{3cm} \text{Eq 2.7}$$

Detection of the gases CO_2, H_2O, N_2 and SO_2 in the product mixture is achieved by gas chromatographic separation followed by quantification with a thermal conductivity detector (TCD).
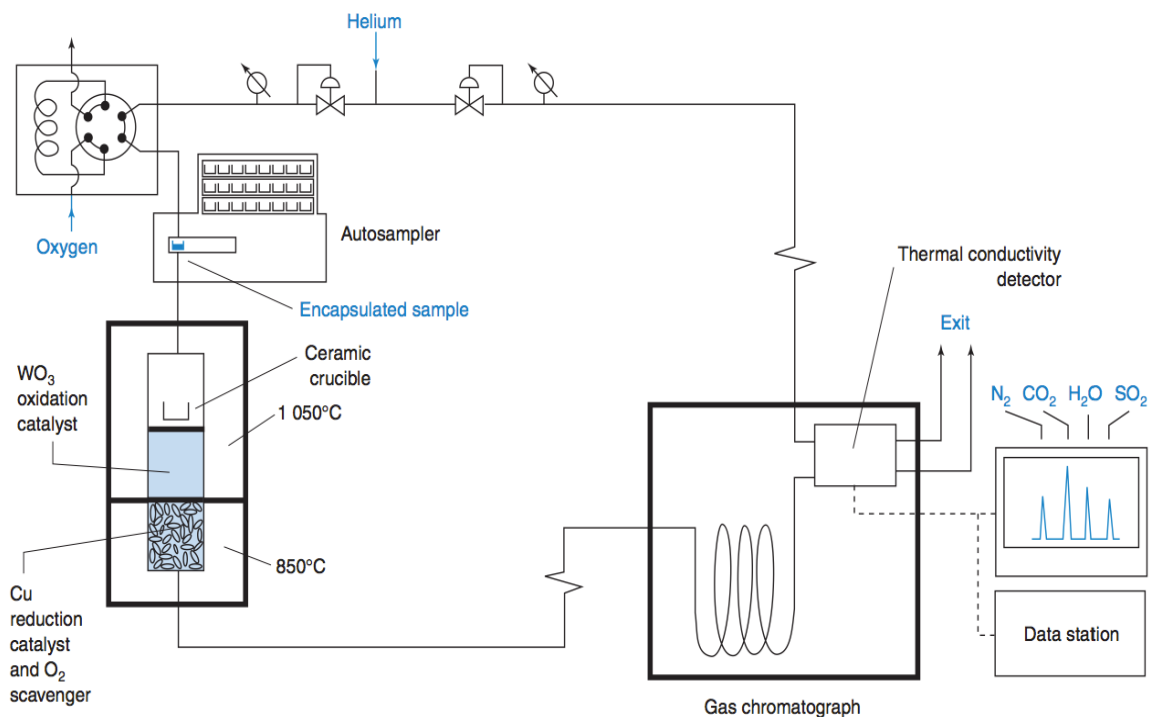
Figure 2.6: Diagram of CHN analyser with gas chromatograph and thermal conductivity detector (TCD).[102]

2.4 Solid phase extraction

Solid phase extraction (SPE) is a sample preparation method used to selectively isolate, enrich and / or clean – up target analytes from aqueous samples prior to analysis. [105-107] Although sample preparation consisting of sample dissolution, purification and extraction was traditionally carried out with liquid-liquid extraction (LLE),[108] this method had several disadvantages which includes the use of large volumes of solvent and the creation of emulsion in aqueous samples that were difficult to extract, resulting in low analyte recoveries and high cost.[105, 106] Furthermore, the presence of interfering compounds in liquid mixtures or extracts obtained from solid matrices capable of co-eluting with the analyte of interest created the need to employ a technique that aided the removal of interferences prior to analysis and subsequently minimised potential co-elution problems. These difficulties were, in part, overcome by the SPE technique.

In SPE, the aqueous sample is introduced onto a solid sorbent (stationary phase) which is packed into a small cartridge. This results in the selective adsorption of the target analytes onto the sorbent's surface prior to elution.[105] The most common SPE arrangement involves the use of a cartridge and a syringe barrel. SPE cartridges are usually made of polypropylene with an opening for sample introduction and an exit for the sample leaving the cartridge as shown in Figure 2.7.[105]
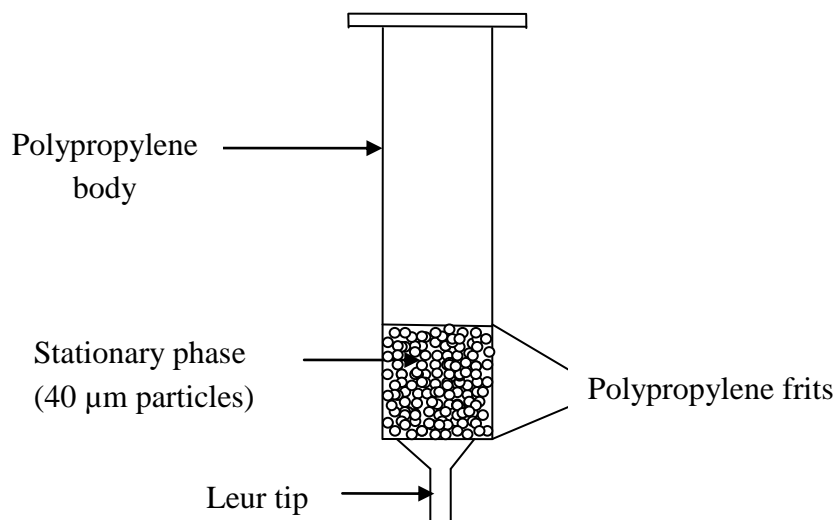
Figure 2.7: Schematic diagram of a solid phase extraction cartridge.[105]

The sorbent material employed (mass of 50 mg – 10 g) is held in between two frits placed at the bottom of the cartridge.[105] The frits are made from polypropylene and have a pore size of 20 µm which helps retain both the sorbent and filter out particles.[105] The flow rate of SPE cartridges typically ranges from 3 - 10 $cm^3 min^{-1}$. A single cartridge or multiple cartridges can be used and a vacuum pump can also be used to facilitate solvent/sample flow through the sorbent if required. A side - arm flask apparatus can also be used to effect solvent flow through a single cartridge and a vacuum manifold for multiple cartridges.

2.4.1 Sorbents used in SPE

In order to facilitate the SPE process, the proper SPE sorbent must be carefully selected so that it retains only the analytes of interest without binding the contaminants.[105] However, further optimisation of extraction conditions may be required in many situations as SPE sorbents are not that selective.[106, 107] Sorbents used in SPE are of three types: polymer based sorbents, silica-based sorbents and graphitised or porous carbon.[106, 109] However, the most commonly used SPE sorbents are silica particles which are chemically modified with functional groups bonded to silanol groups at the surface.[105] These particles are irregular in shape with a diameter ranging from 30 - 60 µm. Although modification of the silica surface is highly essential to alter its retentive properties, unmodified silica is sometimes used in SPE.

The sorbents used in SPE can be grouped into three categories based on their primary interactions or retention mechanism with target analytes which include normal phase, reversed phase and ion exchange sorbents.[105-107] Table 2.1 contains a summary of silica-bonded sorbent types commonly used in SPE.[105]

Normal phase (NP) SPE involves adsorption of the target analytes from a non-polar mobile phase to the polar surface of the sorbent.[105] Sorbents used in NP SPE essentially are generally more polar than the sample matrix or mobile phase; a solvent such as water which is highly polar in nature is not usually employed.[106] Thus, NP SPE is commonly used to extract polar analytes from non-polar organic solvents.[105, 107] Sorbents used in NP SPE have polar functional groups such as amino (NH_2), cyano (CN) or diols, which

are chemically bonded to silica gel.[105] Their mechanism of interaction includes hydrogen bonding, dipole-dipole interactions, induced dipole-dipole interactions and $\pi - \pi$ interactions.[105] [106] Unmodified silica (bare silica) which is extremely polar can also be used in NP SPE.[105] Since NP sorbents are polar in nature, they have the ability to retain polar analytes. Silica, alumina (Al_2O_3) and florisil ($MgSiO_3$) are examples of the most commonly used normal phase sorbents.[105, 106] Although silica and florisil are used in the sequestration of low to moderately polar analytes from non-aqueous solutions, alumina is employed for the removal of polar solutes from non-aqueous solutions.[105]

Reversed phase (RP) SPE involves adsorption of the organic analytes from an aqueous phase which is polar in nature into a non-polar solid phase.[105, 106] In contrast to normal phase sorbents, reversed-phase sorbents are more hydrophobic than the sample.[106] Thus, they are commonly used in SPE to retain non-polar organic analytes from aqueous samples. Reversed-phase sorbents are characterised by non-polar functional groups such as octadecyl (C18), octyl (C8) and methyl bonded to silica with mechanism of interaction that includes van der Waals or dispersion forces.[105] The attachment of a saturated hydrocarbon such as a C_{18} group to bare silica makes its surface become non-polar (hydrophobic). However, a small amount of unreacted or free silanol groups may still be present in silica-based sorbents after completion of the initial bonding reaction as complete bonding of the functional group may not be achieved initially. These unreacted silanols provide polar and acidic sites which could result in complex interactions with compounds and subsequently undesirable/low recoveries. To minimise these interactions, the bonded phase is usually end-capped by reacting the exposed silanols with trimethylsilane (TMS). Nevertheless, non-endcapped phases with unreacted silanols can be used to retain polar analytes in RP SPE since they contain both hydrophobic alkyl chains and polar acidic silanol moieties.[105]

Ion-exchange SPE is typically used to separate either cationic or anionic compounds from either a polar or non-polar mobile phase to an ion-exchange sorbent with an opposite charge.[105] Ion-exchange sorbents are thus made of functional groups which have either cationic or anionic properties bonded to silica gel.[105-107] This causes them to attract compounds of opposite charge when in the ionised form.[105, 108] The ion-exchange sites for strong cation-exchangers consists of sulfonic acid groups while that of weak

cation-exchangers consists of carboxylic acid groups.[105, 106] Strong anion-exchangers are quaternary amines and weak anion-exchangers are primary, secondary and tertiary amines.[105, 106] Thus, ionic compounds can be isolated from aqueous and non-aqueous solutions using cation and anion exchange resins. However, care must be taken in the use of strong acid and bases to avoid exceeding the ion-exchange capacity of the sorbent.[105] A typical example of ion exchange SPE is the retention of cations (amines) on cation exchangers (sulfonic/carboxylic acids) or the retention of anions (sulfonic acid or carboxylic acid groups) on anion exchangers containing any of the different amino groups.[105, 106]

Table 2.1: Summary of Commonly used sorbents in SPE.[106]

Sorbent	Bonded Moiety	Physical properties
Normal phase Cyano (CN) Amino (NH$_2$) Diol (2OH) Silica gel Florisil Alumina	Si-(CH$_2$)$_3$CN Si-(CH$_2$)$_3$NH$_2$ Si-(CH$_2$)$_3$OCH$_2$CHOHCH$_2$OH -SiOH -MgSiO$_3$ -Al$_2$O$_3$	Polar
Reversed phase Octadecyl (C-18), ODS Octyl (C-8) Ethyl (C-2) Cyclohexyl (CH) Phenyl (PH)	Si-(CH$_2$)$_{17}$CH$_3$ Si-(CH$_2$)$_7$CH$_3$ Si-CH$_2$-CH$_3$ Si-CH$_2$CH$_2$-cyclohexyl Si-CH$_2$CH$_2$CH$_2$-phenyl	Non polar
Ion Exchangers Amino propyl, (primary amine) Trimethyl ammoniopropyl, (quartenary amine) Carboxylic acid Ethyl benzene sulfonic acid	Si-(CH$_2$)$_3$NH$_2$ Si-(CH$_2$)$_3$N$^+$ (CH$_3$)$_3$ Si-(CH$_2$)$_2$ COOH Si-(CH$_2$)$_3$-C$_6$H$_4$-SO$_3$H	Weak anion exchange Strong anion exchange Weak anion exchange Strong cation exchange

2.4.2 Solvent Selection in SPE

In SPE, the tendency of the target analyte to be retained by the sorbent and subsequently eluted from the sorbent is determined by the solvent employed.[105] The ability of the solvent to elute target analytes from the sorbent is also governed by its polarity.[105, 106] The different solvent strengths for normal and reversed phase sorbents are displayed in Table 2.2.[105] A mixture of solvent system is usually employed when an individual solvent is inadequate.[105]

Table 2.2 Solvent strengths for normal and reversed phase sorbents.[105]

Solvent strength for normal phase sorbents		Solvent strength for reverse phase sorbents
Weakest	Hexane	**Strongest**
	Iso-octane	
	Toluene	
	Chloroform	
	Dichloromethane	
	Tetrahydrofuran	
	Ethyl ether	
	Ethyl acetate	
	Acetone	
	Acetonitrile	
	Isopropyl alcohol	
	Methanol	
Strongest	Water	**Weakest**

2.4.3 Method of Operation in SPE

The SPE method of operation generally consists of four basic steps: sorbent conditioning, sample addition, interference elution and analyte elution as shown in Figure 2.8.[105, 107, 108] The first step which involves conditioning the sorbent consists of

two sub steps: an initial solvation step and an equilibration step. In the solvation step, the SPE column is initially wetted with a solvent of intermediate strength before the sample is loaded.[105, 106] This facilitates solvation of the bonded alkyl chains thereby promoting interactions between the target analytes and sorbent during adsorption.[105] This is followed by an equilibration step in which a solvent/buffer of similar composition is passed through the sorbent.[106] This aids the removal of residual solvent from the solvation step.[105] In addition, the sorbent is equilibrated in a solvent capable of maximising interactions with target analytes which is necessary for promoting retention.[106] It is essential that the sorbent bed is prevented from drying at this stage or poor recoveries could result. During sample addition, the sample is allowed to pass through the sorbent under suction so that target analytes are retained in preference to impurities.[105] This is followed by interference elution where the sorbent is subsequently washed with a solvent that facilitates isolation of extraneous material without causing elution of the target analyte.[105, 106] Therefore, the solvent used during interference elution should be of intermediate polarity; neither weak nor strong as the solvent used during sample addition and elution respectively.[105, 106] However, it is essential that the wash solvent be miscible with the sample and solvent used for elution so that drying the column in between steps is avoided.[105, 106] The wash step is strongly influenced by the solvent employed and interaction of the target analyte with the sorbent. It is of crucial importance to the entire process as it provides significant improvements in purity.[105] Finally, elution of the target analyte is achieved using a sufficient amount of solvent.[105, 106]

A strong solvent capable of disrupting the analyte-sorbent interactions should be applied in the elution step to facilitate the selective desorption/elution of target analytes from the sorbent.[105] In some cases, a mixture of solvents that can effectively break primary interactions and any other secondary retention mechanisms responsible for analyte binding could be employed during elution.[105] Successful SPE (high analyte recoveries, highly purified extracts and analyte concentration) requires careful selection of the sorbent, solvent systems being used and influence of the analyte of interest.
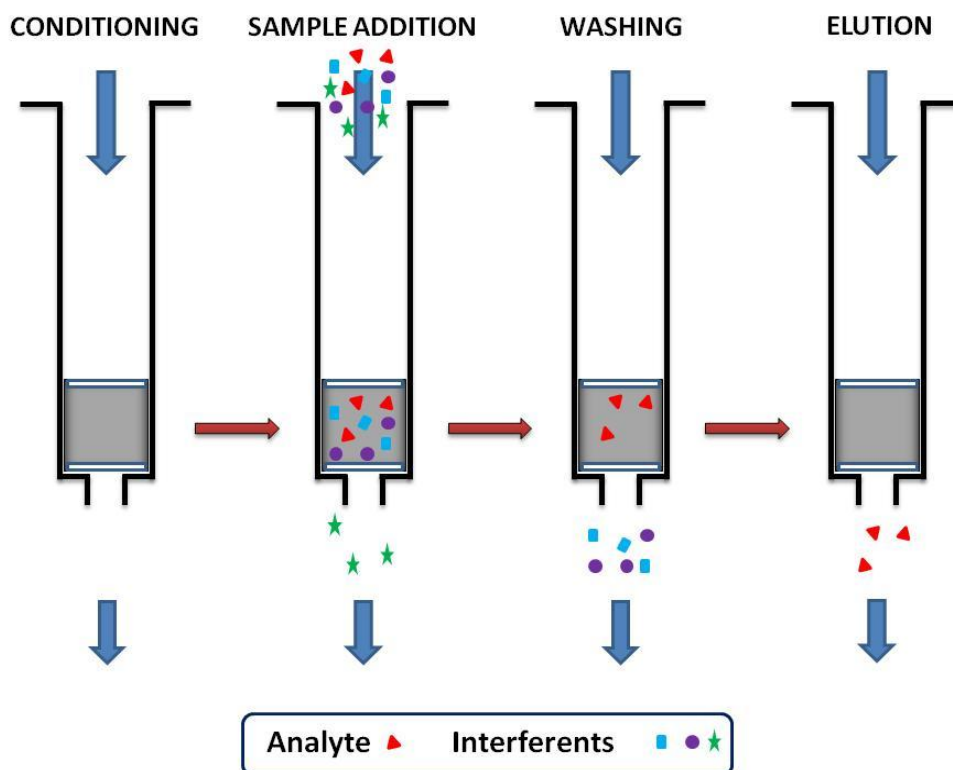
Figure 2.8: The four stages of operation of solid phase extraction.[110]

2.5 Accelerated solvent extraction

Accelerated solvent extraction (ASE) is an extraction technique that uses organic solvents at high temperatures (100 - 180 °C) and pressures (1500 - 2000 psi) to enhance the recovery of organic analytes from solid or semi-solid matrices.[105, 108, 111] This technique is also referred to as pressurised fluid extraction (PFE) or pressurised liquid extraction (PLE).[105, 108] ASE overcomes several limitations inherent in classical extraction techniques such as soxhlet extraction and sonication extraction which require large volumes of organic solvents and long extraction time (up to 24 h).[112, 113] Thus, it has been widely applied in environmental research for extracting a wide variety of organic compounds such as polyaromatic hydrocarbons (PAHs), polychlorinated biphenyls (PCBs), dioxins, furans, pesticides and herbicides from semi-solid and solid matrices.[105, 114] The elevated temperatures and pressures utilised in ASE have a significant effect on the solvent, sample and their interactions.[112] Elevated temperatures result in solubility and mass transfer effects as the capacity of solvents to solubilise

39

analytes increases and mass transfer becomes faster.[112] Similarly, high temperatures and pressures cause disruption of surface equilibria.[108, 112, 115] Elevated temperatures weaken the strong analyte-matrix interactions caused by van-der Waals forces, hydrogen bonding and dipole attractions.[112] In addition, elevated temperatures decrease the viscosity and surface tension of the solvent, solutes and matrix thereby enhancing solvent penetration into the matrix and subsequently extraction.[108, 112] The high pressures at which ASE is carried out facilitates an increase in the boiling point of solvents and helps to maintain the organic solvents as liquids above their boiling points.[112] Thus, the advantages derived from the use of elevated temperatures for ASE would be precluded if elevated pressures are not employed.[112, 116] High pressures also promote the extraction of analytes trapped in matrix pores as the ability of the organic solvent to penetrate certain areas in the sample matrix that would otherwise not be contacted under atmospheric conditions is enhanced.[108, 112] Hence, ASE provides improved extraction efficiencies due to the combination of high temperatures and pressures applied during extractions compared to extractions carried out at or near room temperatures.[112]

2.5.1 The ASE process

The ASE system comprises of a solvent pump, nitrogen tank, heating oven, collection vial and three high pressure valves (pump valve, purge valve and static valve).[112, 117] The sample cells used for extraction are usually made of stainless steel which is capable of withstanding high temperature and pressure required for extractions.[105] Extraction cells are usually lined with cellulose or glass filters to prevent the discharge of suspended particles in extracts into the collection vial. Sample sizes can range from 1 to 100 cm^3. The ASE process involves the use of a dynamic and static flow of solvent to extract analytes from the sample in an extraction cell as illustrated in Figure 2.9.[112] In the first step, the extraction cell containing the sample is loaded onto the cell tray and the oven is heated to the preprogrammed set point. ASE can be performed using two methods: the prefill method and preheat method.[108, 112] In the prefill method, the sample cell is filled with solvent before the cell is heated to the desired temperature and pressure while the preheat method involves heating the sample cell to the desired temperature before the solvent is added.[108, 112] Using the preheat method, the solvent is pumped into

the cell with the static valve closed and extractions carried out.[108] A dynamic or static flow of solvent or a combination of both can be used to facilitate extractions at this stage. In the dynamic mode, the extraction solvent flows through the system while in the static mode, no solvent flows through the system.[108, 112] Although the dynamic mode of extraction may result in higher extraction efficiency, solvent consumption is usually high. Hence, static extractions of 5 - 99 min are commonly employed. After heating and static extractions, the static valve opens and extracts are subsequently flushed into collection vials with fresh solvents.[112] The amount of solvent flushed through the extraction cell after the static state is expressed as a percentage of the cell volume and an equal amount used in each cycle.[108] Flush volumes range from 5 to 150 % of the cell volume and static cycles range from 1 to 5. Once the final solvent flush is finished, the solvent is purged into the collection vial with nitrogen gas usually from 20 to 90 s depending on the cell size.[112] At this stage, the collection vessels contain all the solvent and analytes extracted from the sample. This is referred to as purging. Residual pressure is released from the cell and pressure vented from the system.
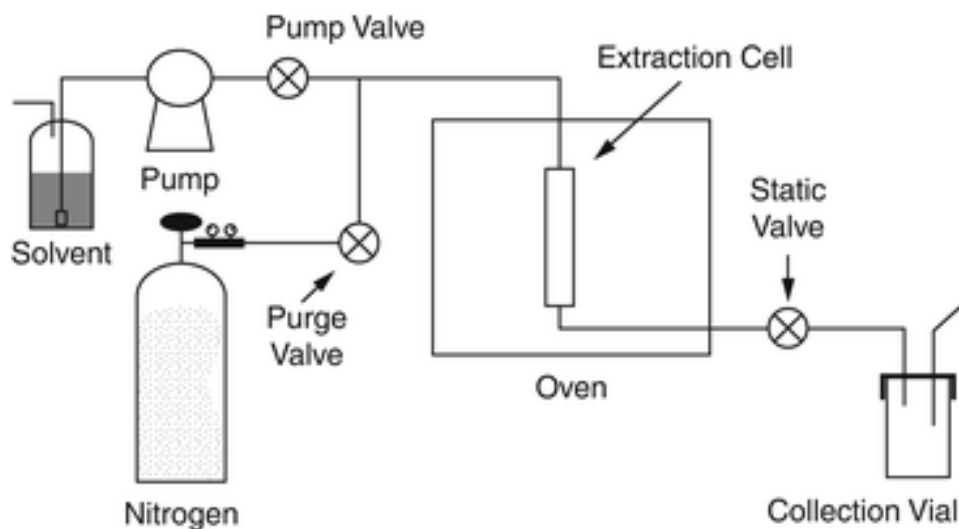
Figure 2.9: Schematic diagram of an Accelerated solvent extraction system.[112]

Samples must be properly prepared prior to extractions to ensure that efficient and reproducible extractions are obtained. Thus, the ideal sample for extraction is a dried, finely divided solid which allows the extraction solvent to flow through and penetrate the matrix pores.[108] Drying or dispersing agents can be added to wet samples to reduce the moisture content.[108] The solvent and temperature used for extractions have a

significant effect on extraction efficiency obtained. Thus, the extraction solvent used in ASE is that which is capable of solubilising the target analyte without degrading the sample matrix.[112] Similarly, ASE is usually performed at a temperature of 75 - 150 °C which is sufficient to disrupt solute-matrix interactions without causing thermal degradation of the target analytes. The pressure selected should be sufficient to maintain the solvent in its liquid state at a temperature above its boiling point at atmospheric pressure.[108, 112] A summary of the ASE process is given in Figure 2.10.
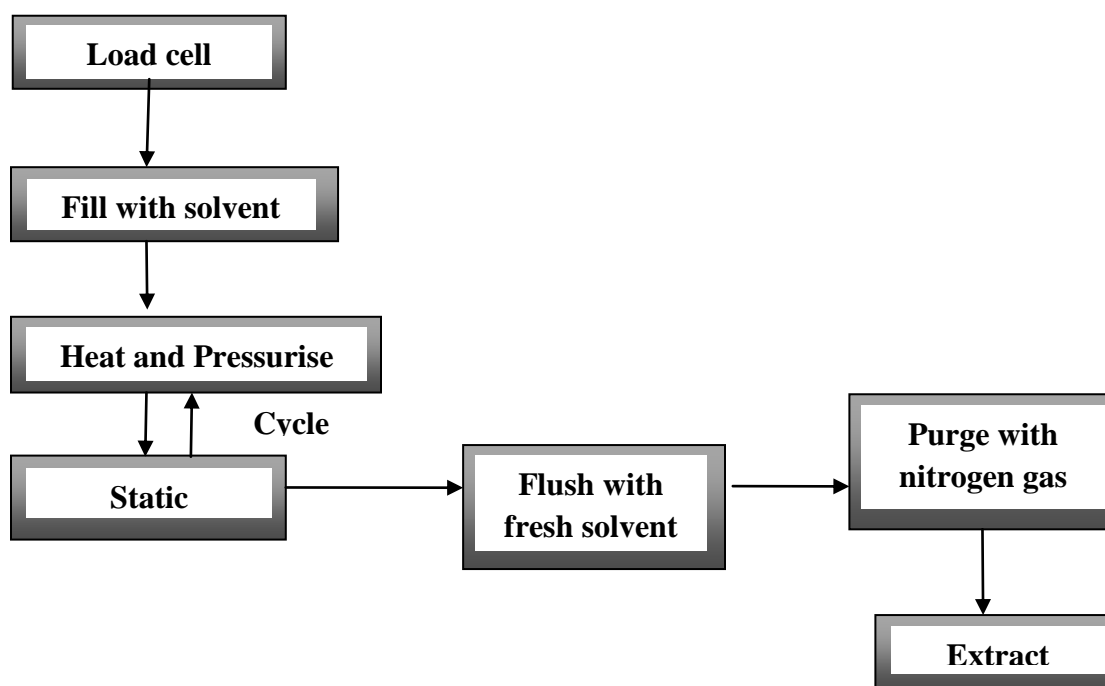
Figure 2.10: Schematic diagram of the ASE process.[108]

2.6 Microwave-assisted extraction

Microwave-assisted extraction (MAE) is a technique that utilises microwave energy to cause molecular movement and dipole rotation of molecules; giving rise to rapid heating of the solvent and samples.[105, 108, 118, 119] Microwaves are electromagnetic radiation that occur between the radio frequency and infrared regions of the electromagnetic spectrum with frequencies ranging from 0.3 - 300 GHz.[108, 118, 120] However, microwave heaters designed for laboratory use are operated at 2.45 GHz.[118] In comparison to conventional

heating where the transfer of thermal energy from the source to the object is achieved via conduction and convection, ionic conduction and dipole rotation are the phenomena responsible for transforming electromagnetic energy into heat during microwave heating.[108] In ionic conduction, ions formed in a solution move under the influence of an electromagnetic field such that heat is generated from the resultant friction between the solution and the ions.[108] In dipole rotation, dipoles of a molecule realign with the changing electric field. Heat is generated due to the inability of the solvent molecules to be realigned with the changing electric field.[108]

The ability of a material to transform electromagnetic energy into thermal energy is generally defined by the value of its dissipation factor (tan δ) given as[108]:

$$\tan \delta \; = \frac{\varepsilon''}{\varepsilon'} \hspace{5cm} \text{Eq 2.8}$$

where tan δ is the dissipation factor; a measure of the efficiency with which solvents heat up under microwave energy, ε'' is the dielectric loss co-efficient; a measure of the efficiency of a material to convert electromagnetic energy to thermal energy and ε' is the dielectric constant; a measure of the ability of the material to absorb microwave energy.[108, 118] As the dielectric constant value ε' increases, the ability of the solvent to become hot also increases. The temperature used in MAE must be carefully selected such that analyte degradation doesn't occur during extraction.

In MAE, dielectric materials or solvents with a permanent dipole get heated under microwave irradiation.[105, 108, 115] Thus, the organic solvent selected for MAE must be capable of absorbing microwave radiation and becoming hot. In addition, the solvent or solvent mixture should be capable of efficiently extracting the target analytes from the sample matrix without extracting the matrix material or degrading analytes of interest.[105] Organic solvents commonly used in MAE include acetone, acetonitrile, dichloromethane and methanol.[105] Non-polar organic solvents like benzene, hexane and toluene which lack dipoles do not absorb microwaves and as a result of this cannot be heated. However, binary mixtures such as hexane: acetone with only one solvent absorbing microwave can be employed. In order to obtain reproducible results and prevent excessive heating in MAE, the moisture content of the sample matrix must be carefully

controlled.[115, 118] This can be achieved by drying the sample matrix or adding a drying agent to the sample matrix prior to extraction.[108]

2.6.1 The MAE process

A microwave system consists of a magnetron (microwave generator), waveguide for transmission, resonant cavity and power supply.[105, 115, 117, 121] A magnetron is a special oscillation tube that generates microwaves that are transported to resonant cavities (oven) by waveguides.

The two distinct types of microwave devices for MAE are the open-vessel and closed-vessel systems (Figure 2.11).[118, 122] Open-vessel systems are usually operated under atmospheric pressure while closed-vessel systems are operated under elevated pressures in a controlled manner.

In open-vessel MAE units, the sample and solvent are placed in an open vessel.[105] Microwaves are then directed to the sample/solvent system by a focused waveguide causing heating and contact with the reflux system.[105, 108] The extraction is repeated for a short period of time enabling recovery of the organic analytes from the sample matrix.[105] This technique is also known as focused microwave-assisted extraction (FMAE).[108]

In closed-vessel systems, the sample and solvent are placed in sealed vessels.[105] Microwaves entering the cavity are diffused by a mode stirrer which results in uniform distribution of microwave energy within the cavity.[105, 108] In contrast to open vessels which require minimal cooling time prior to handling vessels after extraction, a cooling time is required prior to opening vessels after pressurised extraction since the vessels are sealed.[105] Closed-vessel MAE is also referred to as pressurised microwave-assisted extraction (PMAE).[105]
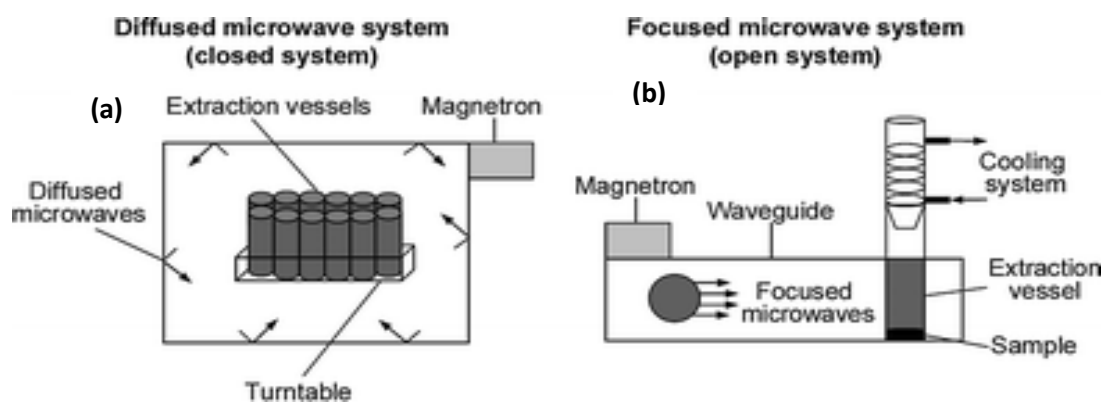
Figure 2.11: Schematic diagram of (a) open and (b) closed MAE systems.[123]

2.7 General theory of gas chromatography

Chromatography is generally used to describe the separation of compounds into their individual components which is based upon the partition or distribution of analytes between two phases termed the stationary phase and the mobile phase.[102, 124] In gas chromatography (GC), the separation of a mixture into its constituents is achieved by introducing the vapourised sample into a gaseous mobile phase which is a stream of inert gas referred to as the carrier gas via an injection port.[104] This is subsequently pumped through a stationary phase held within a column and the effluent finally transferred to a detector. Analytes with a higher affinity for the stationary phase are held within the column for a longer period compared to those with a lower affinity which elute quickly from the system.[124] Liquid or gaseous sample introduction into an injection port is done using a calibrated micro syringe either in the manual or automatic injection mode. The injector temperature is usually 50 °C higher than the boiling point of the least volatile component in the sample.[102, 125] The column is usually enclosed in a temperature controlled oven and the rate at which analytes travel through the column is influenced by their physical properties, composition of stationary phase and column temperature. For a compound to be suitable for GC analysis, it must have a reasonable volatility (200 - 400 °C), high thermal stability and low molecular mass. Hence the GC finds widespread use for the separation and analysis of volatile and semi volatile compounds.[102]

The mobile phase in GC is a gas. Unlike most other types of chromatography, the gaseous mobile phase doesn't interact with molecules of the sample; it simply transports the sample species through the column and is thus referred to as the carrier gas.[126, 127] Therefore, the carrier gas used in GC must be chemically inert and of high purity (free from moisture and oxygen) which is highly crucial in preventing column degradation. Helium, hydrogen, nitrogen and argon are the most commonly used carrier gases in GC with flow rates typically between 0.5 to 50 cm^3 min^{-1}.[128]

The stationary phase used in GC is selected based on its polarity which is determined by the relative polarities of the solutes; a non-polar stationary phase will interact more with a non-polar compound and vice versa. [102] However, in order to successfully achieve separation in GC, the stationary phase must meet certain criteria.[95] It must be thermally and physically stable since high temperatures are often required in GC analysis, chemically inert to solute molecules to prevent the solutes from being lost during the analysis and capable of generating different partition ratios in different sample components at a useful temperature since most stationary phases have a temperature below which they become unable to partition the solute molecules with the carrier gas.[126] The most common stationary phases for fused silica capillary columns in GC are polysiloxanes (silicones) and polyethylene glycol (carbowax) with the former being the most widely used due to the good flexibility possessed by its polymer backbone (Figure 2.12) which allows high diffusion rates of solute molecules into the polymer to be achieved.[125] In addition, it has a good thermal stability with only a slight decrease in viscosity at high temperatures.
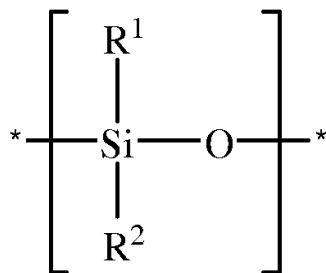
Figure 2.12: Backbone of polysiloxanes.

R^1 and R^2 are functional groups that determine the polarity of polysiloxanes and could either be methyl, phenyl or cyanopropyl. Thus, examples of the most commonly used

polysiloxanes include dimethylpolysiloxane, diphenyl dimethylpolysiloxane and cyanopropylphenyl dimethylpolysiloxane as illustrated in Figures 2.13 - 2.15.[126]
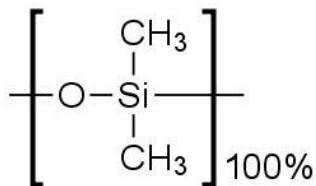
Figure 2.13: Chemical structure of dimethylpolysiloxane.[126]
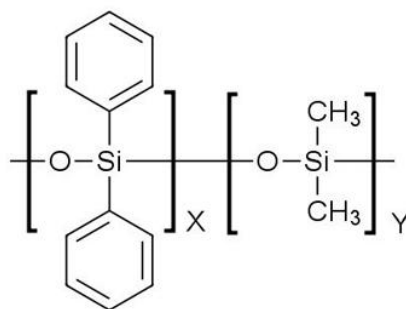
Figure 2.14: Chemical structure of diphenyl dimethylpolysiloxane.[126]
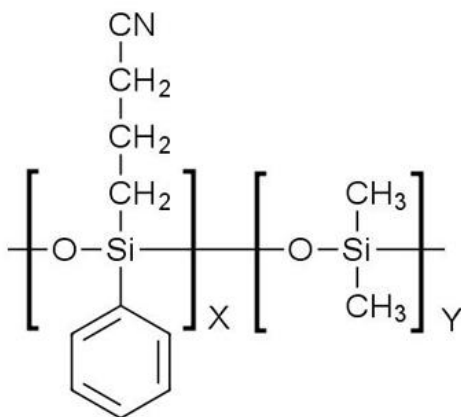
Figure 2.15: Chemical structure of cyanopropylphenyl dimethylpolysiloxane.[126]

2.7.1 Temperature Selection in GC

Selecting the appropriate temperature is highly critical to achieving a successful separation of analytes in GC. This is often a compromise between several factors such as speed, sensitivity and resolution.[102, 104] The temperature employed in sample injection should be sufficient for the sample to travel through the column in the shortest possible time without causing thermal degradation of the sample. This is essential as it decreases spreading and increases resolution. The column temperature should be sufficiently high to enable sample components travel through the column at a reasonable speed preferably below the boiling point of the sample. At high column temperatures, sample components are eluted quickly from the column as they spend most of their time in the gaseous mobile phase but resolution is poor.[104, 126] On the contrary, higher resolution is obtained at low column temperatures as analytes spend most of their time in the stationary phase and are subsequently eluted more slowly; although this results in a decreased sensitivity which arises from an increasing speed of peaks.[124]

Sample analysis can be performed in GC either at a constant column temperature (isothermally) or linear increase of column temperature with time (programmed temperature). However, the separation of sample mixtures which have a wide range of boiling points cannot be achieved using an isothermal program as the least volatile compounds will have longer retention times and very broad peaks at lower temperatures and vice versa.[124] Hence, they require the use of a programmed temperature to facilitate analyte separation.[124, 126] In temperature programming, the temperature is automatically increased at a preselected rate so that the elution of analytes is in order of increasing boiling point.[126, 129] Analytes with low affinity for the stationary phase are resolved by initially using low temperatures which is later increased to allow an increase in migration rate of analytes which have a high affinity for the stationary phase.[129] Thus, the GC method can be optimised to achieve the greatest efficiency and resolution by the oven temperature, ramp rate (rate of temperature change) throughout the chromatographic run in a systematic manner.

2.7.2 GC Columns

The two types of columns generally used in a GC system are packed and capillary columns.[130] Packed columns are commonly fabricated from glass or metal tubing and have a typical length of 2 to 3 m and internal diameter of 2 to 4 mm.[126, 127] The columns are packed with small, uniform, spherical particles coated with a liquid stationary phase which have a particle size of 60 to 80 mesh (250 – 170 µm) or 80 to 100 mesh (170 – 149 µm). This gives rise to a large surface area for supporting the stationary phase (1 m^2/g). Capillary columns are open tubular columns with long lengths up to 100 m.[102] Wall coated open tubular (WCOT) columns are capillary columns made of fused silica and have a thin film (0.1 - 5 µm) coated onto and supported by the internal wall of the capillary.[104] They provide the highest resolution of all GC columns due to their dimensions 0.10 - 0.53 mm internal diameter, 15 - 100 mm long and film coating thickness of 0.1 - 5 µm. Another type of capillary column is the support coated open tubular (SCOT) column which contains inert solid microparticles coated with the liquid stationary phase fused to the inner capillary wall.[104] They have a higher surface area and sample capacity than the thin films of the WCOT columns.[126] However, cross linking techniques have provided stable thick films for WCOT columns with greater sample capacity.[126, 129]

The unparalleled resolution provided by capillary columns has resulted in their use in a large variety of industrial and research applications.[126] In comparison to packed columns which can withstand a higher sample mass (20 µL), capillary columns can only withstand sample masses of 10^{-3} µL.[129] Hence the use of a split/splitless injector is usually employed to avoid overloading the column.[102, 124] In split injection mode, the sample is injected into the injection port using a standard syringe and rapidly vaporised.[129] Only a fraction (1 - 2 %) of the vapour is transported by the carrier gas into the column. The sample left after vaporisation is vented to waste through the split flow valve. This provides high resolution separations as neat samples can be introduced but limits trace analysis since only a fraction of the sample enters the column.[126, 129] As a consequence, splitless injection techniques are used for trace analysis.[126] In the splitless injection mode, the injected sample is vaporised and carried slowly onto a cold column usually at a flow rate of 1 cm^3 min^{-1} where both the sample and solvent condense.[125] The

split valve is opened after a few seconds and residual vapours left in the injection port are swept out.[126] A temperature programme subsequently heats the column initially causing solvent vaporisation.[126, 129] The analytes are then vaporised by the hot column and chromatographed as a narrow band.[126]

2.7.3 Band broadening and Chromatographic Efficiency

In GC, efficiency is a measure of the magnitude of band broadening that occurs as the analyte moves through the column.[95, 102] Resolution is a measure of the amount of band broadening that occurs as analytes travel through the column because each solute band will broaden as it passes through the column.[104, 126] Thus, the longer the analyte remains in the column, the broader the analyte zone. This process results in a loss of column efficiency and is referred to as band broadening. The efficiency of a chromatographic column depends on several parameters such as diameter, length, film thickness, carrier gas type and its average linear velocity (flow rate).[126] This can be expressed in two ways: in terms of number of theoretical plates (N) and the height equivalent to a theoretical plate (HETP).[126] [124] The higher the number of theoretical plates in a column, the higher the column efficiency and vice versa.[129]

$$N = 5.545 . [\frac{t_R}{W_h}]^2$$

Where N = number of theoretical plates, t_R = retention time of peak and W_h = peak width at half height.[126]

$$HETP = {^L}/_N$$

Where HETP is the height equivalent of a theoretical plate, L is the column length (mm) and N represents the number of theoretical plates.[126]

According to Van Deemter and co-workers, eddy diffusion, longitudinal diffusion and mass transfer were identified as the three effects responsible for band broadening in packed columns. [124, 131]

The Van Deemter Equation[131] is generally expressed as: $H = A + \dfrac{B}{u} + Cu$

Eddy diffusion (the A term) can be described as a phenomenon in which molecules of an analyte leave the column at different times because they travel through the columns by pathways which have different lengths (Figure 2.16).[124] As molecules of an analyte pass through a packed column, the distribution of path lengths tend to be shorter for some than others. Molecules with the shortest path length move through the column more quickly than those with longer path lengths.[124] This results in the separation of molecules from each other and consequently broadening of analyte peak.

The A term is given as: $A = 2\lambda dp$

Where A is the eddy diffusion, λ is the packing uniformity and dp is the particle diameter. Since capillary columns commonly used in GC have no solid support, the A term = 0. This is one advantage that capillary columns have over packed columns.[126]

Molecules enter
the column at
the same time

Molecules leave the
column at different
times because of
different paths.
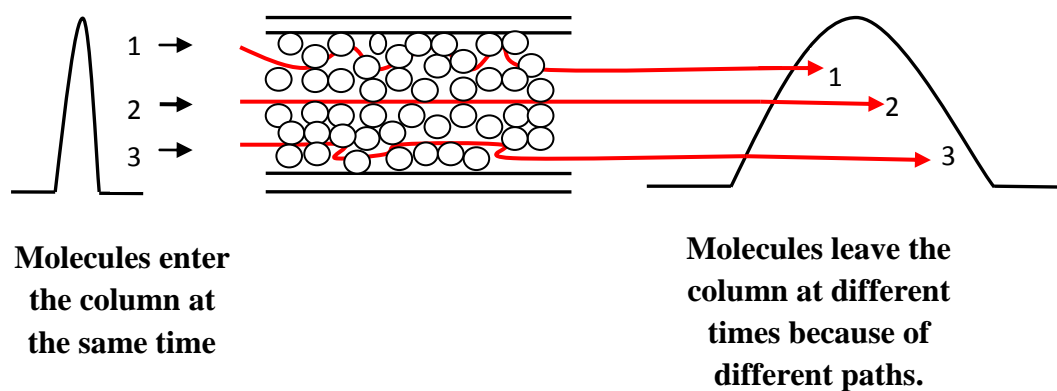
Figure 2.16: Schematic of the different paths taken by three different molecules travelling through a packed column.[126]

Longitudinal diffusion, the B term, results in band broadening when a solute diffuses from a region of high concentration (the concentrated centre of the band) to one of low concentration (more dilute regions) as illustrated in Figure 2.17.[124] A molecule flows through a column in two ways: the physical flow that's taking place and the ability to diffuse randomly. Hence, all compounds travelling through a chromatographic column do exhibit some degree of longitudinal diffusion broadening.[124] This is usually higher for

substances with fast diffusion rates than those with slow diffusion rates. Hence, longitudinal diffusion is likely to cause broadening of chromatographic peaks in GC but this can be minimised by varying the type, pressure and flow rate of carrier gas so that the solute band passes through the column quickly before it diffuses and broadens.[124, 131]

Sample in a region of high concentration
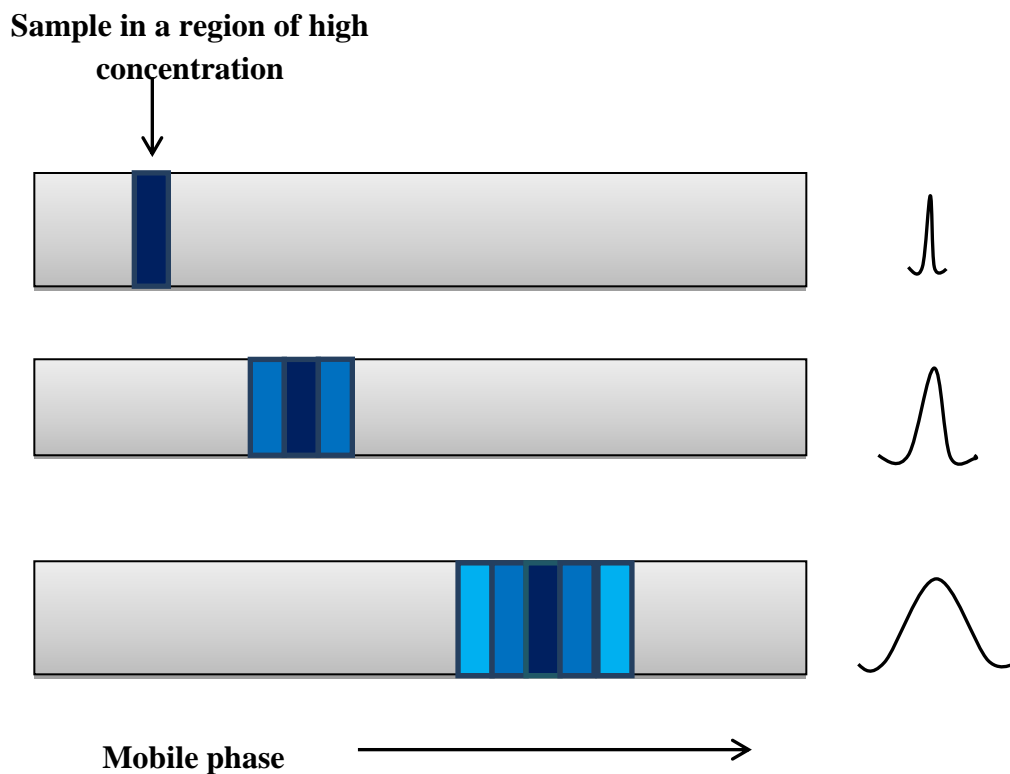
Mobile phase

Figure 2.17: Longitudinal diffusion of analyte band in a column.[126]

The C term (mass transfer) is the time taken for the solute to establish equilibrium as it moves from the mobile phase to the stationary phase and vice versa.[124] As a consequence, molecules in the stationary phase tend to move slower than their counterparts in the mobile phase. The slower the rate at which this takes place, the higher the tendency for broadening to occur and vice versa. Mass transfer effect can be minimised by an increase in temperature and solubility of solute molecules in the stationary phase, decrease in film thickness of stationary phase and flow rate of mobile phase.[126]

A combination of the three terms (A, B and C) gives the Van Deemter plot as illustrated in Figure 2.18.
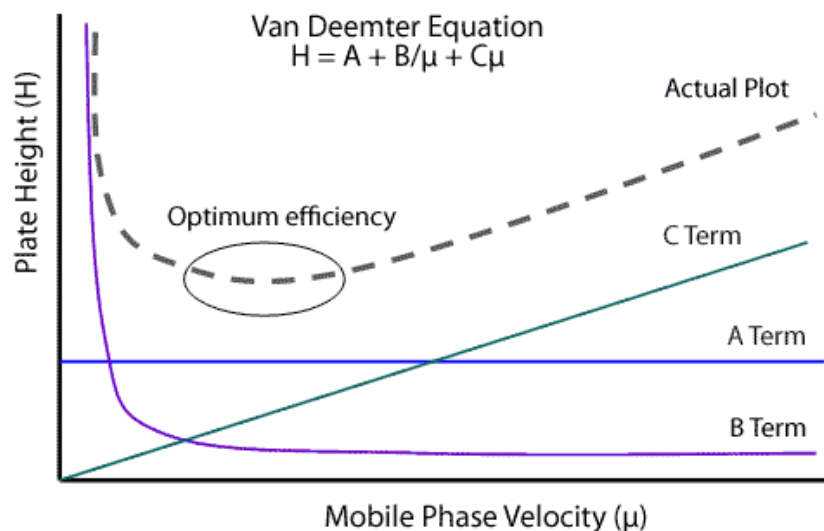
Figure 2.18: Typical van Deemter plot.[124]

The A term is constant over different flow rates since it is independent of the mobile phase velocity.[124, 131] The B term is strongly influenced by low mobile phase velocities which make a significant contribution to broadening. However, this decreases at higher flow rates.[124] The C term is directly proportional to the velocity of the mobile phase; it increases as the flow rate increases.[131] Since each of these three effects contributes to broadening in a chromatographic column, they must be minimised to the barest minimum to maximise column efficiency.[126]

2.8 Mass Spectrometry

Mass spectrometry is an analytical technique used for structural investigation and molecular identification of unknown compounds.[95, 132] The mass spectrometer separates and detects molecular ions based on their mass to charge (m/z) ratio.[132] Mass spectrometers consist of three main sections: an ion source (ionisation chamber) which

produces ions, a mass analyser which separates ions according to their m/z ratio and an ion detector (see Figure 2.19).[132, 133] They are usually maintained under high vacuum of 10^{-6} Torr (low pressure) to ensure that ions reach the detector without being deflected off their intended path due to ion-molecule collisions. This is critical as collisions between ions and gaseous molecules under low vacuum could result in the production of unwanted reactions and complexity of the spectrum.

Sample Introduction

Inlet

Ion source

Mass Analyser

Detector

High Vacuum

Data system
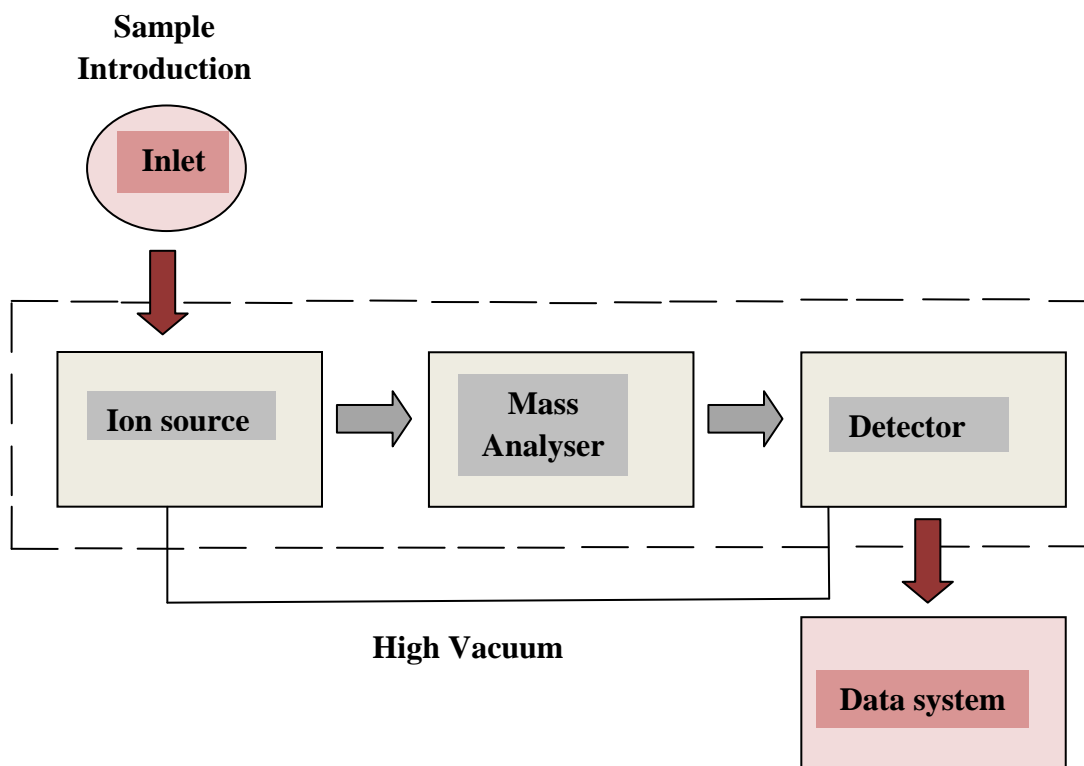
Figure 2.19: Basis of a mass spectrometer.

2.8.1 The ion source

In the ion source, sample molecules are ionised by bombardment with electrons to produce ionised sample molecules. Techniques employed in mass spectrometry could be highly energetic thereby producing extensive fragments or softer thereby producing only ions characteristic of the molecular species.[134] Electron ionisation (EI) and chemical ionisation (CI) techniques are commonly used in mass spectrometry because of their

suitability for gas-phase reactions particularly gaseous molecules with sufficient volatility and thermal stability.[132]

The electron ionisation (EI) technique involves the use of an electron ionisation (EI) source which consists of a heated filament that produces electrons of 70 volts. Sample molecules introduced into the EI source are bombarded with these high energy electrons resulting in the formation of a high energy, singly charged ion which loses its excess energy by extensive fragmentation and produces a collection of fragment ions characteristic of the compound.[134, 135] The gas phase reaction describing the electron ionisation process is as follows: $M + e^- \rightarrow M^{+\cdot} + 2e$, where M is the sample molecule to be ionised, e^- is the electron and $M^{+\cdot}$ is the ion formed.[134]

In EI, most molecules can be sufficiently ionised by approximately 10 eV energy.[136] Thus, the excess energy usually results in an extensive fragmentation which is very useful in providing structural information for elucidation of unknown analytes. The mass generated by the EI process consists of a spectrum correlation of the mass and abundance of ions formed from both the intact sample molecule and its fragments. Identical EI spectra can be produced from various types of EI mass spectrometers provided the electron energy employed is the same.[125, 132] This has resulted in the compilation of extensive libraries of 70 eV containing tens of thousands of substances which form the basis of users spectral libraries. A typical example of this is the National Institute of Standard and Technology (NIST) library.[125, 137] The reproducible fragmentation patterns of the EI mass spectra make them the most widely used ionisation technique for identifying unknowns, determining molecular structure and confirming the identity of target analytes.[132, 136]

Although the EI technique generates reproducible mass spectra, it leads to extensive fragmentation which prevents the molecular ion from being detected or observed for many compounds.[125, 134, 136] This can be overcome by employing the CI technique which uses a lesser amount of excess energy; thereby presenting the advantage of producing a spectrum with less fragmentation and molecular species that can be easily observed. In CI, collision between sample molecules and primary ions in the source results in the generation of ions.[134] The ion source is located in a small cell which has slits that allows the reagent gas, electron beam and sample to enter.[125] This cell is charged with the

reagent gas at a pressure of 10 Pa; higher than the typical pressure (10^{-3}) of a mass spectrometric source which permits collisions between the reagent gas and sample molecules. This is followed by ionisation of the reagent gas with an electron beam to produce a cloud of ions that react to yield adduct ions which serve as excellent proton donors.[132] Thus, analyte molecules introduced into the source are subsequently ionised by these reagent gas ions through the transfer of a proton to yield pseudo-molecular ions (M H$^+$ ions). The energy released during proton transfer is generally influenced by the type of reagent gas used.[132] The most commonly used reagent gases are methane, isobutane and ammonia. Amongst these gases, methane has the strongest ability for proton donation due to its proton affinity (PA) of 5.7 eV.[132] Hence, it is widely used for fragmentation compared to isobutane (PA 8.5 eV) and ammonia (PA 9.0 e V) which are mainly used for softer ionisation; producing only a protonated molecular ion with no fragmentation.[134] EI fragmentation yields structural information while CI increases the abundance of the molecular ion; giving little or no information as fragment ions are few and produced with little excess energy. Hence, CI is a complementary technique that is mainly employed to verify the molecular mass of an unknown.[125, 132, 134, 136]

2.8.2 Mass Analysers

Although different types of mass analysers exist, the basic principles of operation are the same. Ions generated in the source are separated according to their mass to charge ratios via acceleration by the electric field into the mass analyser.[132, 134] The mass analyser is selected according to the resolution, mass range, scan rate and detection limits required for an application.[125, 132] Mass analysers are grouped in two types: continuous or pulsed mass analysers.[125, 134] In continuous mass analysers, a single m/z is selected and transmitted to the detector. The analyser is scanned resulting in the detection of ions with different mass to charge ratios.[134] Only ions at the m/z ratio selected are obtained. Continuous mass analysers include quadrupole filters and magnetic sectors. In pulsed mass analysers, ions are transmitted concurrently via collection of the entire spectrum from a single pulse of ions.[134] These analysers include time-of-flight (TOF), ion cyclotron resonance and quadrupole ion trap mass spectrometers.[132, 134]

The most commonly used mass analyser in mass spectrometry is the quadrupole mass analyser. This was employed throughout the course of this investigation.[132] The quadrupole consists of four cylindrical rods aligned parallel to each other and connected electrically in opposite pairs as shown in Figure 2.20.[134] It is a component of the mass spectrometer responsible for filtering ions based on their m/z ratio. In the quadrupole, the separation of ions is governed by the radio frequency (RF) and direct current (DC) applied to the rods.[134] The oscillating fields produced by these voltages serves as a band pass that filters and transmits only the m/z values selected. To achieve ion separation in the quadrupole, an RF voltage is initially applied between two pairs of rods.[134] This results in the rejection or transmission of ions according to their m/z ratio by alternately focusing them in different planes.[134] In the first half of the RF cycle, the left and right electrodes have a negative potential while electrodes at the top and bottom have a positive potential.[132, 134] However, the polarity of the electrodes is reversed in the second half of the RF cycle.[134] Thus, positive ions are squeezed into the horizontal plane while negative ions are squeezed into the vertical plane in the first half of the RF cycle and vice versa in the second half of the RF cycle. As ions travel through the mass analyser, a three dimensional wave which results in transmission of selected ions is produced from a continuous change of the quadrupole field.[134] Once the appropriate RF frequency and potential is selected, the quadrupole acts like a high pass filter allowing only high m/z ions to be transmitted.[125, 132, 134] Low m/z ions are rejected because their high acceleration rate and amplitude of wave causes the ions to collide with the electrodes and subsequently prevents them from reaching the detector. The application of a DC voltage combined with an RF voltage makes the quadrupole act like a low pass filter; transmitting only low m/z ratios and rejecting high m/z ratios. Hence, the RF and DC potentials are adjusted such that only ions with the selected m/z values are transmitted.[132, 134] The quadrupole can function in two modes: the full scan mode and "single ion monitoring" (SIM) mode. In the full scan mode, a range of masses (m/z) are monitored typically 50 - 500 m/z.[132] This mode is very useful for identifying unknown compounds in a sample.[132, 134] In SIM mode, only ions of specific masses are monitored; providing an increased sensitivity relative to the full scan mode.[132]
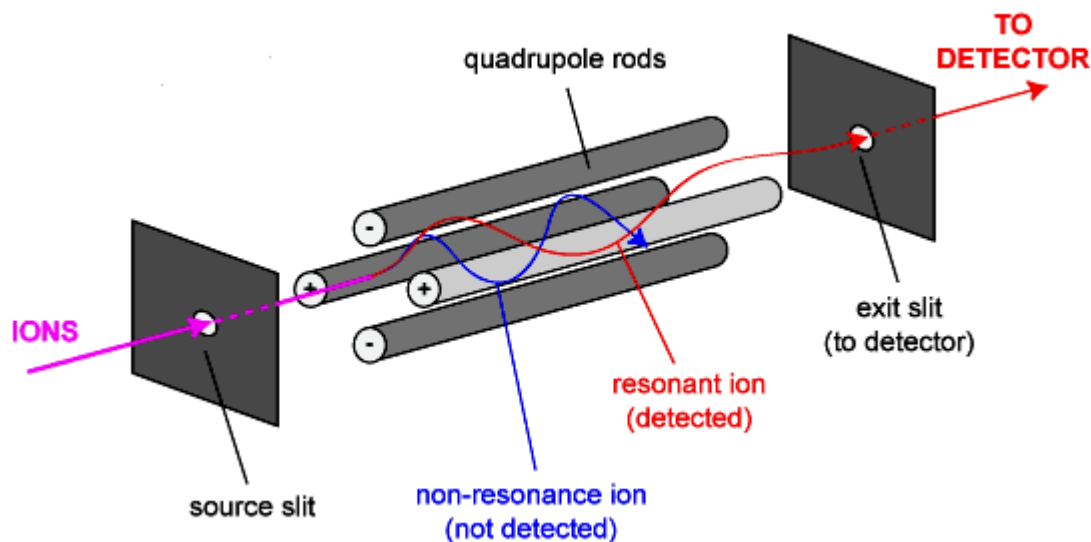
Figure 2.20: Schematic diagram of a quadrupole mass analyser.[138]

2.8.3 The MS detector

Once ions from the mass analyser strike the surface of the detector, they are detected and transformed into a signal usable by the detector. Detectors have the ability to generate an electric current that's proportional to the abundance of incident ions.[132, 134] Ion detectors are generally grouped into two categories.[134] Detectors in the first category have the ability to measure the direct current generated when an ion strikes the surface and is neutralised. An example of this is the Faraday cup detector. The second category of detectors has the ability to transfer kinetic energy of incident ions derived when they strike the surface and their subsequent generation of secondary electrons which is further amplified to produce an electric current.[134] Typical examples of these are electron multipliers or electro-optical ion detectors.

In electron multipliers, ions emitted from the analyser are accelerated to a high speed in order to improve its detection efficiency by holding the conversion dynode at a high potential ($\pm$ 3 to $\pm$ 30 kV) and charge opposite to that of detected ions.[134] As a consequence, several secondary particles (positive ions, negative ions, electrons and neutrals) are emitted when a positive or negative ion strikes the conversion dynode.[134]

In the positive mode, positive ions strike the negative high-voltage conversion dynode resulting in the formation of negative ions and electrons.[134] However, in the negative mode, positive ions are formed when negative ions strike the positive high-voltage conversion dynode.[134] The positive ions formed are converted to electrons at the first dynode and subsequently amplified by a cascade effect to produce a current.[134] Unlike the electron multipliers, electro-optical ion detectors also known as photomultiplier detectors make use of ion and photon detection devices.[134] They operate by converting ions to electrons and subsequently to photons.[134] Thus, they allow the detection of both positive and negative ions. These detectors consist of two conversion dynodes, a phosphorescent screen and a photomultiplier.[134] Like the electron multiplier, ions from the mass analyser strike a conversion dynode.[134] In the positive mode, ions are propelled towards the negative conversion dynode and vice versa.[134] This is followed by acceleration of the secondary electrons produced towards the phosphorescent screen and subsequent emission of photons. In order to prevent charge formation which could prevent new electrons from reaching the phosphorescent screen, its surface is usually covered with a thin layer of aluminium conductor.[132, 134] Emitted photons are then detected by the photomultiplier and converted into an electric current amplified by a cascade effect. The major advantage of photomultiplier detectors over the electron multiplier detectors is that they have a longer lifetime because they are kept sealed in glass and held under vacuum; thereby preventing contamination and prolonging the life span of the detector and making then the most widely used detectors in modern mass spectrometry.[132, 134]

3. Experimental and safety

3.1 Materials and Reagents

The nineteen and five polychlorinated biphenyl (PCB) standard solutions were supplied by Thames Restek UK Ltd and Sigma Aldrich respectively. Acetone (99 %), hexane (99 %) and florisil cartridges were purchased from Sigma Aldrich. C18 (EC) solid phase extraction (SPE) cartridges were purchased from Biotage.

3.2 Preparation of PCB solutions

In order to develop a method for analysing PCB congeners in a solution, two sets of PCB congener mixtures were used: a nineteen and five PCB congener standard mixture. The nineteen PCB congener standard mixture consists of PCB - 1, PCB - 5, PCB - 18, PCB - 31, PCB - 44, PCB - 52, PCB - 66, PCB - 87, PCB - 101, PCB - 110, PCB - 151, PCB - 153, PCB - 141, PCB - 138, PCB - 187, PCB - 183, PCB - 180, PCB - 170 and PCB - 206. The five PCB congener standard mixture consists of PCB -1, 3, 7, 14 and 12.

To establish resolution of the analytes, a 20 µg cm^{-3} standard solution was used for each congener set. For the nineteen PCB mixture, the standard solution (20 µg cm^{-3}) was prepared by transferring a 200 µL aliquot of the stock solution (100 µg cm^{-3}) into a 1 cm^3 volumetric flask which was made up to mark with hexane. For the five PCB mixture, the 20 µg cm^{-3} standard solution was prepared from an 80 µg cm^{-3} PCB stock solution. The 80 µg cm^{-3} PCB stock solution was prepared from individual PCB stock solutions as described below.

A 501.4 µg cm^{-3} stock solution containing PCB - 1 was prepared by dissolving 25.07 mg of the standard in hexane in a 50 cm^3 volumetric flask and made up to mark with hexane. The concentration of stock solution was obtained using Equation 3.1.

$$\text{Concentration (µg cm}^{-3}) = \frac{\text{mg of solute}}{\text{cm}^3 \text{ of solvent}} \times 10^3 \qquad \text{Eq. 3.1}$$

Similarly, concentrations of 501.2, 500.2, 500.8 or 500 µg cm^{-3} were obtained by dissolving 25.06, 25.01, 25.04 and 25.00 mg of PCB - 3, 7, 12 and 14 with hexane in

four 50 cm^3 volumetric flasks and made up to mark with hexane. Thus, the 80 µg cm^{-3} stock solution was prepared by transferring 3200 µL of each PCB stock solution into a 20 cm^3 volumetric flask and hexane was added to the 20 cm^3 mark. All standard solutions were stored in dark amber vials and sealed with PTFE/Silicone caps prior to analysis to prevent any form of photo degradation.

3.3 Analysis of PCB standard solutions by automatic injection into the GC-MS

3.3.1 GC-MS Operating parameters

To establish resolution of the nineteen and five target PCB congeners, a Perkin Elmer Auto System XL gas chromatograph (GC) coupled to a Perkin Elmer Turbo mass spectrometer (MS) was used. The operating conditions for the GC and MS are listed in Tables 3.1 and 3.2. However, the MS scan range and MS scan run time were adjusted to 50 - 250 amu and 3.40 – 6.00 min respectively for the five PCB congeners.

Table 3.1: Operating conditions of the GC for separation of PCBs

Inlet line temperature	250 °C
Inlet pressure	10.794 psi
Oven temperature program (for nineteen PCB congeners).	100 °C for 1 min. Ramped to 200 °C at 20 °C min^{-1}. Ramped to 220 °C at 4 °C min^{-1}. Ramped to 240 °C at 5 °C min^{-1} and held for 10 min; giving an overall GC run time of 25 min.
Oven temperature program (for five PCB congeners).	140 °C for 1 min. Ramped to 200 °C at 20 °C min^{-1}. Ramped to 208 °C at 4 °C min^{-1}; giving an overall GC run time of 6 min.
Column	Perkin Elmer Elite-5MS capillary column, (95 % dimethyl polysiloxane 5% diphenyl), 30 m × 0.25 mm i.d and 0.25 µm thickness
Carrier gas	Helium
Carrier gas flow	1.5 cm^3 min^{-1}

Table 3.2: Operating conditions of the MS for the detection of PCBs

Electron Energy (eV)	Trap Emission (eV)	Multiplier (V)	Scan Run Time	Scan Time (s)	Inter Scan Delay (s)	m/z Range (amu)	Solvent Delay (min)
70	100	315	25	0.2	0.1	50 - 500	3.0

3.3.2 Preparation of PCB calibration solutions

The GC-MS was calibrated for identification and quantification of detected analytes with a 20 µg cm^{-3} PCB standard solution containing the nineteen PCB congeners prepared in hexane as described in Section 3.2. For the five PCB congeners, a set of calibration solutions: 20, 30, 40, 50 or 60 µg cm^{-3} was prepared from the 80 µg cm^{-3} stock solution by transferring 2500, 3750, 5000, 6250 or 7500 µL repectively into five 10 cm^3 volumetric flasks and hexane was added to the calibration mark.

To determine the detection limit of the instrument, 15, 10, 5, 2.5 or 1.25 µg cm^{-3} PCB standard solutions were prepared by transferring 150, 100, 50, 25 or 12.5 µL of the 100 µg cm^{-3} PCB stock solution (containing nineteen PCB congeners) into five 1 cm^3 volumetric flasks respectively. For the five PCB congeners, 15, 10, 5, 2.5 or 1.25 µg cm^{-3} PCB standard solutions were prepared by transferring 938, 625, 312.5, 156 or 78 µL of the 80 µg cm^{-3} PCB stock solution described in Section 3.2 into a 5 cm^3 volumetric flask which was made up to mark with hexane. Each solution was made up to mark with hexane. All standard solutions were stored in dark amber vials and sealed with PTFE/Silicone caps prior to analysis to prevent any form of photo degradation.

3.3.3 Analysis of PCB Solutions

To establish resolution of nineteen PCB congeners, 3 µL of the 20 µg cm^{-3} PCB standard solution was analysed. Calibration of the GC-MS was done by injecting 1, 2, 3, 4 or 5 µL of the 20 µg cm^{-3} standard solution into the GC column via an auto sampler; giving masses 20, 40, 60, 80 or 100 ng respectively. A blank containing only hexane was analysed by injecting 3 µL of the blank into the GC column. The peak areas obtained were used to prepare calibrations for each analyte under examination. To establish the

instrument detection limit, 1 µL of 15, 10, 5, 2.5 or 1.25 µg cm^{-3} PCB standard solutions were injected into the GC column respectively using an autosampler giving masses of 15, 10, 5, 2.5 or 1.25 ng, respectively.

To establish resolution of the five PCB congeners, 1 µL of the 20 µg cm^{-3} PCB standard solution was analysed. The GC-MS was calibrated by injecting 1 µL of the 20, 30, 40, 50 and 60 µg cm^{-3} PCB standard solution into the column via an autosampler. A blank containing only hexane was analysed by injecting 1 µL of the blank into the GC column. To establish the instrument detection limit, 1 µL of 15, 10, 5, 2.5 or 1.25 µg cm^{-3} PCB standard solutions were injected into the GC column respectively using an autosampler giving masses of 15, 10, 5, 2.5 or 1.25 ng, respectively.

3.4 Solid phase extraction (SPE) method for PCBs

To test the ability of the solid phase extraction (SPE) cartridges to retain PCB congeners, a 60 µg cm^{-3} solution containing five PCB congeners: PCB - 1, 3, 7, 12 and 14 was used. In addition, the ability of the SPE cartridges to retain PCBs when present in a mixture of solvents commonly used as extraction solvents for PCBs was examined using a 30 µg cm^{-3} PCB standard solution was employed. This was prepared by diluting 2000 µL of the 60 µg cm^{-3} PCB standard solution with 2000 µL of acetone. All stock and standard solutions were stored in dark amber bottles and sealed with PTFE caps prior to analysis to prevent loss of analyte or photodegradation.

3.4.1 Method of SPE operation

A Supelco Visiprep SPE Vacuum Manifold was used for solid phase extraction of the samples. This was a 12- Port Model capable of extracting 12 samples simultaneously, coupled to an SPE vacuum pump trap kit as shown in Figure 3.1. The SPE process was conducted under a pressure of 15'' Hg Vacuum. The SPE cartridges used had PTFE frits, a sorbent mass of 500 mg and volume of 3 cm^3. Prior to loading the sample solution, the SPE cartridge was conditioned with hexane to ensure good contact between the analyte and sorbent in the adsorption stage. 1 cm^3 of hexane was loaded onto the

cartridge, allowed to pass through it and go to waste (Step 1). 1 cm^3 of the sample was then loaded onto the SPE cartridge. This was allowed to pass through the cartridge and the solution containing the unretained analytes collected for analysis (Step 2). The analytes of interest (retained analytes) were subsequently eluted from the sorbent using 1 cm^3 of hexane and the eluate collected for analysis (Step 3). The elution stage was repeated and eluate collected for analysis (Step 4). Similarly, a blank was prepared using only hexane following the process described above. 1 µL of the solution containing the unretained analytes and eluates was then analysed using the GC-MS described in Section 3.3.1 under the operating conditions given in Section 3.3.1.

Figure 3.1: Solid phase extraction set-up; consisting of an SPE vacuum manifold with 12 ports for SPE cartridges and SPE pump.

Similarly, solid phase extraction of the 30 µg cm^{-3} PCB standard solution was performed using the same process and operating conditions. However, only the eluates were collected for analysis as the solution containing the unretained analytes was allowed to go to waste. 1 µL of the solution was analysed using the GC-MS described in Section 3.3.1 under the operating conditions given in Section 3.3.1.

3.5 Characterisation of adsorbents

3.5.1 BET Isotherm

Nitrogen adsorption-desorption isotherms were measured at 77 K using a Micrometrics ASAP 2420 surface area and porosity analyser. Approximately 0.3 g of each sample was accurately weighed into a gas adsorption sampling tube. The weight of each sampling tube before and after sample addition was recorded. Prior to analysis, sample tubes were attached to the degas port of the nitrogen sorption instrument and degassed at 200 °C for 6 h. The experimental points obtained at relative pressures (P/Po) of 0.05 - 0.25 were used to calculate the Brunauer-Emmett Teller (BET) surface areas. The total pore volume was calculated using the amount of nitrogen adsorbed at P/Po of 0.99 while the average pore size distribution was calculated using the Barrett-Joyner-Halenda (BJH) model from a 30-point BET surface area plot. Pore diameters were calculated using the desorption branch of the isotherms.

3.6 Safety

All work involving chemical substances and apparatus were conducted in a safe and controlled manner according to the experimental risk assessments. The substances used and their associated hazards are given in Table 3.3. Due to their hazardous chemical nature, personal protective equipment such as safety glasses and a laboratory coat were worn at all times. Gloves were used to handle these substances in a fume cupboard. All substances were sealed and stored in appropriate cupboards when not in use.

Table 3.3: Hazardous substance associated with experimental methods

Substance	Very Toxic	Toxic	Carcinogenic	Mutagenic	Harmful	Flammable	Corrosive	Irritant
Tetraethylorthosilicate (TEOS)					√	√		
Cetyltrimethylammoniumbromide(CTAB)								√
Hydrogen peroxide		√			√			
Sodium metasilicate							√	√
Polychlorinated biphenyl (PCB) standard	√				√	√		√
Pentaethylenehexamine (PEHA)					√			
Iron nitrate								√
Ammonia		√			√	√		
Hydrochloric acid							√	√
Sodium Hydroxide						√	√	
Methanol		√				√		
Hexane		√				√		√
Acetone						√		√

Part A: Development of analytical techniques for detection and assessment of polychlorinated biphenyls in soil and water

4. Development of GC-MS method for determination of polychlorinated biphenyls in solution

4. Development of GC-MS method for determination of PCBs in solution

4.1 Selection of PCB standards

To develop a GC-MS method for identifying and quantifying PCBs in unknown sample solutions, two individual sets of PCB mixtures: nineteen and five PCB congener mixtures were selected for investigation in this study. The nineteen PCB congeners were selected as target analytes because they represent technical mixtures of PCBs formerly used as dielectric fluids in electrical transformers. However, the stock solutions were expensive and supplied at very low volumes. Therefore, method validation was carried out using the five PCB congeners. The selected PCB congener mixtures with their corresponding CAS Registry Nos and IUPAC names are given in Tables 4.1 and 4.2.

Table 4.1: CAS Registry No and IUPAC Names of nineteen PCB congeners

PCB Congener	CAS Registry No	IUPAC Name
PCB - 1	2051-60-7	2-Chlorobiphenyl
PCB - 5	16605-91-7	2,3-Dichlorobiphenyl
PCB - 18	37680-65-2	2,2',5-Trichlorobiphenyl
PCB - 31	16606-02-3	2,4',5-Trichlorobiphenyl
PCB - 44	41464-39-5	2,2',3,5'-Tetrachlorobiphenyl
PCB - 52	35693-99-3	2,2',5,5'-Tetrachlorobiphenyl
PCB - 66	32598-10-0	2,3',4,4'-Tetrachlorobiphenyl
PCB - 87	38380-02-8	2,2',3,4,5'-Pentachlorobiphenyl
PCB - 101	37680-73-2	2,2',4,5,5'-Pentachlorobiphenyl
PCB - 110	38380-03-9	2,3,3',4',6-Pentachlorobiphenyl
PCB - 151	52663-63-5	2,2',3,5,5',6-Hexachlorobiphenyl
PCB - 153	35065-27-1	2,2',4,4',5,5'-Hexachlorobiphenyl
PCB - 138	35065-28-2	2,2',3,4,4',5-Hexachlorobiphenyl
PCB - 141	52712-04-6	2,2',3,4,5,5'-Hexachlorobiphenyl
PCB - 187	52663-68-0	2,2',3,4',5,5',6-Heptachlorobiphenyl
PCB - 183	52663-69-1	2,2',3,4,4',5',6-Heptachlorobiphenyl
PCB - 180	35065-29-3	2,2',3,4,4',5,5'-Heptachlorobiphenyl
PCB - 170	35065-30-6	2,2',3,3',4,4',5-Heptaachlorobiphenyl
PCB - 206	40186-72-9	2,2',3,3',4,4',5,5',6-Nonachlorobiphenyl

Table 4.2: CAS Registry No and IUPAC Names of five PCB Congeners

PCB Congener	CAS Registry No	IUPAC Name
PCB – 1	2051 - 60 - 7	2 - Chlorobiphenyl
PCB – 3	2051 - 62 - 9	4 - Chlorobiphenyl
PCB – 7	33284 - 50 - 3	2,4 - Dichlorobiphenyl
PCB – 12	2974 - 92 - 7	3,4 - Dichlorobiphenyl
PCB – 14	34883 - 41 - 5	3,5 - Dichlorobiphenyl

4.2 Resolution of PCB congeners in solution

In order to establish resolution of the nineteen PCB congeners, the GC-MS was used to analyse the 20 ng μL^{-1} PCB standard solution in hexane as specified in Section 3.3.3 under the operating conditions outlined in Section 3.3.1. A blank was analysed using hexane as the solvent with no added PCBs. It can be seen from the chromatogram obtained in Figure 4.1 that the GC-MS method of analysis provided a complete resolution of the entire nineteen PCB congeners with high sensitivities. The nineteen PCB congeners were eluted in the following order: PCB -1 > PCB - 5 > PCB -18 > PCB - 31 > PCB - 44 > PCB - 52 > PCB - 66 > PCB - 87 > PCB - 101 > PCB - 110 > PCB -151 > PCB - 153 > PCB - 138 > PCB - 141 > PCB - 187 > PCB -183 > PCB -180 > PCB - 170 > PCB - 206.

Resolution of the five PCB congeners was established by analysis of the 20 ng μL^{-1} PCB standard solution using the GC-MS as specified in Section 3.3.3. The operating parameters of the GC-MS were modified as outlined in Section 3.3.1. The chromatogram shown in Figure 4.2 illustrates that the five congeners under investigation were eluted in the order: PCB - 1 > PCB - 3 > PCB - 7 > PCB - 14 > PCB - 12. The five analytes were completely resolved and high sensitivities were obtained.
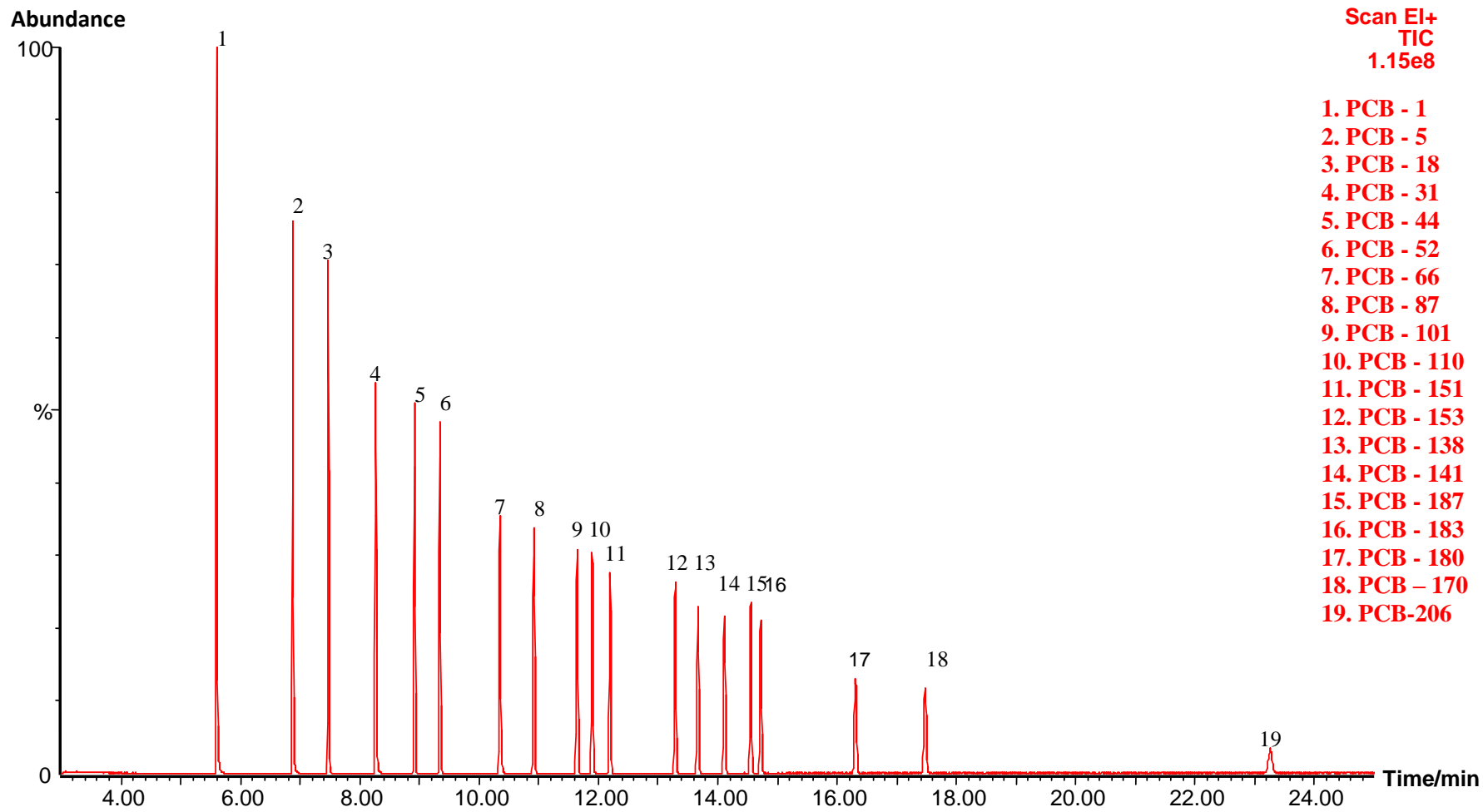
Figure 4.1: GC-MS chromatogram for nineteen PCB congeners
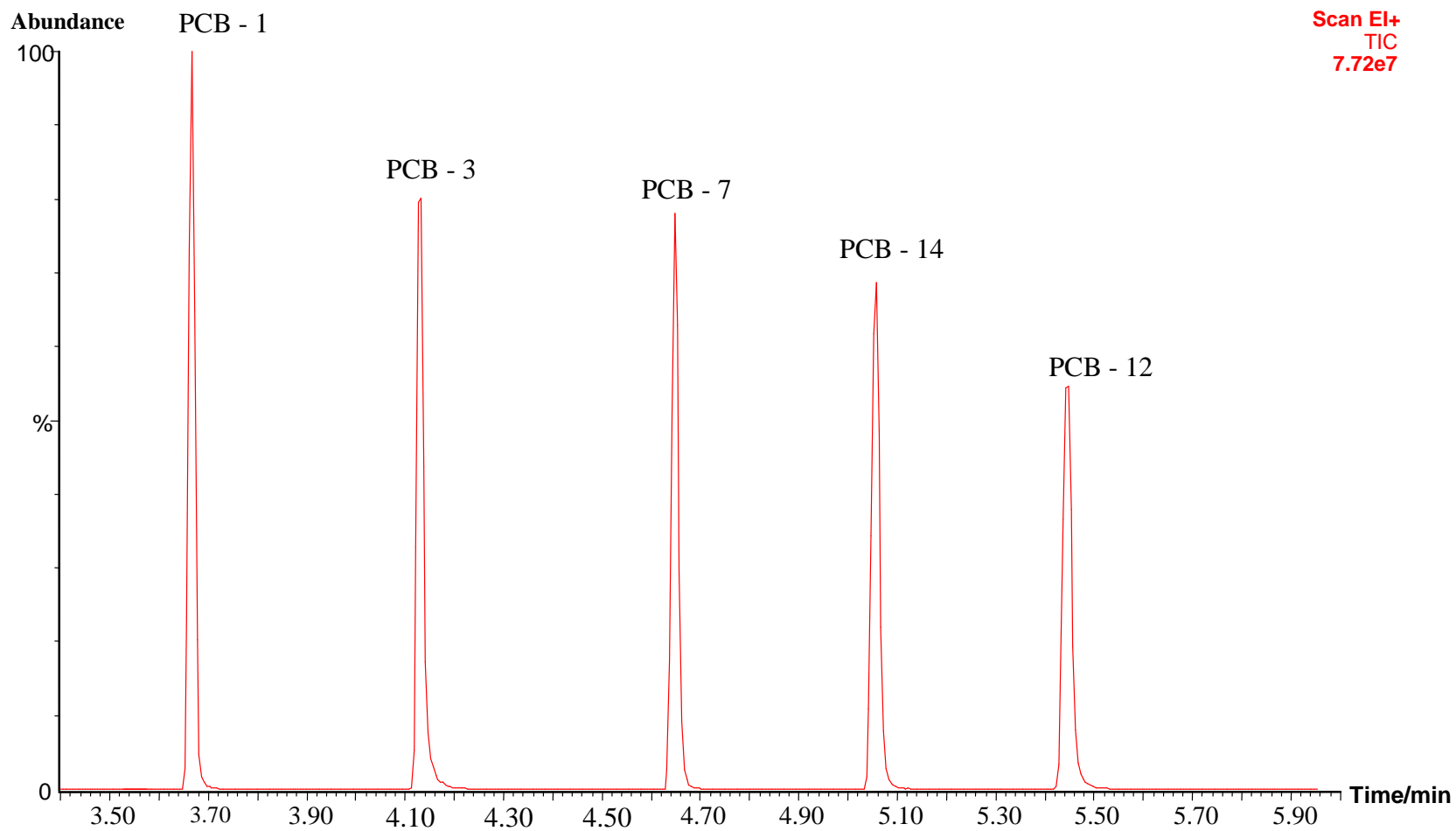
Figure 4.2: GC-MS chromatogram of five PCB congeners

4.3 Calibration of the GC-MS for nineteen PCB congeners in solution

Calibration of the GC-MS instrument involved analysis of increasing volumes of the 20 ng μL^{-1} standard solution as described in Section 3.3.3 using the operating conditions specified in Section 3.3.1. Prior to analysis of the calibration solution, a blank was analysed as specified in Section 3.3.3 under the same conditions. Calibration curves obtained for each analyte were obtained by plotting the respective peak areas against the mass of each PCB injected onto the GC column. The results obtained for each PCB congener using the GC-MS are shown in Appendix 1 (Figures A1.1 - A1.19), with a specimen calibration curve for PCB - 1 illustrated in Figure 4.3.
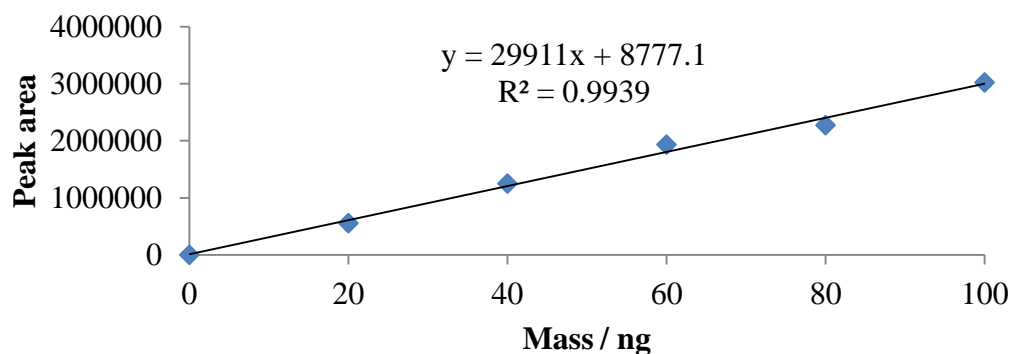
Figure 4.3: Calibration curve for PCB - 1

An examination of the regression lines and correlation co-efficient values for the nineteen PCB congeners showed that signal responses for the eleven congeners: PCB - 1, 5, 18, 31, 44, 52, 66, 87, 101, 110 and 151 were linear over the specified ranges with R^2 values greater than or equal to 0.9901. R^2 values obtained for the remaining eight congeners: PCB - 153, 138, 141, 187, 183, 180, 170 and 206 were less than or equal to 0.9863. This could be attributed to the fact that the abundance of these highly chlorinated congeners was relatively small (approximately 2%) and close to the background noise region especially for PCB - 206 compared to the abundance of the lowly chlorinated congeners. However, all calibrations were shown to be analytically acceptable and thus the instrument used was shown to provide excellent resolution and could be used to quantify the concentration of the nineteen PCB congeners in unknown sample solutions.

4.3.1 Repeatability of the calibration method

The repeatability of the method was determined by injecting 3 µL of the 20 ng µL^{-1} PCB standard solution in triplicate using the autosampler. A blank was analysed by injecting 3 µL of hexane in a similar manner. The results obtained are shown in Table 4.3.

Table 4.3: GC-MS results from analysis of nineteen PCB congeners

Std 180 ng (Peak area)						
Compound	Replicate 1	Replicate 2	Replicate 3	Mean	Std Deviation	% RSD
PCB - 1	1822742	1815477	1883625	1840615	37425	2.0
PCB - 5	1605161	1600294	1682170	1629208	45931	2.8
PCB - 18	1624780	1548377	1654768	1609308	54857	3.4
PCB - 31	1487027	1459712	1530758	1492499	35838	2.4
PCB - 44	1438878	1373824	1454208	1422303	42678	3.0
PCB - 52	1394633	1339408	1419980	1384674	41199	3.0
PCB - 66	1208486	1129144	1230174	1189268	53186	4.5
PCB - 87	1142653	1066301	1138301	1115752	42881	3.8
PCB - 101	1099348	1058009	1103538	1086965	25164	2.3
PCB - 110	1099348	1058009	1114873	1090743	29392	2.7
PCB - 151	981991	930910	1005763	972888	38248	3.9
PCB - 153	926913	890290	934532	917245	23653	2.6
PCB - 138	887965	837384	893990	873113	31089	3.6
PCB - 141	891087	834067	875088	866747	29411	3.4
PCB - 187	813920	750630	803551	789367	33945	4.3
PCB - 183	818831	754064	824847	799247	39245	4.9
PCB - 180	627115	594806	626831	616251	18572	3.0
PCB - 170	600952	549494	596567	582338	28528	4.9
PCB - 206	240869	238353	257453	245558	10378	4.2

The results in Table 4.3 indicate that the % relative standard deviation (RSD) values obtained across the peak areas for each PCB congener were ≤ 4.9 %; thus demonstrating

a small level of imprecision for the measured peak area of each analyte. This suggests good repeatability and precision for the method.

4.3.2 Reproducibility of the calibration method

To establish reproducibility of the method, the calibration of PCB congeners described in Section 4.5 was repeated on two different days. The results obtained for each PCB congener over the three days are given in Appendix 2 (Tables A2.1 - A2.5). In general, the RSD values for the repeated injection of standard solutions ranged from 3.1 - 22 %, with an average RSD value of 12.2 ± 12.4 % (note that this error is based on a Gaussian application). The highest level of imprecision was measured for the lowest mass of PCB standard solution in each case containing 20 ng of all nineteen PCB congeners with RSD values ranging from 22 - 65 %. The reason for the high level of imprecision was attributed to the direct relationship observed between precision and mass of each analyte; the precision increased for each analyte as the mass increased. Hence, the highest level of imprecision was obtained for the 20 ng standard which was the lowest mass standard. Indeed if the PCB mass is plotted against RSD % values, it is evident that the precision is directly proportional to increased mass; see Figure 4.4.
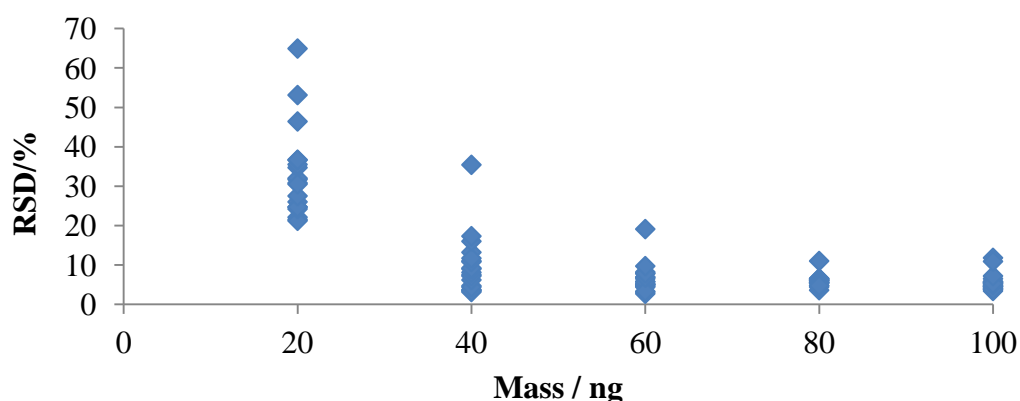
Figure 4.4: Correlation between precision and analyte mass.

There also appeared to be a trend with increasing precision and decreasing molecular weight or degree of chlorination of each PCB analyte as shown in Figures 4.5 - 4.7

which illustrates the most pronounced example for the PCB congeners at a mass of 20 ng.
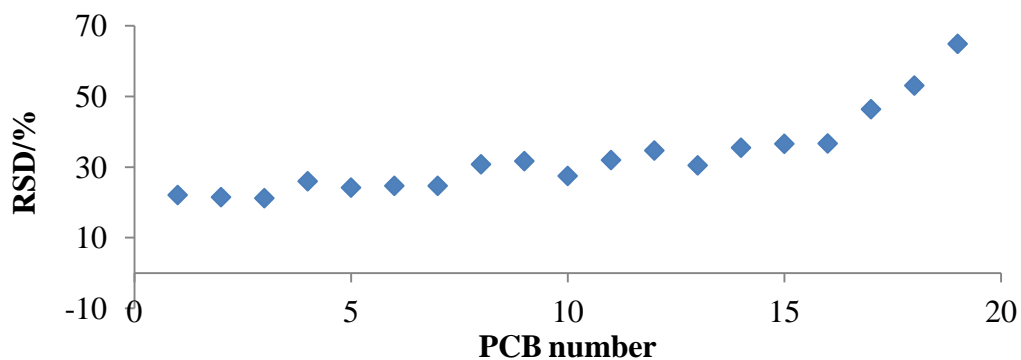
Figure 4.5: Correlation between precision and PCB standard
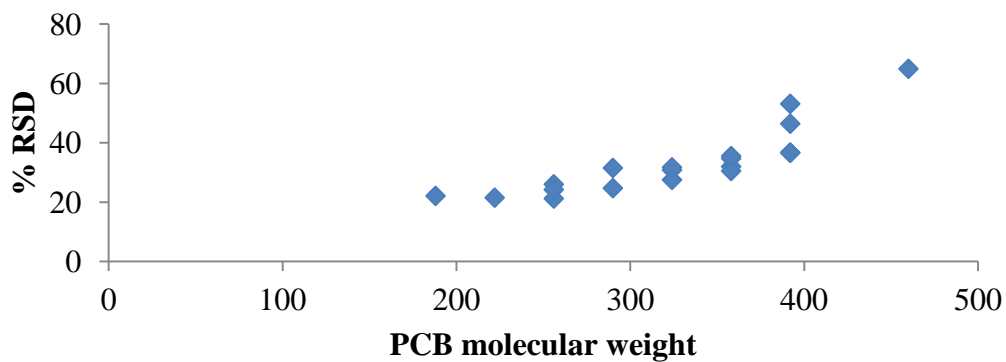
Figure 4.6: Correlation between precision and PCB molecular weight
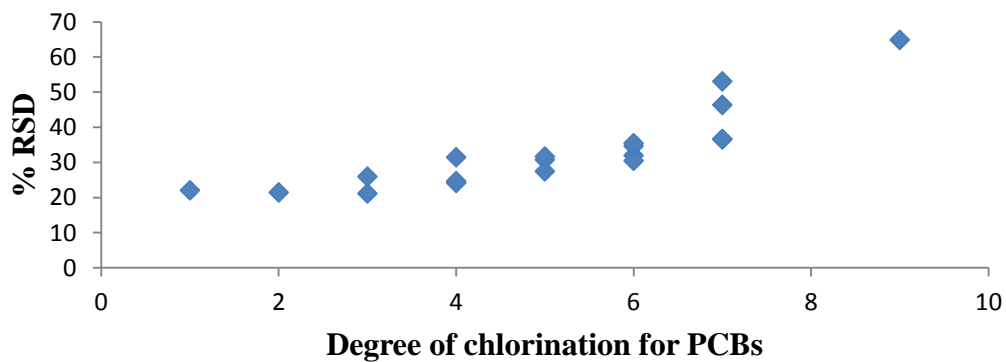
Figure 4.7: Correlation between precision and degree of chlorination for PCBs

Finally, the calibration data (slopes and RSD values obtained) are given in Tables 4.4 and 4.5. Although it was difficult to obtain a linear response for the entire nineteen PCB congeners over the 3 days, % RSD values obtained for slope were $\leq$ 7.7%. This therefore illustrates a good reproducibility for the method and establishes confidence in results obtained from further studies. However, as demonstrated above, care needs to be taken to ensure good precision of analysis when analyte concentrations are low. Similarly higher imprecision will be observed for the larger PCBs. As the level of imprecision was extremely high for the 20 ng μL^{-1} standard solution, the detection limit of the instrument was examined further.

Table 4.4: Slope of 19 PCB Congeners on three different days

PCB Congeners	Day 1	Day 2	Day 3	Mean	Std Deviation	% RSD
PCB – 1	29911	31753	30499	30721	941	3.1
PCB – 5	27647	30182	29677	29169	1342	4.6
PCB – 18	27100	29157	28430	28229	1043	3.7
PCB – 31	26023	27984	28000	27336	1137	4.2
PCB – 44	24681	27024	25965	25890	1173	4.5
PCB – 52	24690	26591	25933	25738	965	3.8
PCB – 66	22840	24078	23472	23463	619	2.6
PCB – 87	20891	22327	22165	21794	786	3.6
PCB - 101	20127	21770	21798	21232	957	4.5
PCB - 110	20826	21790	21822	21479	566	2.6
PCB - 151	18777	19675	19312	19255	452	2.3
PCB - 153	18245	19103	18666	18671	429	2.3
PCB - 138	19270	18702	21576	19849	1522	7.7
PCB - 141	17477	17905	18062	17815	303	1.7
PCB - 187	15966	16934	16738	16546	512	3.1
PCB - 183	16525	16887	16973	16795	238	1.4
PCB - 180	13657	13877	13934	13823	146	1.1
PCB - 170	13057	13041	13520	13206	272	2.1
PCB - 206	6230	6034	6293	6186	135	2.2

Table 4.5: Correlation Coefficients of 19 PCB Congeners on three different days

PCB Congeners	Day 1	Day 2	Day 3	Mean	Std Deviation	% RSD
PCB – 1	0.9939	0.9971	0.9893	0.9934	0.004	0.4
PCB – 5	0.9962	0.9956	0.987	0.9929	0.005	0.5
PCB - 18	0.9950	0.9956	0.9873	0.9926	0.005	0.5
PCB - 31	0.9949	0.9932	0.982	0.9900	0.007	0.7
PCB - 44	0.9958	0.993	0.9836	0.9908	0.006	0.6
PCB - 52	0.9947	0.9922	0.981	0.9893	0.007	0.7
PCB - 66	0.9919	0.9865	0.9719	0.9834	0.010	1.1
PCB - 87	0.9924	0.9857	0.9677	0.9819	0.013	1.3
PCB - 101	0.9922	0.9835	0.966	0.9806	0.013	1.4
PCB - 110	0.9901	0.9869	0.9686	0.9819	0.012	1.2
PCB - 151	0.9905	0.984	0.9659	0.9801	0.013	1.3
PCB - 153	0.9873	0.9799	0.9589	0.9754	0.015	1.5
PCB - 138	0.9863	0.9819	0.9586	0.9756	0.015	1.5
PCB - 141	0.9869	0.9804	0.9591	0.9755	0.015	1.5
PCB - 187	0.9851	0.9758	0.9521	0.9710	0.017	1.8
PCB - 183	0.9845	0.9772	0.9509	0.9709	0.018	1.8
PCB - 180	0.9756	0.9707	0.9359	0.9607	0.022	2.3
PCB - 170	0.9726	0.9673	0.9257	0.9552	0.026	2.7
PCB - 206	0.9500	0.9354	0.8603	0.9152	0.048	5.3

4.3.3 Examination of the GC-MS detection limit for the PCB standards.

In this study, the detection limit was considered as the point where the signal response obtained for each analyte could not be easily distinguished from the background noise of the instrument; signal to noise (3:1). As described in Section 3.3.3, standard solutions with decreasing concentrations of PCB congeners were analysed. The detection limit of each PCB congener is given in Table 4.6. The data demonstrated that the detection limit of each PCB congener varied at different masses. PCB - 206 could not be detected at a

mass ≤ 15 ng while PCB - 180 and 170 could not be detected at a mass ≤ 5 ng. Analyte signals for PCB - 183, 187, 141, 138, 153, 151, 110, 101, 87, 66, 52 and 44 disappeared completely into noise at a mass of 2.5 ng. Although signal responses were obtained for PCB - 1, 5, 18 and 31 at a mass of 1.25 ng, these responses were closely associated with noise. Hence, the detection limit of the instrument below which any PCB congener could not be reliably detected occurred at a mass of 1.25 ng.

Table 4.6: GC-MS detection limit for nineteen PCB congeners

PCB Congeners	PCB Homologue	Detection Limit / ng
PCB - 1	MonoCB	1.25
PCB - 5	DiCB	1.25
PCB - 18	TriCB	1.25
PCB - 31	TriCB	1.25
PCB - 44	TetraCB	2.50
PCB - 52	TetraCB	2.50
PCB - 66	TetraCB	2.50
PCB - 87	PentaCB	2.50
PCB - 101	PentaCB	2.50
PCB - 110	PentaCB	2.50
PCB - 151	HexaCB	2.50
PCB - 153	HexaCB	2.50
PCB - 138	HexaCB	2.50
PCB - 141	HexaCB	2.50
PCB - 187	HeptaCB	2.50
PCB - 183	HeptaCB	2.50
PCB - 180	HeptaCB	5.00
PCB - 170	HeptaCB	5.00
PCB - 206	NonaCB	15.00

*In a concentration of ng μL^{-1}

4.4 Calibration of the GC-MS for five PCB congeners in solution

The GC-MS was calibrated for quantification of the five PCB congeners specified in Section 4.1 by analysing 1µL of the 20, 30, 40, 50 or 60 ng µL^{-1} PCB standard solutions described in Section 3.3.3 under the operating conditions outlined in Section 3.3.1. The peak areas obtained for each analyte were plotted against the mass of each PCB congener injected onto the GC column. The calibration curves are shown in Figures 4.8 and 4.9. It can be deduced from the calibration curves that signal responses for the five PCB congeners were linear over the specified ranges with R^2 values greater than or equal to 0.9920.

PCB - 1
y = 18880x + 4636.1
R² = 0.9939

PCB - 3
y = 18077x - 18260
R² = 0.9932
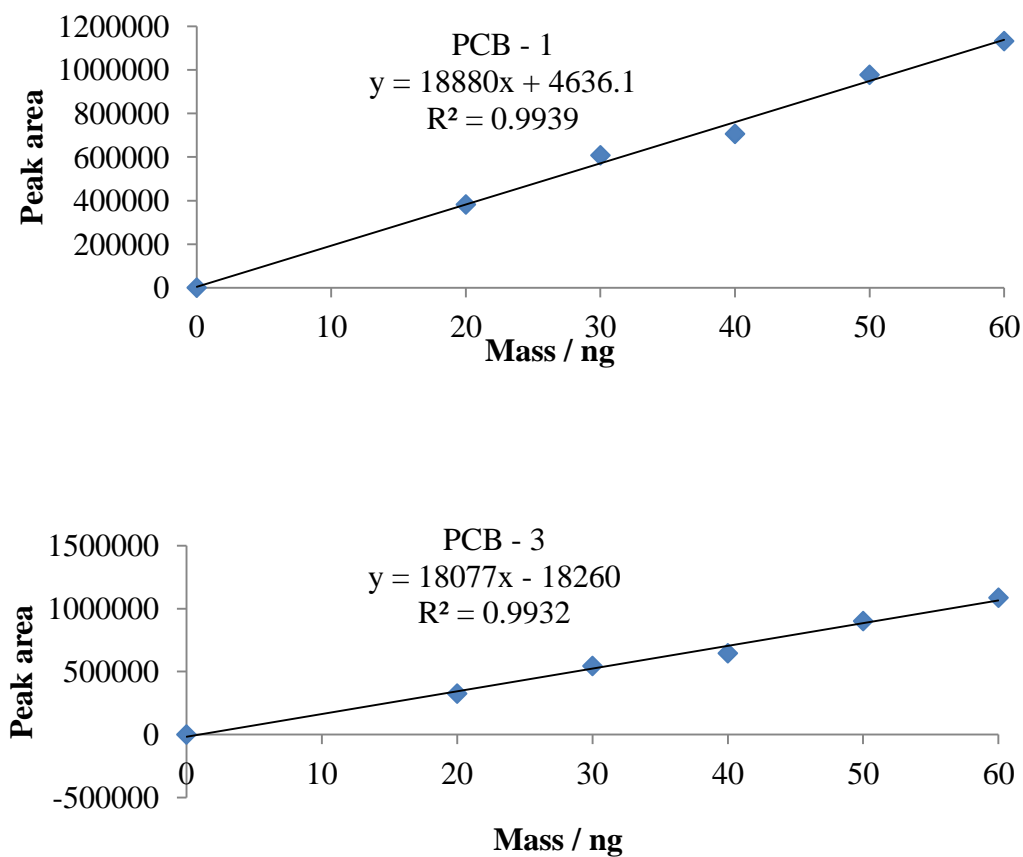
Figure 4.8: Calibration curves for PCB - 1 and 3.
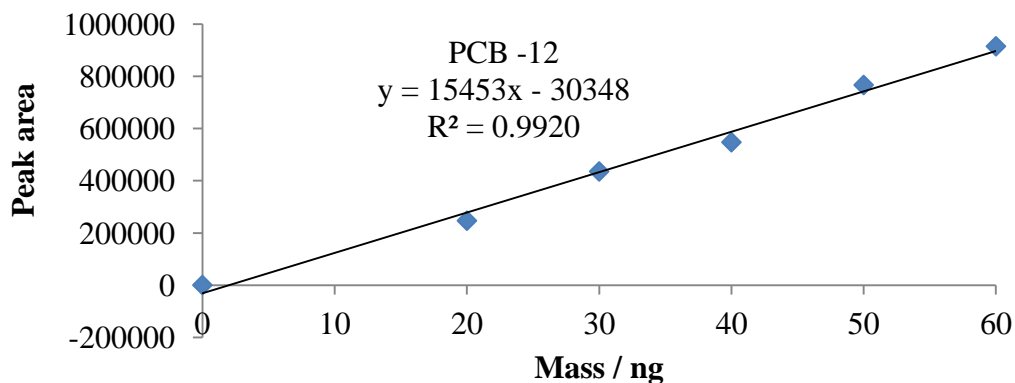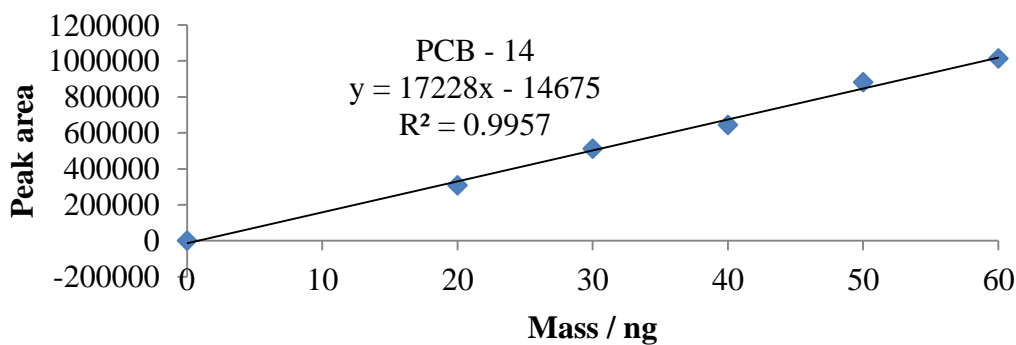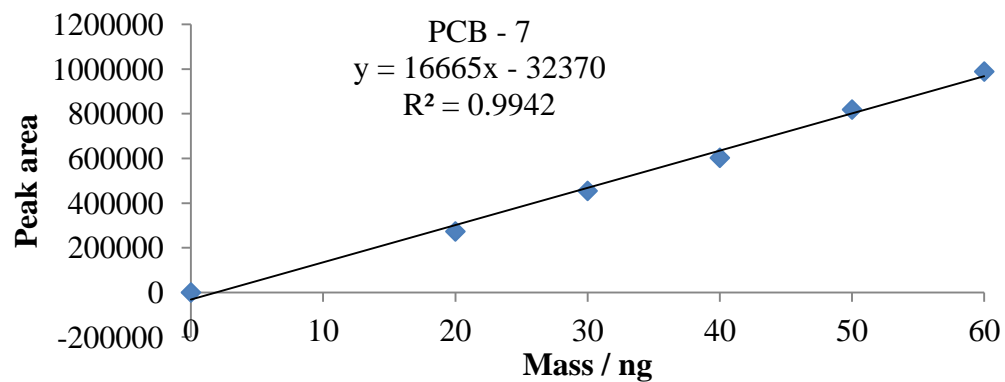
Figure 4.9: Calibration curves for PCB - 7, PCB - 14 and PCB - 12

From the regression line and correlation co-efficients in Figures 4.8 and 4.9, it can be seen that the performance of the instrument was satisfactory and similar to previous

performances as signal responses obtained for the five PCB congeners were linear over the specified ranges with R^2 values greater than or equal to 0.9942.

4.4.1 Repeatability of the method

The repeatability of the method was determined by injecting 1µL of the 60 µg cm^{-3} PCB standard solution in triplicate using the autosampler. A blank was analysed by injecting 1 µL of hexane in a similar manner. The results obtained are shown in Table 4.7.

Table 4.7: Repeatability of GC-MS method for five PCB congeners

Std 60 ng repeat	PCB-1	PCB-3	PCB-7	PCB-14	PCB-12
Replicate 1	1131709	1087491	989059	1013521	914262
Replicate 2	1101612	1065261	967036	1002150	912242
Replicate 3	1112424	1044221	945121	1033110	913361
Mean	1115248	1065658	967072	1016260	913288
Std dev	15246	21638	21969	15661	1012
% RSD	1.37	2.03	2.27	1.54	0.11

As shown in Table 4.7, a good repeatability was obtained as % RSD values across the peak areas of the five PCB congeners were ≤ 2.27 %.

4.4.2 Detection Limit

The detection limit of the PCB congeners were determined by analysing the dilute standard solutions as described in Section 3.3.3. As shown in Table 4.8, the detection limit obtained for PCB congeners was 1.25 ng which was similar to detection limit obtained for congeners in the diCB homologue.

Table 4.8: GC-MS detection limit for five PCB congeners

PCB Congeners	PCB Homologue	Detection Limit / ng
PCB - 1	MonoCB	1.25
PCB - 3	DiCB	1.25
PCB - 7	DiCB	1.25
PCB - 14	DiCB	1.25
PCB - 12	DiCB	1.25

* In a concentration of ng μL^{-1}

4.5 Conclusion

The key objective of this work was to develop a method for identifying and quantifying PCB congeners in solutions using gas chromatography-mass spectrometry (GC-MS). The results obtained in this study demonstrated that the GC-MS method of analysis provided an excellent resolution of the nineteen and five pre-selected PCB congener mixtures. The automatic injection of PCBs onto the GC-MS was successfully used to resolve the nineteen and five PCB congener set under 24 min and 6 min respectively. For the nineteen PCBs, the calibration curves obtained for masses 20 - 100 ng were linear with R^2 values > 0.9901 for PCB - 1, 5, 18, 31, 52, 66, 87, 101, 110 and 151. Other curves for the highly chlorinated congeners, PCB - 153, 138, 141, 187, 183, 180, 170 and 206, still had a good correlation with R^2 values $\leq$ 0.9863. This method was shown to be repeatable (% RSD < 5%, n = 3) and reproducible (% RSD of slope < 7.7 %); although the precision improved for higher masses of PCBs due to the direct relationship observed between precision and mass of each analyte. The GC-MS method of analysis has also been used to resolve the 19 PCB congeners in hexane under 26 min in a study conducted by Cachada et.al.[139] For the five PCB congeners, the calibration curves obtained were linear with R^2 values $\geq$ 0.9942 and repeatability $\leq$ 2.27. The two sets of PCB congeners studied had detection limits of 1.25 – 15 ng μL^{-1}.

5. Development of extraction methods for polychlorinated biphenyls in soil

5.1 Introduction

Soil is a major component of the earth's ecosystem responsible for supporting plants and animals which are essential to human survival.[35] However, industrialisation has resulted in the release of persistent organic pollutants such as PCBs into the soil.[35] Soil has been identified as a major reservoir for PCBs in the environment [8, 15, 39, 140] and primary pathway for their release into the atmosphere.[8, 12, 27, 37] The tendency for PCBs to accumulate in soil and be retained for long periods ranging from 3 months to 47 years coupled with their capacity to undergo long range atmospheric transport from soil matrices to places far from their point of release is a global environmental problem. This has led to an extensive research on the levels of PCBs in soils with indicator congeners (PCB - 28, 52, 101, 118, 138, 153 and 180) and dioxin-like congeners (PCB - 77, 81, 105, 114, 123, 126, 156, 167 and 169) being the most widely examined.[42, 44, 50 33, 36, 44, 52, 140-150]

Domotorova *et. al.*[50] examined the levels of both dioxin-like and indicator-PCBs in soils taken from five specific sites in Slovakia. A good correlation was obtained for all dioxin-like and indicator PCB levels indicating that the sites were most likely contaminated with the same PCB mixtures (Delor 103, 104, 105 and 106) commercially produced in eastern Slovakia; formerly used in open systems. Identical congener patterns were found for all the samples analysed. The dominant dioxin-like PCB congener was PCB-118 and subsequently PCB - $156 > 167 \approx 105 > 189 > 157 \approx 77$. However, this was not the case for one of the samples where the dominant indicator congener was PCB - 156. The most abundant indicator congeners were PCB - 153, 138 and 180; seemingly corresponding to the use of Delor. In the same vein, high concentrations of PCBs found in a suburban site from Canada were reported to be likely due to spills from technical mixtures used in an old local transformer or contaminated fills used for the site.[151]

An estimated 93 % of the contemporary UK environmental burden of PCBs was found to be associated with soils.[15] There is a general consensus that the sources of PCBs in urban soils are mainly due to local sources and long range atmospheric transport as signs of PCB deposition are still present in the urban soils of some European countries in spite of their ban for several decades.[139].[139, 142, 152] A study on the level of PCBs in urban soils

from five major European cities Uppsala (Sweden), Ljubljana (Slovenia), Aveiro (Portugal), Torino (Italy) and Glasgow (Scotland) showed that hotspots (concentrations greater than the Dutch target value of 20 µg kg^{-1}) were present in all of the cities particularly in Glasgow and Torino.[139]

PCB levels in soil have been determined using several analytical methods; a wide range of these methods have been summarized in Table 5.1. The classical soxhlet extraction technique involving the use of n-hexane and acetone (20 - 75 % on a volume basis) and extraction times of 7 - 48 h is the most commonly used method for extracting PCBs from soil samples.[139, 140, 144, 146, 153] Although high recoveries have been obtained via this method, the large volume of solvents and long extraction times required have resulted in the use of other extraction techniques such as ultrasonic extraction, soxtec extraction, accelerated solvent extraction and microwave-assisted extraction with shorter extraction times and smaller solvent volumes.[33, 154, 155] The extraction efficiencies of these techniques have been compared with the classical soxhlet extraction using a mixture of n-hexane/acetone (1:1 v/v) as extraction solvents for soxhlet, soxtec, microwave-assisted extraction, (3:1 v/v) for ultrasonic extraction and CO_2 for supercritical fluid extraction.[150] The results obtained indicated that PCB recoveries from soil were dependent upon the extraction conditions selected.

Clean up of soil extracts is commonly performed using either a silica gel, alumina or florisil column which involves several rigorous and lengthy steps while GC-MS is observed to be the most widely employed analytical technique for analysis of PCBs in extracts. [141, 146, 156] From the review of literature, it has been observed that most studies focus on assessing the levels of PCBs in urban soils of various European countries with very few studies in developing countries particularly Africa.[51] In addition, it is further observed that limited number of studies have focused on the comparison of PCB recoveries from soils using two or more solvent extraction methods. [150, 157]

Hence, the key objective of this study was to develop an analytical method that can be easily applied for determination of PCBs in soils and eliminates the use of a lengthy clean up step. Two different extraction methods: the accelerated solvent extraction method and the microwave-assisted extraction method were assessed under optimum conditions. In this study, soil samples were collected from two power stations (Site A

and B) in Lagos, Nigeria which is notably the hub of commercial activities in Nigeria. Site A (Ijora power station) is a defunct power station that's currently being employed as a repair station for transformers while Site B is a power station that's being used for power generation and transmission. Whilst PCBs have never been manufactured in Nigeria, they were employed as dielectric fluids in transformers for power generation. These power operating plants are generally classified into two types; the thermal/fossil fuel power plants which are either coal or natural gas fired and hydroelectric power plants. The eleven operational thermal power stations which are gas fired include the Aba, Afam, Egbin, Geregi, Ibom, Ihovbor, Okpai, Olorunsogo, Omotosho, Sapele and Ughelli power stations while the four operational hydroelectric power stations include the Kainji, Jebba, Shiroro and Zamfara power stations. The Power Holding Company of Nigeria was reportedly the largest user of dielectric fluids and owners of equipment that possibly contained PCBs. Although these sites have been deemed to be potentially contaminated with PCBs, there is no actual data on the level of PCBs in soils from sites or records of historical waste containing PCBs. Therefore, another objective of this study was to investigate the level of PCBs in soil samples collected from the aforementioned sites using the developed method.

Table 5.1: A review of analytical methods used for determination of PCBs in soils

PCBs analysed and Standards used	Solvent Extraction Technique	Clean up Technique	Technique, Column Used, Operating Conditions and Results obtained
I. PCBs: 28, 52, 101, 118, 153, 138 and 180.	Ultrasonication: 7.5 g of freeze-dried soil sample was extracted using 20 cm^3 hexane, 10 cm^3 methanol and 5 cm^3 deionised water and sonicated in an ultrasonic bath for 1 h. The resulting mixture was centrifuged and extracts collected. 20 cm^3 of n-hexane was subsequently added to the residue. The process was repeated once and extracts concentrated using a rotary evaporator.	Extracts were cleaned up using a 6 cm^3 silica gel column containing a 0.5 g layer of anhydrous sodium sulfate at the top. Elution from the column was done with 7 cm^3 hexane and eluate concentrated to 1 cm^3 using a gentle stream of pure nitrogen.	GC–ECD equipped with an HP-5 capillary column (30 m × 0.32 m i.d × 0.25 μm film thickness). Oven temperature: 60 °C for 1 min, ramped to 170 °C at 25 °C min^{-1}, to 190 °C at 4 °C min^{-1}, to 270 °C at 10 °C min^{-1} and kept at 270 °C for 5 min. Injector and detector temperatures: 220 °C and 270 °C respectively. High PCB concentrations were found in urban soils compared to those in country side areas. The $\sum$7 PCBs for all urban and rural soils were > 1.5 μg kg^{-1} and < 0.5 μg kg^{-1} respectively. Peak value for urban soils was 9.87 μg kg^{-1} (lower than the Dutch target value of 20 μg kg^{-1}).[141]

PCBs analysed and Standards used	Solvent Extraction Technique	Clean up Technique	Technique, Column Used, Operating Conditions and Results obtained
II. Dioxin like and Indicator PCBs	Pressurised liquid extraction: 10 g of dried soil sample mixed with 2 g of copper and 3 g of anhydrous sodium Na_2SO_4 were packed in the extractor cells. Extraction was carried out using hexane at 100 °C, 10 MPa, 5 min static time in 2 cycles.	Concentrated extracts were cleaned using silica gel column made up of 1.5 g 3.3 % Ag NO_3 on silica, 1.5 g base modified silica gel (KOH/silica), 4 g of 44 % H_2SO_4/silica, 2 g anhydrous Na_2SO_4 (all separated by a thin layer of silica gel). Hexane was used as the eluent and the eluate concentrated to a small volume using a semi-automated power pump system.	HR GC-MS equipped with a DB-5 MS column (60 m $\times$ 0.25mm i.d $\times$ 0.25 µm film thickness). Oven temperature: 120 °C for 1.5 min, ramped to 200 °C at 30 °C min^{-1}, to 287 °C at 3 °C min^{-1}, and 325 °C at 10 °C min^{-1}. The average sum of dioxin like and indicator PCBs were between 0.21 to 3.8 ng g^{-1} and 2.0 to 46 ng g^{-1}. The most abundant PCB congeners were PCB 118 and 153.[50]

PCBs analysed and Standards used	Solvent Extraction Technique	Clean up Technique	Technique, Column Used, Operating Conditions and Results obtained
III. PCBs: 18, 28, 52, 101, 118, 153, 138, 149, 153, 170, 180 and 194.	Ultrasonication: 15 g of soil homogenised with 1 g of copper and anhydrous sodium sulfate was placed in a centrifuge tube and sonicated for 20 min using 60 cm^3 hexane/acetone (1:1 v/v). Sample was separated by centrifugation and extracts concentrated.	Clean up was done using a column consisting of 3 g silica gel at the bottom and 2 g anhydrous sodium sulfate at the top. Hexane was used as the eluting solvent and eluate concentrated using a gentle stream of nitrogen	GC-ECD equipped with an HP-5 fused silica capillary column (30 m × 0.32 m i.d × 0.25 μm film thickness). Oven temperature: 90 °C for 1 min, ramped to 140 °C at 20 °C min^{-1}, to 240 °C at 3 °C min^{-1}, to 240 °C at 3 °C min^{-1} and kept at 300 °C at 10 °C min^{-1} for 10 min. The highest concentration of PCBs found in surface soils was 32.83 ng g^{-1}. A weak correlation between soil organic matter and PCB congeners was observed.[49]

PCBs analysed and Standards used	Solvent Extraction Technique	Clean up Technique	Technique, Column Used and Operating Conditions Results Obtained
IV. PCBs: 1, 5, 18, 31, 44, 52, 66, 87, 101, 110, 138, 141, 151, 153, 170, 180, 183, 187 and 206.	Soxhlet extraction: 10 g of air-dried soil was extracted with a mixture of hexane: acetone (1:1 v/v) for 6 h at a rate of 4 - 6 cycles/h. Extracts were concentrated using a rotary vapour at 30 °C.	Resultants extracts were cleaned using a 6 cm^3 column containing 1 g of neutral alumina, 0.5 g of Na_2SO_4 at the upper layer. Elution was done using 8 cm^3 hexane: DCM (9:1) and 4 cm^3 hexane: DCM (12:1). Eluate was concentrated using a rota vapour and subsequently dried under a gentle stream of nitrogen. Solvent was changed to isooctane prior to GC-MS analysis.	GC-MS equipped with a DB-5 fused capillary column. Oven temperature: 40 °C for 2 min, ramped to 290 °C at 10 °C min^{-1} and held for 8 min. Injector and detector temperatures: 280 °C and 300 °C respectively. Hotspots were found in all cities studied as soil samples had values higher than the 20 µg kg^{-1} Dutch target value. [139]

PCBs analysed and Standards used	Solvent Extraction Technique	Clean up Technique	Technique, Column Used, Operating Conditions and Results Obtained
V. PCBs: 8, 18, 28, 44, 52, 66, 77, 101, 118, 123, 128, 138, 153, 156, 180 and 189.	Accelerated solvent extraction: 14 g of soil sample was extracted with 30 cm^3 hexane: acetone (1:1 v/v) at 100 °C and 1500 psi. The process was repeated three times and extracts combined.	A column containing 2 g of silver nitrate silica, 1 g of activated silica gel, 3 g of basic silica gel, 4 g of acid silica gel, 1 g of activated silica gel and 2 g of anhydrous sodium sulfate was used to clean up extracts. Elution was done with 100 cm^3 hexane. Eluate was concentrated with a rotary evaporator and reduced under a gentle stream of nitrogen.	GC-MS equipped with a DB-5 MS capillary column (30 m × 0.25 mm i.d × 0.25 µm film thickness). Oven temperature: 80 °C for 2 min, ramped to 160 °C at 10 °C min^{-1} (held for 1 min), to 230 °C at 1.5 °C min^{-1} (held for 15 min), to 280 °C at 20 °C min^{-1} (held for 15 min). PCB concentrations in urban soils met the Dutch standard values (0.02 mg kg^{-1}) with tetra-CBs being the most toxic contaminants.[143]

PCBs analysed and Standards used	Solvent Extraction Technique	Clean up Technique	Technique, Column Used, Operating Conditions and Results obtained
VI. PCBs: 77, 81, 105, 114, 118, 123, 156, 167 and 169.	Soxhlet extraction: 60 g of soil sample was homogenised with anhydrous sodium sulfate. Activated copper granules with hydrochloric acid were added to remove elemental sulfur. Sample was extracted for 24 h with 400 cm^3 n-hexane: acetone (1:1 v/v).	Clean up was done using a silica gel column filled with 1 cm layer of anhydrous sodium sulfate. Elution was done with n-hexane and eluate concentrated using a rotary evaporator and reduced with a gentle stream of pure nitrogen.	GC-ECD equipped with a DB-5 fused silica capillary column (60 m × 0.25 mm i.d × 0.25 μm film thickness). Oven temperature: 100 °C for 2 min, ramped to 240 °C at 1 °C min^{-1}, to 280 °C at 10 °C min^{-1}, held for 20 min. PCB levels were strongly dependent on the proximity to major emission sources indicating that industrial activities could likely be due to the emission sources of PCBs. The predominant PCB homologues were the penta and tri CBs.[153]

PCBs analysed and Standards used	Solvent Extraction Technique	Clean up Technique	Technique, Column Used ,Operating Conditions and Results Obtained
VII. Di-PCB, tri-CB, penta-CB, hexa-CB and hepta-CB.	Soxhlet extraction: Soil samples were extracted with n-hexane: acetone (1:1 v/v) for 10 h.	Two columns: a gel permeation column filled with bio-bead S-X3 and a column filled with 3 g silica, 3 g aluminium oxide and 3 g anhydrous Na_2SO_4 were used for cleaning up extracts. Extracts were concentrated using a gentle stream of N_2.	GC-ECD equipped with a DB-5 capillary column (60 m × 0.25 mm i.d × 0.25 µm film thickness). Oven temperature: 90 °C for 2 min, ramped to 170 °C at 22 °C min^{-1}, to 280 °C at 1.32 °C min^{-1}, held for 17 min. PCB pollution was found in soils from both background and urban areas. The concentration of lowly chlorinated congeners in rural and background soils were higher than those for urban areas. A significant correlation between soil and organic matter and lowly chlorinated congeners was found.[158]

PCBs analysed and Standards used	Solvent Extraction Technique	Clean up Technique	Technique, Column Used, Operating Conditions and Results Obtained
VIII. Di-CB, tri-CB, penta-CB, hexa-CB and hepta-CB.	Soxhlet extraction: 20 g of soil sample was extracted with 100 cm^3 n-hexane/acetone (1:1 v/v).	Extracts were dried by filtering through a funnel filled with anhydrous Na$_2$SO$_4$ and concentrated using a rotary evaporator and subsequently a gentle stream of N$_2$. A 10 g silica gel column was used to clean extracts and a 70 cm^3 mixture of a DCM and hexane (1:1 v/v) was used as the eluting solvent. Eluates were rotary evaporated and reduced using a gentle stream of N$_2$.	GC-MS equipped with an HP-5 MS capillary column (60 m × 0.25 mm i.d × 0.25 µm film thickness). Oven temperature: 70 ^{o}C for 1 min, ramped to 160 ^{o}C at 10 °C min^{-1}, to 280 °C at 2 °C min^{-1}, held for 10 min. Relatively high PCB concentrations (2.24 ± 1.64 ng/g dw) > (1.59 ±1.02 ng/g dw) > (0.64 ± 0.29 ng/g dw) > (0.30 ng/g dw) were found for urban, rural, suburban and background soils respectively. High positive correlations between PCBs and soil organic matter were obtained.[142]

PCBs analysed and Standards used	Solvent Extraction Technique	Clean up Technique	Technique, Column Used, Operating Conditions and Results Obtained
IX. Di-CB, tri-CB, penta-CB, hexa-CB and hepta-CB.	Soxhlet extraction: 20 g of soil sample was extracted for 24 h using a 200 cm^3 mixture of n-hexane: acetone (1:1v/v).	Extracts were cleaned using a column filled with 5 g of anhydrous Na_2SO_4 at the top and 10 g silica gel at the bottom. Elution was done using 50 cm^3 hexane: DCM (1:1 v/v).	GC-MS equipped with an HP-5MS capillary column (60 m × 0.25 mm i.d × 0.25 μm film thickness). Oven temperature: 80 °C for 2 min, ramped to 160 °C at 10 °C min^{-1} (held for 1 min), to 230 °C at 1.5 °C min^{-1} (held for 15 min), to 280 °C at 20 °C min^{-1} (held for 10 min). Average PCB concentrations in urban soils (3.037 μg/kg dw) were much higher than those in rural soils (1.337 μg/kg dw). There was no significant correlation between total PCB concentration and total organic carbon content in soil.[140]

PCBs analysed and Standards used	Solvent Extraction Technique	Clean up Technique	Technique, Column Used, Operating Conditions and Results obtained
X. PCBs: 28, 52, 101, 118, 138, 153 and 180.	Accelerated solvent extraction: 15 g of freeze dried soil samples were extracted with hexane: acetone (1:1 v/v) under 1500 psi at 100 °C. Extraction was done in 2 cycles with 5 min heating, followed by 5 min static extraction. Extracts were dried using anhydrous Na_2SO_4 and concentrated to 1 cm^3 using a gentle stream of N_2.	Clean up was done by passing extracts through a glass column (30 cm × 10 mm i.d) filled with 1.5 g Na_2SO_4, 1.5 g copper powder and 3 g activated florisil. 100 ml hexane: acetone (9:1 v/v) was used as the eluent. Eluate was reduced to a final volume of 1 cm^3 under a gentle stream of N_2.	GC-ECD equipped with an HP-5MS fused capillary column (30 m × 0.25 mm id × 0.25 μm film thickness). Oven temperature: 120 °C for 2 min, ramped to 180 °C at 30 °C min^{-1}, to 200 °C at 4 °C min^{-1} (held for 2 min), to 270 °C at 2 °C min^{-1} (held for 10 min). The average total PCB concentration was 46.2 μg kg^{-1}. PCB pollution stemmed mainly from industrial point sources.[155]

PCBs analysed and Standards used	Solvent Extraction Technique	Clean up Technique	Technique, Column Used, Operating Conditions and Results Obtained
XI. PCBs: 1, 5, 18, 28, 31, 44, 52, 66, 87, 101, 110, 118, 138, 141, 151, 153, 170, 180, 183, 187 and 206.	Soxhlet extraction: 10 g of soil was extracted with 90 cm^3 hexane: acetone (2:1 v/v) for 8 h at a rate of 10 cycles/ h using a prewashed glass filter thimble and extracts concentrated with a rotary evaporator at 30 °C.	Solid phase extraction cartridges filled with 1 g silica, 2 g neutral alumina, 3 % deactivated and 0.5 g Na_2SO_4 at the upper layer. Eluate was concentrated to 2 cm^3 using a rotary evaporator and volume reduced under a gentle stream of N_2. Extracts were redissolved in hexane and further cleaned using 2 g acidic silica (30 % conc H_2SO_4 w/w.	GC-MS equipped with an SPB-5 fused capillary column. Oven temperature: 40 °C for 2 min, ramped to 290 °C at 10 °C min^{-1} and held for 8 min. High PCB concentrations were found in cities studied. The mean concentrations were 4.1 µg kg^{-1} and 1.7 µg kg^{-1} for $\sum$7 PCBs and 7.0 µg kg^{-1} and 4.6 µg kg^{-1} for $\sum$21 PCBs studied. PCB retention in soils was strongly influenced by organic carbon.[146]

PCBs analysed and Standards used	Solvent Extraction Technique	Clean up Technique	Technique, Column Used, Operating Conditions and Results Obtained
XII Di-CB, tri-CB, tetra CB, penta-CB, hexa-CB, hepta-CB, octa-CB, nona-CB and deca-CB.	Microwave extraction: 10 g of soil was extracted with 30 cm^3 hexane: acetone (1:1 v/v) at 100 °C for 20 min. Extract was filtered through a glass funnel containing 5 g anhydrous Na_2SO_4 followed by washing with n-hexane:acetone (1:1 v/v) three times.	Extracts were cleaned using a florisil column. 10 cm^3 n- hexane: acetone (9:1 v/v) was used as the eluent. Eluate was concentrated to 1 cm^3 by evaporation in a water bath under a gentle stream of N_2.	GC-MS equipped with a DB-5 MS capillary column (30 m × 0.25 mm i.d × 0.25 μm film thickness). Oven temperature: 40 °C ramped to 280 °C at 35 °C min^{-1}, held for 5 min. PCB 118 had the highest concentration amongst the PCBs studied.[154]

5.2 Materials and Reagents

PCB extractions were carried out using HPLC grade n-hexane and acetone supplied by Fisher Scientific and Sigma Aldrich respectively. Individual PCB congener standards (PCB - 1, 3, 7, 14 and 12) and anhydrous sodium sulfate were purchased from Sigma Aldrich. Horticultural peat (pH - 4.51, organic matter - 93 %) was purchased from Northern Peat and Moss Company. Syringe filters, pelletised diatomaceous earth and cellulose filters were obtained from Thames Restek UK Ltd.

5.3 Experimental

5.3.1 Sample collection and preparation

As mentioned earlier, soil samples were collected from two sites – the Ijora power station (Site A) and the Egbin power station (Site B) which were open-field sites. Information on the geographical location and site description is given in Table 5.2.

Table 5.2: Geographical Information and Site Description

Sample ID	Matrix	Geographical coordinates of sampling points	Site Description
A1	Soil	$6^{\circ}28'11.5''$N $3^{\circ}22'32.4''$E	Transformer repairs had been recently undertaken
A2	Soil	$6^{\circ}28'18.9''$N $3^{\circ}22'\,32.4''$E	Disused/old transformer storage area
A3	Soil	$6^{\circ}28'16.1''$N $3^{\circ}22'32.8''$E	Disused/old transformer storage area
A4	Soil	$6^{\circ}28'14.3''$N $3^{\circ}22'31.6''$E	No transformer repairs had been undertaken for a long time
B1	Soil	$6^{\circ}33'48.3''$N $3^{\circ}36'54.9''$E	Power generating plant on site
B2	Soil	$6^{\circ}33'45.0''$N $3^{\circ}36'54.9''$E	Working transformers on site
B3	Soil	$6^{\circ}33'42.8''$N $3^{\circ}36'48.4''$E	Working transformers on site

*A and B represent samples taken at Ijora and Egbin power stations respectively

Composite samples of soil (0 - 10 cm) were obtained using a stainless steel spade and stored in aluminium foil pre-rinsed with hexane. Prior to extraction, all soil samples

collected were homogenised by air drying and sieving using a 2 mm stainless steel sieve. In order to obtain a representative sample, soil samples (< 1 mm size fractions) were subjected to coning and quartering on a piece of aluminium foil. Representative samples obtained were stored in dark amber glass bottles and sealed with Teflon caps for extraction.

5.3.2 Soil characterisation

5.3.2.1 Soil pH

The pH of soil samples was determined using standard method (ISO10390, 2005).[159] 5 g of soil was weighed into a sample bottle and 25 cm^3 of distilled water was added. The suspension was shaken for 60 min using a mechanical shaker and allowed to settle for 2 h. The pH meter was calibrated using buffer solutions 4.00, 7.01 and 10.00 at 20 °C (VWR chemicals). This was done in triplicate. The pH of the supernatant solution was measured using a Mettler Toledo Seven Multi pH meter (GmbH Schwerzenbach, Switzerland).

5.3.2.2 Moisture content

The British standard method (ISO 12880, 2000)[160] was used to determine the moisture content of soil samples. 0.5 g of soil was weighed into a crucible and dried in air using an oven at 105 °C for 24 h. This was allowed to cool in a dessicator before weighing. The loss in weight was determined and moisture content calculated using Equation 5.1 as follows:

$$\% \text{ moisture by mass} = \frac{\text{initial weight} - \text{dry weight}}{\text{initial weight}} \times 100 \qquad \text{Eq 5.1}$$

5.3.2.3 Soil organic matter content (weight loss on ignition)

Soil organic matter (SOM) content was determined according to British Standard method (ISO 12879, 2000). The air-dried soil samples were placed in a muffle furnace

and ashed at 550 °C for 24 h in air. After ashing, the samples were cooled in a dessicator and reweighed. The SOM content was calculated using Equation 5.2 as shown:

$$\% \text{ SOM} = \frac{\text{dry weight of soil} - \text{ashed weight of soil}}{\text{dry weight of soil}} \times 100 \qquad \text{Eq. 5.2}$$

5.3.2.4 Particle size distribution

Particle size distribution was obtained using the procedure described as follows: 50 g of soil sample was weighed into a 500 cm^3 beaker. 50 cm^3 of sodium hexametaphosphate (5 %) solution and 100 cm^3 of distilled water were added into the beaker and mixed thoroughly for 30 min using a stirring rod. The entire solution (soil suspension) was transferred into a 1000 cm^3 measuring cylinder and made up to mark with distilled water. The top of the cylinder was sealed with parafilm and the cylinder was manually inverted for 30 min resulting in a uniform suspension. The resulting suspension was gently placed on a bench and the density and temperature readings were taken after 40 s using a hydrometer and thermometer respectively. The suspension was allowed to stand for 3 h and density and temperature readings were taken. A blank sample was prepared by transferring 50 cm^3 of the sodium hexametaphosphate solution into a 1000 cm^3 measuring cylinder which was made up to mark with distilled water. The hydrometer readings were corrected by subtracting 0.2 units for every 1 °F below 68 °F obtained. The particle size distribution (percentage of clay, silt and sand) was calculated using Equations 5.3 - 5.5.

$$\% \text{ clay} = \text{corrected hydrometer reading at 3 h} \times \frac{100}{\text{weight of sample}} \qquad \text{Eq. 5.3}$$

$$\% \text{ silt} = \text{corrected hydrometer reading at 40 s} \times \frac{100}{\text{weight of sample}} \qquad \text{Eq 5.4}$$

$$\% \text{ sand} = 100 - (\% \text{ silt} + \% \text{ clay}) \qquad \text{Eq 5.5}$$

5.3.3 Spiking procedure for soil samples

Soil samples were spiked with a 60 ng µL^{-1} congener mixture containing the five PCB congeners (Section 3.3.3). 0.5 g of dried soil or horticultural peat was weighed into an amber glass vial and spiked with a 500 µL aliquot of the PCB congener mixture. This was done in triplicate. A control sample was prepared by spiking 0.5 g of dried soil with 500 µL of hexane in an amber glass vial. All extraction vessels were loosely capped and analytes were allowed to equilibrate with the soil for 24 h. The spiked samples were subsequently transferred into extraction vessels for extraction.

The procedural detection limit (DL$_{pro}$) of each PCB congener was determined using Equation 5.6.

$$\text{DL}_{\text{pro}} = \frac{\text{DL } (\mu\text{g cm}^{-3}) \times \text{volume of extract (cm}^3) \ \times* \text{ preconc factor}}{\text{mass of dry sample (g)}} \qquad \text{Eq 5.6}$$

*preconc denotes preconcentration

5.3.4 Sample extraction

5.3.4.1 Microwave-assisted extraction

Microwave assisted extraction (MAE) of soil samples was conducted using a CEM MARS Xpress Microwave Accelerated Reaction System (CEM Corporation, Matthews, NC, USA). Prior to extraction, 5 g of sodium sulfate was weighed into the extraction vessels containing the spiked soil and 30 cm^3 of n-hexane: acetone (1:1 v/v) was added as the extraction solvent to each vessel respectively. A procedural blank was prepared by transferring 5 g of anhydrous sodium sulfate and 30 cm^3 of n-hexane: acetone (1:1 v/v) into an extraction vessel. The MAE vessels were sealed, placed in the system and subjected to extraction under the operating conditions outlined as follows: the temperature was ramped to 130 °C in 15 min at a microwave power of 800 W, held for 20 min and allowed to cool down for 10 min. The supernatant obtained from the extracts was subjected to clean up as described in Section 5.3.5 prior to GC-MS analysis.

5.3.4.2 Accelerated solvent extraction

Accelerated solvent extraction (ASE) of soil samples was performed on a Dionex ASE 350 Accelerated Solvent Extractor (Dionex Corporation, Sunnyvale, CA, USA). Prior to extraction, the bottom of each stainless steel extraction cell (10 cm^3) was lined with a piece of cellulose filter (27 mm). Each extraction cell was filled with a layer of pelletised diatomaceous earth (DE), the soil sample and another layer of pelletised DE at the top. The procedural blank was prepared by filling an extraction cell with only pelletised DE. All extraction cells were sealed, loaded onto the ASE system and extractions performed at a temperature of 100 °C and pressure of 1500 psi in 3 cycles using a mixture of hexane: acetone (1:1 v/v). Heating and static extractions were conducted for 5 min and 10 min respectively. 100 % of the extraction cells were flushed with fresh solvent after each cycle and extracts purged with nitrogen for 50 s. The resulting extracts (30 cm^3) were collected in glass vials (60 cm^3) lined with Teflon septa and subsequently subjected to clean-up as described in Section 5.3.5 prior to GC-MS analysis.

5.3.5 Sample clean-up

Prior to clean up, a 25 mm, 0.22 µm PTFE syringe filter with a luer lock inlet was used to filter the supernatant obtained from the MAE process to remove any suspended particles. The resulting MAE filtrates and ASE extracts were subsequently evaporated to dryness under a gentle stream of nitrogen at 30 °C for 2 h using a Techne Inc Sample Concentrator (NJ, USA). The samples were reconstituted with 2 cm^3 of hexane and cleaned by loading onto a disposable Pasteur pipette packed with a layer of glass wool, 100 - 200 mesh silica gel and anhydrous sodium sulfate conditioned with 1 cm^3 of n-hexane. The resulting solution obtained was analysed using the GC-MS.

5.4 Results and Discussion

5.4.1 Physicochemical properties of soil samples

Characterisation of soil samples (pH, soil organic matter content and particle size distribution) was conducted as described in Section 5.3.2 and results obtained given in Table 5.3. In general, soil samples were neutral except sample B3 which was slightly acidic in nature. All samples had a soil organic matter (SOM) content ≤ 40.6 % except for sample A4 which had an SOM content of 91.6 %. A higher percentage of sand compared to silt and clay was generally present in all samples.

Table 5.3: Physicochemical properties of soil samples collected from sites A and B in Lagos, Nigeria

Sample ID	pH	SOM content	% clay	% silt	% sand
A1	6.91	25.2	12.4	7.8	79.8
A2	7.98	15.8	10.4	2.4	87.2
A3	6.77	27.6	8.4	5.4	86.2
A4	7.36	91.6	12.4	4.4	83.2
B1	6.36	14.4	4.4	0.4	95.2
B2	6.18	11.9	6.4	2.4	91.2
B3	4.84	40.6	2.4	0.4	97.2

5.4.2 Extraction efficiency of MAE for soil samples

To assess the extraction efficiency using MAE, 1 µL of the resulting solution obtained after the clean up process (Section 5.3.5) was analysed using the GC-MS via injection with an autosampler using the operating conditions described in Section 3.3.1. All MAE extractions were conducted in triplicate to establish the repeatability and precision of the method. Linear regression analysis (LRA) was used to obtain unknown masses of each PCB congener by fitting the peak areas of each analyte into their respective calibration data and the results obtained given in Table 5.4. No PCBs were found in procedural

blanks analysed. For soil samples (horticultural peat) spiked directly with PCBs in MAE vessels, average recoveries obtained for PCBs ranged from 29.3 – 43.3 %. This may be due to the method used for spiking resulting in vaporisation of the target analytes from the sample via openings on the MAE vessels during the 24 h equilibration period. High RSD values of 23.1 – 58 % obtained were consistent with the low recoveries obtained.

Table 5.4: MAE results for soil samples spiked directly in MAE vessels

	Std 15 ng repeat	PCB - 1	PCB - 3	PCB - 7	PCB - 14	PCB - 12
% Recovery	**Replicate 1**	12	20	27	32	24
	Replicate 2	46	51	50	51	46
	Replicate 3	29	40	42	47	40
	Mean	29.3	37.0	39.7	43.3	36.7
	Std dev	17.0	15.7	11.7	10.0	11.4
	% RSD	58.0	42.5	29.4	23.1	31.0

Therefore, to improve the recoveries and precision obtained using MAE, soil samples were spiked in dark amber vials and subsequently transferred to extraction vessels as described in Section 5.3.4.1. The resulting solutions obtained after clean up (Section 5.3.5) were analysed and LRA was used to obtain unknown masses of target analytes. In contrast to low recoveries previously obtained using MAE, the results displayed in Table 5.5 indicate that there was a significant improvement in recoveries and precision obtained as average recoveries for each PCB congener ranged from 68 - 75.3 % while RSD values ranged from 8.2 - 9.6 % except for PCB - 1 and 3 which had relatively high RSD values of 18.3 and 13.9 % respectively. This high level of imprecision may perhaps be attributed to the high volatility of PCB - 1 and 3 which belong to the monochlorobiphenyl (mono CB) homologue compared to PCB congeners in the dichlorobiphenyl (diCB) homologue which had a relatively lower volatility. As a consequence, vapourisation of these analytes from their respective vessels would vary leading to a variation in recoveries obtained. The variation in results may also be due in part to the filtration of extracts conducted prior to preconcentration and clean up.

Table 5.5: MAE results for soil samples spiked in dark amber glass vials

	Std 15 ng repeat	PCB - 1	PCB - 3	PCB - 7	PCB - 14	PCB - 12
	Replicate 1	70	75	73	71	69
	Replicate 2	85	86	79	79	74
% Recovery	Replicate 3	59	65	67	67	61
	Mean	71.3	75.3	73.0	72.3	68.0
	Std dev	13.1	10.5	6.0	6.1	6.6
	% RSD	18.3	13.9	8.2	8.4	9.6

5.4.3 Recovery of PCB congeners from ASE

To assess the recovery of PCB congeners from soil samples using ASE, 1μL of the solution obtained was analysed using the GC-MS via injection with an autosampler under the operating conditions specified in Section 3.3.1. The experiment was conducted in triplicate to establish the repeatability and precision of the method. Unknown masses of each PCB congener were obtained using LRA. Results obtained are given in Table 5.6.

Table 5.6: ASE results for soil samples spiked in amber glass vials

	Std 15 ng repeat	PCB - 1	PCB - 3	PCB - 7	PCB -14	PCB - 12
	Replicate 1	87	93	86	86	81
% Recovery	Replicate 2	85	94	83	88	81
	Replicate 3	84	95	87	86	82
	Mean	85.3	94.0	85.3	86.7	81.3
	Std dev	1.5	1.0	2.1	1.2	0.6
	% RSD	1.8	1.1	2.4	1.3	0.7

From Table 5.6, it can be deduced that average recoveries obtained for each PCB congener ranged from 81.3 - 94 %. This was significantly higher than average recoveries

obtained using MAE suggesting that the ASE method gives better recoveries of PCBs from soil samples than the MAE method. Furthermore, in comparison to the MAE method where relatively high RSD values were obtained, RSD values obtained for each PCB congener using the ASE method were ≤ 2.4 %; indicating that PCB masses recovered did not vary significantly for each extraction performed. This demonstrates that repeatable results and high precisions were achieved for the ASE extraction method. This is similar to the findings by Wang et al[161] in a study based on evaluation of soxhlet extraction, ASE and MAE for PCBs in soil samples which showed that MAE gave larger relative standard deviations than ASE.

5.4.4 Procedural detection limit

For the nineteen PCB congeners, the detection limit (Equation 5.6) was 0.006 µg kg^{-1} for PCB - 1, 5 and 18, 0.01 µg kg^{-1} for PCB - 44, 52, 66, 87, 101, 110, 151, 153, 138, 141, 187 and 183, 0.02 µg kg^{-1} for PCB - 170 and 206. The detection limit obtained for the five PCB congeners was 0.006 µg kg^{-1}.

5.4.5 Analysis of real soil samples

From the results obtained, the optimised method which had higher extraction efficiency for PCBs was the ASE method. Hence, the soil samples (A1-A4, B1-B3) collected from Lagos, Nigeria were extracted using the optimised ASE method. The resulting solutions obtained after clean up were screened for the nineteen target PCB congeners. However, none of the target PCB congeners were present in the samples analysed. Therefore, to further validate the developed method, the samples were spiked with PCBs (Section 5.3.3) and the results obtained are given in Table 5.7. PCB recoveries obtained ranged from 60 - 101 % with RSD values ≤ 12 %; indicating that the developed method can be satisfactorily applied to real environmental samples.

Table 5.7: PCB recoveries for real soil samples spiked with PCBs

Analyte	Std 60 ng	Sample ID						
		A1	**A2**	**A3**	**A4**	**B1**	**B2**	**B3**
PCB-1	Replicate 1	74	65	61	62	75	65	64
	Replicate 2	80	58	65	71	75	55	71
	Replicate 3	87	57	71	64	70	61	73
	Mean	80.3	60.0	65.7	65.7	73.3	60.3	69.3
	Std dev	6.5	4.4	5.0	4.7	2.9	5.0	4.7
	% RSD	8.1	7.3	7.7	7.2	3.9	8.3	6.8
PCB-3	Replicate 1	81	84	68	62	91	73	87
	Replicate 2	94	85	66	66	88	67	88
	Replicate 3	92	87	64	52	82	71	99
	Mean	89.0	85.3	66.0	60.0	87.0	70.3	91.3
	Std dev	7.0	1.5	2.0	7.2	4.6	3.1	6.7
	% RSD	7.9	1.8	3.0	12.0	5.3	4.3	7.3
PCB-7	Replicate 1	80	94	69	68	97	74	101
	Replicate 2	83	94	67	67	89	68	111
	Replicate 3	92	97	66	65	83	68	92
	Mean	85.0	95.0	67.3	66.7	89.7	70.0	101.3
	Std dev	6.2	1.7	1.5	1.5	7.0	3.5	9.5
	% RSD	7.3	1.8	2.3	2.3	7.8	4.9	9.4
PCB-14	Replicate 1	85	99	69	67	96	76	90
	Replicate 2	84	98	66	69	89	71	101
	Replicate 3	95	102	71	62	85	75	94
	Mean	88.0	99.7	68.7	66.0	90.0	74.0	95.0
	Std dev	6.1	2.1	2.5	3.6	5.6	2.6	5.6
	% RSD	6.9	2.1	3.7	5.5	6.2	3.6	5.9
PCB-12	Replicate 1	81	100	69	101	93	75	87
	Replicate 2	97	99	75	102	88	69	88
	Replicate 3	91	104	71	89	91	69	99
	Mean	89.7	101.0	71.7	97.3	90.7	71.0	91.3
	Std dev	8.1	2.7	3.0	7.1	2.4	3.7	6.7
	% RSD	9.0	2.6	4.3	7.4	2.8	4.9	7.3

5.5 Conclusion

A simple and efficient method involving the use of ASE was developed for extraction of PCBs from soil samples with recoveries of 81.3 - 94 % and % RSD values ≤ 2.4 %. This method eliminates the use of a lengthy and rigorous clean up step which is commonly used as a post extraction step for PCBs. Soil samples collected from Lagos, Nigeria were investigated for any possible PCB contamination using the developed method but none of the nineteen target PCB congeners were present in samples analysed. Therefore, in order to further validate the developed method, the soil samples were spiked with PCBs and extracted using the optimised ASE method. The recoveries obtained (60 - 101%) indicate that the developed method could be applied for trace analysis of PCBs in environmental samples with satisfactory results.

6: Development of extraction methods for polychlorinated biphenyls in water

6.1 Introduction

The presence of PCBs in water is a serious global environmental concern because of their aforementioned toxicity and tendency to be transported to other environmental matrices far from their point of release. Accidental spills, leakages and discharges from poorly managed hazardous waste sites with PCB containing equipment have been recognised as sources of PCBs in water bodies.[12] However, atmospheric deposition remains the primary pathway for global transport of PCBs from land to waters.[162]

Although the manufacture and use of PCBs was banned in the mid 1970s, they have been detected in water in several countries.[8] In a study conducted on the Mississippi river in New Orleans, USA, significant levels of PCBs were detected.[163] In the same vein, significant levels of PCBs have also been found in surface and river water samples from China.[164-168]

Several extraction techniques such as the classical liquid-liquid extraction (LLE), solid-phase extraction (SPE), solid-phase microextraction (SPME), dispersive liquid-liquid microextraction (DLLME) and stir-bar sorptive extraction have been used to extract PCBs from water.[99, 163-165, 169, 170] In a study conducted by Shi et al[171] on quantifying PCB levels in water, a membrane-assisted solvent extraction system with recovery values of 76.9 % - 104.6 % was used to extract PCBs from water with n-hexane : acetone as the extraction solvent. In another study conducted by Wolska et al[169] for investigating PCB levels in water, a special filtration device was designed to facilitate both the isolation of suspended particulate matter (SPM) and preconcentration of seven target PCB congeners using a solid phase extraction (SPE) cartridge. A post-extraction sonication step was applied to the SPM obtained using dichloromethane and total PCB recoveries of 48 - 70 % were obtained by combining the extracts derived from both phases.

The SPE method has been developed and applied for the determination of PCB congeners in water using n-pentane as the extraction solvent and methanol for conditioning the cartridges.[172] The entire SPE process, cleanup and preconcentration was achieved following 19 steps and recovery values of 71 % obtained for PCBs were attributed to too much sample manipulation. PCBs have been extracted from water using

SPE disks consisting of two layers (C18 and SDB-XC); this involved the use of methane, acetone and dichloromethane as elution solvents.[163] In a similar manner, a combination of SPE and super critical fluid extraction (SFE) was used for the extraction of PCBs in waste waters.[173] In this study, SPE was conducted using SPE disks placed on glass fibre filters and SFE was achieved by extracting the disks and fibres obtained from SPE in a series of steps. Average recovery values obtained were > 94 % for untreated waste waters and > 75 % for cleaned waste waters. The removal of PCBs from environmental waters has also been achieved using stir-bar sorptive extraction with recovery values of 73 - 121 %.[174] This involved the use of a polyaniline/$\propto$- cyclodextrin coated stir bar for sorption and methanol for desorption. Rezeai et al[99] developed a dispersive liquid-liquid microextraction procedure (DLLME) for extraction of PCB congeners from water samples in trace levels with recovery values greater than 92 %. This was achieved using small volumes of acetone and chlorobenzene as the dispersion and extraction solvent respectively.

Although these developed methods provided reasonable recoveries, they are lengthy and time consuming; involving several lengthy steps and subsequently larger amount of solvent consumption. In addition, very few studies have been carried out to assess PCB levels in water samples particularly in developing countries. Hence the objective of this study was to develop a simple and efficient method for extraction and preconcentration of PCBs from water. This involved an assessment of two different types of SPE - florisil and C18 (EC) cartridges for their ability to extract and preconcentrate PCBs from water. Water samples collected from the two sites described in Section 5.3.1 were subsequently screened for target PCB congeners using the developed method.

6.2 Materials and Reagents

C18 (EC) SPE cartridges were obtained from Biotage. Disposable SPE liners and florisil SPE cartridges were supplied by Sigma Aldrich.

6.3 Experimental

6.3.1 Sample collection

Water samples were collected from two sites described in Section 5.3.1 using a grab sampler and stored in amber glass bottles with Teflon caps. The collected samples were refrigerated at 4 °C prior to extraction. Information on sampling sites and sample type is given in Table 6.1.

Table 6.1: Geographical Information of water samples

Sample ID	Matrix	Geographical coordinates of sampling points	Site Description
A5	Water	$6°27'25.4''$N $3°22'57.0''$E	Drainage channel close to the repair station
A6	Water	$6°28'08.9''$N $3°22'35.2''$E	Underground water
B4	Water	$6°33'42.0''$N $3°36'55.2''$E	Water inlet
B5	Water	$6°33'50.3''$N $3°36'52.8''$E	Water outlet

*A and B represent samples taken at Ijora and Egbin power stations respectively

6.3.2 Preparation of PCB standard solutions for SPE

To test the ability of the SPE cartridges to retain PCB congeners, standard solutions (60 ng μL^{-1}) containing five PCB congeners: PCB - 1, 3, 7, 12 and 14 were used. The solution was prepared in hexane as described in Section 3.2.

The ability of the SPE cartridges to retain PCBs when present in a mixture of solvents commonly used as extraction solvents for PCBs was examined using a 30 ng μL^{-1} PCB standard solution. This was prepared by diluting 2000 μL of the 60 ng μL^{-1} PCB standard solution with 2000 μL of acetone. All stock and standard solutions were stored in dark amber bottles and sealed with PTFE caps prior to extraction and analysis to prevent loss of analyte or any form of photodegradation.

6.3.3 Preparation of aqueous solutions containing PCBs

Aqueous solutions (20 ng μL^{-1}) containing PCBs were prepared by spiking 2 cm^3 of distilled water or real water samples with 1 cm^3 of the PCB congener mixture (60 ng μL^{-1}) in a 3 cm^3 volumetric flask which was made up to mark with distilled water. This was shaken for 3 min and allowed to equilibrate for 1 h. In a similar manner, another set of aqueous PCB solutions : 6.7, 10, 13.3 and 16.7 ng μL^{-1} was prepared by spiking with 1 cm^3 of 20, 30, 40 and 50 ng μL^{-1} PCB standard solution. A control sample was prepared in a similar manner by spiking the water sample with 1cm^3 of hexane. Target analytes were subsequently extracted using florisil and C18 (EC) SPE cartridges.

6.3.4 SPE procedure for PCBs using SPE cartridges

The SPE procedure described in Section 3.4.1 was applied to assess the recovery of PCB congeners from SPE cartridges. Both florisil and C18 (EC) cartridges had a sorbent mass of 500 mg and volume of 3 cm^3. To examine PCB recoveries from florisil cartridges, 1 cm^3 of the 60 ng μL^{-1} PCB standard solution was loaded onto the cartridge. Elution of the target analytes was carried out using hexane and eluates collected from steps 2, 3 and 4. A procedural blank containing only hexane was extracted under the same conditions. The recovery of PCBs present in a mixture of solvents (hexane: acetone 1:1 v/v) was assessed using florisil cartridges by loading 1 cm^3 of PCB standard solutions (30 ng μL^{-1}) onto the cartridge. The target analytes were eluted using hexane and eluates from steps 3 and 4 were collected for GC-MS analysis. A procedural blank containing only hexane and acetone was extracted in the same manner.

To assess the recovery of PCB congeners from aqueous solutions containing PCBs, florisil or C18 (EC) SPE cartridges were used. 1 cm^3 of the aqueous solution (20 ng μL^{-1}) was loaded onto the SPE cartridge. Hexane was used as the eluent and the resulting eluate from step 3 was collected for GC-MS analysis. An aqueous solution containing distilled water spiked with only hexane was used as the procedural blank.

All extractions were conducted in triplicate to establish the repeatability of the method. 1 μL of all eluates obtained were analysed using the GC-MS under the operating conditions specified in Section 3.3. The unknown masses of each PCB congener were

obtained using LRA by fitting the peak areas obtained for each analyte into their respective calibration data.

6.3.5 Procedure for preconcentration using the Buchi Syncore Analyst System

10 cm^3 of distilled water was spiked with 1 cm^3 of the PCB congener mixture (60 ng μL^{-1}). This was shaken for 3 min and transferred into glass vessels. The glass vessels were placed in the Buchi Syncore Analyst system and operated at a speed of 180 rpm, the cooling unit (recirculation chiller) and the bottom heater were operated at temperatures of 10 ºC and 45 ºC respectively. The samples were evaporated to dryness for 2 h and reconstitution was done using 2 cm^3 hexane.

6.4 Results and Discussion

6.4.1 Extraction of PCBs from water using florisil and C18 (EC) cartridges

On this occasion, the GC-MS had been shut down for routine maintenance; therefore the instrument was calibrated to ensure that it was performing well. The results obtained (Appendix 3.1 and 3.2) were similar to previous performances with R^2 values > 0.9921. PCB recoveries from florisil cartridges were assessed as described in Section 6.3.2.

From Table 6.2, it can be seen that the PCB recovery values from the first elution (step 3) ranged from 57 - 70 %. This was thought to be reasonable recovery rates for the first attempt as more than 57 % of the PCBs introduced onto the SPE cartridges were retained by the sorbent (florisil). However, it was also noted that during the loading step (Step 2) a reasonably high concentration of PCBs passed through the SPE column without being retained by the adsorbent. As much as 28 % of the analyte passed through the column unretained and this was attributed to the competition between the mobile phase (hexane) and the stationary phase (florisil) for the PCBs in solution. The cartridge was eluted for a second time (Step 4) and lower recovery values of approximately 7%, or less, were measured suggesting that most of the PCBs retained by the cartridge were successfully eluted in the first elution (Step 3).

Table 6.2: Solid phase extraction (SPE) results for five PCB congeners using florisil SPE congeners

Std 60 ng Repeat	PCB Congeners	Peak area			Calculated mass / ng			Recovery / %		
		Step 2 (Load)	Step 3 (Elute 1)	Step 4 (Elute 2)	Step 2 (Load)	Step 3 (Elute 1)	Step 4 (Elute 2)	Step 2 (Load)	Step 3 (Elute 1)	Step 4 (Elute 2)
Replicate 1	PCB – 1	160305	768306	42502	8	40	2	13	67	3
	PCB – 3	152865	687997	18605	9	39	2	15	65	3
	PCB – 7	115603	596285	13656	9	38	3	15	63	5
	PCB – 14	271761	596672	1226	17	35	1	28	58	2
	PCB – 12	208349	625916	6543	15	42	2	25	70	3
Replicate 2	PCB – 1	142795	713645	74754	7	38	4	12	63	7
	PCB – 3	131712	673902	41320	8	38	3	13	63	5
	PCB – 7	100553	565441	31985	8	36	4	5	60	7
	PCB – 14	239156	585585	8517	15	35	1	25	58	2
	PCB – 12	178555	608972	19997	14	41	3	23	68	5
Replicate 3	PCB – 1	145981	767883	55271	7	40	3	12	67	5
	PCB – 3	134981	718111	27161	8	41	3	13	68	5
	PCB – 7	101537	599647	23406	8	38	3	13	63	5
	PCB – 14	231729	575530	4116	14	34	1	23	57	2
	PCB – 12	175757	621016	13250	13	42	3	22	70	5

Table 6.3: Variation between replicates for PCBs in steps 2, 3 and 4 using florisil cartridges

	Std 60 ng	PCB - 1	PCB - 3	PCB - 7	PCB - 14	PCB - 12
	Calculated mass / ng					
Step 2	**Replicate 1**	8	9	9	17	15
	Replicate 2	7	8	8	15	14
	Replicate 3	7	8	8	14	13
	Mean	7.3	8.3	8.3	15.3	14.0
	Std dev	0.6	0.6	0.6	1.5	1.0
	% RSD	7.9	6.9	6.9	10.0	7.1
Step 3	**Replicate 1**	40	39	38	35	42
	Replicate 2	38	38	36	35	41
	Replicate 3	40	41	38	34	42
	Mean	39.3	39.3	37.3	34.7	41.7
	Std dev	1.2	1.5	1.2	0.6	0.6
	% RSD	2.9	3.9	3.1	1.7	1.4
Step 4	**Replicate 1**	2	3	3	1	2
	Replicate 2	4	2	4	1	3
	Replicate 3	3	3	3	1	3
	Mean	3.0	2.7	3.3	1.0	2.7
	Std dev	1.0	0.6	0.6	0.0	0.6
	% RSD	33.3	21.7	17.3	0.0	21.7

An assessment of the results displayed in Table 6.3 showed that the % RSD values obtained were all < 10 % for Step 2 and < 3.9 % for Step 3. This demonstrates a good repeatability and high precision for the SPE method as the high % RSD values of 17.3 - 33.3 % in Step 4 were consistent with the low recoveries obtained.

6.4.2 Recovery of PCB congeners in a mixture of solvents from SPE florisil cartridges

PCB recoveries obtained from a mixture of solvents (hexane: acetone 1:1 v/v) commonly used as extraction solvents obtained are shown in Table 6.4 and the results of the replicate analysis for step 3 are given in Table 6.5.

Table 6.4: SPE Results from GC-MS Analysis of PCB standards

Std 30 ng Repeat	PCB Congeners	Peak area	Calculated mass / ng		Recovery / %	
		Step 3 Elute 1	Step 3 Elute 1	Step 4 Elute 2	Step 3 Elute 1	Step 4 Elute 2
Replicate 1	PCB – 1	310571	16	-	53	-
	PCB – 3	267915	16	-	53	-
	PCB – 7	246175	17	-	57	-
	PCB – 14	255251	16	-	53	-
	PCB – 12	214349	16	-	53	-
Replicate 2	PCB – 1	307707	16	-	53	-
	PCB – 3	263737	16	-	53	-
	PCB – 7	257551	17	-	57	-
	PCB – 14	260722	16	-	53	-
	PCB – 12	224596	16	-	53	-
Replicate 3	PCB – 1	317882	17	-	57	-
	PCB – 3	263957	16	-	53	-
	PCB – 7	255695	17	-	57	-
	PCB – 14	261622	16	-	53	-
	PCB – 12	229803	17	-	57	-

Table 6.5: Variation between replicates for each PCB congener in Step 3

	Calculated mass /ng of PCB Congeners					
	Std 30 ng	PCB – 1	PCB - 3	PCB - 7	PCB - 14	PCB - 12
Step 3	Replicate 1	16	16	17	16	16
	Replicate 2	16	16	17	16	16
	Replicate 3	17	16	17	16	17
	Mean	16.3	16.0	17.0	16.0	16.3
	Std deviation	0.6	0.0	0.0	0.0	0.6
	% RSD	3.5	0.0	0.0	0.0	3.5

The results displayed in Tables 6.4 and 6.5 indicate that recoveries of approximately 57% were achieved at the first elution (Step 3). This was relatively lower than recoveries obtained for PCBs prepared using a single solvent (hexane). It would therefore appear that the affinity of PCBs for the solvent mixture (hexane: acetone 1:1 v/v) was higher than their affinity for the single solvent (hexane) and thus a higher mass of analytes washed through the cartridge during the loading procedure (Step 2); consequently resulting in a reduction in the mass of PCBs retained by the sorbent of the SPE cartridge. In contrast to results previously obtained in Step 4 for PCBs prepared in hexane, no PCBs were recovered from Step 4 which indicated that all the PCBs that had been retained in the cartridge were eluted in Step 3. The % RSD values for each PCB in Step 3 were less than 3.5 % which demonstrated that the masses recovered did not vary significantly for each extraction performed. This illustrates that repeatable results and high precisions were achieved for the SPE method; although it is clear that the recovery values are lower than would be hoped.

6.4.3 Recovery of PCBs from water using florisil and C18 (EC) SPE cartridges (volume: 3ml, 500 mg sorbent)

Florisil SPE cartridges were assessed for their ability to retain PCBs from water based on PCB recoveries previously obtained from standard solutions. The results obtained are given in Table 6.6.

Table 6.6: PCB recoveries from water using Florisil SPE cartridges

% PCB Recovery / 20 ng	PCB - 1	PCB - 3	PCB - 7	PCB - 14	PCB – 12
Replicate 1	8	11	14	15	16
Replicate 2	10	13	14	15	16
Replicate 3	8	8	14	14	16
Mean	8.7	10.7	14.0	14.7	16.0
Std dev	1.2	2.5	0.0	0.6	0.0
% RSD	13.3	23.6	0.0	3.9	0.0

It can be deduced from Tables 6.6 that PCB recoveries (≤16 %) from water were significantly lower than that obtained from standard solutions. This may be attributed to the polar nature of florisil which favours the isolation of low to moderately polar species from non-aqueous solutions. Since PCBs are non-polar in nature and characterised by low water solubility, there is a tendency for recoveries to be low. Therefore, to further improve the recoveries obtained for PCBs, C18 (EC) SPE cartridges were assessed for their ability to retain PCBs and the results obtained are displayed in Table 6.7.

Table 6.7: PCB recoveries from water using C18 (EC) SPE cartridges

% PCB recovery / 20 ng	PCB - 1	PCB - 3	PCB - 7	PCB - 14	PCB - 12
Replicate 1	48	50	41	41	46
Replicate 2	47	48	40	38	50
Replicate 3	47	48	42	43	48
Mean	47.3	48.7	41.0	40.7	48.0
Std dev	0.6	1.2	1.0	2.5	2.0
% RSD	1.2	2.4	2.4	6.2	4.2

In contrast to the low PCB recoveries obtained from water using florisil cartridges, a significant improvement in recoveries (41 − 48.7 %) was obtained from water using C18 (EC) cartridges. This may be due to hydrophobic nature of the sorbent which facilitates sorption of non-polar organic analytes such as PCBs from a polar mobile phase such as water; thereby giving a stronger affinity to PCBs in solution. In addition, % RSD values obtained using C18 (EC) cartridges were significantly lower (≤ 6.2 %) than % RSD values obtained using florisil cartridges (3.9 − 23.6 %); thereby demonstrating a better repeatability and precision for the method. Since C18 (EC) SPE cartridges provides higher extraction efficiencies, recoveries across different concentrations were evaluated and results obtained displayed in Tables 6.8 and 6.9. Recovery values were consistent for PCB concentrations at 6.7 - 20 ng μL^{-1}; which means a recovery factor can be used to determine accurate concentrations of recovered PCBs within this concentration range. Although an ANOVA (analysis of variance) test showed that recovery values were statistically significantly different when comparing different concentrations, the average recovery obtained for the full congener set was 45 ± 3.8 %.

Table 6.8: PCB recoveries across different concentrations using C18 (EC) SPE cartridges

Conc / ng µL⁻¹	PCB Congeners	Recovery / %				
		PCB - 1	PCB - 3	PCB - 7	PCB - 14	PCB - 12
6.7	Replicate 1	47	47	38	39	43
	Replicate 2	45	48	36	37	41
	Replicate 3	47	45	38	40	44
	Mean	46.3	46.7	37.3	38.7	42.7
	Std dev	1.2	1.5	1.2	1.5	1.5
	% RSD	2.5	3.3	3.1	4.0	3.6
10	Replicate 1	48	56	42	44	50
	Replicate 2	46	52	44	40	46
	Replicate 3	50	54	40	44	49
	Mean	48.0	54.0	42.0	42.7	48.3
	Std dev	2.0	2.0	2.0	2.3	2.1
	% RSD	4.2	3.7	4.8	5.4	4.3
13.3	Replicate 1	45	45	36	38	45
	Replicate 2	43	42	40	39	43
	Replicate 3	42	47	38	38	42
	Mean	43.3	44.7	38.0	38.3	43.3
	Std dev	1.5	2.5	2.0	0.6	1.5
	% RSD	3.5	5.6	5.3	1.5	3.5
16.7	Replicate 1	51	55	46	46	52
	Replicate 2	49	57	45	44	53
	Replicate 3	52	53	45	47	53
	Mean	50.7	55.0	45.3	45.7	52.7
	Std dev	1.5	2.0	0.6	1.5	0.6
	% RSD	3.0	3.6	1.3	3.3	1.1

Table 6.9: PCB recoveries across different concentrations using C18 (EC) SPE cartridges

Conc / ng µL^{-1}	PCB Congeners	Recovery / %				
		PCB-1	PCB-3	PCB-7	PCB-14	PCB-12
20	Replicate 1	48	50	41	41	46
	Replicate 2	47	48	40	38	50
	Replicate 3	47	48	42	43	48
	Mean	47.3	48.7	41.0	40.7	48.0
	Std dev	0.6	1.2	1.0	2.5	2.0
	% RSD	1.2	2.4	2.4	6.2	4.2

It is important to mention that the low water solubility of PCBs can make their recovery from water difficult as both substances are completely immiscible. However, C18 (EC) SPE cartridges provide stable recovery values and higher extraction efficiencies than florisil cartridges; although it is evident that the recovery values were lower than expected.

6.4.4 Recovery of PCBs using the Buchi Syncore Analyst System

The feasibility of extracting and preconcentrating PCB congeners from water was assessed using the Buchi Syncore Analyst System as described in Section 6.3.5. However, no PCB congeners were recovered from the resulting solution analysed. Perhaps, this could be attributed to the high volatility of the PCB congeners being examined.

6.4.5 Analysis of real water samples

Since higher recoveries were obtained using C18 (EC) cartridges, real water samples collected from Lagos, Nigeria (Section 6.1) were screened for PCBs using C18 (EC) cartridges. However, none of the nineteen target PCB congeners were present in the samples. Therefore, the method was further validated using real water samples spiked

with PCBs. Analyses were conducted in triplicate and results obtained are displayed in Table 6.10.

Table 6.10: Recovery of PCBs spiked on real water samples using C18 (EC) SPE cartridges

Sample ID	PCB Congeners	PCB-1	PCB-3	PCB-7	PCB-14	PCB-12
A5	Replicate 1	35	40	32	36	41
	Replicate 2	36	42	34	34	37
	Replicate 3	38	39	34	33	39
	Mean	36.3	40.3	33.3	34.3	39.0
	Std dev	1.5	1.5	1.2	1.5	2.0
	% RSD	4.2	3.8	3.5	4.4	5.1
A6	Replicate 1	37	37	31	33	39
	Replicate 2	36	39	33	34	38
	Replicate 3	36	40	32	33	39
	Mean	36.3	38.7	32.0	33.3	38.7
	Std dev	0.6	1.5	1.0	0.6	0.6
	% RSD	1.6	4.0	3.1	1.7	1.5
B4	Replicate 1	42	45	38	38	44
	Replicate 2	40	44	36	38	45
	Replicate 3	39	43	35	39	43
	Mean	40.3	44.0	36.3	38.3	44.0
	Std dev	1.5	1.0	1.5	0.6	1.0
	% RSD	3.8	2.3	4.2	1.5	2.3
B5	Replicate 1	39	41	36	37	43
	Replicate 2	36	41	35	36	41
	Replicate 3	37	40	33	35	40
	Mean	37.3	40.7	34.7	36.0	41.3
	Std dev	1.5	0.6	1.5	1.0	1.5
	% RSD	4.1	1.4	4.4	2.8	3.7

Table 6.11: Recovery of PCB-1, 3 and 7 from real water samples at different concentrations using C18 (EC) SPE cartridges

Conc / ng µL^{-1}	Sample ID	% Recovery											
		PCB - 1				PCB - 3				PCB - 7			
		A5	A6	B4	B5	A5	A6	B4	B5	A5	A6	B4	B5
6.7	Replicate 1	34	34	40	42	33	31	46	39	27	33	37	31
	Replicate 2	33	35	43	40	34	32	44	36	25	32	37	30
	Replicate 3	36	34	41	40	32	31	47	38	28	35	38	32
	Mean	34.3	34.3	41.3	40.7	33.0	31.3	45.7	37.7	26.7	33.3	37.3	31.0
	Std dev	1.5	0.6	1.5	1.2	1.0	0.6	1.5	1.5	1.5	1.5	0.6	1.0
	% RSD	4.4	1.7	3.7	2.8	3.0	1.8	3.3	4.1	5.7	4.6	1.5	3.2
10	Replicate 1	36	39	45	45	34	33	50	44	29	33	42	35
	Replicate 2	39	38	43	45	35	36	49	44	30	34	40	34
	Replicate3	40	38	47	44	37	34	47	43	27	32	39	35
	Mean	38.3	38.3	45.0	44.7	35.3	34.3	48.7	43.7	28.7	33.0	40.3	34.7
	Std dev	2.1	0.6	2.0	0.6	1.5	1.5	1.5	0.6	1.5	1.0	1.5	0.6
	% RSD	5.4	1.5	4.4	1.3	4.3	4.4	3.1	1.3	5.3	3.0	3.8	1.7
13.3	Replicate 1	39	41	39	43	34	34	44	48	28	34	38	38
	Replicate 2	40	37	42	41	37	33	42	50	27	33	36	36
	Replicate3	38	38	41	39	35	34	43	46	29	34	35	37
	Mean	39.0	38.7	40.7	41.0	35.3	33.7	43.0	48.0	28.0	33.7	36.3	37.0
	Std dev	1.0	2.1	1.5	2.0	1.5	0.6	1.0	2.0	1.0	0.6	1.5	1.0
	% RSD	2.6	5.4	3.8	4.9	4.3	1.7	2.3	4.2	3.6	1.7	4.2	2.7

Table 6.12: Recovery of PCB-1, 3 and 7 from real water samples at different concentrations using C18 (EC) SPE cartridges

Conc / ng μL^{-1}	Sample ID	% Recovery											
		PCB - 1				PCB - 3				PCB - 7			
		A5	A6	B4	B5	A5	A6	B4	B5	A5	A6	B4	B5
16.7	Replicate 1	36	34	41	40	35	32	44	48	29	31	37	40
	Replicate 2	35	35	42	40	38	33	42	50	28	30	37	41
	Replicate3	35	37	41	43	36	32	45	48	30	32	36	40
	Mean	35.3	35.3	41.3	41.0	36.3	32.3	43.7	48.7	29.0	31.0	36.7	40.3
	Std dev	0.6	1.5	0.6	1.7	1.5	0.6	1.5	1.2	1.0	1.0	0.6	0.6
	% RSD	1.6	4.3	1.4	4.2	4.2	1.8	3.5	2.4	3.4	3.2	1.6	1.4
20	Replicate 1	36	36	41	38	36	32	44	48	32	38	36	35
	Replicate 2	38	35	40	38	34	31	46	49	30	36	39	36
	Replicate3	35	36	40	40	37	33	42	48	33	40	38	35
	Mean	36.3	35.7	40.3	38.7	35.7	32.0	44.0	48.3	31.7	38.0	37.7	35.3
	Std dev	1.5	0.6	0.6	1.2	1.5	1.0	2.0	0.6	1.5	2.0	1.5	0.6
	% RSD	4.2	1.6	1.4	3.0	4.3	3.1	4.5	1.2	4.8	5.3	4.1	1.6

Table 6.13: Recovery of PCB-14 and 12 from real water samples at different concentrations using C18 (EC) SPE cartridges

Conc / ng µL^{-1}	PCB Congeners	PCB - 14				PCB - 12			
	Sample ID	A5	A6	B4	B5	A5	A6	B4	B5
6.7	Replicate 1	28	31	39	32	28	38	44	36
	Replicate 2	27	30	39	33	31	36	45	36
	Replicate 3	30	31	40	30	30	35	44	37
	Mean	28.3	30.7	39.3	31.7	29.7	36.3	44.3	36.3
	Std dev	1.5	0.6	0.6	1.5	1.5	1.5	0.6	0.6
	% RSD	5.4	1.9	1.5	4.8	5.1	4.2	1.3	1.6
10	Replicate 1	29	34	42	39	34	38	48	38
	Replicate 2	31	33	40	37	33	39	47	37
	Replicate3	31	35	44	36	34	36	45	40
	Mean	30.3	34.0	42.0	37.3	33.7	37.7	46.7	38.3
	Std dev	1.2	1.0	2.0	1.5	0.6	1.5	1.5	1.5
	% RSD	3.8	2.9	4.8	4.1	1.7	4.1	3.3	4.0
13.3	Replicate 1	30	34	41	38	35	39	40	45
	Replicate 2	29	33	39	40	34	36	42	45
	Replicate3	30	36	38	42	33	38	44	44
	Mean	29.7	34.3	39.3	40.0	34.0	37.7	42.0	44.7
	Std dev	0.6	1.5	1.5	2.0	1.0	1.5	2.0	0.6
	% RSD	1.9	4.4	3.9	5.0	2.9	4.1	4.8	1.3
16.7	Replicate 1	30	34	39	42	34	34	44	50
	Replicate 2	30	34	39	42	34	34	44	50
	Replicate3	31	31	36	41	35	35	41	48
	Mean	30.3	33.0	38.0	41.7	34.3	34.3	43.0	49.3
	Std dev	0.6	1.7	1.7	0.6	0.6	0.6	1.7	1.2
	% RSD	1.9	5.2	4.6	1.4	1.7	1.7	4.0	2.3

Table 6.14: Recovery of PCB-14 and 12 from real water samples at different concentrations using C18 (EC) SPE cartridges

Conc / ng µL^{-1}	PCB Congeners	PCB - 14				PCB - 12			
	Sample ID	A5	A6	B4	B5	A5	A6	B4	B5
20	Replicate 1	32	35	37	34	38	37	44	42
	Replicate 2	33	34	41	36	38	38	43	41
	Replicate3	33	36	39	39	39	40	44	40
	Mean	32.7	35.0	39.0	36.3	38.3	38.3	43.7	41.0
	Std dev	0.6	1.0	2.0	2.5	0.6	1.5	0.6	1.0
	% RSD	1.8	2.9	5.1	6.9	1.5	4.0	1.3	2.4

As shown in Table 6.10, C18 (EC) SPE cartridges provided good and stable quantitative recoveries (32 - 44 %) for PCBs in real water samples similar to previous results; thereby demonstrating that the method could be used to analyse environmental water samples containing PCBs. PCB recoveries across different concentrations were also evaluated and results obtained are shown in Tables 6.11 - 6.14. An ANOVA test applied to evaluate recoveries obtained at different concentrations showed that recoveries were statistically significantly different when comparing different concentrations. However, average recoveries obtained for the entire congener set was 33, 35, 41 and 40 ± 3.3, 1.8, 3.6 and 3.3 % for samples A5, A6, B4 and B5 respectively.

6.5 Conclusion

The overall objective of this work was to develop a simple and efficient method for the extraction and preconcentration of PCBs from water. A comparison of florisil and C18 (EC) SPE cartridges showed that higher recoveries (41 – 48.7 %) of PCBs were obtained using C18 (EC) cartridges with RSD values ≤ 6.2 %. In addition, PCB recoveries obtained from water across different concentrations (6.7 - 20 ng) were consistent indicating that a recovery factor could be applied to determine the concentration of PCBs in unknown samples. Although none of the nineteen target PCB congeners were found in the real water samples screened, further validation of the developed method using the real water samples spiked with PCBs showed that

C18 (EC) cartridges could be applied for determination of PCBs in environmental samples.

Part B: Environmental remediation of polychlorinated biphenyls in water

7. Use of silica platforms as adsorption surface for polychlorinated biphenyls in water

7.1 Introduction

7.1.1 Mesoporous materials

Ordered mesoporous silicates can be referred to as materials which have both the amorphous properties of gels and ordered porosity of crystalline materials such as zeolites.[175] They consist of extended inorganic or inorganic-organic hybrid networks with long channels, robust structure, controlled pore size and geometry, textural and surface properties that can be modified.[176-178] By virtue of these properties, they have been widely used as adsorbent platforms for adsorption of toxic organic pollutants in liquids.[179-182]

The manufacture of mesosilica materials involves the use of both silica sol-gel chemistry and molecular surfactant assemblies as framework templates. Sol-gel materials are metastable solids formed from molecular precursors which have the building blocks of the desired products under kinetically controlled reactions. A sol is a stable suspension of colloidal particles in a liquid which can be amorphous or crystalline with dense, porous or polymeric substructures.[183] Gels consist of a porous three-dimensional extended solid network surrounding a liquid phase. The method used for synthesis of sol-gel oxides is similar to that used for preparing mesoporous molecular sieves. Although both materials have amorphous frameworks, the surfactant template used in preparing mesoporous molecular sieves provides the materials with an ordered porosity, uniform pore sizes and large surface areas compared to porous sol-gel oxides which are completely disordered.

7.1.2 The silica gel process

The silica sol-gel process (see Figure 7.1) involves a series of hydrolysis and condensation steps which require a silica source (precursor), catalyst, template and solvent.[128, 184] In the first step, silanol groups are formed from hydrolysis of the silica precursor (alkoxysilane) under acidic (HCl) or basic (NaOH, NH_3) conditions.[183] The rate of hydrolysis obtained at this stage depends on the type of silica precursor used as hydrolysis rate generally decreases as the hydrophobicity of the precursor increases. In addition, partial or complete hydrolysis may occur where all the alkoxy (OR) groups are replaced depending on the water/alkoxide ratios, quantity and nature of catalysts and synthetic conditions. Hydrolysis is followed by condensation of the

silanol group with an alkoxide or self-condensation with a silanol group. In the sol-gel process, the hydrolysis and condensation reactions occur simultaneously once the hydrolysis reaction is initiated and soluble higher weight polysilicates are formed. The resulting colloidal suspension formed is the "sol" while the "gel' is formed when the polysilicates connect together to form a three dimensional network filled with solvent molecules.[128]
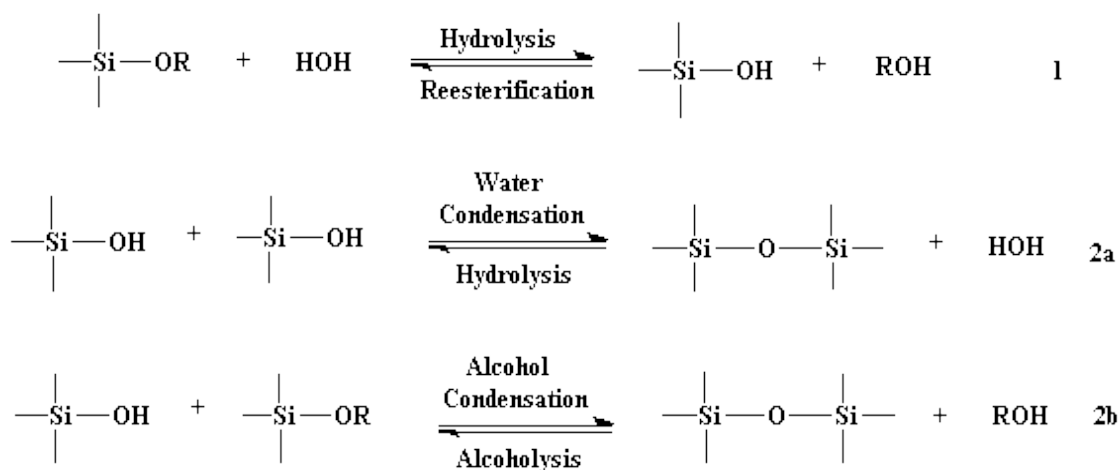

Figure 7.1: The sol-gel process, (1) hydrolysis of silicon alkoxide, (2a) self condensation of silanol groups, (2b) condensation of silanol group with silicon alkoxide.[184]

7.1.3 The role of surfactants

Surfactant molecules are generally amphiphilic in nature as they possess a hydrophobic tail at one end and hydrophilic head at the other end.[185] Depending on the nature of the hydrophilic headgroup, they can be categorised as cationic (quaternary ammonium), anionic (sulfate), zwitterionic (phospholipids) or neutral (amines) for small molecule surfactants.[114, 176, 185-187] In addition, polymeric surfactants with a polar head group can be used to obtain larger self-assembled structures of mesoporous materials. The hydrophobic tail of polymeric substances usually have less soluble polymers while the hydrophobic region for small molecule surfactants is typically a single alkyl chain. One of the commonly used cationic surfactant for synthesis of MCM-41 is cetyltrimethylammonium bromide – CTAB

(Figure 7.2). Other types of surfactants used to template silica include sodium dodecylsulfate (anionic) or pluronic series (triblock copolymeric surfactant); their chemical structures are displayed in Figures 7.3 and 7.4 respectively.
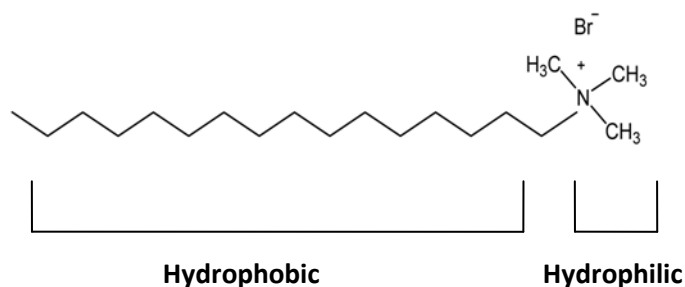
Figure 7.2: Chemical structure of a cationic surfactant – CTAB.[185]
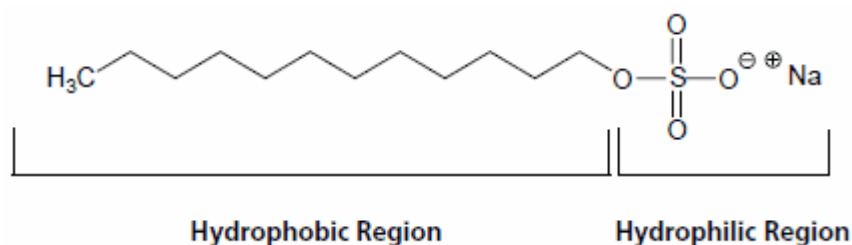
Figure 7.3: Chemical structure of an anionic surfactant - sodium dodecylsulfate.[185]
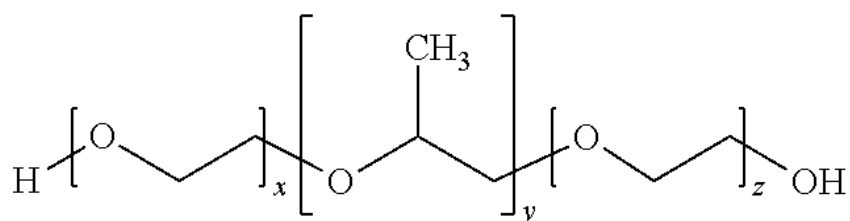
Figure 7.4: Chemical structure for triblock copolymer P123.[188]

The amphiphilic nature of surfactant molecules makes their arrangement at interfaces in solutions possible such that the hydrophobic part is removed from water and aggregates are formed in the bulk solution above a certain concentration known as the "critical micelle concentration" (CMC). The aggregates formed have stable

structures capable of partitioning between the micelle and solution such that a uniform size and shape are achieved under certain solution conditions (pH, temperature, ionic strength and concentration).

7.1.4 The silica source

Various types of silica precursors such as silicon alkoxides; tetramethoxysilane (TMOS) or tetraethoxysilane (TEOS) can be employed in preparing mesoporous silica materials. Alternatively, sodium silicate is a cheaper precursor that can be used alone or in combination with alkoxides. Amongst these precursors, TEOS is the most commonly used as its low reactivity during hydrolysis makes it possible to control the reaction. The hydrolysis and condensation of TEOS under acidic and basic conditions is illustrated in Figure 7.5.

Condensation reactions occurring during silica formation can be influenced by acidic, alkaline or neutral conditions. Under neutral conditions, the surfactant itself functions as a catalyst, since the formation of the template materials occurs more rapidly than precipitation.[189] Under acidic conditions ≤ pH 2 (the isoelectric point of silica), silica condensation reactions are slow requiring several hours depending on the surfactant used.[190] However, the formation of mesoporous silicates with different structures is accelerated at very low pH as the solution is precipitated within minutes.[185, 191] In alkaline conditions (pH 9.5 - 12.5), the precipitation of mesoporous silica occurs rapidly immediately the silica source is added to the surfactant solution.[192] In contrast to acidic conditions, the polymerisation and cross linkage mechanisms are reversible such that the structure of the resulting material can be altered by changing the conditions employed in synthesis. Hence, a wide variety of silica precursors such as silica gel, sodium silicate, colloidal sols, silica aerogels or TEOS which are readily soluble in alkaline solutions can be used. Bases such as ammonia, potassium hydroxide, tetramethyl ammonium hydroxide and sodium hydroxide can also be employed.
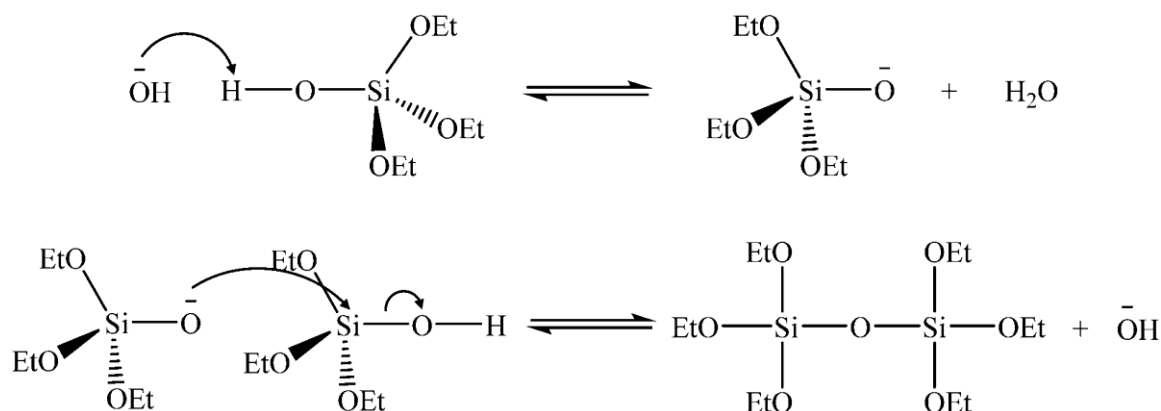
Acidic:
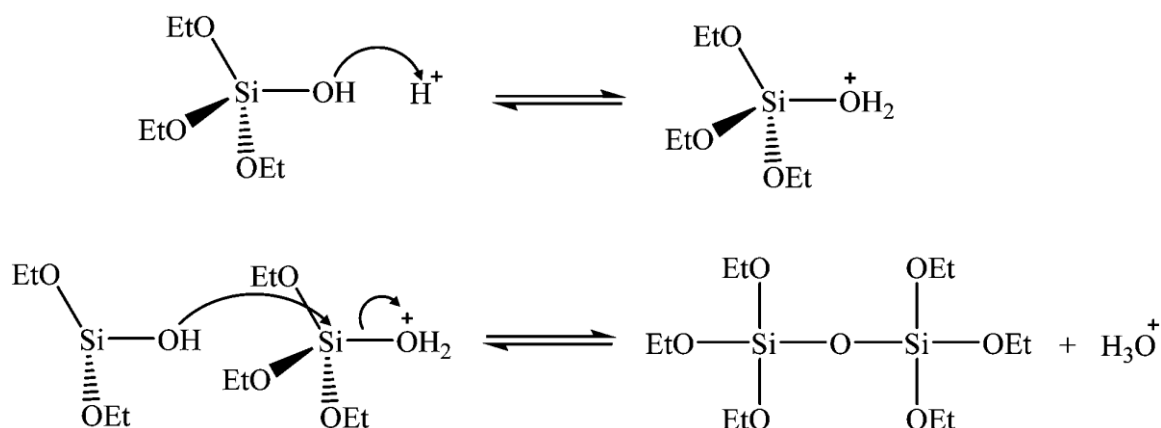
Basic:

Figure 7.5: Hydrolysis and condensation reactions of tetraethylorthosilicate (TEOS) under acidic and alkaline conditions.[193]

7.1.5 Template removal

Once the mesoporous material has been synthesised, the removal of the surfactant template from the initial inorganic-surfactant mesostructured material is necessary in order to open up the pores. This can be done using several methods: calcination, solvent extraction and microwave digestion.[185] One of the most commonly used methods for template removal is calcination due to ease of operation and complete template removal. In the calcination process, the organic template is combusted at high temperatures in an ashing furnace either in the presence of air or nitrogen.[194]

Calcination can also be carried out using a sequential flow of nitrogen and oxygen. Calcination temperatures used for template removal generally range from 500 - 600 ºC for several hours with a temperature ramping rate of 1 - 2 ºC min^{-1}. Although Bagshaw and colleagues reported that the porosity of some materials could be improved by heating them at much rapid rates[195], the pore spacings could contract at high temperatures as a result of further condensation of the silicate species in the walls.[196] Several studies have shown that template removal for ionic and polymeric surfactants is achieved in several steps particularly at temperatures below 200 ºC.[197]

Solvent extraction is another method that is commonly used for template removal. This is achieved by placing the materials in acidic ethanol and extracting for a few hours using the reflux or soxhlet extraction method.[198, 199 200] However, a major drawback of this method is that the pore structures of the solvent extracted materials obtained may not be different from that of the as-synthesised materials.[201] In addition, the particle sizes of the solvent extracted materials can also be reduced or residual solvents left in the final product.[202] Surfactant removal can also be conducted under milder conditions using supercritical fluids (CO_2) although the addition of a modifier is required to improve the extraction efficiency for ionic surfactant templates.[203 204]

Microwave digestion is another effective method for removing templates from mesoporous materials.[205] In this process, the powdered materials are suspended in aqueous solutions containing a mixture of nitric acid (HNO_3) and hydrogen peroxide (H_2O_2), followed by digestion in a microwave system at 1200 W for 2 min. In contrast to conventional template removal methods, the resulting products are characterised by highly ordered inorganic frameworks, larger pore volumes and reduced structural shrinkage, higher surface areas and increased number of silanol groups.[185]

Although zeolites are well known members of the microporous class with excellent catalytic properties resulting from their crystalline aluminosilicate network, their use in several applications (adsorbents, catalyst and catalyst supports) is limited by their relatively small pore openings.[179, 206, 207] As a consequence, mesoporous materials are of great interest due to their large and ordered pore sizes, which allows sterically hindered molecules to diffuse easily to internal active sites.[208]

Although mesoporous materials are typically amorphous or paracrystalline solids with pores that are irregularly spaced and broadly distributed in size, the M41S series represents a new family of silicate/aluminosilicate mesoporous molecular sieves characterised by high surface areas, tunable pore diameters, uniform pores and a narrow pore size distribution (nm) similar to zeolites.[79, 209-211] M41S materials are formed via a liquid crystal templating mechanism (Figure 7.6) involving aggregation of organic template molecules; cationic alkyltrimethylammonium surfactants with amorphous pore walls that differentiate them from microporous zeolites.[79] These materials were discovered by the Mobil Research & Development Corporation in 1992 and consist of three members: MCM-41, MCM-48 and MCM-50 (MCM stands for Mobil Composition of Matter) which are classified based on the difference in the order of their pores in three dimensional spaces.[177] A variation in the condition of synthesis, surfactant/silica ratio would result in the production of any of these materials.[181, 210] MCM-41 and MCM-48 are reportedly the most popular members of the M41S series.
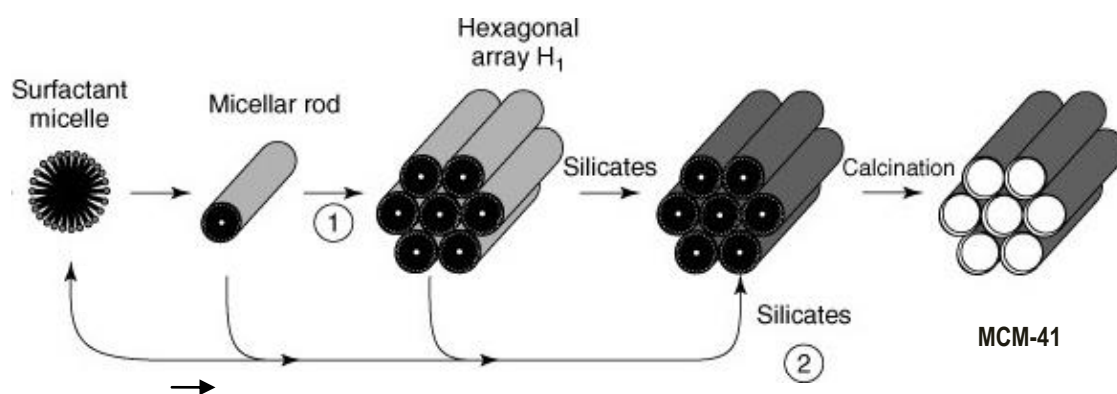
Figure 7.6: Liquid-crystal templating mechanism showing two possible pathways for the formation of MCM-41 (1) Liquid crystal initiated 2) silicate initiated.[177]

MCM-41 materials generally exhibit a honeycomb structure resulting from a one-dimensional, hexagonal arrangement of uniform cylindrical mesopores.[177, 206] They have uniform channels with pores that are long, parallel and isolated from each other. Their pore diameters can be varied by changing the alkyl chain lengths of the cationic surfactants employed during synthesis.[176] In comparison to other members

of the M41S series, MCM-41 has attracted more research attention due to its thermodynamic stability, high hydrocarbon sorption capacity and ease of synthesis. Hence, they have been widely used in catalysis,[212-215] adsorption media [216-218] and chemical separations.[219]

MCM-48 materials have a three dimensional cubic ordered pore structure with two non intersecting networks of mesoporous channels intricately attached together.[220] In contrast to their hexagonal counterparts (MCM-41) where the surfactant/silica ratio is <1, MCM-48 is usually the resulting structure when larger surfactant/silica ratios are employed.[210, 211] MCM-48 materials have also been used in catalytic and separation applications although they have been far less studied than MCM-41 due to the difficulty encountered in synthesis procedures. [211, 221] In order to obtain reliable synthesis of cubic materials, Huo et al.[222] have carried out systematic investigations using different surfactants.

MCM-50 materials have an unstable lamellar structure. These materials are characterised by poor thermal stability such that their structure collapses into a dense phase with little order of porosity upon template removal by thermal treatment.[223] Hence, they have been given little attention due to this limitation. The structures of M41S materials are given in Figure 7.7.
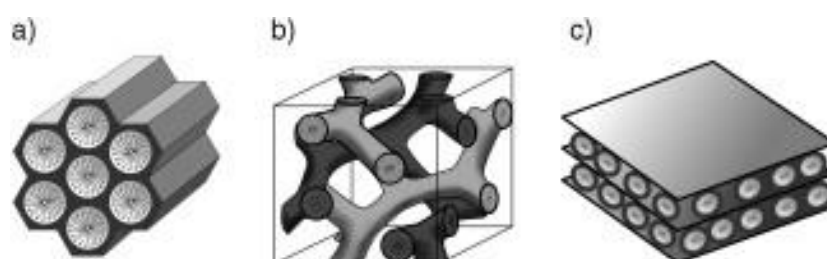
Figure 7.7: Structures of M41S materials (a) MCM-41 (b) MCM-48 (c) MCM-50.[175]

7.1.6 Biosilicification

The process of biosilicification also known as "biological silica formation" is defined as "the movement of silicic acid from environments in which its concentration does not exceed its solubility (2 mmol L^{-1}) to intracellular or systemic compartments where it is accumulated for subsequent deposition as amorphous hydrated silica".[224]

Biological organisms such as diatoms, grasses and sponges are responsible for the formation of the aforementioned biogenic silica structures.[225, 226] Nevertheless, diatoms (unicellular microalgae) are known to be predominant contributors to biosilica formation in several length scales ranging from nanoscale to microscale.[227]

In contrast to the synthetic preparation of precipitated silica via sol-gel routes where poor control over the structure and processing of the product is obtained, a high control of morphology is achieved in this process as the biological organisms which take up and store soluble silicon (silicic acid) are capable of processing it with great sophistication into ornate hierarchical patterned biosilica structures.[225, 228] Another outstanding feature associated with biological silica formation is that it takes place under mild pH (mildly acidic to near neutral) and ambient temperatures (< 40 ℃) compared to silica formation using synthetic approaches where low hydrolysis rates and longer gelation periods are derived at neutral pH and low temperature (< 100 ℃) conditions.[82, 183, 229] In addition, the use of unsaturated silicic acid; a soluble and non-toxic form of silica in an all-aqueous environment for biosilica formation provides a significant advantage over sol-gel syntheses where alkoxysilanes which are toxic in nature and relatively insoluble in water are employed.[226, 230] By virtue of this, biosilification is generally referred to as an environmentally friendly ("green") process.[227]

7.1.7 Bioinspired silica synthesis

In order to develop novel materials and/or technologies for various applications, detailed investigations were carried out to mimic the knowledge derived from *in vivo* formation of biological silica ("biosilica") materials for *in vitro* synthesis of biologically inspired silica materials known as "bioinspired silica".[227]

Organic biomolecules such as proteins and propylamines from diatoms responsible for *in vivo* silica formation have demonstrated the ability to control *in vitro* formation of silica in aqueous systems under mild physicochemical conditions.[231, 232] Similarly, *in vitro* silica formation was also successfully achieved using bioextracts such as silicatein proteins isolated from sponges.[233, 234] However, analogues have also been employed due to the complex nature of bioextracts. The abundance of cationically charged moieties or ability of additives to undergo self-assembly before and during

silica polymerisation were identified as rules governing silica formation.[227] Investigations on the influence of customised additives such as polymers, small amines (ethyl or propyl amines) and proteins during silica polymerisation for biosilica and bioinspired silica formation have been conducted. These additives reportedly have the ability to control the condensation rates, morphology and porosity of the silica formed under mild conditions compared to that obtained via the sol-gel route.[183, 231, 235] For instance, the use of polyamines with long chains (six or seven amines) such as pentaethylenehexamine (PEHA) at low concentrations (30 mM) results in rapid precipitation of silica particles within 30 s.[236] Silica particles ranging from nanoscale to microscale have also been synthesised using cyclic amines and bioextracts from diatoms. As a consequence, bioinspired silica materials have found vast applications in sensors, catalysis, coatings and adsorption.

7.1.8 Advanced Oxidation Processes (AOPs)

Advanced oxidative processes (AOPs) are basically environmentally friendly methods that involve the use of hydroxyl radicals generated in situ for degradation of toxic pollutants into harmless products.[237] These processes generally include cavitation,[238] photocatalytic oxidation [239] and the Fenton method. [240] [241] Amongst these processes, the Fenton method is regarded as the most popular and economically attractive AOP for water/waste water treatment due to the non-toxic nature and abundance of iron, ease of handling hydrogen peroxide and mild operating conditions which result in environmentally safe products with no related disposal problems.[242] This process involves the formation of hydroxyl radicals ($OH^\bullet$) in the presence of Fenton's reagent: a mixture of hydrogen peroxide (H_2O_2) and ferrous iron (Fe^{2+}).[240, 242]

$$Fe^{2+} + H_2O_2 \rightarrow Fe^{3+} + OH^- + OH^\bullet \qquad \text{Eq. 7.1}$$

$$Fe^{3+} + H_2O_2 \rightarrow Fe^{2+} + HOO^\bullet + H^+ \qquad \text{Eq. 7.2}$$

In the initial stage, Fe^{2+} is oxidised to Fe^{3+} by H_2O_2, the $OH^\bullet$ radical and OH ion are formed (Equation 7.1). This is followed by reduction of the Fe^{3+} formed to Fe^{2+} by another molecule of H_2O_2 and subsequent formation of a hydroxyperoxy radical and proton (Equation 7.2).[243] However, the oxidation efficiency of the Fenton reagent is strongly accelerated by irradiation with UV-VIS light at wavelengths greater than

300 nm as photolysis of Fe^{3+} complexes allows the regeneration of Fe^{2+} and subsequently $OH^\bullet$ generation (Equation 7.3) in a process referred to as the "Photoassisted Fenton process".

$$Fe(OH)^{2+} \xrightarrow{h\nu} Fe^{2+} + HO^\bullet \qquad\qquad Eq.\,7.3$$

Although homogeneous Fenton systems have been widely used for water/wastewater treatment, they are difficult to recycle and often associated with additional operational costs for separation and recovery of iron ions from solution or treated sludge. In addition, the reaction is limited by narrow range of pH (2.5 - 3.5). Therefore, in order to overcome these limitations, heterogeneous Fenton and photo-Fenton catalysts where an extended working pH range (near pH 7) is possible was developed.

7.1.9 Applications

The removal of organic pollutants such as PCBs from water has attracted increasing global attention due to their aforementioned adverse health and environmental effects. The presence of PCBs in water at trace concentrations can prevent the use/reuse of water. Hence, there is a critical need to provide methods for sequestering these pollutants from water. Numerous methods such as hydrolysis, liquid-liquid extraction, coagulation, filtration, reverse osmosis, biological removal, and adsorption have been used to remove organic pollutants from water.[244][180, 245, 246] However, the ease of operation and maintenance, low energy consumption and scaling up associated with the use of adsorption makes it a desirable method for the removal of toxic organic pollutants from water.[247]

As mentioned previously, mesoporous materials have shown to be promising adsorbents for the removal of several organic pollutants from contaminated water systems due to its useful properties which include high surface area, large pore size, highly tunable surface and textural properties and ease of regeneration. Whilst MCM-41 has been widely applied for sequestering organic pollutants from water, the potential application for PCB removal from water has not been reported in literature. Therefore, an objective of this study was to prepare MCM-41 materials and assess their feasibility for sequestering PCBs from aqueous solutions. However, in contrast

to synthesis of MCM-41 materials which is usually lengthy and associated with use of reagents that are not environmentally friendly, the synthesis of bioinspired silica is achieved via a simple, faster, milder, greener and more economical route. Hence, there has been a growing interest to assess their potential application for decontaminating water systems containing organic pollutants. Several studies have employed iron catalysts supports on zeolites and silica materials such as MCM-41 in heterogeneous Fenton systems.[248, 249] Therefore, another objective of this research was to prepare iron incorporated bioinspired silica materials (Fe-GN) and assess the potential of this material to decontaminate water containing PCBs via the photo-Fenton process.

7.2 Experimental

7.2.1 Materials and Reagents

Tetraethoxysilane (TEOS), iron nitrate, aqueous ammonia (30 %, NH_3), absolute ethanol, pentaethylenehexaamine ($C_{10}H_{28}N_6$) and hydrogen peroxide were supplied by Sigma Aldrich. Cetyltrimethylammonium bromide (98 %, CTAB) was obtained from BDH chemicals. Sodium metasilicate ($Na_2SiO_3.5H_2O$) and 1M hydrochloric acid (HCl) was obtained from Fisher Scientific.

7.2.2 Synthesis of MCM-41

MCM-41 was synthesised using the method reported by Idris et al.[250] 8.8 g of CTAB was dissolved in a mixture containing 208 cm^3 of distilled water and 96 cm^3 of aqueous ammonia under slight heating at 35 °C. 40 cm^3 of TEOS was added dropwise to the clear solution under stirring. The solution was continuously stirred for 3 h. After stirring, the gel was aged for 24 h in a closed container. The product obtained was filtered, washed with distilled water and dried in air at room temperature. The material obtained is referred to as As-syn MCM-41. Organic template removal was carried out using a conventional calcination rig by heating the resulting material in air at 550 °C for 8 h. The material obtained is referred to as Calc MCM-41.

7.2.3 Synthesis of iron incorporated on bioinspired silica (Fe-GN) materials

6.62 g of sodium metasilicate was dissolved in 500 cm^3 of distilled water. 1.160 g of PEHA was dissolved in 400 cm^3 of distilled water. The PEHA solution was added to the sodium metasilicate solution and stirred at 250 rpm until a stable pH was obtained. 5.54 g of iron nitrate was added to the solution mixture which was continuously stirred at 300 rpm and the reaction solution neutralised with 1M HCl within 5 min. Prior to this, the amount of acid needed for neutralisation within the 5 min reaction time was determined and observed to be 28 cm^3. Hence, the final volume of the reaction solution was made up to the 1000 cm^3 mark using 72 cm^3 of distilled water. The change in pH solution was monitored using a pH meter, after 5 min, a stable pH reading of 7.0 ± 0.1 was obtained. The reaction solution was filtered immediately and the precipitate obtained washed with distilled water and subsequently dried overnight in an oven at 85 °C. The resulting "as-synthesised iron green nanomaterial" was denoted as "as-syn Fe-GN" and the organic template present was removed by heating in air using a calcination rig at 550 °C for 8 h to give a "calcined iron green nanomaterial" denoted as "calc Fe-GN".

7.2.4 FTIR analysis

An MB 3000 ABB Miracle ATR-FTIR was used to obtain the infrared spectra of sample materials. A small amount of the sample was placed on the surface of the crystal and the pressure handle was screwed onto the sample to allow contact between the sample and surface of the crystal. Infrared transmission and absorbance spectra were obtained from the sample materials over a wavelength range of 500 - 4000 cm^{-1}, 32 scans and a resolution of 4 cm.

7.2.5 Batch adsorption experiments

To assess the feasibility of as-syn MCM-41 or calc MCM-41 to remove PCBs from water, a 5 cm^3 solution containing 60 μg of the PCB congener mixture was used. The aqueous PCB solution was placed in amber glass vials and 10 mg of each sorbent added to each vial. A procedural blank was prepared in the same manner without any sorbent. Each solution was stirred for 2 h at 250 rpm and the resulting solution

centrifuged at 4000 rpm for 5 min using an Eppendorf centrifuge 5804 R. The supernatant obtained was preconcentrated using the SPE process described in Section 3.4.1 and 1 µL of the eluate obtained was subjected to GC-MS analysis using the operating conditions specified in Section 3.3.1.

The removal efficiency was calculated as follows: $(C_o - C_1)/C_o \times 100$ Eq. 7.4

where C_o and C_1 represent the initial and final concentrations of PCB congeners in the aqueous solutions respectively.

7.2.6 Photo-Fenton reactions

The performance of as-syn and calc Fe-GN materials as heterogeneous catalysts for degradation of PCBs from water was examined using a photoreactor set up. 5 cm^3 of the aqueous PCB congener mixture was placed in a 15 cm^3 cylindrical quartz vessel and 10 mg of each catalyst suspended in the solution. A procedural blank was prepared in a similar manner without the addition of any catalyst. Two UV/VIS light sources : 8 and 4 W blacklight blue lamps from UVITEC and UVP ltd, Cambridge UK respectively which emit photons with wavelengths of 300 - 425 nm were used in place of the commonly used UV lamps (254 nm) for irradiation. The quartz vessel was placed in between the two lamps separated by a distance of 40 mm and the reaction was initiated by the addition of 200 mM H_2O_2. This was allowed to proceed for 2 h at a speed of 300 rpm. The resulting solution was centrifuged at 4000 rpm for 5 min using an Eppendorf centrifuge 5804 R and the supernatant preconcentrated using C18 (EC) cartridges following the procedure described in Section 3.4.1. 1 µL of the eluate obtained was analysed using the GC-MS under the operating conditions described in Section 3.3.1.

The percentage of degradation was calculated as follows: $(Co - C_1)/C_o \times 100$

Where C_o and C_1 are the initial and final concentrations of PCBs in the aqueous solution respectively.

7.3 Results and Discussion

7.3.1 FTIR analysis

The FTIR spectra obtained for As-syn MCM-41 and Calc MCM-41 are given in Figure 7.8.
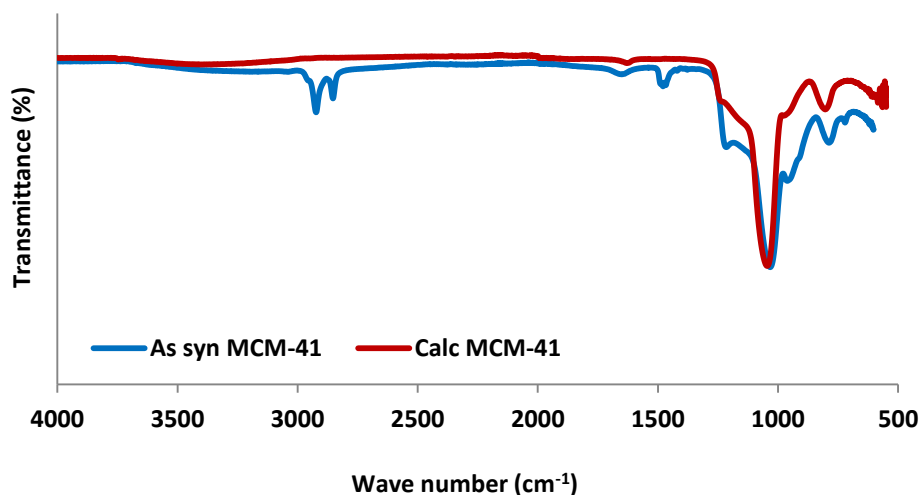
Figure 7.8: FTIR spectra of MCM-41 materials

Both samples had similar spectra peculiar to silica containing materials. In both materials, the absorption band due to Si–O–Si (siloxane) stretching is observed at 1030 - 1200 cm^{-1}, the water bending band is observed at 1650 cm^{-1} and the broad band at 3200 - 3500 cm^{-1} can be ascribed to –OH stretching of the silanol group and some absorbed water. In addition, absorption bands corresponding to C–H and C–N stretching were observed at 2850 - 2930 cm^{-1} and 1490 cm^{-1} respectively in the spectrum of as-syn MCM-41; indicating the presence of the surfactant template. Hence, the absence of these bands in calc MCM-41 confirms the successful removal of the surfactant template.

From Figure 7.9, it can be deduced that similar data was obtained for the Fe-GN materials. The siloxane (Si-O-Si) peaks observed at 1100 and 800 cm^{-1} correspond to silica formation while amine peaks observed at 1500 - 1700 cm^{-1} can be attributed to the presence of PEHA in the both materials (as-syn and calc Fe-GN). For as-syn Fe-GN, the broad band at 3200 - 3500 cm^{-1} is due to the –OH stretching of the silanol group and some absorbed water. However, a sharp decrease of this broad band in

147

calc Fe-GN can be ascribed to a significant loss of the adsorbed water during calcination.
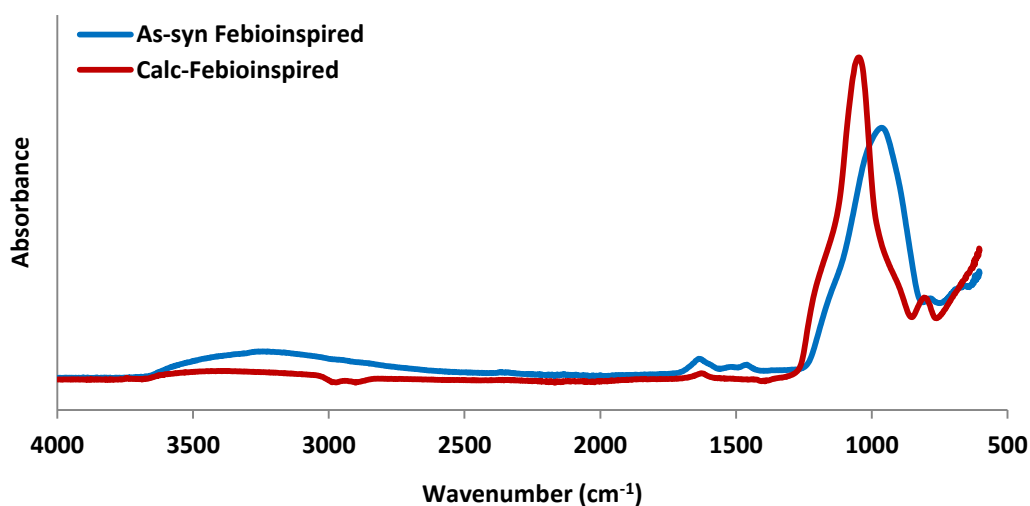
Figure 7.9: FTIR spectra of Fe-GN materials

7.3.2 Material characterisation using N_2 sorption isotherms

The characteristic data (surface area, average pore size and pore volume) of MCM-41 and Fe-GN materials were obtained from nitrogen sorption isotherms as described in Section 3.5.1. The results obtained are summarised in Table 7.1.

Table 7.1: Characterisation data for MCM-41 and Fe-GN materials

Sample Name	BET Surface Area $(m^2\ g^{-1})^a$	A.P.S $(nm)^b$	T.P.V $(cm^3\ g^{-1})^c$
As-syn MCM-41	11 ± 0.11	11.5	0.03
Calc MCM-41	930 ± 1	3.0	0.90
As-syn Fe-GN	233 ± 2	11.4	0.67
Calc Fe-GN	201 ± 1.2	11.9	0.55

A.P.S: Average Pore Size (pore diameter), T.P.V: Total pore volume

[a] Calculated by the BET model from sorption data in a relative pressure range from 0.05-0.29.
[b] Calculated by the BJH model from the desorption branches of isotherms.
[c] Calculated from N_2 amount adsorbed at relative pressure P/Po of 0.99.

The low surface area (11 m^2 g^{-1}) exhibited by as syn MCM-41 is due to a lack of porosity prior to template removal. However, the surface area (930 m^2 g^{-1}) increased significantly and a reduction in pore size (3.0 nm) was observed for calc MCM-41 after template removal. Perhaps, the decrease in pore size could be an indication that smaller and well defined pores were obtained after template removal. The surface areas for as-syn and calc Fe-GN were 233 and 201 m^2 g^{-1} respectively. The relatively large surface area and pore volume of as syn Fe-GN compared to calc Fe-GN may be attributed to the use of mild conditions for material synthesis and the presence of iron resulting in a change in assembly of the material during synthesis. In addition, it is evident that the incorporation of iron into the silica material resulted in a porous material (as-syn Fe-GN) prior to removal of the surfactant template. However, the influence of Fe^{3+} ions on the structure of the material requires further investigation.

The nitrogen adsorption-desorption isotherms for MCM-41 and Fe-GN materials are given in Figures 7.10 and 7.11 respectively. A type II isotherm was exhibited by as-syn MCM-41 with H4 hysteresis which is characteristic of non porous adsorbents; indicating that the surfactant template was still present. A type IVb isotherm with H1 hysteresis was exhibited by calc MCM-41 which is characteristic of mesoporous materials with smaller widths and corresponds to the presence of well defined cylindrical pores. A type IVa isotherm with H4 hysteresis was exhibited by both as-syn and calc Fe-GN materials which is characteristic for mesoporous materials with pore widths greater than a certain critical width (~ 4 nm) such that capillary condensation occurs simultaneously with hysteresis. In addition, both Fe-GN materials exhibited a type II isotherm which is associated with small contributions of microporosity at lower relative pressures as a sharp rise wasn't seen at lower relative pressures.
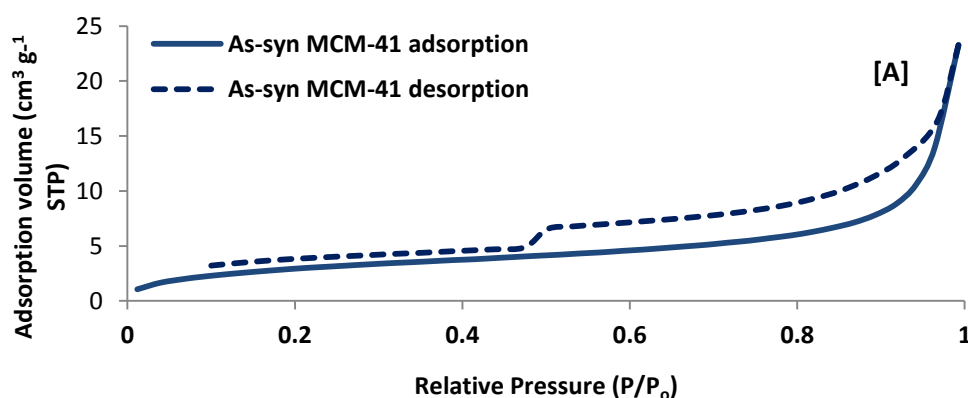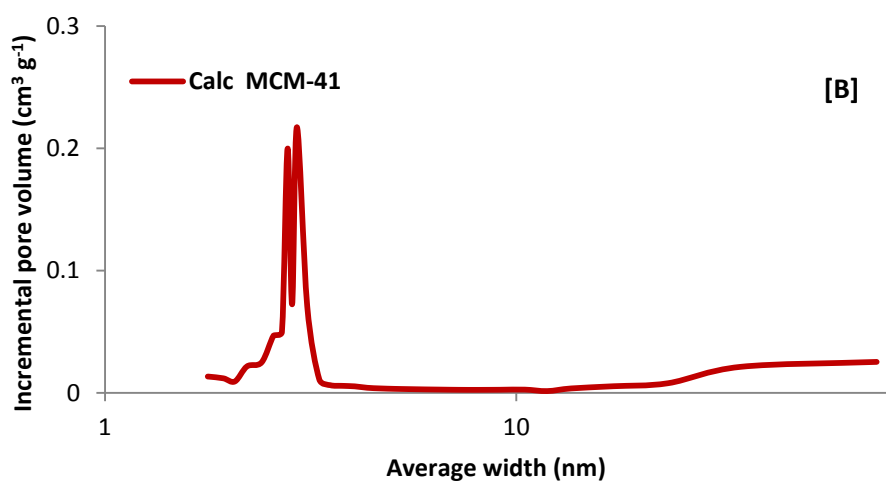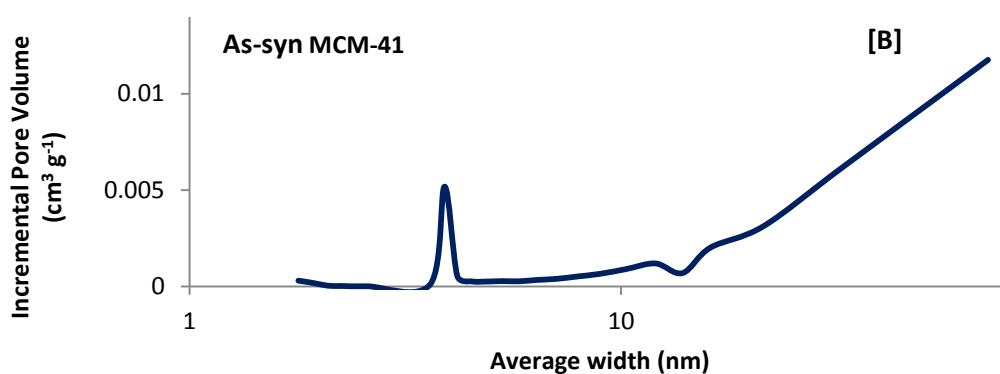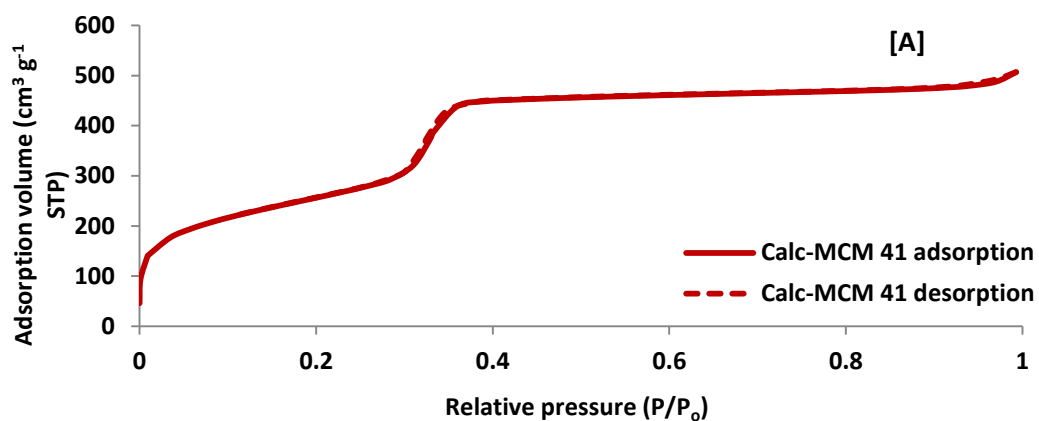
Figure 7.10: **[A] Nitrogen sorption isotherms and [B] average pore size distribution for as-syn and calc MCM-41 respectively.**
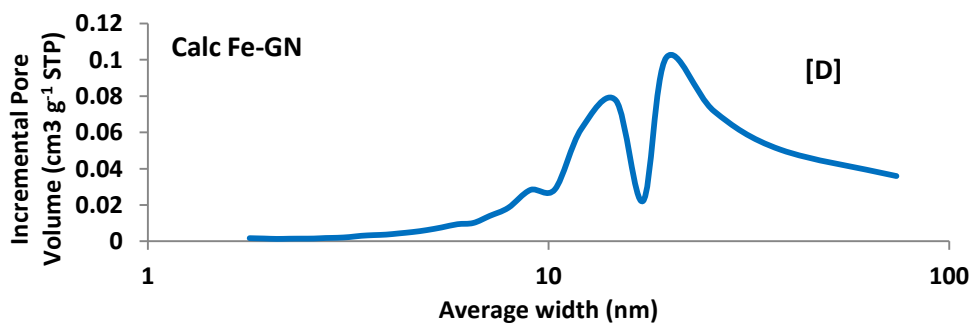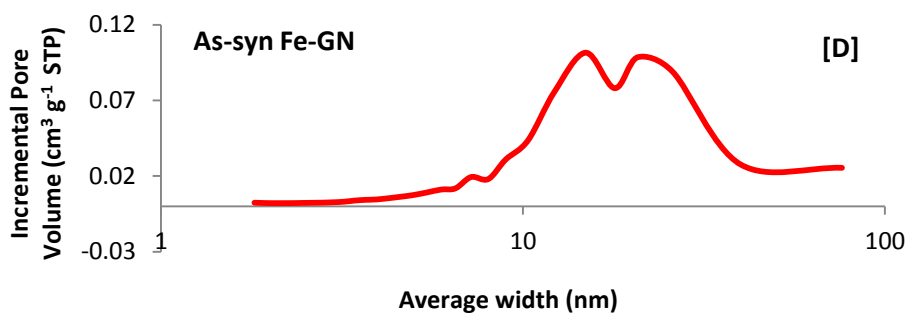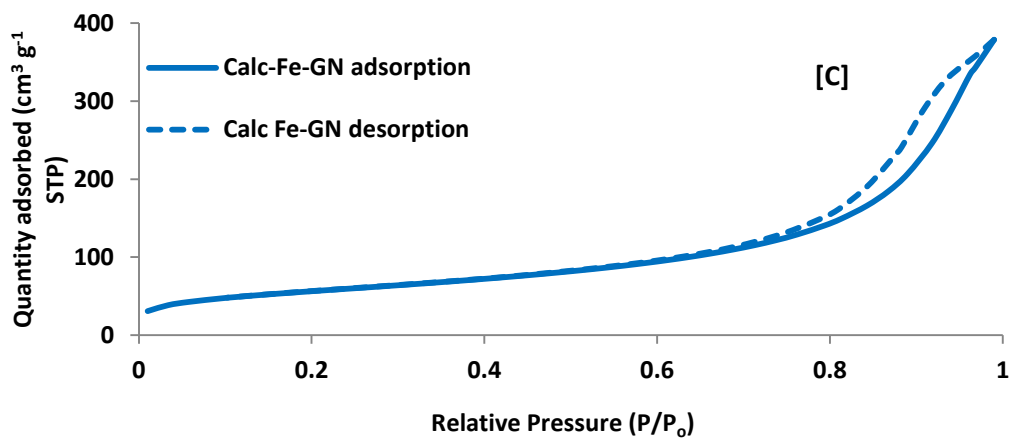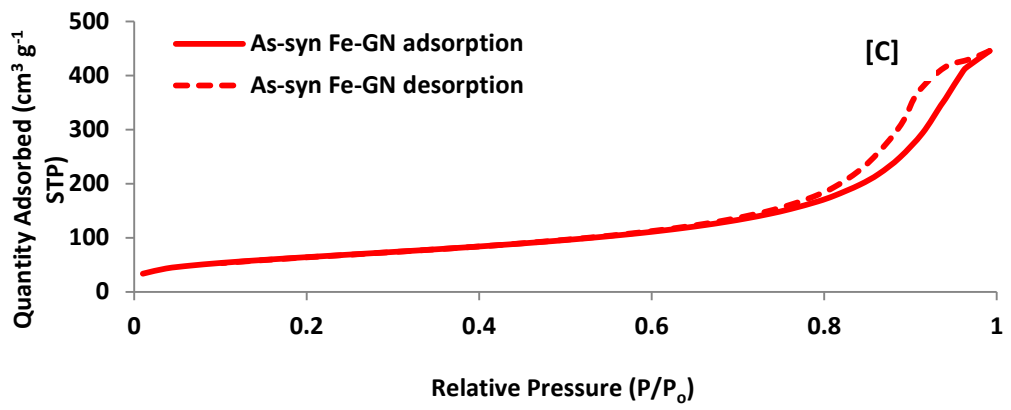
Figure 7.11: **[C] Nitrogen sorption isotherm and [D] average pore size distribution for as-syn and calc MCM-41 respectively.**

7.3.3 Adsorption of PCBs from water using MCM-41 materials

The performance of as-syn and calc MCM-41 materials for sequestration of PCBs from water was examined as described in Section 7.2.5 and the results obtained are displayed in Table 7.2. It can be deduced from Table 7.2 that average recoveries obtained for all PCB congeners were ≤ 46.7 % which corresponds to the expected average recovery of PCB congeners from aqueous solutions without the addition of a sorbent (Section 6.4.3). This therefore suggests that both materials had 0 % removal efficiency for the PCB congeners in aqueous solutions. The recoveries obtained for procedural blanks corresponded to expected PCB recoveries (45 ± 3 %) from water without sorbent addition.

Table 7.2: Recovery of PCB congeners from water using MCM-41 materials

Sorbent used (10 mg) / 2 h		Recovery %				
		PCB-1	PCB-3	PCB-7	PCB-14	PCB-12
As-syn MCM-41	Replicate 1	48	46	44	43	47
	Replicate 2	45	46	45	45	43
	Replicate 3	44	44	49	48	45
	Mean	45.7	45.3	46.0	45.3	45.0
	Std dev	2.1	1.2	2.6	2.5	2.0
	% RSD	4.6	2.5	5.8	5.6	4.4
Calc MCM-41	Replicate 1	46	43	48	45	47
	Replicate 2	44	45	47	44	47
	Replicate 3	44	47	43	45	46
	Mean	44.7	45.0	46.0	44.7	46.7
	Std dev	1.2	2.0	2.6	0.6	0.6
	% RSD	2.6	4.4	5.8	1.3	1.2

As-syn MCM-41 have similar characteristics to micelles as they possess hydrophobic cavities which have hydrophilic surfaces and hydrophobic pores.[193] On the other hand, calc MCM-41 is characterised by the presence of unreacted silanol groups which have the tendency to form hydrogen bonds with water molecules.[193] Hence, as-syn MCM-41 is reportedly a more useful adsorbent for the removal of organic molecules as the surfactant template present provides pockets of hydrophobic sites

for preferential diffusion of target organic molecules.[179, 193, 251] Since the surface of as-syn and calc MCM-41 consists of hydroxyl and silanol groups with the former consisting of the surfactant template which serves as a hydrophobic pocket, the adsorbent-adsorbate interactions would be mainly influenced by hydrophobic interactions between the aromatic molecule and surfactant head or electron donor interactions between the oxygen group on the siloxane surface and pi-system of the aromatic ring for as-syn MCM-41 and calc MCM-41 respectively. However, both sorbents did not show any affinity for the PCB congeners in aqueous solutions; thereby suggesting these interactions were not strong enough to effect the removal of PCB congeners from aqueous solutions. Furthermore, an increase in sorbent mass or contact time did not result in any significant increase in the affinity of both sorbents for PCB congeners in solution as shown in Tables 7.3 - 7.5.

Table 7.3: Recovery of PCBs congeners from water using a higher sorbent mass (20 mg) of MCM-41 materials for 2 h

Sorbent used (20 mg) / 2 h		Recovery %				
		PCB-1	PCB-3	PCB-7	PCB-14	PCB-12
As-syn MCM-41	Replicate 1	47	48	47	44	47
	Replicate 2	46	45	46	43	45
	Replicate 3	43	47	45	47	45
	Mean	45.3	46.7	46.0	44.7	45.7
	Std dev	2.1	1.5	1.0	2.1	1.2
	% RSD	4.6	3.3	2.2	4.7	2.5
Calc MCM-41	Replicate 1	48	46	47	44	48
	Replicate 2	45	43	47	46	45
	Replicate 3	48	47	45	45	46
	Mean	47.0	45.3	46.3	45.0	46.3
	Std dev	1.7	2.1	1.2	1.0	1.5
	% RSD	3.7	4.6	2.5	2.2	3.3

Table 7.4: Recovery of PCBs congeners from water using as-syn MCM-41 after an increase in contact time from 2 h to 3 h

Sorbent (10 mg) / 3 h		Recovery %				
		PCB-1	PCB-3	PCB-7	PCB-14	PCB-12
As-syn MCM-41	Replicate 1	47	47	45	47	43
	Replicate 2	46	45	46	45	45
	Replicate 3	44	48	45	45	46
	Mean	45.7	46.7	45.3	45.7	44.7
	Std dev	1.5	1.5	0.6	1.2	1.5
	% RSD	3.3	3.3	1.3	2.5	3.4

Table 7.5: Recovery of PCBs congeners from water using calc MCM-41 after an increase in contact time from 2 h to 3 h

Sorbent (10 mg) / 3 h		Recovery %				
		PCB-1	PCB-3	PCB-7	PCB-14	PCB-12
Calc MCM-41	Replicate 1	46	47	46	44	43
	Replicate 2	47	45	45	46	45
	Replicate 3	43	47	43	46	46
	Mean	45.3	46.3	44.7	45.3	44.7
	Std dev	2.1	1.2	1.5	1.2	1.5
	% RSD	4.6	2.5	3.4	2.5	3.4

7.3.4 Degradation of PCBs in water using the Photo-Fenton process

The degradation efficiencies of as-syn and calc Fe-GN as heterogeneous catalysts were assessed using the photo Fenton process as described in Section 7.2.6 and the results obtained are given in Table 7.6. As shown in Table 7.5, average recoveries obtained using both silica based sorbents were ≤ 46.3 % for all PCB congeners which corresponds to the expected recovery for each PCB congener without the addition of a sorbent. It was therefore evident that none of the PCBs congeners were degraded using the photo-Fenton process.

Table 7.6: Recovery of PCB congeners from water using Fe-GN materials

Sorbent used / 10 mg		Recovery %				
		PCB-1	PCB-3	PCB-7	PCB-14	PCB-12
As-syn Fe-GN	Replicate 1	46	46	45	44	47
	Replicate 2	46	44	46	43	45
	Replicate 3	43	47	45	47	45
	Mean	45.0	45.7	45.3	44.7	45.7
	Std dev	1.7	1.5	0.6	2.1	1.2
	% RSD	3.8	3.3	1.3	4.7	2.5
Calc Fe-GN	Replicate 1	48	46	46	43	47
	Replicate 2	45	43	47	46	45
	Replicate 3	46	48	43	45	46
	Mean	46.3	45.7	45.3	44.7	46.0
	Std dev	1.5	2.5	2.1	1.5	1.0
	% RSD	3.3	5.5	4.6	3.4	2.2

7.4 Conclusion

The objective of this study was to assess the feasibility of MCM-41 materials to remove PCBs from water and Fe-GN materials to degrade PCBs in water. The results obtained showed that neither MCM-41 materials nor Fe-GN materials were suitable for the removal or degradation of PCBs in aqueous solutions respectively. This may be attributed to poor interactions between the sorbents and the analyte. However, further investigations would be required to examine the ability of surface modified silica materials with specific functional groups to selectively remove PCBs from aqueous solutions.

Chapter 8: Sequestration of polychlorinated biphenyls from water using activated carbon

8.1 Introduction

The removal of PCBs from water systems using efficient and effective adsorbents is highly critical due to their aforementioned toxicity. Several porous carbonaceous adsorbents like fullerenes, nanoplastics, microplastics, graphene oxide, carbon nanotubes (CNT), multiwalled carbon nanotubes (MWCNTs) and activated carbon have been applied for the sequestration of organic pollutants from water.[252-256] However, activated carbon still remains the most widely used adsorbent due to its adsorption properties such as high porosity, physicochemical stability, adsorptive capacity, mechanical strength, degree of surface reactivity and large surface area (500 - 1500 m^2 g^{-1}).[69, 257-262] In addition, organic materials which are non polar in nature are usually preferentially sorbed to ACs than polar species.[263, 264]

Activated carbons (ACs) are porous carbonaceous adsorbents which are amorphous and microcrystalline. They are also referred to as activated charcoal, activated coal or solid sponge and characterised based on their physical properties as they do not have any distinctive chemical formula.[263, 265] ACs are commonly classified as powdered activated carbon (PAC), granular activated carbon (GAC), fibrous activated carbon, activated carbon cloths and pelletised activated carbon commonly referred to as extruded activated carbon (EAC).[266-269] According to the IUPAC, ACs can be classified into three types based on their pore sizes; micropore (< 2 nm), mesopore (2 - 50 nm) and macropore (> 50 nm).[266] A further subdivision of micropores into ultramicropore (< 0.5 nm) and supermicropore (1 - 2 nm) can also be obtained.[270] Elements such as sulfur (S), oxygen (O), hydrogen (H), nitrogen (N) and halogens are usually associated with AC as functional groups or chemically bonded atoms.[265, 266] However, O is the most predominant atom associated with AC usually as carboxyl, carbonyl, phenols and lactone functional groups as depicted in Figure 8.1.[265, 271] The type of oxygen surface groups found on AC generally depends on the starting material used and type of activation employed.[272]

Two different processes known as physical or chemical activation are generally applied for the preparation of ACs.[261, 273-278] In physical activation or thermal activation, AC is prepared following a two-step process known as carbonisation and activation.[263] In the first step, carbonisation is achieved by heating the starting material (precursor) in an inert atmosphere at a temperature ranging from 400 - 850 ℃.[263] This is followed by activation of the resulting charcoal in the

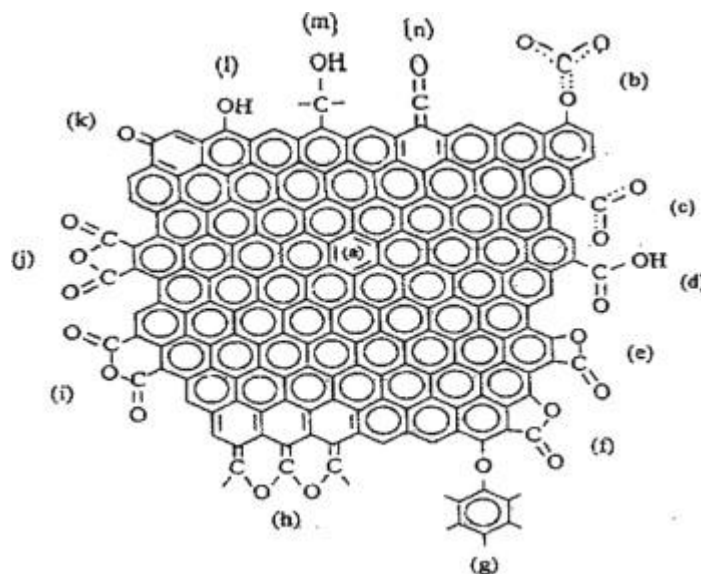presence of suitable oxidising agents such as steam, air, carbon dioxide or any mixture of these gases.[263]

Figure 8.1: IR active groups on carbon surface; (a) aromatic C=C stretching (b, c), carboxyl carbonates (d), carboxylic acid (e, f), lactone - 4 MR, 5 MR (g), ether bridge (i, j), cyclic anhydride-5 MR, 6 MR (k), quinine (i), phenol (m), alcohol (m), and ketene (n).[265] ; MR denotes membered ring.

The major aim of carbonisation is to reduce the volatile content of the precursor such that the resulting char has a higher content of fixed carbon (80 % or higher) suitable for activation.[263] In addition, rearrangement of carbon atoms into the graphitic-like structure is also achieved during carbonisation.[265] The activation process results in the formation of a highly porous activated carbon and an extended surface area by developing further porosity and creating some ordering of the structure.[279]

The process of chemical activation or wet oxidation is generally applied for the conversion of uncarbonised cellulosic material such as wood into AC.[259, 263] In this process, the precursor is usually impregnated with the activating agent and subsequently heated in an inert atmosphere at temperatures ranging from 300 - 800 °C.[265] The function of the activating agent is to dehydrate the precursor thereby giving rise to charring and aromatisation of the carbon skeleton; creating a porous structure and an extended surface area.[265] The resulting AC is finally washed with acid or alkali followed by water to remove any chemical components and develop porosity in the activated carbon.[270 275, 280] In contrast to physical activation,

the resulting product derived from chemical activation usually has a higher surface area as the pores are less susceptible to volume contraction upon heating at relatively lower temperatures.[265] In addition, the activating reagents employed in chemical activation have the ability to dissolve the cellulosic components of the precursor and consequently promote the formation of cross-links.[261, 281, 282] However, chemically activated carbon has been reported to have a higher amount of acidic surface functional groups than thermally activated carbon which results in pore surfaces which are less hydrophobic.[265] Hence, higher adsorption capacities for organics have been obtained using thermally activated carbon compared to chemically activated carbon. The addition of binders to PAC can also result in the formation of carbon granules and pellets thereby enhancing their environmental application.[257, 258] Nevertheless, the properties of the final material obtained using either of the two processes are largely influenced by the precursor used during preparation.[283, 284]

The precursors commonly used for AC production are coal and agricultural by products (lignocellulosic materials) such as sugar cane bagasse, rice husk, corn cob, coconut shell, oil palm trunks, grape seeds, walnut shell and apricot stone characterised by high carbon and low inorganic content.[257, 258, 285-289] However, precursors such as wood, coal, peat and lignite are widely employed in the manufacture of commercial ACs.[265, 290] Activating reagents such as phosphoric acid, zinc chloride, sulfuric acid, sodium carbonate, sodium hydroxide, calcium hydroxide, nitric acid and hydrogen peroxide are usually employed in chemical activation.[261, 263, 270, 291] Nevertheless, zinc chloride and phosphoric acid are the most commonly used chemical agents.[265]

Several studies have been carried to investigate the adsorptive properties of carbonaceous adsorbents for PCBs in water. Fe_3O_4 grafted graphene oxide has been reported to be an effective adsorbent for removing PCB-28 in aqueous solutions.[254] Bradley et al.[252] studied the efficacy of five different carbonaceous adsorbents: activated carbon (AC), charcoal (BC), carbon nanotubes (CNT), graphene (GE) and graphene oxide (GO) as sorbent materials for eleven PCB congeners in aqueous solutions. Amongst all the materials studied, AC was found to have the highest sorption capacity for PCBs in aqueous solution. In a study conducted on the use of MWCNTs for preconcentration of PCBs from aqueous solutions, high adsorption capacities were obtained.[253] However, in another study, β-cyclodextrin grafted on MWCNTs were reported to have higher adsorption capacities than MWCNTs for the

removal of PCBs (4,4′-dichlorobiphenyl and 2,3,3′-trichlorobiphenyl) from aqueous solutions.[292]

Although AC has been widely applied for the removal of hydrophobic organic contaminants (HOCs) from water, its use for PCB removal from water has not been explored in detail. In addition, the specific mechanism by which adsorption of PCBs occurs on ACs with different textural properties still remains ambiguous. As a consequence, data on adsorption of PCBs in water using AC is sparse in literature. Therefore, the objective of this work was to examine the efficacy of three different types of ACs: powdered activated carbon (PAC), granular activated carbon (GAC) and extruded activated carbon (EAC) with different textural properties for the sequestration of PCB congeners from aqueous solutions at trace concentrations. Adsorption kinetics was conducted to determine the mechanism of adsorption of the target PCB congeners onto the three sorbents. The effect of solution pH on the removal efficiency of three sorbents for PCBs in aqueous solutions was also investigated.

8.2 Experimental

8.2.1 Materials and reagents

Norit CA1 (PAC), Darco (GAC) and Norit CNR-150 (EAC) were obtained from Sigma Aldrich and used for adsorption experiments without any further modifications. Distilled water was used for all experiments. C18 (EC) SPE cartridges were supplied by Biotage.

8.2.2 Ultimate and proximate analysis

Ultimate (elemental) analysis of materials under investigation was carried out using an Exeter analytical CE440 elemental analyser to determine the amount of carbon (C), hydrogen (H), nitrogen (N) and oxygen (O) present in each sample. A small amount of the sample was accurately weighed into a tin capsule and combusted at 950 ℃ in an oxygen enriched environment. This was followed by an increase in combustion temperature resulting in the vaporisation of the sample and subsequent formation of CO_2, H_2O, N_2 and NO_x as combustion products and gaseous

by-products. The combustion products were swept through a reduction tube (metallic Cu) to convert oxides of nitrogen and any unused oxygen remaining from the initial combustion process. A small fraction of the product mixture (CO_2, H_2O, N_2) was then separated in the gas chromatograph and CHN quantified by the thermal conductivity detector (TCD).

Proximate analysis was carried out using a Netzsch STA 449 F3 Jupiter thermogravimetric (TGA) analyser to determine the moisture content, fixed carbon, volatile matter and ash content. Prior to analysis, the sample was degassed under N_2 for 2 h at ambient temperature. A small amount of the sample material was placed in the crucible and the sample degassed for a few minutes under N_2 until a stable weight was obtained. The sample was subsequently heated as follows; 30 ºC (held for 10 min), increased to 900 ºC at 20 ºC min^{-1} (held for 40 min) under N_2 at a flow rate of 20 cm^3 min^{-1}. After decomposition, the gas flow was switched to O_2 at a flow rate of 20 cm^3 min^{-1} and final temperature held at 900 ºC for 45 min for combustion. The protective N_2 was kept constant at a flow rate of 50 cm^3 min^{-1} in both N_2 and O_2 atmospheres.
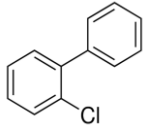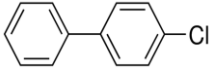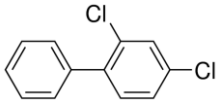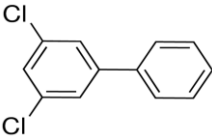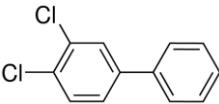
8.2.3 Batch adsorption experiments

Batch adsorption experiments were conducted using the five PCB congeners specified in Section 4.2. 3 cm^3 of distilled water was placed in a 5 cm^3 volumetric flask, spiked with 1 cm^3 of the PCB congener mixture (60 µg cm^{-3}) and made up to mark with distilled water. The molecular structures and some physicochemical properties of these target PCB congeners are depicted in Table 8.1.

To assess the performance of the three ACs (PAC or GAC or EAC) for PCBs in aqueous solutions, the spiked solution (12 µg cm^{-3}) was placed in 15 cm^3 amber glass bottles and 10 mg of each sorbent added. A procedural blank was prepared in a similar manner without the addition of any sorbent. The bottles were sealed with PTFE screw caps and the mixture stirred for 2 h at 250 rpm. Each mixture was then centrifuged at 4000 rpm for 5 min using an Eppendorf centrifuge 5804 R centrifuge and the supernatant preconcentrated using C18 (EC) SPE cartridges following the SPE process described in Section 3.4.1. A 1 µL aliquot of the resulting solution was analysed using the GC-MS under the operating conditions described in Section 3.3.1.

The removal efficiency of each AC for the target PCB congeners was calculated using Equation 7.4.

Table 8.1 Characteristics of target PCB congeners

PCB congeners	Chemical structure	Homologue	Type of PCB	Log K_{ow} [293]
PCB - 1		monoCB	Mono-*ortho* PCB	4.46
PCB - 3		monoCB	Non-*ortho* PCB	4.69
PCB - 7		diCB	Mono-*ortho* PCB	5.07
PCB - 14		diCB	Non-*ortho* PCB	5.22
PCB - 12		diCB	Non-*ortho* PCB	5.28

8.2.4 Adsorption isotherms

Adsorption isotherms were obtained by varying the initial concentrations of the PCBs in the mixed solution: 12, 16, 20 and 24 µg cm^{-3} and batch experiments conducted following the procedure described in Section 8.2.3. The amount of PCBs adsorbed per unit mass of sorbent (AC) at equilibrium can be calculated using Equation 8.1.

$$q_e = \frac{C_o - C_e}{W} V \qquad \text{Eq. 8.1}$$

C_o and C_e (mg L^{-1}) are the initial and equilibrium concentrations of PCBs in the aqueous solution, V is the volume of solution (L) and W is the mass of sorbent (g).

The resulting experimental data was subsequently applied to the Langmuir and Freundlich models. The Langmuir model is based upon the assumption that the adsorbent surface is homogeneous and maximum adsorption corresponds to a saturated monolayer of adsorbate molecules on the adsorbent surface with no side interactions occurring between the adsorbed molecules.[67, 294, 295] The Langmuir model is mathematically expressed as shown in Equation 8.2.

$$\frac{C_e}{q_e} = \left(\frac{1}{q_m b}\right) + \left(\frac{1}{q_m}\right) C_e \qquad\qquad \text{Eq. 8.2}$$

Where q_e (mg g^{-1}) is the amount of PCB adsorbed per unit mass of sorbent, C_e (mg L^{-1}) is the equilibrium concentration of PCB in the solution. A plot of $\frac{C_e}{q_e}$ vs C_e gives a straight line where q_m (mg g^{-1}) and b (L mg^{-1}) are the maximum monolayer capacity and Langmuir constants which can be deduced from the slope and intercept respectively.

The Langmuir model corresponds to homogeneous adsorption and the favourability of the adsorption system can be expressed using a dimensionless separation factor R_L (Equation 8.3) where $R_L > 1$ or 0, $R_L = 1$, $0 < R_L < 1$ and $R_L = 0$ describe unfavourable, linear, favourable and irreversible adsorption isotherms respectively.[296]

$$R_L = \frac{1}{1 + C_O b} \qquad\qquad \text{Eq. 8.3}$$

The Freundlich adsorption model is based upon the assumption that adsorption occurs on a heterogeneous surface with side interactions via a multilayer adsorption mechanism.[67, 296] The Freundlich model is expressed in Equation 8.4.

$$\ln q e = \ln k_f + \left(\frac{1}{n}\right) \ln c_e \qquad\qquad \text{Eq. 8.4}$$

Where k_f (mg g^{-1}) and n (L mg^{-1}) are the Freundlich constants related to the adsorption capacity and intensity respectively. The Freundlich model corresponds to heterogeneous adsorption and a large n value indicates stronger adsorbent-adsorbate interaction.[296] The adsorption process is considered favourable and feasible when 1/n ranges from 0 - 1.

8.2.5 Adsorption kinetics study

Kinetic studies was undertaken to examine the rate of PCB removal from water using the three different ACs. The aqueous solutions (5 cm^3) containing the same initial concentration (12 µg cm^{-3}) of PCBs and 10 mg of each sorbent were stirred for different time intervals: 5, 15, 30, 45, 60, 90, 105 and 120 min. Procedural blanks were prepared in a similar manner without the addition of any sorbent. After each time interval, solutions were centrifuged at 4000 rpm for 5 min using an Eppendorf centrifuge 5804 R and the supernatant preconcentrated using C18 (EC) SPE cartridges following the SPE method described in Section 3.4.1. The concentration of PCBs remaining after time (t) was determined by GC-MS analysis of the solution using the operating conditions outlined in Section 3.3.1. Kinetics of PCB adsorption onto the sorbents was analysed using the pseudo first-order and pseudo second-order models given in Equations 8.5 and 8.6 respectively.[254, 297]

The pseudo-first order equation of Lagergren is generally expressed as:

$$\log(q_e - q_t) = \log(qe) - \frac{K_1}{2.303}\ t \qquad\qquad \text{Eq 8.5}$$

Where q_e and q_t are the adsorption capacities at equilibrium and time t respectively (mg g^{-1}), k_1 is the pseudo-first order rate constant (L min^{-1}). A plot of log (q_e-q_t) against t gives a linear relationship where k_1 (slope) and q_e (intercept) can be deduced.

The pseudo-second order equation is generally expressed as:

$$\frac{t}{q_t} = \frac{1}{k_2 q_e^2} + \frac{1}{q_e}t \qquad\qquad \text{Eq. 8.6}$$

A plot of $\dfrac{t}{q_t}$ vs t gives a straight line, where q_e (mg g^{-1}) and k_2 which is the pseudo-second order rate constant (g mg^{-1} min^{-1}) can be deduced from the intercept and slope respectively.

In order to confirm whether the sorption of PCBs onto ACs was due to chemisorption or physisorption, the spent ACs obtained from adsorption experiments were brought in contact with 5 cm^3 of distilled water for 30 min and the supernatant subjected to FTIR analysis using the procedure specified in Section 7.4.3.

8.2.6 Effect of solution pH on removal efficiencies of ACs for PCBs in aqueous solutions

To investigate the effect of solution pH on sorption of PCB congeners onto the ACs, the pH of the solution was altered to 3, 5, 7, 9 and 11 using 0.1 M HCl and 0.1 M NaOH. The resulting aqueous solution was spiked as described in Section 8.2.3. Thereafter, adsorption experiments, solution preconcentration and eluate analysis were conducted as described in Section 8.2.3.

8.2.7 Removal efficiency of EAC for PCBs in real water samples

The efficiency of EAC for sorption of PCBs in real water samples was investigated using the water samples collected from Lagos, Nigeria (Section 6.1). The water samples (5 cm^3) were spiked with PCB congeners as described in Section 8.2.3. The adsorption experiments were conducted using EAC (10 mg) following the same procedure specified in Section 8.2.3 and 1 μL aliquot of the resulting solution was analysed using the GC-MS under the operating conditions outlined in Section 3.2.1.

8.3 Results and discussion

8.3.1 Ultimate and proximate analysis

Ultimate analysis of PAC, GAC and EAC was conducted to determine the elemental composition: carbon (C), hydrogen (H) and nitrogen (N) contents of the studied materials. The oxygen content was calculated by difference. Proximate analysis was carried out to measure the moisture, volatile matter, fixed carbon and ash content of the sample materials. A summary of the results obtained is given in Table 8.2 and TGA curves displayed in Fig 8.1. Ultimate analysis of the three ACs showed that EAC had the highest carbon and lowest oxygen content. The H contents obtained were less than 5 % with no N except for EAC which had 0.8 % N content.

Table 8.2: Ultimate and proximate analysis of PAC, GAC and EAC

Ultimate analysis – wt / %				
Sorbent	**C**	**H**	**N**	**O***
PAC	69.3	3.9	-	26.8
GAC	70.1	1.4	-	28.5
EAC	72.2	3.0	0.8	23.9
Proximate analysis – wt / %[a]				
Sorbent	**Moisture**	**Ash**	**Volatile matter**	**Fixed Carbon**
PAC	2.3	5.4	18.4	73.9
GAC	2.1	16.0	5.2	76.7
EAC	2.8	9.2	15.4	72.6

 a: calculated on dry basis, *: calculated by difference

Four distinct regions of weight loss were obtained from proximate analysis of the three ACs as shown in Figure 8.2. The first region corresponds to weight loss of absorbed water molecules present in the sample at a temperature range of 30 - 180 ºC. The next region of weight loss was due to the percentage of volatile matter in the sample material via decomposition at temperatures ranging from 180 - 700 ºC in an inert atmosphere using N_2 gas. The third region of weight loss corresponds to the percentage of fixed carbon in the sample material obtained under combustion in air at a temperature of 900 ºC. Finally, the last region can be ascribed to the percentage of ash content present in the sample material.

Results obtained from proximate analysis indicate that the three ACs had a high amount of fixed carbon > 70 % and low amount of moisture < 5 % which are desirable properties for use in adsorption. However, GAC had the highest amount of ash content (16 %) and lowest amount of volatile matter (5.2 %) compared to PAC and EAC. The high ash content obtained for GAC may be attributed to the use of binders for extrusion or reconstitution of powdered material during the manufacturing process.
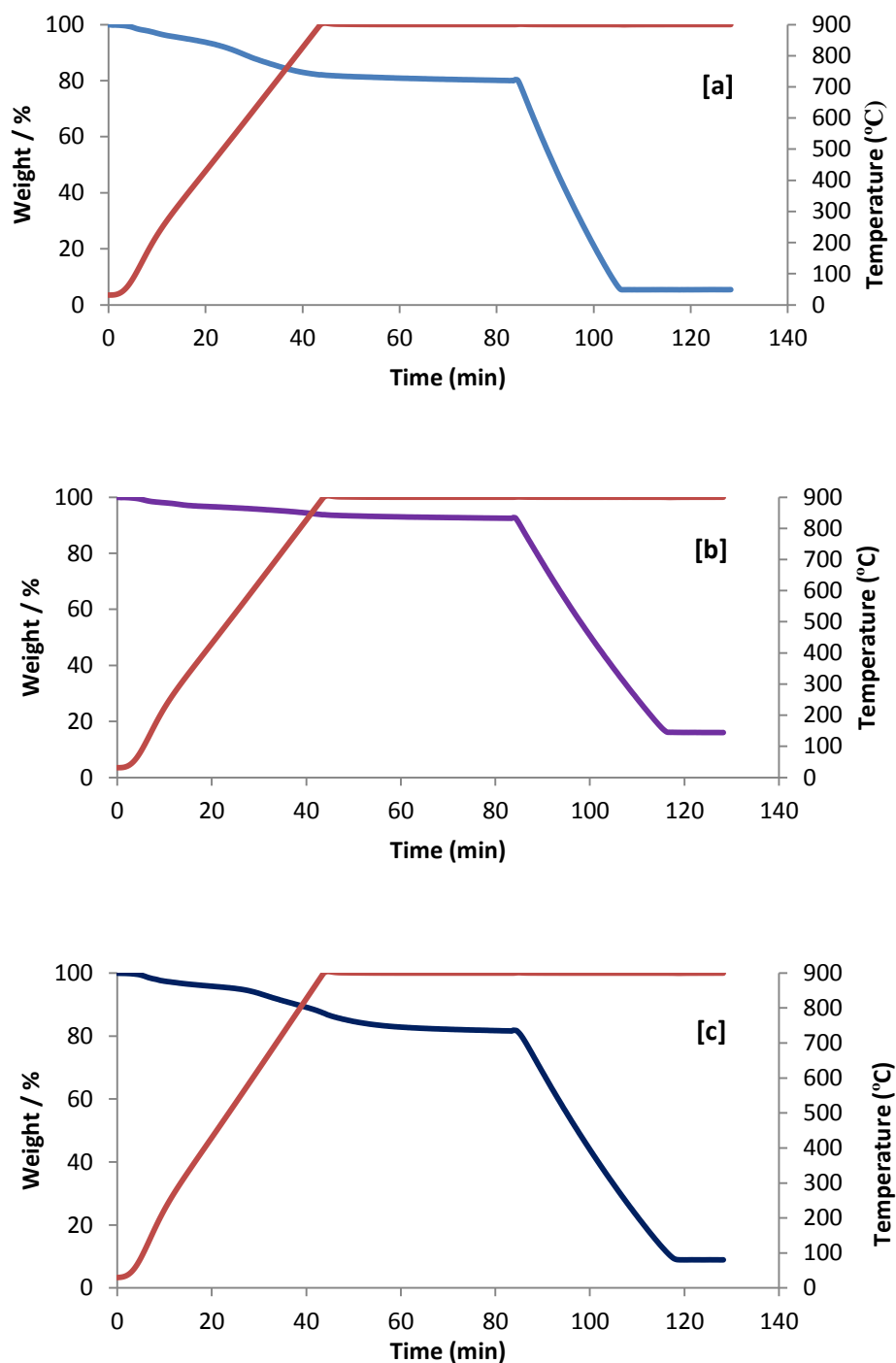
Figure 8.2: TGA curves for (a) PAC (b) GAC (c) EAC respectively

8.3.2 Material characterisation

The textural properties (surface area, pore volume and average pore diameter) of the three ACs were obtained from the nitrogen sorption isotherms as described in Section 3.5.1 and the results displayed in Table 8.3.

Table 8.3: Characterisation data for ACs

Sorbent	BET Surface Area [a] / $m^2 \, g^{-1}$	A.P.S [b] / nm	T.P.V [c] / $cm^3 \, g^{-1}$	M.P.V [c] / $cm^3 \, g^{-1}$	M.A [d] / $m^2 g^{-1}$
PAC	1207 ± 11	5.4	1.05	0.31	698
GAC	569 ± 5	5.8	0.52	0.14	311
EAC	1395 ± 28	2.8	0.85	0.47	938

A.P.S: Average Pore Size, T.P.V: Total pore volume, M.P.V: Micropore volume, M.A: Micropore area

[a] Calculated by the BET model from sorption data in a relative pressure range from 0.05-0.29.
[b] Calculated by the BJH model from the desorption branches of isotherms.
[c] Calculated from N_2 amount adsorbed at relative pressure P/Po of 0.99.
[d] Calculated by t-plot analysis using the Harkins and Jura equation.

Amongst the three ACs, EAC had the highest surface area (1395 $m^2 \, g^{-1}$) compared to PAC and GAC which had surface areas of 569 and 1207 $m^2 \, g^{-1}$ respectively. The total micropore area deduced for EAC (938 $m^2 g^{-1}$) was higher than that obtained for PAC (698 $m^2 g^{-1}$) and GAC (311 $m^2 g^{-1}$) respectively. PAC, GAC and EAC had total pore volumes of 1.05, 0.52 and 0.85 with micropore volumes which were 30 %, 27 % and 55 % their total pore volumes respectively.

The nitrogen adsorption-desorption isotherms obtained for the three ACs are displayed in Figures 8.3 and 8.4. A type IVa isotherm with H4 hysteresis was exhibited by PAC which is typical for mesoporous adsorbents with wider pores as capillary condensation is accompanied by hysteresis. The type II isotherm with H4 hysteresis exhibited by GAC is associated with the presence of mesopores with small contributions of microporosity (monolayer adsorption) occurring at lower relative pressures. The type Ib isotherm observed for EAC corresponds to the presence of wider micropores in the material while the H4 hysteresis is an indication of the presence of mesopores in addition to the micropores already present.
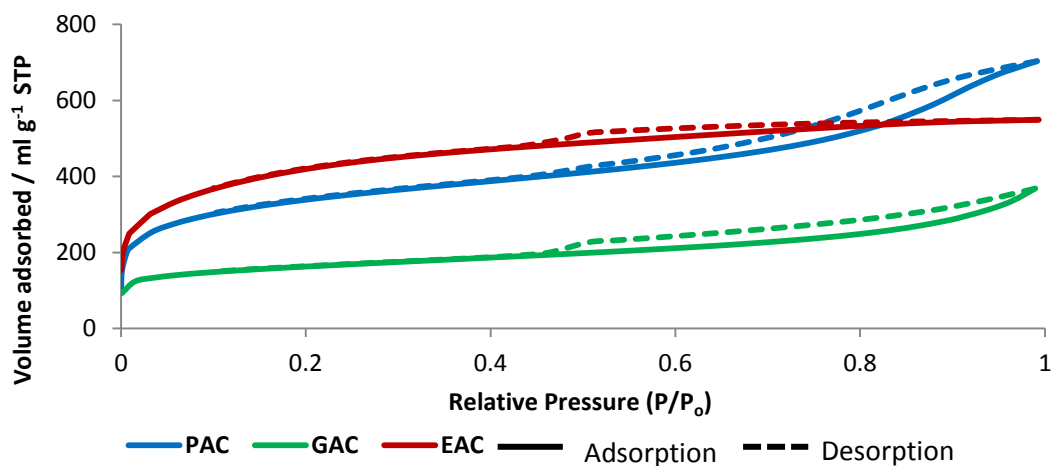
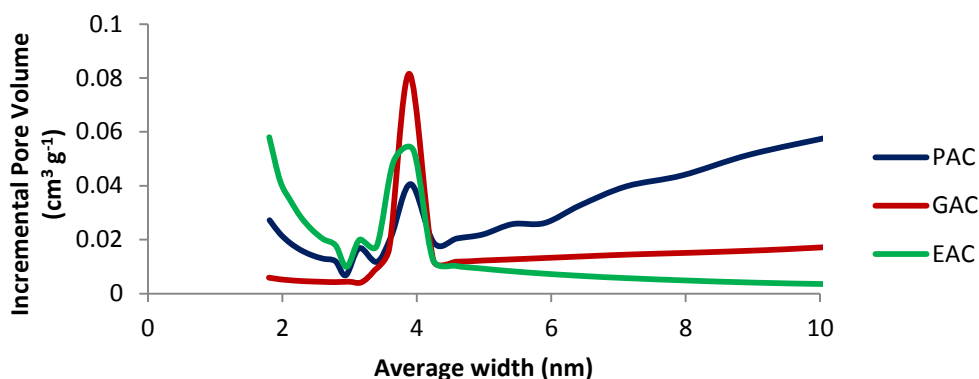**Figure 8.3: Nitrogen sorption isotherms of PAC, GAC and EAC**

Figure 8.4: Average pore size distribution of PAC, GAC and EAC

8.3.3 Removal efficiency of PCBs in water samples

The performance of the three ACs for the removal of PCBs from aqueous solution was examined as described in Section 8.2.3. Since the resulting solutions obtained after extraction were preconcentrated using the SPE method (Section 3.4.1), a recovery factor of 0.45 was applied to the final PCB concentrations obtained at equilibrium (C_e) and the results obtained are displayed in Figure 8.5.
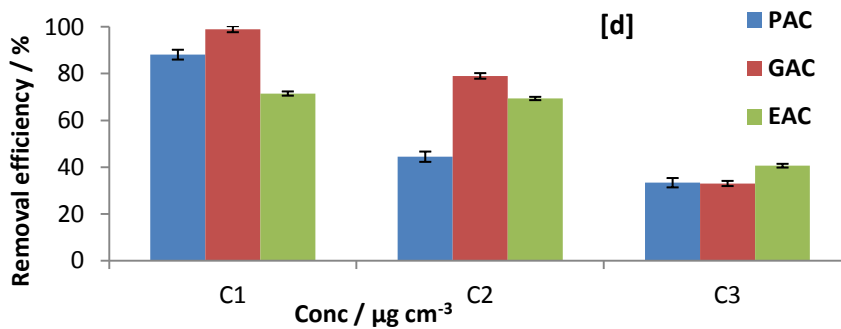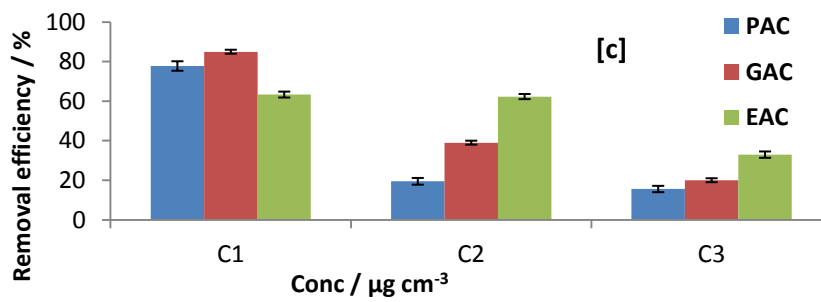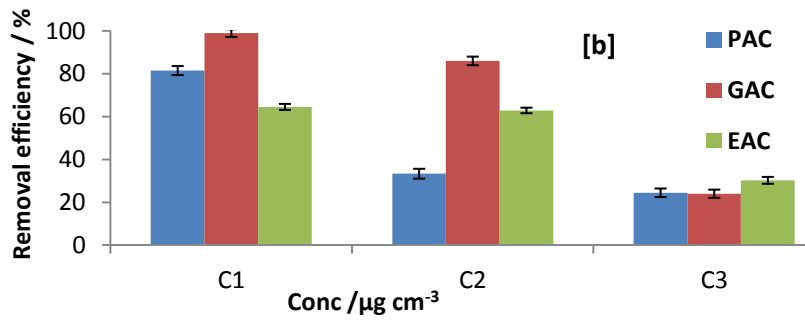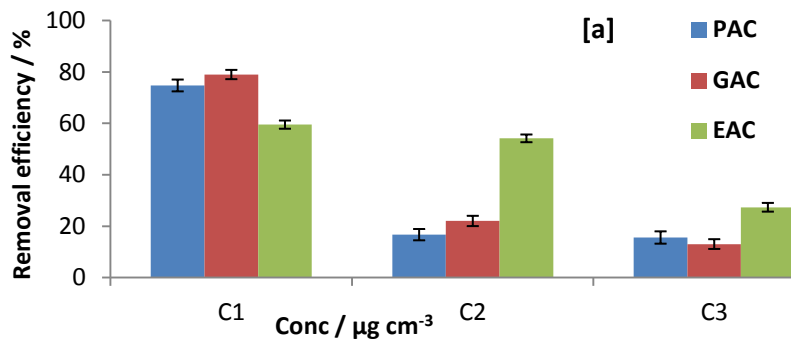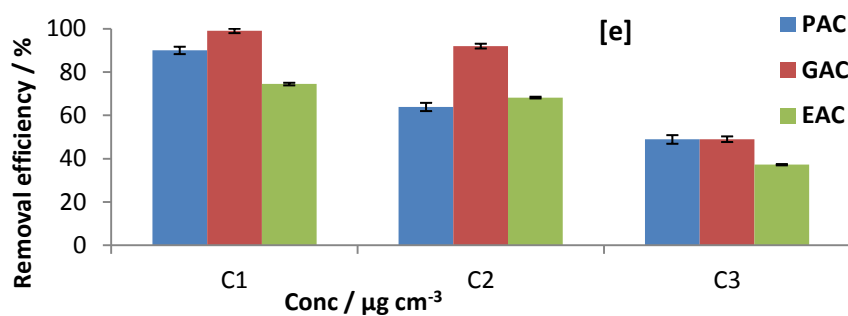
Figure 8.5: Removal efficiencies (a, b, c, d, e) of PAC, GAC and EAC for PCB 1, 3, 7, 14 and 12 (n=3) respectively; C1, C2 and C3 represent concentrations - 12, 16 and 20 µg cm^{-3} of the aqueous solutions containing PCBs respectively.

As shown in Figure 8.5, the removal efficiencies of PAC, GAC and EAC for PCBs in aqueous solutions were 75 - 90 % and 79 - 99 % and 60 - 74 % respectively; thereby indicating that GAC had higher removal efficiency for PCBs than PAC and EAC. In contrast to EAC where only a slight decrease in removal efficiency for PCBs was obtained as the concentration of aqueous solution increased, a significant decrease in removal efficiency was obtained for both PAC and GAC respectively.

Although ACs are known to be suitable materials for adsorption of several aromatic compounds, ACs with lower surface oxygen contents have been reported to have higher adsorption capacities than their counterparts as the reduction in surface oxygen content promotes specific interactions between the π-electron rich regions of AC and aromatic rings of the compound.[264, 298, 299] This could be attributed to the fact that an increase in the surface oxygen content on AC results in an increase in the polarity of the AC surface and subsequently an increase in preference for water molecules over the organic analyte.[264] As a consequence, water clusters are formed which have the tendency to block the carbon pores and prevent access of the organic analyte to the hydrophobic region on the surface of AC.[66] Therefore, the higher removal efficiency of EAC observed for all PCB congeners with an increase in concentration of aqueous solution can be attributed to the presence of a lower surface oxygen content compared to PAC and GAC; thereby favouring specific π-π interactions and resulting in a lower saturation of its pores at higher PCB concentrations. In general, the sorption efficiencies of the three ACs were higher for

non-*ortho* PCBs than mono-*ortho* PCBs particularly PCB - 1. PCBs are known to have a complex range of structures which can either assume a planar or twisted conformation and the tendency of a PCB molecule to assume any of these conformations depends on two interactive forces: π electron conjugation and steric repulsion.[300] Hence, the presence of a π electron conjugated system in a PCB molecule results in a planar conformation while steric repulsion between chlorine atoms in the ortho position of a PCB molecule results in a twisted conformation.[300] ACs are known to consist of a highly disorganised network of graphite-like crystallites which are randomly oriented.[256, 263] As a result of this, the adsorption of PCBs onto AC is achieved by $\pi - \pi$ interactions between the phenyl rings and graphite-like surface of the adsorbent pore. Therefore, the higher removal efficiencies of the three ACs for non-ortho PCBs compared to mono-ortho PCBs can be attributed to their ability to easily assume planar conformations and consequently achieve stronger $\pi - \pi$ interactions.[255] This is similar to findings by Ayato et al.[256] in a study based on the relationship between the adsorption of dioxin-like PCBs and physicochemical properties of AC where non-ortho PCBs had higher adsorption ratios compared to mono-ortho PCBs.

8.3.4 Adsorption isotherms for PCBs on ACs

To examine the maximum adsorption capacity of the three ACs: PAC, GAC and EAC for PCB congeners in aqueous solutions, the Langmuir and Freundlich isotherms were applied to the equilibrium data obtained. The measured concentrations obtained at equilibrium are given in Tables 8.4 - 8.6. The Langmuir and Freundlich isotherms for PAC, GAC and EAC are displayed in Figures 8.6 and 8.7 respectively while the corresponding isotherm parameters are given in Tables 8.7 and 8.8.
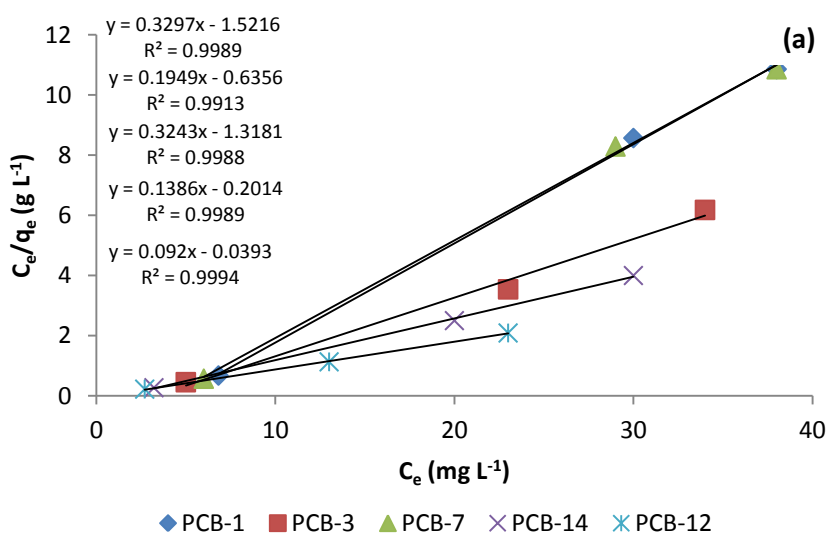
Table 8.4: Initial concentrations (C_o) and equilibrium concentrations (C_e) of PCBs in water after adsorption with PAC

C_o / µg cm^{-3}		C_e / µg cm^{-3}			
	PCB - 1	PCB – 3	PCB - 7	PCB - 14	PCB – 12
12	3.1	2.25	2.7	1.4	1.2
16	13.5	10.8	13.1	9.0	5.9
20	17.1	15.3	17.1	13.5	10.4

Table 8.5: Initial concentrations (C$_o$) and equilibrium concentrations (C$_e$) of PCBs in water after adsorption with GAC

C$_o$ / µg cm^{-3}		C$_e$ / µg cm^{-3}			
	PCB - 1	PCB – 3	PCB - 7	PCB - 14	PCB – 12
12	2.6	0.06	1.8	0.07	0.05
16	12.6	2.3	9.9	3.6	1.4
20	17.6	15.3	16.2	13.5	10.4

Table 8.6: Initial concentrations (C$_o$) and equilibrium concentrations (C$_e$) of PCBs in water after adsorption with EAC

C$_o$ / µg cm^{-3}		C$_e$ / µg cm^{-3}			
	PCB - 1	PCB – 3	PCB - 7	PCB - 14	PCB – 12
12	4.9	4.3	4.4	3.4	3.1
16	7.4	5.9	6.0	4.9	5.1
20	14.5	13.9	13.4	11.9	12.6

It can be deduced from Figures 8.6 and 8.7 that interactions between the PCB congeners in aqueous solutions and the three ACs best fit the Langmuir model in the linear form as correlation co-efficients obtained were higher than that obtained from the Freundlich model. As mentioned earlier, the Langmuir and Freundlich models correspond to homogeneous and heterogeneous adsorption respectively. Therefore, the results obtained suggest that monolayer adsorption occurred between the liquid phase and solid adsorbent phase.
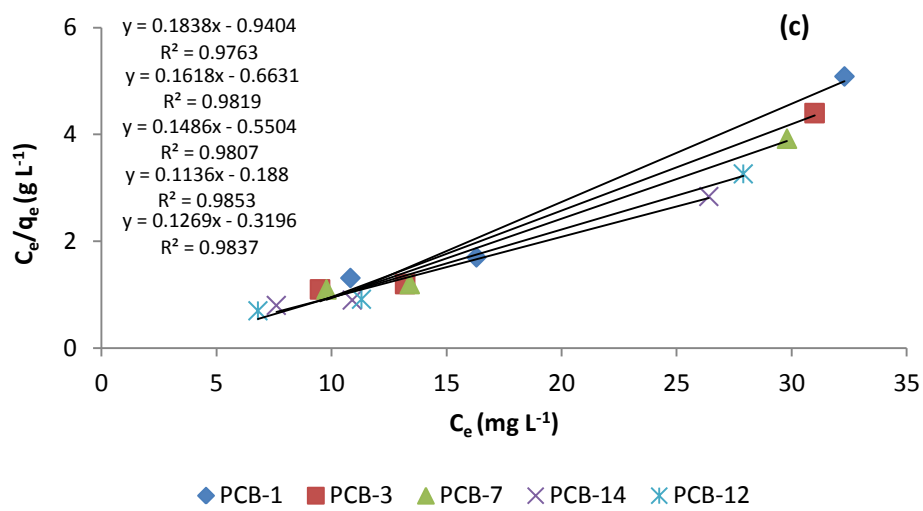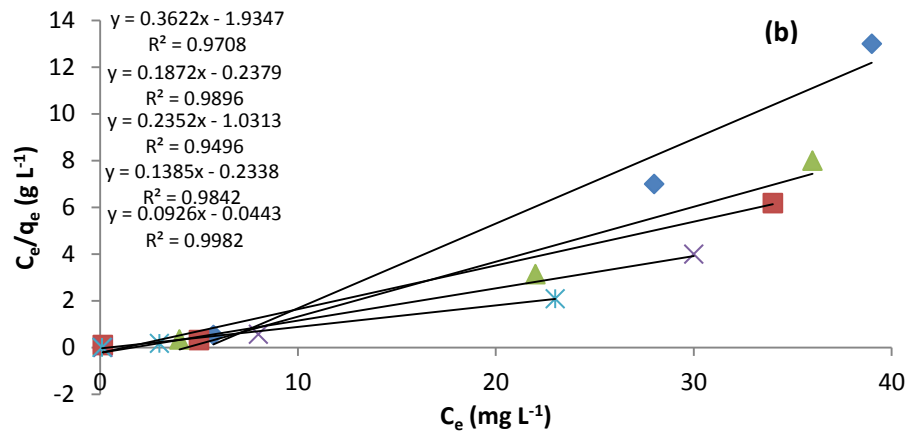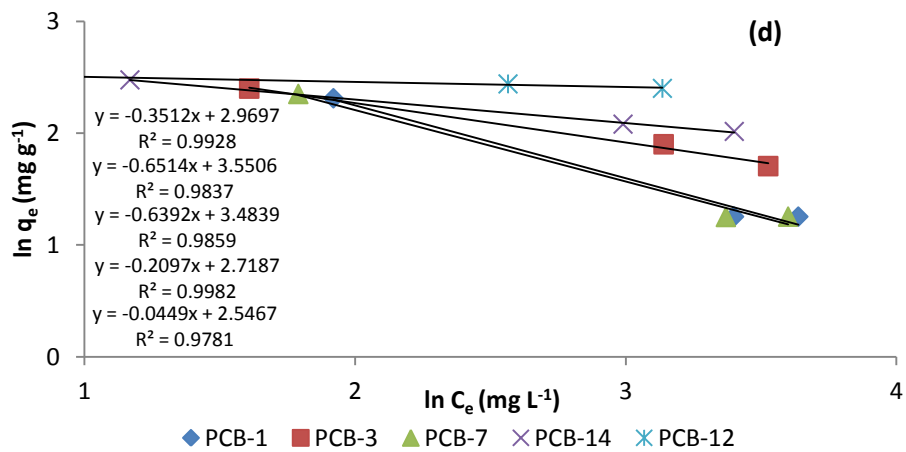
(b)

$y = 0.3622x - 1.9347$
$R^2 = 0.9708$
$y = 0.1872x - 0.2379$
$R^2 = 0.9896$
$y = 0.2352x - 1.0313$
$R^2 = 0.9496$
$y = 0.1385x - 0.2338$
$R^2 = 0.9842$
$y = 0.0926x - 0.0443$
$R^2 = 0.9982$

◆ PCB-1   ■ PCB-3   ▲ PCB-7   ✕ PCB-14   ✱ PCB-12

(c)

$y = 0.1838x - 0.9404$
$R^2 = 0.9763$
$y = 0.1618x - 0.6631$
$R^2 = 0.9819$
$y = 0.1486x - 0.5504$
$R^2 = 0.9807$
$y = 0.1136x - 0.188$
$R^2 = 0.9853$
$y = 0.1269x - 0.3196$
$R^2 = 0.9837$

◆ PCB-1   ■ PCB-3   ▲ PCB-7   ✕ PCB-14   ✱ PCB-12

Figure 8.6: Langmuir isotherms (a, b, c) of PAC, GAC and EAC for PCB -1, 3, 7, 14 and 12 respectively.

(d)

$y = -0.3512x + 2.9697$
$R^2 = 0.9928$
$y = -0.6514x + 3.5506$
$R^2 = 0.9837$
$y = -0.6392x + 3.4839$
$R^2 = 0.9859$
$y = -0.2097x + 2.7187$
$R^2 = 0.9982$
$y = -0.0449x + 2.5467$
$R^2 = 0.9781$

◆ PCB-1   ■ PCB-3   ▲ PCB-7   ✕ PCB-14   ✱ PCB-12

(e)

y = -0.057x + 2.7039
R² = 0.1472
y = -0.2531x + 2.767
R² = 0.6476
y = -0.7595x + 3.9068
R² = 0.989
y = -0.1895x + 2.783
R² = 0.5823
y = -0.4798x + 3.302
R² = 0.8954

◆ PCB-1   ■ PCB-3   ▲ PCB-7   ✕ PCB-14   ✱ PCB-12

(f)

y = -0.276x + 2.9147
R² = 0.2729
y = -0.1909x + 2.7605
R² = 0.2907
y = -0.2035x + 2.7857
R² = 0.2357
y = -0.0964x + 2.5988
R² = 0.1231
y = -0.1516x + 2.7115
R² = 0.3458

◆ PCB-1   ■ PCB-3   ▲ PCB-7   ✕ PCB-14   ✱ PCB-12

Figure 8.7: Freundlich isotherms (d, e, f) of PAC, GAC and EAC for PCB -1, 3, 7, 14 and 12 respectively.

As shown in Tables 8.7 and 8.8, the calculated R_L values for PAC, GAC and EAC ranged from 0 - 1 for all PCB congeners suggesting favourable adsorption for all PCB species. The total PCB adsorption capacities q_m obtained were 29.3, 30.4 and 35 mg/g for PAC, GAC and EAC respectively; indicating that EAC had a greater maximum adsorption capacity for all PCB congeners than GAC and PAC.

Table 8.7: Langmuir isotherm parameters for PCB sorption on PAC, GAC and EAC

Compound	PAC q_m / mg g^{-1}	b	R_L	GAC q_m / mg g^{-1}	b	R_L	EAC q_m / mg g^{-1}	b	R_L
PCB - 1	3.03	0.22	0.28	2.8	0.19	0.31	5.44	0.20	0.30
PCB - 3	5.13	0.31	0.21	5.3	0.79	0.10	6.18	0.24	0.25
PCB - 7	3.08	0.25	0.25	4.3	0.23	0.27	6.73	0.27	0.24
PCB - 14	7.22	0.69	0.11	7.2	0.59	0.12	8.80	0.60	0.12
PCB - 12	10.87	2.34	0.03	10.8	2.09	0.04	7.88	0.40	0.17

Table 8.8: Freundlich Isotherm parameters for PCB sorption on PAC, GAC and EAC

Compound	PAC K_f / mg g^{-1}	n	1/n	GAC K_f / mg g^{-1}	n	1/n	EAC K_f / mg g^{-1}	n	1/n
PCB - 1	18.1	0.5	2.0	49.7	1.3	0.8	18.4	3.6	0.3
PCB - 3	13.3	4.2	0.2	15.9	3.9	0.2	15.8	5.2	0.2
PCB - 7	28.9	1.7	0.6	27.2	2.1	0.5	16.2	4.9	0.2
PCB - 14	9.6	15.4	0.1	16.2	5.3	0.2	13.4	10.4	0.1
PCB -12	7.0	6.5	0.1	14.9	17.5	0.1	15.1	6.6	0.1

8.3.5 Kinetic study of PCB adsorption onto ACs

The rate of PCB removal from water using PAC, GAC and EAC was examined as described in Section 8.2.5. The pseudo first-order and pseudo second-order models were applied to the data obtained to study the sorption rate of PCB congeners onto the different ACs. The results obtained are displayed in Figures 8.8 and 8.9.
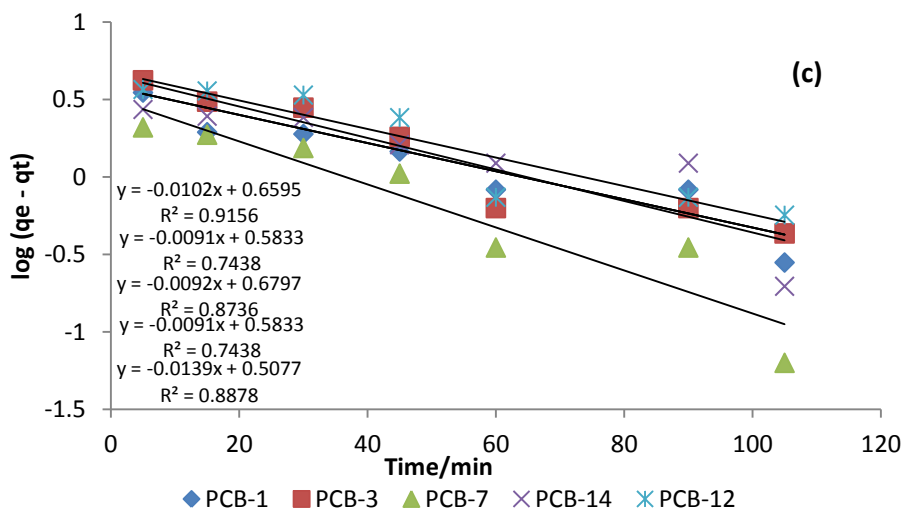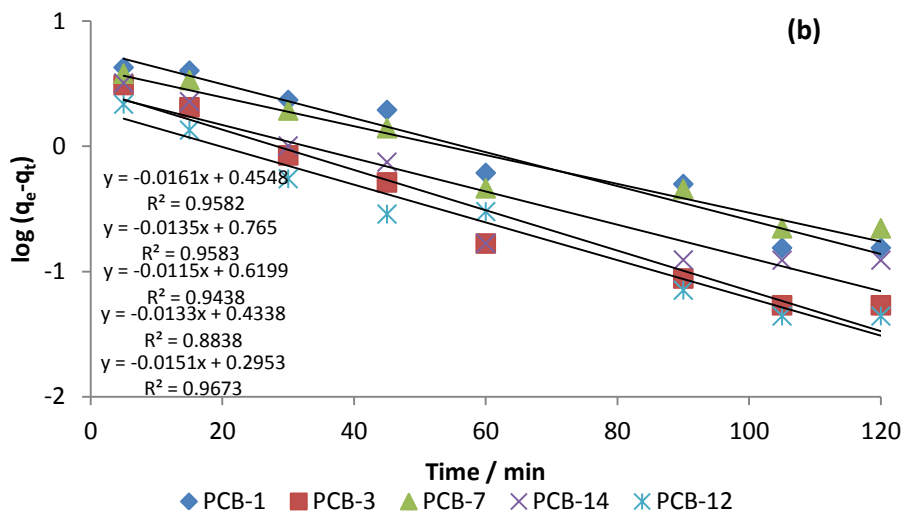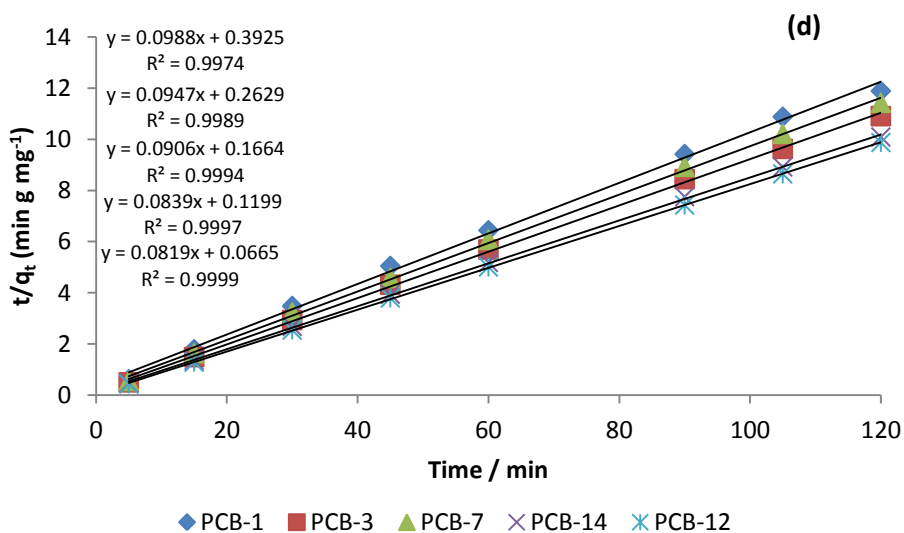
(b)

$y = -0.0161x + 0.4548$
$R^2 = 0.9582$
$y = -0.0135x + 0.765$
$R^2 = 0.9583$
$y = -0.0115x + 0.6199$
$R^2 = 0.9438$
$y = -0.0133x + 0.4338$
$R^2 = 0.8838$
$y = -0.0151x + 0.2953$
$R^2 = 0.9673$

(c)

$y = -0.0102x + 0.6595$
$R^2 = 0.9156$
$y = -0.0091x + 0.5833$
$R^2 = 0.7438$
$y = -0.0092x + 0.6797$
$R^2 = 0.8736$
$y = -0.0091x + 0.5833$
$R^2 = 0.7438$
$y = -0.0139x + 0.5077$
$R^2 = 0.8878$
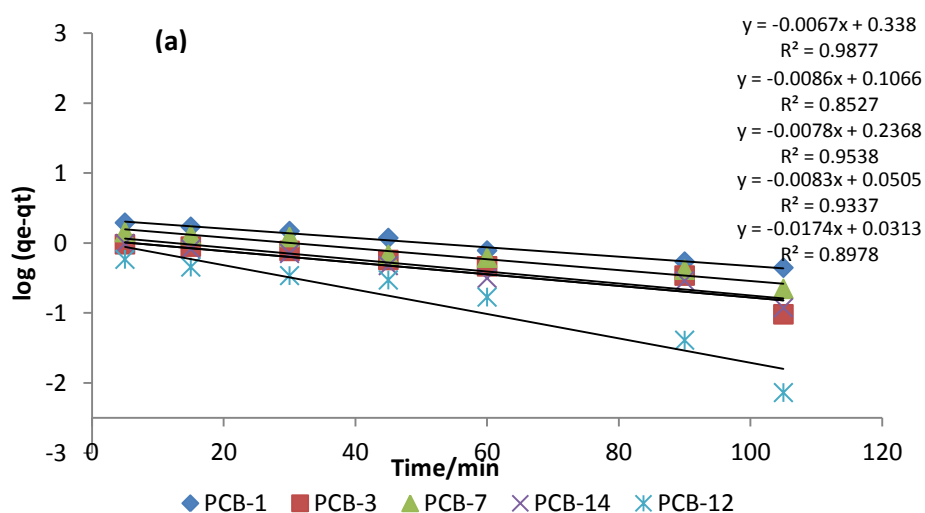
Figure 8.8: Pseudo-first order kinetics (a, b, c) of adsorption for PCB - 1, 3, 7, 14 and 12 onto PAC, GAC and EAC respectively.

(d)

$y = 0.0988x + 0.3925$
$R^2 = 0.9974$
$y = 0.0947x + 0.2629$
$R^2 = 0.9989$
$y = 0.0906x + 0.1664$
$R^2 = 0.9994$
$y = 0.0839x + 0.1199$
$R^2 = 0.9997$
$y = 0.0819x + 0.0665$
$R^2 = 0.9999$

177
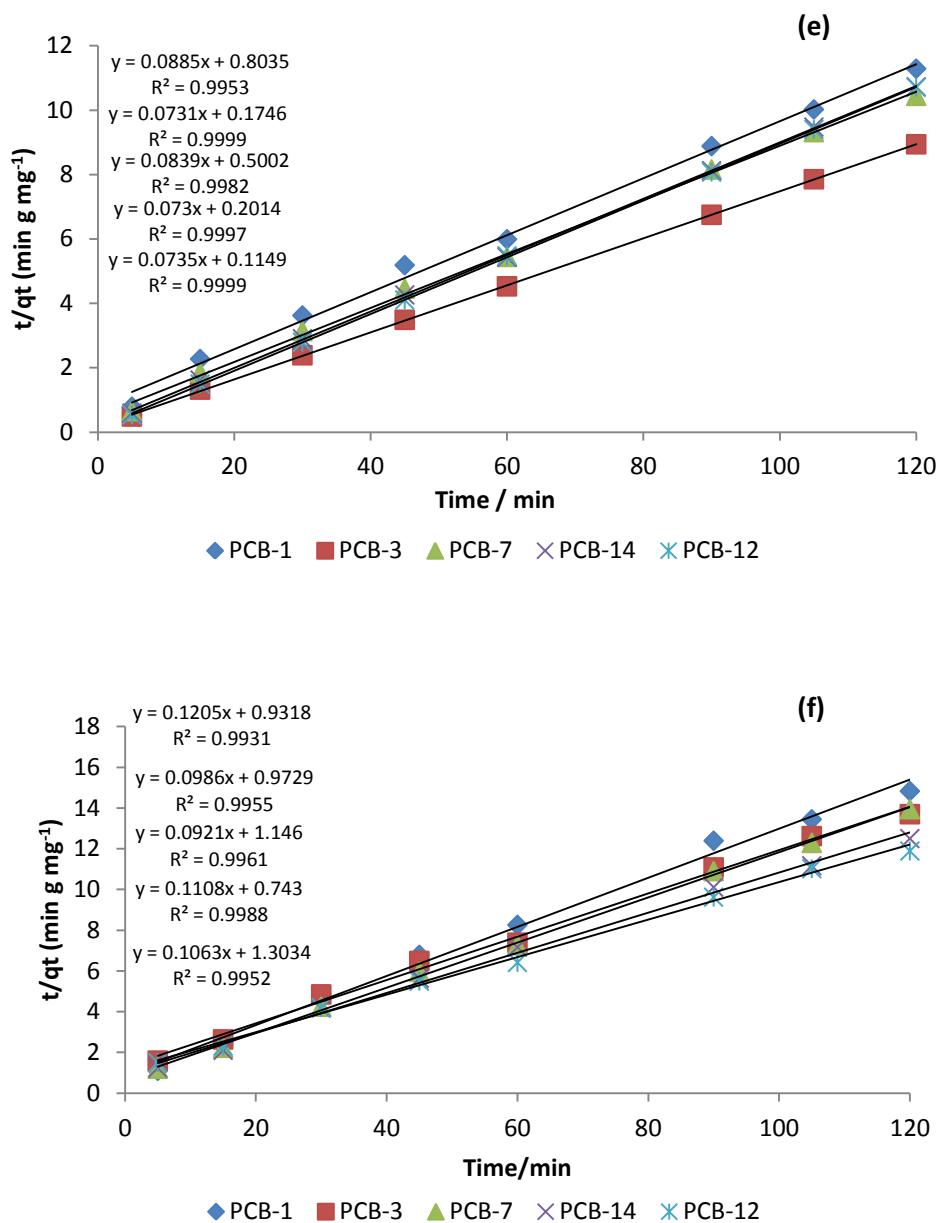
Figure 8.9: Pseudo-second order kinetics (d, e, f) of adsorption for PCB - 1, 3, 7, 14 and 12 onto PAC, GAC and EAC respectively.

First order kinetics is generally used to describe reversible reactions where equilibrium is established between the liquid and solid phases.[301] In second order kinetics, the adsorption process is controlled by chemical interactions which involve binding of the solute ions to the sorbent surface via covalent bonding (sharing or exchange of electrons) which is irreversible.[66] However, pseudo first-order and pseudo second-order kinetics are generally applied to describe the sorption of solute molecules to solid surfaces due to the effects of transport phenomena and chemical reactions which play a major role.[302] As shown in Figures 8.8 and 8.9, the

178

experimental data had a better fit to the pseudo second-order model as R^2 values obtained were $\geq$ 0.9974, 0.9953, 0.9931 for PAC, GAC and EAC respectively. This suggests that the sorption rates of PCBs onto the adsorbents were most likely controlled by the chemical process. The pseudo first-order model was not suitable to describe the adsorption process of PCBs onto the three sorbents as low correlation values were obtained. These findings were similar to previous studies where kinetics of PCBs onto mesoporous AC was found to follow pseudo second-order kinetics.[256] Further investigations were carried out on the spent ACs using FTIR analysis as described in Section 8.2.5 to confirm that interactions between the adsorbed molecules and the adsorbent was due to chemisorption. The FTIR spectra obtained is displayed in Figure 8.10.
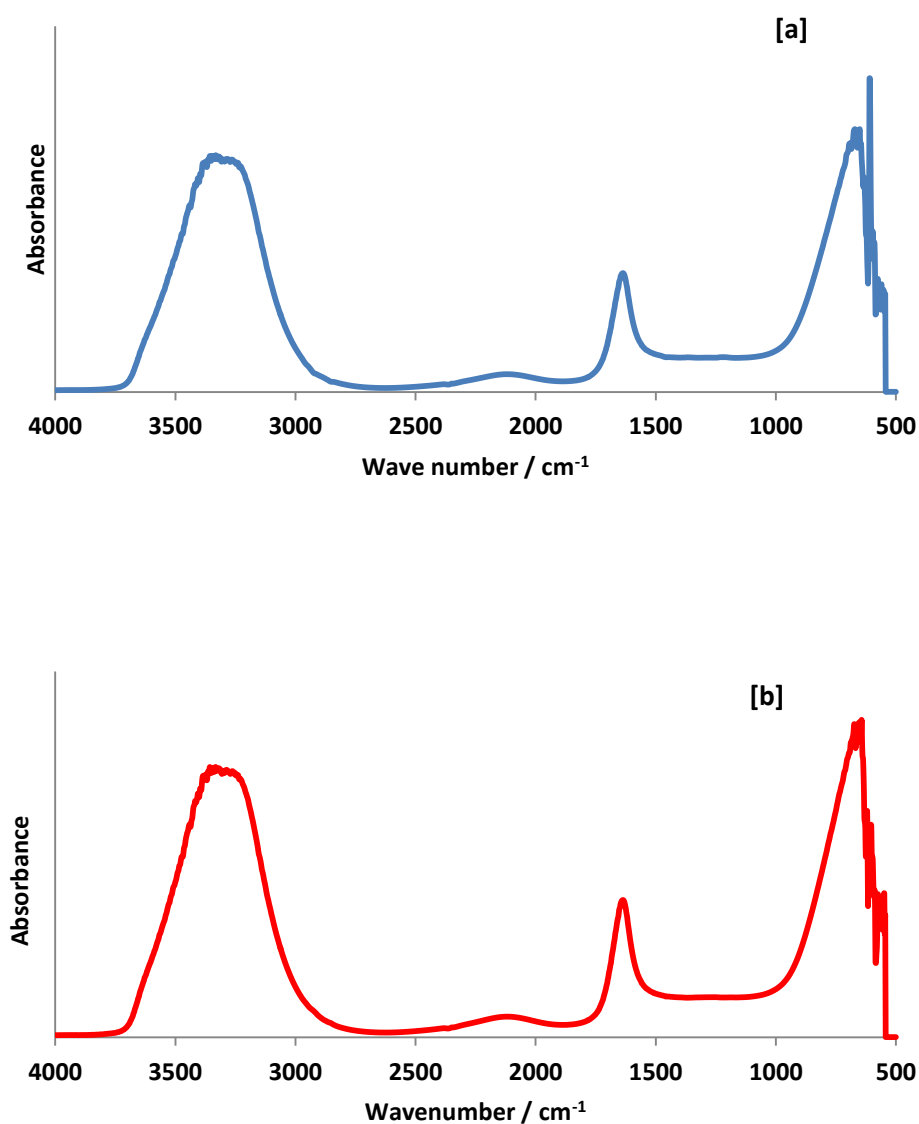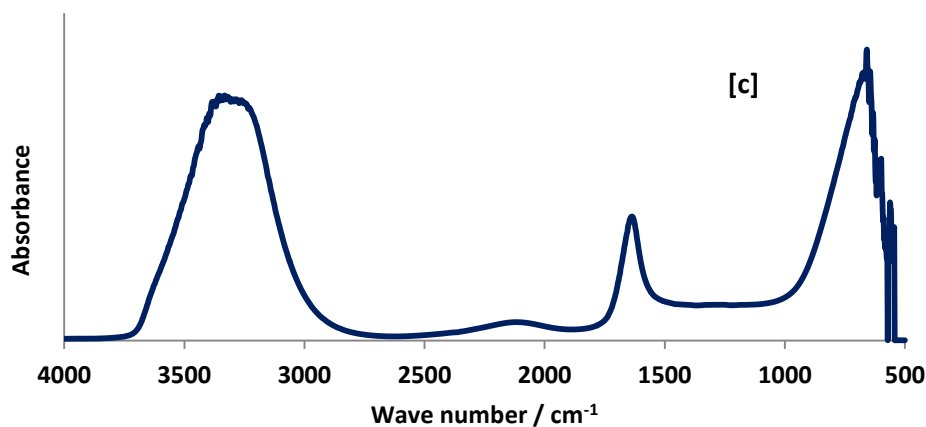
Figure 8.10: (a), (b) and (c); FTIR spectra obtained from supernatant after desorption of spent PAC, GAC and EAC with water respectively.

In physical adsorption, the solute molecules are held to the surface of the adsorbent by weak van der Waals forces such that adsorption is reversible and rapid.[67] The adsorbed molecules are not fixed to a site at the surface but rather move freely on the surface or within the interface such that monolayers or multilayers are formed.[67] In contrast to this, chemisorption is an irreversible process where chemical bonds are formed via electron sharing. The adsorbed molecules do not move freely on the surface or within the interface such that adsorption is limited to only specific sites on the surface; thereby resulting in the formation of monolayers.[66, 67]

As shown in the FTIR spectra displayed in Figure 8.10, the broad band at 3300 - 3400 cm^{-1} can be attributed to the –OH vibrational stretching of hydroxyl groups including hydrogen bonding of the water molecules. The absorption band at 1600 - 1800 cm^{-1} corresponds to the presence of C–O–C groups, C=O stretching of carbonyl groups or aromatic C–C bending vibrations on the surface of AC materials. The peak observed at 640 cm^{-1} corresponds to C–C and conjugated C=C bonds. This suggests that none of the PCB congeners adsorbed by ACs were desorbed by contact with distilled water as none of the absorption bands observed in the FTIR spectra was due to the presence of the PCB congeners; further confirming that the sorption of PCBs onto the three ACs was due to chemisorption and not physisorption.

8.3.6 Effect of solution pH on removal efficiency of ACs for PCB congeners

The effect of solution pH on the removal efficiency of ACs for PCBs was examined over a wide pH range of 3 - 11. The solution pH is an important parameter that can influence the sorption of PCBs onto ACs.[66, 266] ACs generally exhibit amphoteric behaviour in aqueous solutions depending on the surface group present.[271] Acidic groups generally undergo dissociation, donate their protons to the solution which results in a negatively charged surface (deprotonated).[271] In stark contrast to acidic groups, basic groups attract protons from the solution leaving the outer surface more oxidised than the inner surface (protonated).[271]

In general, organic molecules form positive ions at low pH values (higher H^+ ion concentration) and negative ions at high pH values in the liquid phase.[66] Therefore, the adsorption of organic molecules by AC is reportedly higher at lower pH as the negative charges at the surface are neutralised resulting in more active sites for adsorption and vice versa at higher pH.[66] In addition, neutral pH conditions are deemed to be favourable for sorption of organic molecules onto AC.[66] The results displayed in Figure 8.11 indicate that the removal efficiency of the three ACs was generally higher for PCBs at solution pH 3. This may be attributed to neutralisation of negative charges present at the surface of AC under acidic conditions; thereby resulting in more active adsorption sites and preferential sorption of PCB molecules onto the surface of AC. However, in contrast to PAC, a significant increase in sorption efficiency of GAC and EAC was observed for mono-*ortho* PCBs compared to non-*ortho* PCBs at solution pH 3. As the solution pH exceeded 7, a slight decrease in removal efficiency was observed for the three ACs. This may be associated with the introduction of oxygen containing groups resulting in excess OH^- ions and consequently the formation of water clusters which prevent preferential sorption of PCBs onto the surface of AC at higher pH. Nevertheless, the adsorption of non-*ortho* PCBs was generally high compared to mono-*ortho* PCBs regardless of solution pH; corresponding to the ability of non-*ortho* PCBs to easily assume planar conformations and achieve stronger π-π interactions with the three ACs.
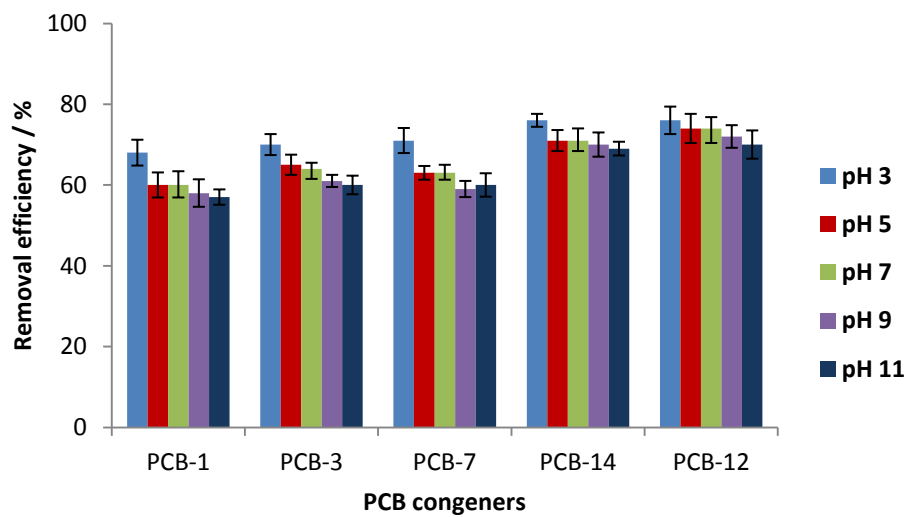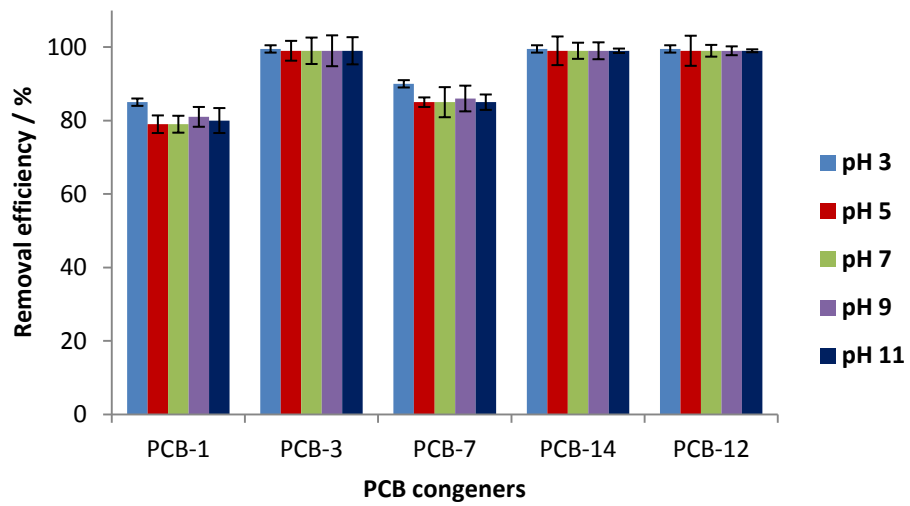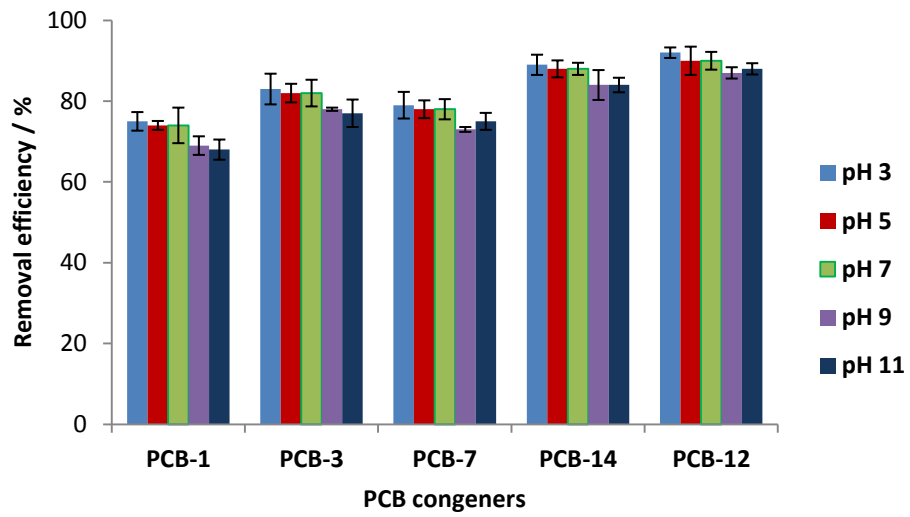
Figure 8.11: Effect of pH for removal efficiency of PCBs using (a) PAC, (b) GAC and (c) EAC.

8.3.7 Assessment of the performance of EAC in real samples

Based on the results obtained, EAC had the highest adsorption capacity for PCBs in aqueous solutions. Hence, its removal efficiency for PCBs in real water samples was examined using the water samples collected from Lagos, Nigeria as described in Section 8.2.7. Recovery factors of 0.33, 0.35, 0.41 and 0.40 for A5, A6, B4 and B5 were applied to final PCB concentrations obtained at equilibrium. The pH values of the water samples were 7.63, 7.96, 7.32 and 7.57 for A5, A6, B4 and B5 respectively. As mentioned earlier (Section 6.8), water samples were analysed to detect the presence of PCB congeners and none of the target PCBs were detected. The removal efficiency obtained for PCBs in real water samples (Figure 8.12) using EAC ranged from 64 - 75 % which was similar to results previously obtained; although a slight increase in the removal efficiency was observed for mono-*ortho* PCBs in real samples. This demonstrates that EAC can be satisfactorily used to remove PCBs from environmental water samples.
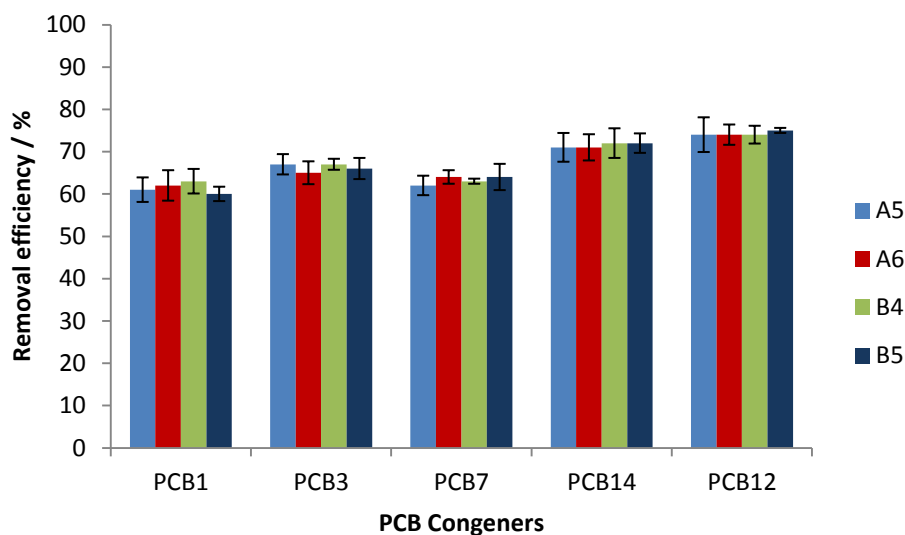

Figure 8.12: Removal efficiency of PCBs from real water samples using EAC.

8.4 Conclusion

The results obtained from this study show that the three ACs investigated were suitable adsorbents for the removal of PCBs from aqueous solutions with removal efficiencies ranging from 75 - 90 % and 79 - 99 % and 60 - 74 % respectively for PAC, GAC and EAC. However, in comparison to PAC and GAC where a significant

decrease in sorption efficiency was obtained as the concentration of the solution increased, only a slight decrease in performance was observed for PCBs using EAC. Equilibrium data obtained for the sorption of PCBs by the three ACs was well described by the Langmuir model indicating that monolayer adsorption occurred on a homogeneous surface containing a finite number of identical adsorption sites. EAC generally had the highest maximum adsorption capacity (35 mg/g) for the entire PCB congeners studied due to its high surface area and low surface oxygen content which resulted in stronger π-π interactions with the PCB congeners. Kinetic experiments showed that the adsorption processes of the entire PCB congeners onto the three ACs followed the pseudo-second order model with correlation co-efficients $\geq$ 0.9974, 0.9953 and 0.9931 for PAC, GAC and EAC respectively. An assessment of the effect of solution pH on the removal efficiency of the three ACs for PCBs in solution indicated that the highest sorption efficiency of PCBs onto ACs was obtained at solution pH 3. A slight decrease in removal efficiency of PAC and EAC was obtained for the entire PCB congeners as the solution pH increased. However, for GAC, a significant decrease in sorption efficiency was observed for mono-*ortho* PCBs compared to non-*ortho* PCBs as the solution pH increased. This could be ascribed to the formation of water clusters which reduce the sites available for sorption of PCB congeners. Based on the adsorption capacity (35 mg g^{-1}) obtained for EAC, its performance in real water samples was examined. The removal efficiency obtained was similar to previous performances demonstrating that EAC could be conveniently applied for the removal of PCBs from contaminated water samples with satisfactory results.

9. Conclusion and further work

9.1 Development of analytical methods for determination of PCBs in soil and water

GC-MS methods were developed for identifying and quantifying PCB congeners in solution. The developed methods provided a good resolution of the nineteen and five pre-selected PCB congener mixtures in 24 min and 5 min respectively. The calibration curves obtained were linear over the specified concentration range (20 - 60 ng μL^{-1}) as indicated by the correlation co-efficients obtained; ≥ 0.9901 for the nineteen PCB congeners and ≥ 0.9942 for the five PCB congeners; although some of the nineteen PCB congeners had R^2 values ≤ 0.9863. The calibration method obtained for the nineteen congeners was repeatable (≤ 4.9 %) and reproducible (≤ 7.7 %) with detection limits ranging from 1.25 - 15 ng μL^{-1}. Similarly, results obtained for the five PCB congeners were repeatable (≤ 2.27 %) with detection limits of 1.25 ng μL^{-1}.

The developed ASE method for extracting PCBs from soil samples gave average recoveries of 81 - 94 % with % RSD values ≤ 2.2 % for replicate analyses which was higher than recoveries obtained using the MAE method (68 - 75 %). In addition, this method eliminated the need for a lengthy post-extraction clean up step; thereby providing a method that's easier to apply than methods which are available. Soil samples collected from Lagos, Nigeria were screened for the nineteen target PCB congeners but none of the congeners were present. However, these samples were spiked with PCBs and the optimized method applied for PCB extractions which gave average recoveries of 60 - 101 % with % RSD values of 2.0 - 12.0 %; demonstrating that the method can be conveniently applied to screen and quantify soil samples contaminated with PCBs.

The extraction and preconcentration of PCBs from water samples was achieved using C18 (EC) SPE cartridges. This provided average recoveries of 41 - 49 % with a precision ≤ 4.3 % which were higher than recoveries obtained using florisil SPE cartridges (9 - 16 %). A further examination of PCB recoveries from water samples across different concentrations gave similar recoveries of 45 $\pm$ 3 %; indicating that a change in PCB concentration did not have any significant effect on recoveries obtained and could be applied to extract and preconcentrate PCBs present in contaminated water samples. A limitation of this study was the low aqueous solubility associated with PCBs which contributed to the low recoveries obtained.

Perhaps, the introduction of several steps and a solvent to further disperse PCBs in the solution could result in improved recoveries although this could be time consuming as well. Although none of the target PCB congeners were found in soil and water samples investigated, the results obtained demonstrate that the developed method can be readily employed for screening sites deemed to be potentially contaminated with PCBs both locally in Nigeria and globally.

9.2 Development of analytical techniques for remediation of PCBs in water samples

MCM-41 materials (as-syn and calc MCM-41) were successfully synthesised and evaluated for their ability to retain PCBs in aqueous solutions. However, both materials were not suitable adsorbents for sequestration of PCB congeners from aqueous solutions as none of the target congeners were successfully removed from aqueous solutions using these sorbents. Therefore an attempt was made to increase the sorbent mass and contact time but no significant improvement in performance of the MCM-41 materials for removal of PCB congeners from solution was obtained. Furthermore, the use of as-syn and calc Fe-GN materials as heterogeneous catalysts in the photo-Fenton process did not result in degradation of any of the target PCB congeners. This indicates that interactions between these adsorbents and PCB congeners were not strong enough to facilitate PCB removal from aqueous solutions. Perhaps, surface modification of these materials using specific functional groups to increase the hydrophobicity may be necessary to facilitate the selective removal of PCBs from aqueous solutions.

In stark contrast to results obtained using MCM-41 and Fe-GN materials, the three ACs (PAC, GAC and EAC) successfully removed PCB congeners from water as removal efficiencies of 75 - 90 %, 79 - 99 %, 60 - 74 % were obtained for PAC, GAC and EAC respectively. However, a decrease in removal efficiency was observed for PAC and GAC as the concentration of the aqueous solution increased compared to EAC where only a slight decrease in performance was observed. This could be attributed to the low surface oxygen content and high surface area of EAC compared to PAC and GAC. Nevertheless, the three ACs had higher removal efficiency for non-*ortho* PCBs than mono-*ortho* PCBs due to the ability of

non-*ortho* PCBs to assume planar configurations and achieve stronger π-π interactions with each AC.

An examination of the adsorption capacity of each AC for PCBs in aqueous solution showed that EAC had the highest adsorption capacity (35 mg/g) compared to PAC and GAC (29.3 and 30.4 mg g^{-1} respectively). In addition, the adsorption isotherms of the three ACs were well described by the Langmuir isotherms indicating that monolayer adsorption occurred between the liquid phase and sorbent phase. The kinetics of adsorption of each PCB congener onto the three ACs was best described by the pseudo second-order kinetic model which indicated that the sorption of each congener onto PAC, GAC and EAC was due to chemisorption. The three ACs were found to have the highest removal efficiencies at solution pH 3 which decreased slightly with an increase in solution pH. However, the decrease in removal efficiency of GAC was significantly higher for mono-*ortho* PCBs than non-*ortho* PCBs as the solution pH increased. Similar performance (64 - 75 %) was obtained for EAC when used to sequester PCBs from real water samples obtained from Lagos, Nigeria.

In general, the results obtained from this study indicate that EAC can be conveniently used in water treatment plants under mildly acidic to neutral conditions to facilitate the removal of PCBs from aqueous solutions. To the best of my knowledge, only few methods involving the use of AC to decontaminate water systems containing PCBs have been reported in literature.[252, 256] Therefore, the developed method serves as a viable and practical solution for remediation of water systems contaminated with PCBs globally since AC materials are readily available; although further investigations under a continuous flow system may be required.

9.3 Further work

In this study, none of the PCB congeners were sequestered from water via adsorption using MCM-41 materials or photodegraded using Fe-GN materials. Therefore, further studies could be carried out to modify MCM-41 or Fe-GN materials using specific functional groups which have the tendency to increase hydrophobicity and examine the feasibility of the modified materials to selectively remove PCB congeners from water.

Although ACs were efficient adsorbents for the removal of PCB congeners from the aqueous phase, their application on a large scale could be limited by high production costs and difficulty in regeneration often associated with capacity loss. Hence, further work could involve preparation of ACs using cheap precursors such as agricultural, industrial and domestic wastes to provide less costly and more sustainable ACs. In addition, other sustainable carbonaceous adsorbents can be explored for their potential to sequester PCBs from aqueous solutions. The type of surface functional groups present on AC is an important parameter that could influence the sorption of PCB congeners onto AC. Hence, further characterisation and investigations of the ACs could be conducted using specific methods to determine the type and amount of surface functional groups. This could be followed by an examination of the effect and kinetic implications of the surface pH on sorption of each PCB congener onto the studied ACs.

References

1. UNEP, *Guidelines for the Identification of PCBs and Materials Containing PCBs*, United Nations Environment Programme, Switzerland, 1999.
2. S. Safe, L. Safe and M. Mullin, *Journal of Agricultural and Food Chemistry*, 1985, **33**, 24-29.
3. C. J. George, G. F. Bennett, D. Simoneaux and W. J. George, *Journal of Hazardous Materials*, 1988, **18**, 113-144.
4. D. E. Metcalfe, G. Zukovs, D. Mackay and S. Paterson, in *Hazards, Decontamination, and Replacement of PCB: A Comprehensive Guide*, ed. J.-P. Crine, Springer US, Boston, MA, 1988, pp. 3-33.
5. EA, UK SHS Report , No.1, Environment Agency, Bristol, 2007.
6. UNEP, United Nations Environment Programme, Switzerland, 2002.
7. K. N. Dimou, T.-L. Su, R. I. Hires and R. Miskewitz, *Journal of Hazardous Materials*, 2006, **136**, 103-110.
8. M. D. Erickson, *Analytical Chemistry of PCB's* CRC Press, Boca Raton, 2nd edn., 2007.
9. J. P. Giesy and K. Kannan, *Crit. Rev. Toxicol.*, 1998, **28**, 511-569.
10. IPCS, , Concise International Chemical Assessment Document (CICAD), No.55, World Health Organization / International Programme on Chemical Safety,, Geneva, 2003.
11. K. Ballschmiter and M. Zell, *Fresenius Zeitschrift fur Analytische Chemie* 1980, **302**.
12. ASTDR, US Department of Health and Human Services, Agency for Toxic substances and Disease Registry, , Atlanta, GA, 2000.
13. C. A. Oliveira Ribeiro, Y. Vollaire, E. Coulet and H. Roche, *Environmental Pollution*, 2008, **153**, 424-431.
14. S. Afful, J. A. M. Awudza, S. K. Twumasi and S. Osae, *Chemosphere*, 2013, **93**, 1556-1560.
15. S. J. Harrad, A. P. Sewart, R. Alcock, R. Boumphrey, V. Burnett, R. Duarte-Davidson, C. Halsall, G. Sanders, K. Waterhouse, S. R. Wild and K. C. Jones, *Environmental Pollution*, 1994, **85**, 131-146.
16. L. Guo, B. Zhang, K. Xiao, Q. Zhang and M. Zheng, *Journal of Environmental Sciences*, 2009, **21**, 468-473.
17. P. Mandal, *Journal of Comparative Physiology B*, 2005, **175**, 221-230.
18. M. Van den Berg, L. Birnbaum and M. Denison, *Journal of Toxicology Science*, 2006, **93**, 223 - 241.
19. E. J. Willman, J. B. Manchester-Neesvig and D. E. Armstrong, *Environmental Science & Technology*, 1997, **31**, 3712-3718.
20. EA, *Soil Guideline values for dioxins, furans and dioxin -like PCBs in soil*, Environment Agency, 2009
21. DEFRA, Consultation document , No. 55 , Department for Environment, Food and Rural Affairs,, London, 2002.
22. DEFRA, Report NCEN/ED48412/R1 , Department for Environment, Food and Rural Affairs, London, 2006a.
23. G. F. Fries, *Journal of Animal Science*, 1995, **73**, 1639-1650.
24. M. E. Harnly, M. X. Petreas, J. Flattery and L. R. Goldman, *Environmental Science & Technology*, 2000, **34**, 1143-1149.
25. P. R. S. Kodavanti, T. R. Ward, E. C. Derr-Yellin, W. R. Mundy, A. C. Casey, B. Bush and H. A. Tilson, *Toxicology and Applied Pharmacology*, 1998, **153**, 199-210.

26. S. Tanabe, *Environmental Pollution*, 1988, **50**, 5-28.
27. R. E. Alcock, A. E. Johnston, S. P. McGrath, M. L. Berrow and K. C. Jones, *Environmental Science & Technology*, 1993, **27**, 1918-1923.
28. K. Breivik, A. Sweetman, J. M. Pacyna and K. C. Jones, *Science of The Total Environment*, 2002, **290**, 181-198.
29. V. Notarianni, M. Calliera, P. Tremolada, A. Finizio and M. Vighi, *Chemosphere*, 1998, **37**, 2839-2845.
30. P. Ruiz, O. Faroon, C. J. Moudgal, H. Hansen, C. T. De Rosa and M. Mumtaz, *Toxicology Letters*, 2008, **181**, 53-65.
31. M. Biterna and D. Voutsa, *Environment International*, 2005, **31**, 671-677.
32. U. G. Ahlborg, A. Brouwer, M. A. Fingerhut, J. L. Jacobson, S. W. Jacobson, S. W. Kennedy, A. A. F. Kettrup, J. H. Koeman, H. Poiger, C. Rappe, S. H. Safe, R. F. Seegal, T. Jouko and M. van den Berg, *European Journal of Pharmacology: Environmental Toxicology and Pharmacology*, 1992, **228**, 179-199.
33. E. Priha, S. Hellman and J. Sorvari, *Chemosphere*, 2005, **59**, 537-543.
34. S. E. Manahan, *Fundamentals of environmental chemistry*, Boca Raton : CRC Press, 2009.
35. M. Radojevic and V. N. Bashkin, *Practical Environmental Analysis*, The Royal Society of Chemistry, Cambridge, UK;, 2006.
36. C. Backe, I. T. Cousins and P. Larsson, *Environmental Pollution*, 2004, **128**, 59-72.
37. T. Harner, D. Mackay and K. C. Jones, *Environmental Science & Technology*, 1995, **29**, 1200-1209.
38. M. Hippelein and M. S. McLachlan, *Environmental Science & Technology*, 2000, **34**, 3521-3526.
39. I. T. Cousins and K. C. Jones, *Environmental Pollution*, 1998, **102**, 105-118.
40. I. T. Cousins, B. Gevao and K. C. Jones, *Chemosphere*, 1999, **39**, 2507-2518.
41. F. Wania and D. MacKay, *Environmental Science & Technology*, 1996, **30**, 390A-396A.
42. S. N. Meijer, W. A. Ockenden, A. Sweetman, K. Breivik, J. O. Grimalt and K. C. Jones, *Environmental Science & Technology*, 2003, **37**, 667-672.
43. S. E. Koslowski, C. D. Metcalfe, R. Lazar and G. Douglas Haffner, *Journal of Great Lakes Research*, 1994, **20**, 260-270.
44. X. Zhao, M. Zheng, B. Zhang, Q. Zhang and W. Liu, *Science of The Total Environment*, 2006, **368**, 744-752.
45. H. Iwata, S. Tanabe, N. Sakai, A. Nishimura and R. Tatsukawa, *Environmental Pollution*, 1994, **85**, 15-33.
46. L. Manodori, A. Gambaro, I. Moret, G. Capodaglio, W. R. L. Cairns and P. Cescon, *Chemosphere*, 2006, **62**, 449-458.
47. R. Duarte-Davidson and K. C. Jones, *Science of The Total Environment*, 1994, **151**, 131-152.
48. U. G. Ahlborg, G. C. Becking, L. S. Birnbaum, A. Brouwer, H. Derks, M. Feeley, G. Golor, A. Hanberg, J. C. Larsen, A. K. D. Liem, S. H. Safe, C. Schlatter, F. Waern, M. Younes and E. Yrjänheikki, *Chemosphere*, 1994, **28**, 1049-1067.
49. J.-y. Zhang, L.-m. Qiu, J. He, Y. Liao and Y.-m. Luo, *Journal of Environmental Sciences*, 2007, **19**, 338-342.
50. M. Dömötörová, Z. Stachová Sejáková, A. Kočan, K. Čonka, J. Chovancová and A. Fabišiková, *Chemosphere*, 2012, **89**, 480-485.
51. D. Muir and E. Sverko, *Anal Bioanal Chem*, 2006, **386**, 769-789.

52. O. Mikes, P. Cupr, S. Trapp and J. Klanova, *Environmental Pollution*, 2009, **157**, 488-496.

53. UNEP, *Stockholm Convention on Persistent Organic Pollutants*, Geneva, 2011.

54. M. Frignani, R. Piazza, L. G. Bellucci, N. H. Cu, R. Zangrando, S. Albertazzi, I. Moret, S. Romano and A. Gambaro, *Chemosphere*, 2007, **67**, 1786-1793.

55. M. Van den Berg, L. Birnbaum, A. T. C. Bosveld, B. Brunstrom, P. Cook, M. Feeley, J. P. Giesy, A. Hanberg, R. Hasegawa, S. W. Kennedy, T. Kubiak, J. C. Larsen, F. X. R. van Leeuwen, A. K. D. Liem, C. Nolt, R. E. Peterson, L. Poellinger, S. Safe, D. Schrenk, D. Tillitt, M. Tysklind, M. Younes, F. Waern and T. Zacharewski, *Environmental Health Perspectives*, 1998, **106**, 775-792.

56. D. Onozuka, T. Yoshimura, S. Kaneko and M. Furue, *American Journal of Epidemiology*, 2009, **169**, 86-95.

57. M. Furue, T. Uenotsuchi, K. Urabe, T. Ishikawa and M. Kuwabara, *Journal of Dermatological Science Supplement*, 2005, **1**, S3-S10.

58. D.-K. Soong and Y.-C. Ling, *Chemosphere*, 1997, **34**, 1579-1586.

59. A. Bernard, F. Broeckaert, G. De Poorter, A. De Cock, C. Hermans, C. Saegerman and G. Houins, *Environmental Research*, 2002, **88**, 1-18.

60. A. Bernard and S. Fierens, *International Journal of Toxicology*, 2002, **21**, 333-340.

61. A. Covaci, S. Voorspoels, P. Schepens, P. Jorens, R. Blust and H. Neels, *Environmental Toxicology and Pharmacology*, 2008, **25**, 164-170.

62. S. Voorspoels, A. Covaci and H. Neels, *Environmental Toxicology and Pharmacology*, 2008, **25**, 179-182.

63. E. Worch, *Adsorption Technology in Water Treatment, Fundamentals, Processes, and Modeling*, 2012.

64. F. Rouquerol, J. Rouquerol, K. S. W. Sing, G. Maurin and P. Llewellyn, in *Adsorption by Powders and Porous Solids (Second Edition)*, ed. F. R. R. S. W. S. L. Maurin, Academic Press, Oxford, 2014, pp. 1-24.

65. F. o. Rouquerol, *Adsorption by powders and porous solids : principles, methodology, and applications*, San Diego : Academic Press, 1999.

66. F. Cecen and O. Aktas, *Activated Carbon for Water and Wastewater Treatment: Integration of Adsorption and Biological Treatment*, Wiley, 2011.

67. Y. C. Sharma, *A Guide to the Economic Removal of Metals from Aqueous Solutions*, United States: John Wiley & Sons Inc, 2012.

68. K. Ishizaki, S. Komarneni and M. Nanko, *Porous Materials : process technology and applications*, Springer Science and Business Applications, US, 1998.

69. D. O. Cooney, *Adsorption Design for Waste water Treatment*, Lewis Publishers, Boca Raton Florida.

70. D. M. Ruthven, *Principles of Adsorption and Adsorption Processes*, John Wiley & Sons, Inc, Canada, 1984.

71. B. M. Lok, T. R. Cannan and C. A. Messina, *Zeolites*, 1983, **3**, 282-291.

72. P. Christophliemk, P. Gerike and M. Potokar, in *Detergents*, ed. N. T. Oude, Springer Berlin Heidelberg, Berlin, Heidelberg, 1992, pp. 205-228.

73. Z. A. Alothman, *Materials*, 2012, **5**, 2874-2902.

74. L. Mahoney and R. T. Koodali, *Materials*, 2014, **7**, 2697-2746.

75. R. M. Barrer, *Zeolites and clay minerals as sorbents and molecular sieves*, Academic press, 1978.

76. D. W. Breck, W. G. Eversole, R. M. Milton, T. B. Reed and T. L. Thomas, *Journal of the American Chemical Society*, 1956, **78**, 5963-5972.

77. P. Behrens, *Adv. Mater.*, 1993, **5**, 127-132.
78. R. Szostak, *Molecular Sieves : Principles of Synthesis and Identification*, Springer, New York, 1989.
79. J. S. Beck and J. C. Vartuli, *Current Opinion in Solid State and Materials Science*, 1996, **1**, 76-87.
80. H. Ferch, *Chemie Ingenieur Technik*, 1980, **52**, 366-366.
81. P. Cool and E. F. Vansant, in *Synthesis*, Springer Berlin Heidelberg, Berlin, Heidelberg, 1998, pp. 265-288.
82. R. K. Iler, *The chemistry of silica : solubility, polymerization, colloid and surface properties, and biochemistry*, New York : Wiley, 1979.
83. S. Lowell, J. E. Shields, M. A. Thomas and M. Thommes, *Characterization of Porous Solids and Powders: Surface Area, Pore Size and Density*, Springer Science and Business Media, LLC, U.S.A, 2004.
84. R.Dales, L.Liu, A.J.Wheeler and N.L.Gilbert, *Canadian Medical Association*, 2008, **147-152**.
85. J. r. U. Keller, *Gas adsorption equilibria : experimental methods and adsorptive isotherms*, New York : Springer, 2005.
86. K. Sing and R. Williams, *Adsorption Science & Technology*, 2004, **22**, 773-782.
87. K. S. W. Sing, D. H. Everett, R. A. W. Haul, L. Moscou, R. A. Pierotti, J. Rouquerol and T. Siemieniewska, *Pure Appl. Chem.*, 1985, **57**, 603-619.
88. M. Thommes, K. Kaneko, V. Neimark Alexander, P. Olivier James, F. Rodriguez-Reinoso, J. Rouquerol and S. W. Sing Kenneth, in *Pure Appl. Chem.*, 2015, vol. 87, p. 1051.
89. S. Brunauer, P. H. Emmett and E. Teller, *Journal of the American Chemical Society*, 1938, **60**, 309-319.
90. K. S. W. Sing, in *Adsorption by Powders and Porous Solids (Second Edition)*, ed. F. R. R. S. W. S. L. Maurin, Academic Press, Oxford, 2014, pp. 237-268.
91. E. P. Barrett, L. G. Joyner and P. P. Halenda, *Journal of the American Chemical Society*, 1951, **73**, 373-380.
92. J. M. Thomas, *Principles and practice of heterogeneous catalysis*, Weinheim ; New York : VCH, 1997.
93. H. Naono, M. Hakuman, T. Tanaka, N. Tamura and K. Nakai, *Journal of Colloid and Interface Science*, 2000, **225**, 411-420.
94. B. C. Smith, *Fundamentals of Fourier transform infrared spectroscopy* Boca Raton, Fla. : CRC Press, 2011.
95. F. Rouessac and A. Rouessac, *Chemical Analysis: Modern Instrumentation Methods and Techniques, 2nd Edition*, John Wiley & Sons, Ltd, 2007.
96. *IR Spectroscopy, Intensive Seminars in Modern Chemistry*, Columbia University, New York, 2007.
97. P. R. Griffiths, *Fourier transform infrared spectrometry* Hoboken, N.J. : Wiley-Interscience ; Chichester : John Wiley distributor, 2007.
98. M. Milosevic, John Wiley & Sons Inc, Hokoben, New Jersey, 2012.
99. F. Rezaei, A. Bidari, A. P. Birjandi, M. R. Milani Hosseini and Y. Assadi, *Journal of Hazardous Materials*, 2008, **158**, 621-627.
100. W. Kemp, *Organic spectroscopy*, Basingstoke : Macmillan, 1991.
101. M. F. Atitar, H. Belhadj, R. Dillert and D. W. Bahnemann, *The Relevance of ATR-FTIR Spectroscopy in Semiconductor Photocatalysis*, 2015.
102. G. D. Christian, *Analytical chemistry*, Hoboken, NJ : Wiley, 2004.
103. M. Thompson, *AMC Technical Briefs, The Royal Society of Chemistry, London*, 2008.

104. G. D. Christian, *Analytical chemistry*, New York : Wiley & Sons, 1994.
105. J. A. Dean, *Extraction techniques in analytical sciences*, Wiley, Chichester, West Sussex, U.K. ;, 2009.
106. E. M. Thurman, *Solid-phase extraction : principles and practice*, New York : Wiley, 1998.
107. N. J. K. Simpson, *Solid-Phase Extraction: Principles, techniques and Applications*, Marcel Dekker Inc, New York, 2000.
108. S. Mitra, *Sample Preparation Techniques in Analytical Chemistry*, John Wiley & Sons, Canada, 2003.
109. A. Żwir-Ferenc and M. b. c. p. g. p. Biziuk, *Polish Journal of Environmental Studies*, 2006, **15**, 677-690.
110. P. Lucci, D. Pacetti, N. G. Frega and O. Núñez, *Current Trends in Sample Treatment Techniques for Environmental and Food Analysis*, 2012.
111. L. Devanand, V. Dutt, N. Kirk and E. John, in *Oil Extraction and Analysis*, AOCS Publishing, 2004.
112. B. E. Richter, B. A. Jones, J. L. Ezzell, N. L. Porter, N. Avdalovic and C. Pohl, *Analytical Chemistry*, 1996, **68**, 1033-1039.
113. Y. Abrha and D. Raghavan, *Journal of Hazardous Materials*, 2000, **80**, 147-157.
114. A. Mitra, A. Bhaumik and B. K. Paul, *Microporous and Mesoporous Materials*, 2008, **109**, 66-72.
115. V. Camel, *Analyst*, 2001, **126**, 1182-1193.
116. J. L. Luque-García, in *Encyclopedia of Analytical Science (Second Edition)*, eds. A. Townshend and C. Poole, Elsevier, Oxford, 2005, pp. 591-597.
117. W. Routray and V. Orsat, in *Natural Products*, eds. K. G. Ramawat and J.-M. Mérillon, Springer Berlin Heidelberg, 2013, pp. 2013-2045.
118. V. Camel, *TrAC Trends in Analytical Chemistry*, 2000, **19**, 229-248.
119. P. Veggi, J. Martinez and M. A. Meireles, in *Microwave-assisted Extraction for Bioactive Compounds*, eds. F. Chemat and G. Cravotto, Springer US, 2013, pp. 15-52.
120. V. Lopez-Avila, *Critical Reviews in Analytical Chemistry*, 1999, **29**, 195-230.
121. E. Destandau, T. Michel and C. Elfakir, in *Natural Product Extraction: Principles and Applications*, The Royal Society of Chemistry, 2013, pp. 113-156.
122. B. Kaufmann and P. Christen, *Photochemical Analysis*, 2002, **105-113**.
123. O. Sticher, *Natural Product Reports*, 2008, **25**, 517-554.
124. H. M. McNair, *Basic gas chromatography*, New York : Wiley, 1998.
125. S. O. David, Z. E. Perton and F. G. Kitson, *Gas Chromatography and Mass Spectrometry : A Practical Guide*, Elsevier, Oxford, UK;, 2011.
126. *Gas chromatography : a practical approach*, Oxford : IRL at Oxford University Press, 1993.
127. *Gas chromatography* S.l. : Elsevier, 2012.
128. *The sol-gel handbook* Weinheim, Germany : Wiley-VCH, 2015.
129. *Modern Practice of Gas Chromatography*, Wiley - Blackwell, New Jersey, 2004.
130. *Analytical chemistry : an introduction*, Fort Worth : Saunders College Pub., 2000.
131. J. J. van Deemter, F. J. Zuiderweg and A. Klinkenberg, *Chemical Engineering Science*, 1956, **5**, 271-289.
132. M. C. Mc Master, *GC/MS : A Practical User's Guide*, Wiley, Hoboken, New Jersey, 2008.
133. J. H. Gross, *Mass Spectrometry*, Springer, Heidelberg, 2011.

134. E. d. Hoffmann and V. Stroobant, *Mass Spectrometry : Principles and Applications*, Wiley, Chichester, West Sussex, England, 2007.

135. O. D. Sparkman, *Introduction to Mass Spectrometry: Instrumentation, Applications and Strategies for Data Application*, Wiley Blackwell, Chichester, West Sussex, England, 2007.

136. F. G. Kitson, B. S. Larsen and C. N. McEwen, *Gas Chromatography and Mass Spectrometry : A Practical Guide*, Academic Press, Inc, U.S.A, 1996.

137. H.-J. Hübschmann, *Handbook of GC/MS : fundamentals and applications*, Weinheim : Wiley-VCH ; Chichester : John Wiley distributor, 2007.

138. P. Gates, *Gas chromatography - mass spectrometry* University of Bristol, England, 2014.

139. A. Cachada, L. V. Lopes, A. S. Hursthouse, M. Biasioli, H. Grcman, E. Otabbong, C. M. Davidson and A. C. Duarte, *Environmental Pollution*, 2009, **157**, 511-518.

140. D.-G. Wang, M. Yang, H.-L. Jia, L. Zhou and Y.-F. Li, *Chemosphere*, 2008, **73**, 38-42.

141. H. B. Zhang, Y. M. Luo, M. H. Wong, Q. G. Zhao and G. L. Zhang, *Geoderma*, 2007, **138**, 244-251.

142. W.-L. Ma, Y.-F. Li, D.-Z. Sun and H. Qi, *Archives of Environmental Contamination and Toxicology*, 2009, **57**, 670-678.

143. S. Wu, X. Xia, L. Yang and H. Liu, *Chemosphere*, 2011, **82**, 732-738.

144. J. M. Armitage, M. Hanson, J. Axelman and I. T. Cousins, *Science of The Total Environment*, 2006, **371**, 344-352.

145. C. S. Creaser, A. R. Fernandes, S. J. Harrad, T. Hurst and E. A. Cox, *Chemosphere*, 1989, **19**, 1457-1466.

146. A. Cachada, P. Pato, T. Rocha-Santos, E. F. da Silva and A. C. Duarte, *Science of The Total Environment*, 2012, **430**, 184-192.

147. L. Turrio-Baldassarri, V. Abate, S. Alivernini, C. L. Battistelli, S. Carasi, M. Casella, N. Iacovella, A. L. Iamiceli, A. Indelicato, C. Scarcella and C. La Rocca, *Chemosphere*, 2007, **67**, 1822-1830.

148. K. C. Jones, *Chemosphere*, 1989, **18**, 1665-1672.

149. B. Kumar, S. Kumar and C. S. Sharma, *Journal of Xenobiotics*, 2012, **2**.

150. S. Sporring, S. Bøwadt, B. Svensmark and E. Björklund, *Journal of Chromatography A*, 2005, **1090**, 1-9.

151. F. Wong, M. Robson, M. L. Diamond, S. Harrad and J. Truong, *Chemosphere*, 2009, **74**, 404-411.

152. A. Jamshidi, S. Hunter, S. Hazrati and S. Harrad, *Environmental Science & Technology*, 2007, **41**, 2153-2158.

153. Z. Li, S. Kong, L. Chen, Z. Bai, Y. Ji, J. Liu, B. Lu, B. Han and Q. Wang, *Chemosphere*, 2011, **85**, 494-501.

154. L. Chen, X. Peng, Y. Huang, Z. Xu, B. Mai, G. Sheng, J. Fu and X. Wang, *Archives of Environmental Contamination and Toxicology*, 2009, **57**, 437-446.

155. H. Hou, L. Zhao, J. Zhang, Y. F. Xu, Z. G. Yan, L. P. Bai and F. S. Li, *Environ Sci Pollut Res*, 2013, **20**, 3366-3380.

156. G. J. Hu, S. L. Chen and Y. G. Zhao, *Bulletin of Environmental Contamination & Toxicology*, 2009, **82**, 48-54.

157. L. Morselli, M. Sabbioni, S. Zappoli and G. Quattroni, *Fresenius Environ. Bull.*, 1995, **4**, 463-468.

158. E. A. Mamontova, A. A. Mamontov, E. N. Tarasova, M. I. Kuzmin, D. Ganchimeg, M. Y. Khomutova, O. Gombosuren and E. Ganjuurjav, *Environmental Pollution*, 2013, **182**, 424-429.

159. *BS EN 10390:2005; Soil quality - Determination of pH.*
160. *BS EN 12880:2000; Characterisation of sludges. Determination of dry residue and water content.*
161. P. Wang, Q. Zhang, Y. Wang, T. Wang, X. Li, L. Ding and G. Jiang, *Analytica Chimica Acta*, 2010, **663**, 43-48.
162. A. H. Knap and M. Kaiser, *The Long Range Atmospheric Transport of Natural and Contaminant Substances*, Kluwer Academic Publishers, U.S.A.
163. S. Zhang, Q. Zhang, S. Darisaw, O. Ehie and G. Wang, *Chemosphere*, 2007, **66**, 1057-1069.
164. Z. Zhang, J. Huang, G. Yu and H. Hong, *Environmental Pollution*, 2004, **130**, 249-261.
165. K. Li, G.-f. Zhao, H.-d. Zhou, M. Zeng, B.-h. Liao, Z.-y. Wu, P.-w. Zhang and H. Hao, *Huanjing Kexue*, 2012, **33**, 1676-1681.
166. K. Li, G.-f. Zhao, H.-d. Zhou, M. Zeng, B.-h. Liao, Z.-y. Wu, P.-w. Zhang and M. Liu, *Huanjing Kexue*, 2012, **33**, 2574-2579.
167. Z. L. Zhang, H. S. Hong, J. L. Zhou, J. Huang and G. Yu, *Chemosphere*, 2003, **52**, 1423-1430.
168. J. Ge, M. Liu, X. Yun, Y. Yang, M. Zhang, Q. X. Li and J. Wang, *Chemosphere*, 2014, **103**, 256-262.
169. L. Wolska, K. Galer, T. Górecki and J. Namieśnik, *Talanta*, 1999, **50**, 985-991.
170. Y. Yang, D. J. Miller and S. B. Hawthorne, *Journal of Chromatography A*, 1998, **800**, 257-266.
171. X. Shi, Z. Tang, A. Sun, L. Zhou, J. Zhao, D. Li, J. Chen and D. Pan, *Journal of Chromatography B*, 2014, **972**, 58-64.
172. R. Westbom, L. Thörneby, S. Zorita, L. Mathiasson and E. Björklund, *Journal of Chromatography A*, 2004, **1033**, 1-8.
173. S. Zorita, R. Westbom, Th, Ouml, L. Rneby, Bj, Ouml, E. Rklund and L. Mathiasson, *Analytical Sciences*, 2006, **22**, 1455-1459.
174. Y. Lei, M. He, B. Chen and B. Hu, *Talanta*, 2016, **150**, 310-318.
175. F. Hoffmann, M. Cornelius, J. Morell and M. Fröba, *Angewandte Chemie International Edition*, 2006, **45**, 3216-3251.
176. C. T. Kresge, M. E. Leonowicz, W. J. Roth, J. C. Vartuli and J. S. Beck, *Nature*, 1992, **359**, 710.
177. J. S. Beck, J. C. Vartuli, W. J. Roth, M. E. Leonowicz, C. T. Kresge, K. D. Schmitt, C. T. W. Chu, D. H. Olson, E. W. Sheppard, S. B. McCullen, J. B. Higgins and J. L. Schenkler, *J. Am. Chem. Soc.*, 1992, **114**, 10835.
178. J. Wen and G. L. Wilkes, *Chemistry of Materials*, 1996, **8**, 1667-1681.
179. P. A. Mangrulkar, S. P. Kamble, J. Meshram and S. S. Rayalu, *Journal of Hazardous Materials*, 2008, **160**, 414-421.
180. P. Prarat, C. Ngamcharussrivichai, S. Khaodhiar and P. Punyapalakul, *Journal of Hazardous Materials*, 2011, **192**, 1210-1218.
181. M. Ghiaci, A. Abbaspur, R. Kia and F. Seyedeyn-Azad, *Separation and Purification Technology*, 2004, **40**, 217-229.
182. A. Sayari, S. Hamoudi and Y. Yang, *Chemistry of Materials*, 2005, **17**, 212-216.
183. C. J. Brinker and G. W. Scherer, *Sol Gel Science : The Physics and Chemistry of Sol Gel Processing*, Academic Press, San Diego, 1990.
184. *Handbook of Sol-Gel Science and Technology*, Springer US, 2005.
185. *Porous materials*, Chichester, West Sussex, U.K. : Wiley, 2011.
186. P. T. Tanev and T. J. Pinnavaia, *Science*, 1995, **267**, 865-867.

187. J. García-Martínez, P. Brugarolas and S. Domínguez-Domínguez, *Microporous and Mesoporous Materials*, 2007, **100**, 63-69.
188. S. Y. Chen, S. H. Hu and H. Y. HUANG, Google Patents, 2012.
189. M. Dubois, T. Gulik-Krzywicki and B. Cabane, *Langmuir*, 1993, **9**, 673-680.
190. T. Brennan, S. J. Roser, S. Mann and K. J. Edler, *Chemistry of Materials*, 2002, **14**, 4292-4299.
191. C. C. Egger, M. W. Anderson, G. J. T. Tiddy and J. L. Casci, *Physical Chemistry Chemical Physics*, 2005, **7**, 1845-1855.
192. Y. Wan and Zhao, *Chemical Reviews*, 2007, **107**, 2821-2860.
193. L. T. Gibson, *Chemical Society Reviews*, 2014, **43**, 5173-5182.
194. P. T. Tanev and T. J. Pinnavaia, *Chemistry of Materials*, 1996, **8**, 2068-2079.
195. S. A. Bagshaw and I. J. Bruce, *Microporous and Mesoporous Materials*, 2008, **109**, 199-209.
196. C.-Y. Chen, H.-X. Li and M. E. Davis, *Microporous Materials*, 1993, **2**, 17-26.
197. M. T. J. Keene, R. D. M. Gougeon, R. Denoyel, R. K. Harris, J. Rouquerol and P. L. Llewellyn, *Journal of Materials Chemistry*, 1999, **9**, 2843-2849.
198. G. Temtsin, T. Asefa, S. Bittner and G. A. Ozin, *Journal of Materials Chemistry*, 2001, **11**, 3202-3206.
199. A. Doyle and B. K. Hodnett, *Microporous and Mesoporous Materials*, 2003, **58**, 255-261.
200. M. A. Wahab, Kim, II and C.-S. Ha, *Microporous and Mesoporous Materials*, 2004, **69**, 19-27.
201. P. Kumar, J. Ida, S. Kim, V. V. Guliants and J. Y. S. Lin, *Journal of Membrane Science*, 2006, **279**, 539-547.
202. Y. Xia, Z. Yang and R. Mokaya, *The Journal of Physical Chemistry B*, 2004, **108**, 19293-19298.
203. S. Kawi and M. W. Lai, *AIChE Journal*, 2002, **48**, 1572-1580.
204. L. Huang, S. Kawi, C. Poh, K. Hidajat and S. C. Ng, *Talanta*, 2005, **66**, 943-951.
205. B. Tian, X. Liu, C. Yu, F. Gao, Q. Luo, S. Xie, B. Tu and D. Zhao, *Chemical Communications*, 2002, 1186-1187.
206. U. Ciesla and F. Schüth, *Microporous and Mesoporous Materials*, 1999, **27**, 131-149.
207. B. P. Kelleher, A. M. Doyle, T. F. O'Dwyer and B. K. Hodnett, *Journal of Chemical Technology & Biotechnology*, 2001, **76**, 1216-1222.
208. D. M. Antonelli and J. Y. Ying, *Current Opinion in Colloid & Interface Science*, 1996, **1**, 523-529.
209. J. S. Beck, J. C. Vartuli, W. J. Roth, M. E. Leonowicz, C. T. Kresge, K. D. Schmitt, C. T. W. Chu, D. H. Olson, E. W. Sheppard, S. B. McCullen, J. B. Higgins and J. L. Schlenker, *Journal of the American Chemical Society*, 1992, **114**, 10834-10843.
210. J. C. Vartuli, K. D. Schmitt, C. T. Kresge, W. J. Roth, M. E. Leonowicz, S. B. McCullen, S. D. Hellring, J. S. Beck and J. L. Schlenker, *Chemistry of Materials*, 1994, **6**, 2317-2326.
211. G. Øye, J. Sjöblom and M. Stöcker, *Advances in Colloid and Interface Science*, 2001, **89–90**, 439-466.
212. M. Xia, C. Chen, M. Long, C. Chen, W. Cai and B. Zhou, *Microporous and Mesoporous Materials*, 2011, **145**, 217-223.
213. N. Masque, R. Marce, F. Borrull, P. Cormack and D. Sherrington, *J Anal Chem*, 2000, **72**, 4122 - 4126.

214. K. R. Kloetstra and H. van Bekkum, *Journal of the Chemical Society, Chemical Communications*, 1995, 1005-1006.

215. U. Junges, W. Jacobs, I. Voigt-Martin, B. Krutzsch and F. Schuth, *Journal of the Chemical Society, Chemical Communications*, 1995, 2283-2284.

216. J. Rathousky, A. Zukal, O. Franke and G. Schulz-Ekloff, *Journal of the Chemical Society, Faraday Transactions*, 1994, **90**, 2821-2826.

217. K. F. Lam, C. M. Fong, K. L. Yeung and G. McKay, *Chemical Engineering Journal*, 2008, **145**, 185-195.

218. R. S. Araújo, D. C. S. Azevedo, C. L. Cavalcante Jr, A. Jiménez-López and E. Rodríguez-Castellón, *Microporous and Mesoporous Materials*, 2008, **108**, 213-222.

219. Y. Miyake, M. Hanaeda and M. Asada, *Industrial & Engineering Chemistry Research*, 2007, **46**, 8152-8157.

220. K. Schumacher, P. I. Ravikovitch, A. Du Chesne, A. V. Neimark and K. K. Unger, *Langmuir*, 2000, **16**, 4648-4654.

221. R. Ryoo, S. H. Joo and J. M. Kim, *The Journal of Physical Chemistry B*, 1999, **103**, 7435-7440.

222. Q. Huo, D. I. Margolese and G. D. Stucky, *Chemistry of Materials*, 1996, **8**, 1147-1160.

223. H. Saputra, R. Othman, A. G. E. Sutjipto, R. Muhida and M. H. Ani, *Materials Research Bulletin*, 2012, **47**, 732-736.

224. C. Exley, in *Marine Molecular Biotechnology*, eds. W. E. G. Muller and M. A. Grachev, Springer-Verlag Berlin, Heidelberger Platz 3, D-14197 Berlin, Germany, 2009, vol. 47, pp. 173-184.

225. S. V. Patwardhan, N. Mukherjee, M. Steinitz-Kannan and S. J. Clarson, *Chemical Communications*, 2003, 1122-1123.

226. M. Hildebrand, *Chemical Reviews*, 2008, **108**, 4855-4874.

227. S. V. Patwardhan, *Chemical Communications*, 2011, **47**, 7567-7582.

228. M. Hildebrand and R. Wetherbee, in *Silicon biomineralization: Biology, biochemistry, molecular biology, biotechnology*, ed. W. E. G. Mueller, Springer-Verlag New York Inc., 175 Fifth Avenue, New York, NY, 10010-7858, USA; Springer-Verlag GmbH & Co. KG, Heidelberger Platz 3, D-14197, Berlin, Germany, 2003, vol. Volume 33, pp. 11-57.

229. E. G. Vrieling, W. W. C. Gieskes and T. P. M. Beelen, *Journal of Phycology*, 1999, **35**, 548-559.

230. M. J. Ellwood, M. Wille and W. Maher, *Science*, 2010, **330**, 1088-1091.

231. N. Kröger, R. Deutzmann, C. Bergsdorf and M. Sumper, *Proceedings of the National Academy of Sciences*, 2000, **97**, 14133-14138.

232. N. Kroger, S. Lorenz, E. Brunner and M. Sumper, *Science*, 2002, **298**, 584-586.

233. K. Shimizu, J. Cha, G. D. Stucky and D. E. Morse, *Proceedings of the National Academy of Sciences*, 1998, **95**, 6234-6238.

234. Y. Zhou, K. Shimizu, J. N. Cha, G. D. Stucky and D. E. Morse, *Angew. Chem.-Int. Edit.*, 1999, **38**, 780-782.

235. S. Masse, G. Laurent and T. Coradin, *Physical Chemistry Chemical Physics*, 2009, **11**, 10204-10210.

236. D. J. Belton, S. V. Patwardhan, V. V. Annenkov, E. N. Danilovtseva and C. C. Perry, *Proc. Natl. Acad. Sci. U. S. A.*, 2008, **105**, 5963-5968.

237. D. Landy, I. Mallard, A. Ponchel, E. Monflier and S. Fourmentin, *Environmental Chemistry Letters*, 2012, **10**, 225-237.

238. P. R. Gogate, *Advances in Environmental Research*, 2002, **6**, 335-358.

239. J.-M. Herrmann, J. Matos, J. Disdier, C. Guillard, J. Laine, S. Malato and J. Blanco, *Catalysis Today*, 1999, **54**, 255-265.

240. R. Venkatadri and R. W. Peters, *Hazard. Waste Hazard. Mater.*, 1993, **10**, 107-149.

241. P. R. Gogate and A. B. Pandit, *Advances in Environmental Research*, 2004, **8**, 501-551.

242. R. Andreozzi, V. Caprio, A. Insola and R. Marotta, *Catalysis Today*, 1999, **53**, 51-59.

243. E. Neyens and J. Baeyens, *Journal of Hazardous Materials*, 2003, **98**, 33-50.

244. M. Anbia, N. Mohammadi and K. Mohammadi, *Journal of Hazardous Materials*, 2010, **176**, 965-972.

245. M. N. Rashed, *Organic pollutants, Monitoring, Risk and Treatment*, InTECH, 2013.

246. F. Orshansky and N. Narkis, *Water Research*, 1997, **31**, 391-398.

247. V. Wernert and R. Denoyel, *Microporous and Mesoporous Materials*, 2016, **222**, 247-255.

248. O. A. Makhotkina, E. V. Kuznetsova and S. V. Preis, *Applied Catalysis B: Environmental*, 2006, **68**, 85-91.

249. G. Satishkumar, M. V. Landau, T. Buzaglo, L. Frimet, M. Ferentz, R. Vidruk, F. Wagner, Y. Gal and M. Herskowitz, *Applied Catalysis B: Environmental*, 2013, **138–139**, 276-284.

250. S. A. Idris, C. M. Davidson, C. McManamon, M. A. Morris, P. Anderson and L. T. Gibson, *Journal of Hazardous Materials*, 2011, **185**, 898-904.

251. H. Zhao, K. L. Nagy, J. S. Waples and G. F. Vance, *Environmental Science & Technology*, 2000, **34**, 4822-4827.

252. B. Beless, H. S. Rifai and D. F. Rodrigues, *Environmental Science & Technology*, 2014, **48**, 10372-10379.

253. E. N. Ndunda and B. Mizaikoff, *Analytical Methods*, 2015, **7**, 8034-8040.

254. S. Zeng, N. Gan, R. Weideman-Mera, Y. Cao, T. Li and W. Sang, *Chemical Engineering Journal*, 2013, **218**, 108-115.

255. I. Velzeboer, C. J. A. F. Kwadijk and A. A. Koelmans, *Environmental Science & Technology*, 2014, **48**, 4869-4876.

256. A. Kawashima, M. Katayama, N. Matsumoto and K. Honda, *Chemosphere*, 2011, **83**, 823-830.

257. Z. Hu and M. P. Srinivasan, *Microporous and Mesoporous Materials*, 1999, **27**, 11-18.

258. N. Tancredi, N. Medero, F. Möller, J. Píriz, C. Plada and T. Cordero, *Journal of Colloid and Interface Science*, 2004, **279**, 357-363.

259. J. i. Hayashi, A. Kazehaya, K. Muroyama and A. P. Watkinson, *Carbon*, 2000, **38**, 1873-1878.

260. Y. Sun, J. P. Zhang, G. Yang and Z. H. Li, *Chem. Biochem. Eng. Q.*, 2006, **20**, 429-435.

261. H. Teng, T.-S. Yeh and L.-Y. Hsu, *Carbon*, 1998, **36**, 1387-1395.

262. P. T. Williams and A. R. Reed, *Biomass and Bioenergy*, 2006, **30**, 144-152.

263. G. J. McDougall, *J. S. Afr. Inst. Min. Metall.*, 1991, **91**, 109-120.

264. C. Moreno-Castilla, *Carbon*, 2004, **42**, 83-94.

265. M. A. Yahya, Z. Al-Qodah and C. W. Z. Ngah, *Renewable and Sustainable Energy Reviews*, 2015, **46**, 218-235.

266. J. M. Dias, M. C. M. Alvim-Ferraz, M. F. Almeida, J. Rivera-Utrilla and M. Sánchez-Polo, *Journal of Environmental Management*, 2007, **85**, 833-846.

267. M. Ahmedna, W. E. Marshall and R. M. Rao, *Bioresource Technology*, 2000, **71**, 113-123.

268. M. Ahmedna, W. E. Marshall and R. M. Rao, *Bioresource Technology*, 2000, **71**, 103-112.

269. J. S. Mattson, *Product R&D*, 1973, **12**, 312-317.

270. A. Ahmadpour and D. D. Do, *Carbon*, 1997, **35**, 1723-1732.

271. J. L. Figueiredo, *Journal of Materials Chemistry A*, 2013, **1**, 9351-9364.

272. L. Li, P. A. Quinlivan and D. R. U. Knappe, *Carbon*, 2002, **40**, 2085-2100.

273. Z. Hu and M. P. Srinivasan, *Microporous and Mesoporous Materials*, 2001, **43**, 267-275.

274. J. i. Hayashi, T. Horikawa, I. Takeda, K. Muroyama and F. Nasir Ani, *Carbon*, 2002, **40**, 2381-2386.

275. A. Ahmadpour and D. D. Do, *Carbon*, 1996, **34**, 471-479.

276. H. Teng and S.-C. Wang, *Carbon*, 2000, **38**, 817-824.

277. Z. Hu, M. P. Srinivasan and Y. Ni, *Carbon*, 2001, **39**, 877-886.

278. W. Tongpoothorn, M. Sriuttha, P. Homchan, S. Chanthai and C. Ruangviriyachai, *Chemical Engineering Research and Design*, 2011, **89**, 335-340.

279. S. Guo, J. Peng, W. Li, K. Yang, L. Zhang, S. Zhang and H. Xia, *Applied Surface Science*, 2009, **255**, 8443-8449.

280. C. J. Kirubakaran, K. Krishnaiah and S. K. Seshadri, *Industrial & Engineering Chemistry Research*, 1991, **30**, 2411-2416.

281. Q. P. Campbell, J. R. Bunt, H. Kasaini and D. J. Kruger, *Journal of the Southern African Institute of Mining and Metallurgy*, 2012, **112**, 37-44.

282. T. Budinova, E. Ekinci, F. Yardim, A. Grimm, E. Björnbom, V. Minkova and M. Goranova, *Fuel Processing Technology*, 2006, **87**, 899-905.

283. A. C. Lua and T. Yang, *Journal of Colloid and Interface Science*, 2005, **290**, 505-513.

284. N. Spahis, A. Addoun, H. Mahmoudi and N. Ghaffour, *Desalination*, 2008, **222**, 519-527.

285. B. S. Girgis, L. B. Khalil and T. A. M. Tawfik, *Journal of Chemical Technology & Biotechnology*, 1994, **61**, 87-92.

286. N. R. Khalili, M. Campbell, G. Sandi and J. Golaś, *Carbon*, 2000, **38**, 1905-1915.

287. O. Ioannidou and A. Zabaniotou, *Renewable and Sustainable Energy Reviews*, 2007, **11**, 1966-2005.

288. T. Wigmans, *Carbon*, 1989, **27**, 13-22.

289. T. M. Alslaibi, I. Abustan, M. A. Ahmad and A. A. Foul, *Journal of Chemical Technology & Biotechnology*, 2013, **88**, 1183-1190.

290. R. Baccar, J. Bouzid, M. Feki and A. Montiel, *Journal of Hazardous Materials*, 2009, **162**, 1522-1529.

291. J. Donald, Y. Ohtsuka and C. Xu, *Materials Letters*, 2011, **65**, 744-747.

292. D. Shao, G. Sheng, C. Chen, X. Wang and M. Nagatsu, *Chemosphere*, 2010, **79**, 679-685.

293. D. W. Hawker and D. W. Connell, *Environmental Science & Technology*, 1988, **22**, 382-387.

294. R. I. Masel, *Principle of adsorption and reaction on soild surfaces*, John Wiley & Sons Inc, Canada, 1996.

295. D. Savova, N. Petrov, M. F. Yardim, E. Ekinci, T. Budinova, M. Razvigorova and V. Minkova, *Carbon*, 2003, **41**, 1897-1903.

296. J. Ren, D. Gou, F. Zhang, L. Tau and M. Zhang, *Environmental Protection and Sustainable Ecological Development Proceedings*, 2015.

297. Y. S. Ho and G. McKay, *Process Safety and Environmental Protection*, 1998, **76**, 332-340.

298. M. A. Lillo-Ródenas, D. Cazorla-Amorós and A. Linares-Solano, *Carbon*, 2005, **43**, 1758-1767.
299. T. García, R. Murillo, D. Cazorla-Amorós, A. M. Mastral and A. Linares-Solano, *Carbon*, 2004, **42**, 1683-1689.
300. O. V. Dorofeeva, V. P. Novikov, N. F. Moiseeva and V. S. Yungman, *Journal of Molecular Structure: THEOCHEM*, 2003, **637**, 137-153.
301. P. Ding, K.-L. Huang, G.-Y. Li and W.-W. Zeng, *Journal of Hazardous Materials*, 2007, **146**, 58-64.
302. Y. S. Ho and G. McKay, *Water Research*, 1999, **33**, 578-584.

Appendix 1

GC-MS calibration curves for 19 PCB congeners
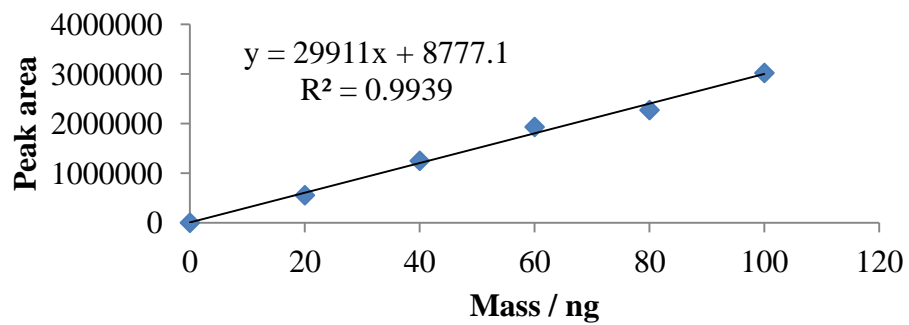
Figure A1.1: Calibration curve for PCB - 1

$y = 29911x + 8777.1$
$R^2 = 0.9939$
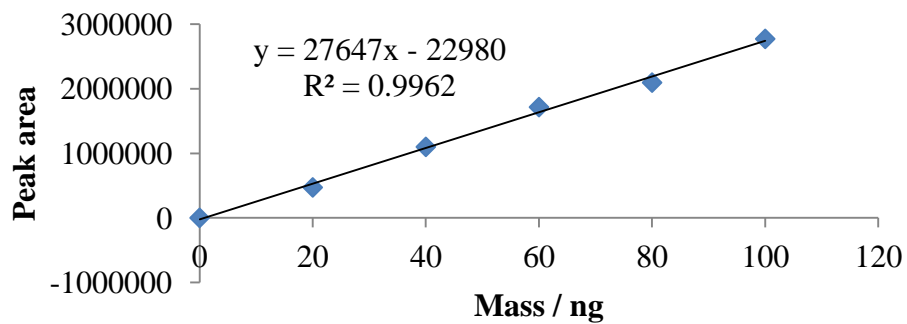
Figure A1.2: Calibration curve for PCB - 5

$y = 27647x - 22980$
$R^2 = 0.9962$
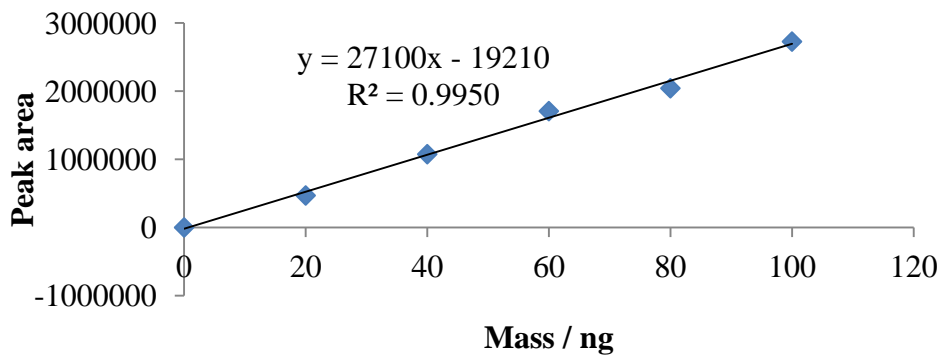
Figure A1.3: Calibration curve for PCB – 18

$y = 27100x - 19210$
$R^2 = 0.9950$
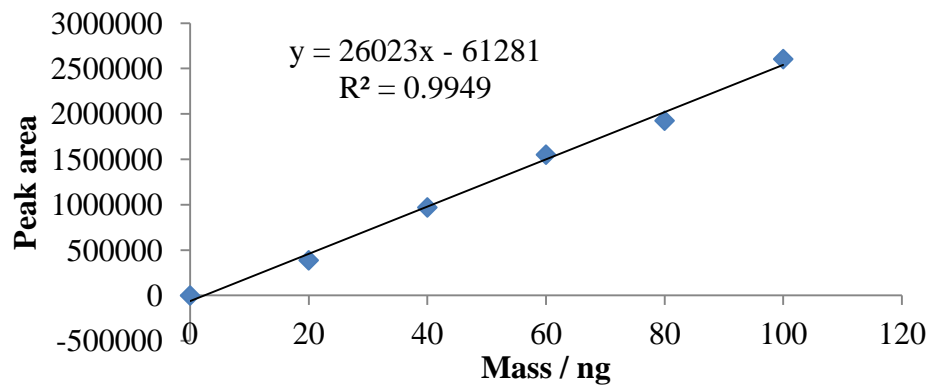
Figure A1.4: Calibration curve for PCB - 31
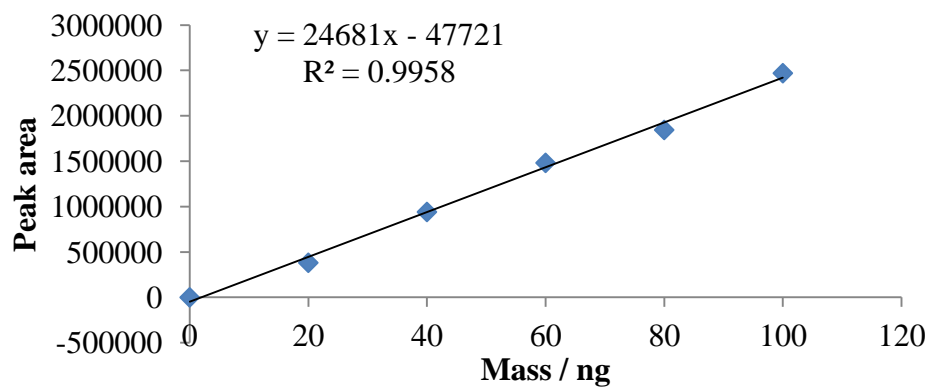
Figure A1.5: Calibration curve for PCB - 44
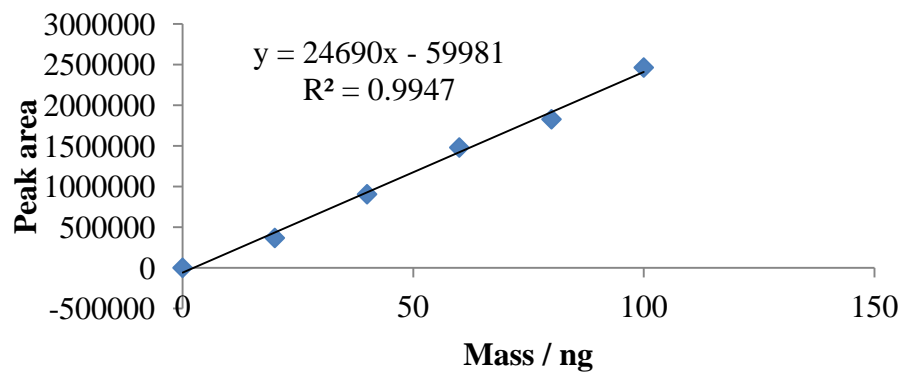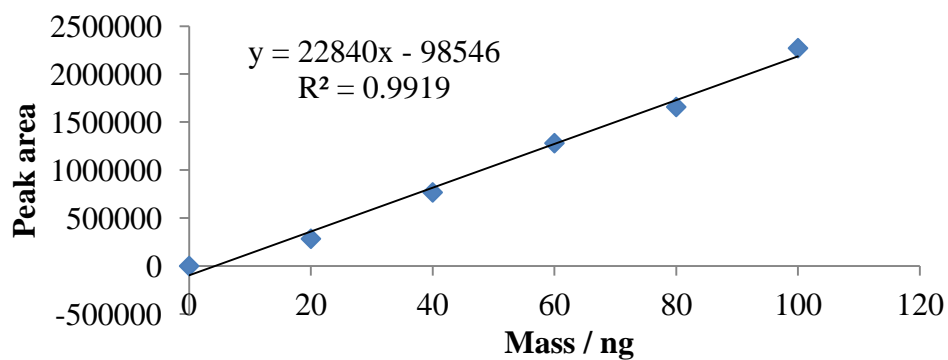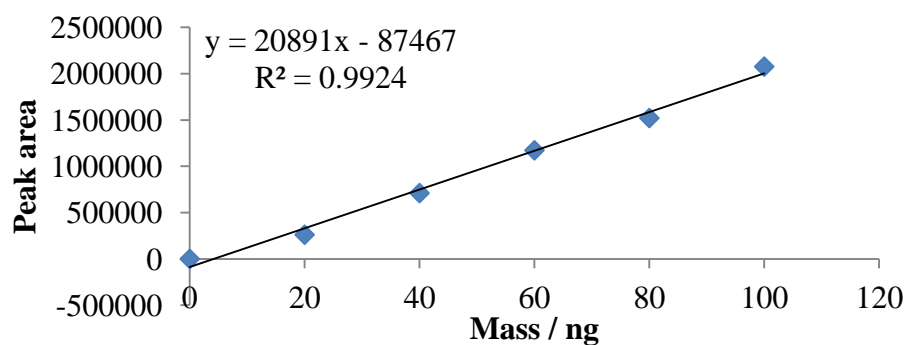

Figure A1.6: Calibration curve for PCB - 52

Figure A1.7: Calibration curve for PCB - 66

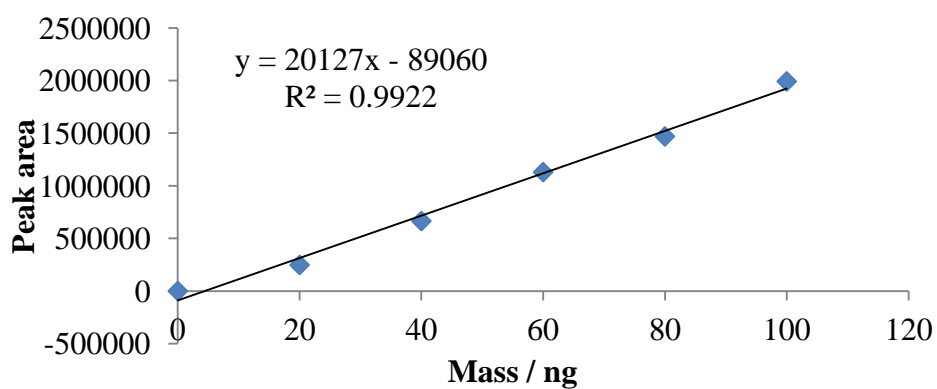**Figure A1.8: Calibration curve for PCB - 87**
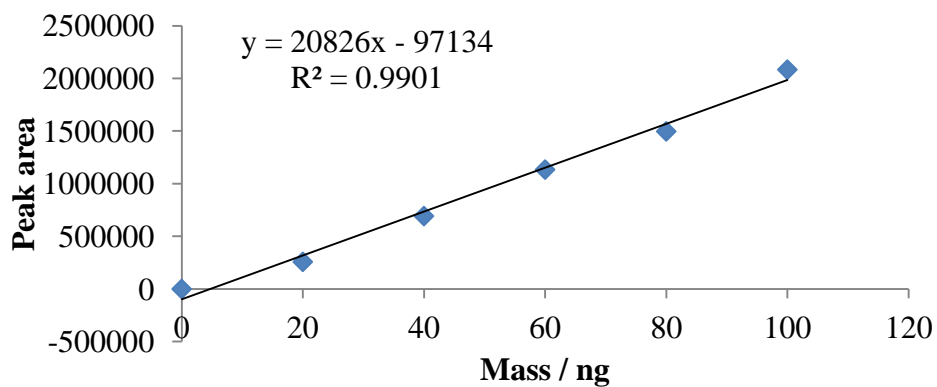

Figure A1.9: Calibration curve for PCB - 101

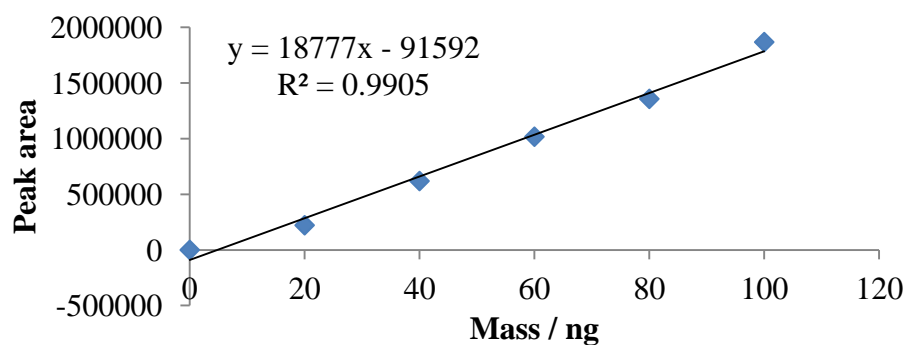**Figure A1.10: Calibration curve for PCB - 110**

Figure A1.11: Calibration curve for PCB – 151
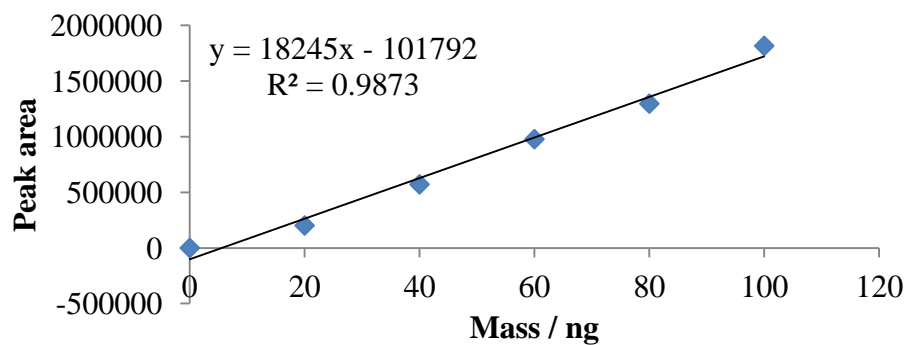

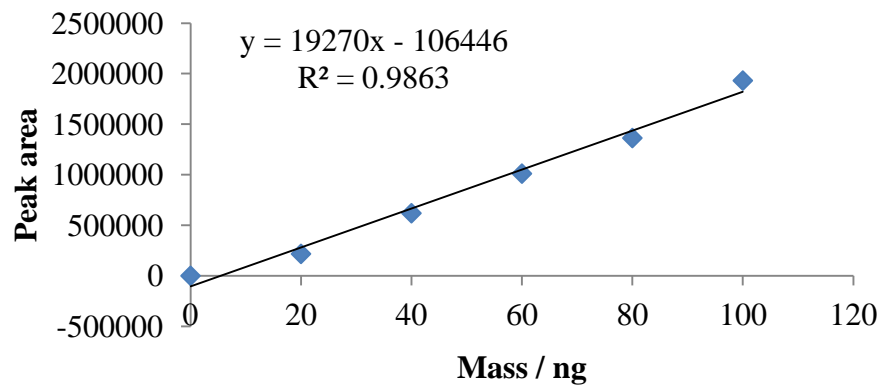**Figure A1.12: Calibration curve for PCB - 153**

Figure A1.13: Calibration curve for PCB - 138
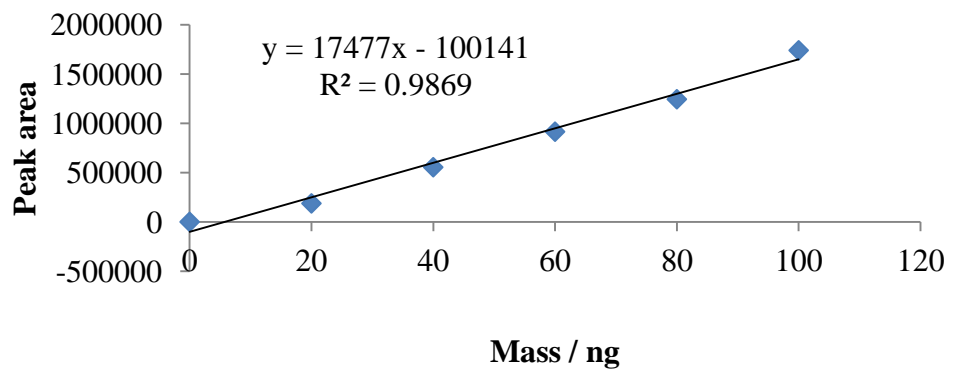

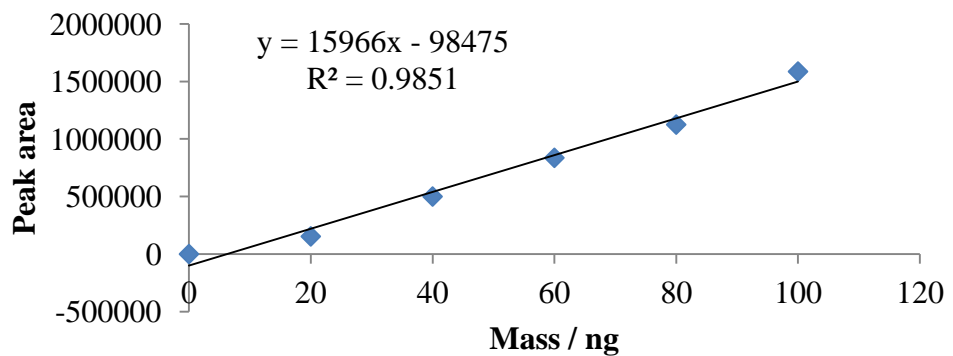**Figure A1.14: Calibration curve for PCB – 141**

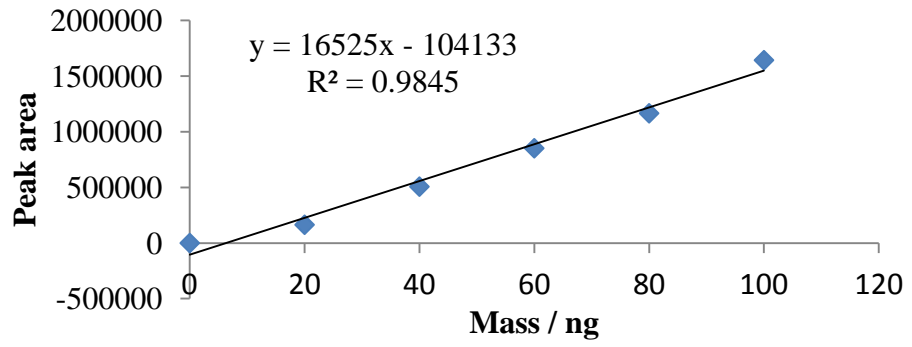**Figure A1.15: Calibration curve for PCB – 187**
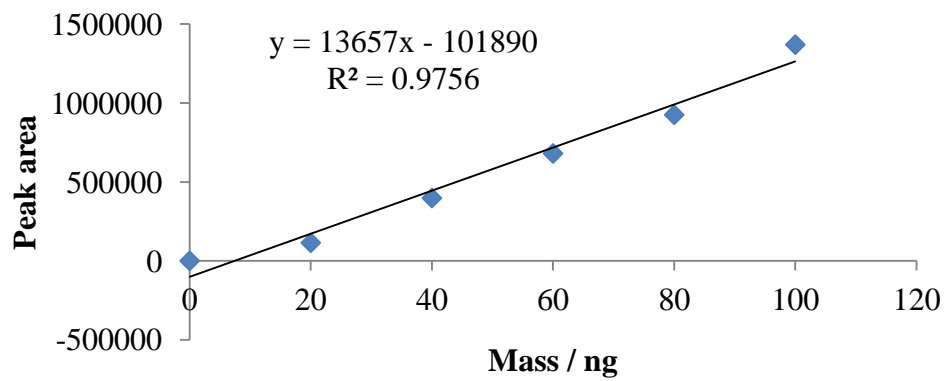
Figure A1.16: Calibration curve for PCB - 183
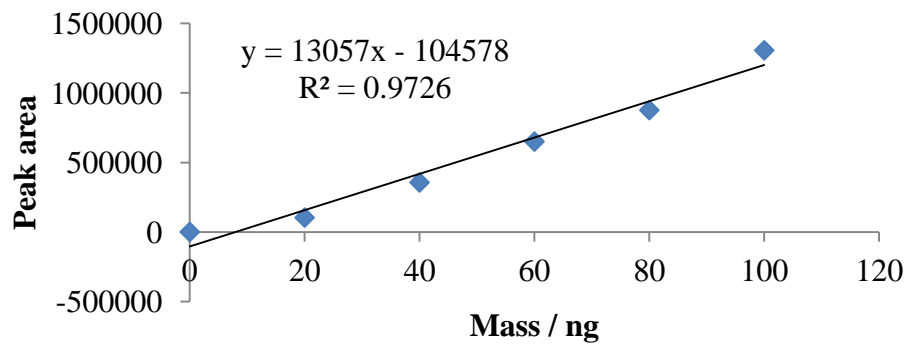

Figure A1.17: Calibration curve for PCB – 180

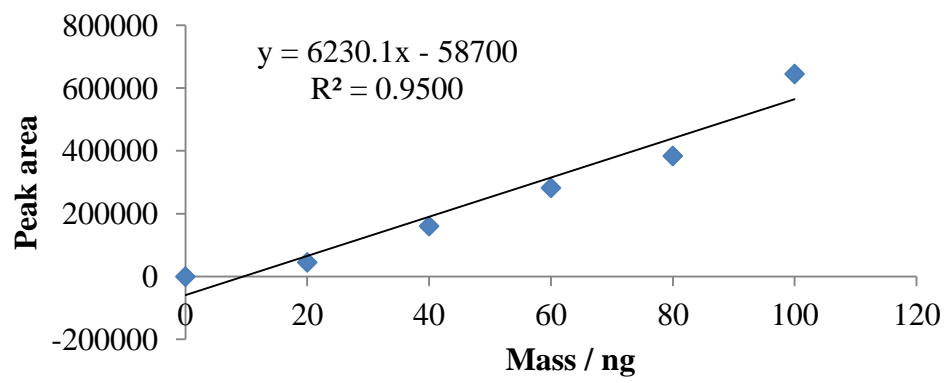**Figure A1.18: Calibration curve for PCB – 170**

Figure A1.19: Calibration curve for PCB – 206

Appendix 2

GC-MS results for 19 PCB congeners

Table A2.1: Variation between replicates for PCB standard over 3 days

PCB Congeners	Mass/ ng	Peak area				
		20	**40**	**60**	**80**	**100**
PCB-1	Day 1	554269	1248259	1931299	2271753	3020493
	Day 2	465498	1174201	1843558	2532442	3071331
	Day 3	717599	1226401	1769213	2279560	3224126
	Mean	579122	1216287	1848023	2361252	3105317
	Std deviation	127875	38051	81135	148307	105985
	% RSD	22.1	3.13	4.4	6.3	3.4
PCB-5	Day 1	471847	1099786	1715894	2095632	2773109
	Day 2	404310	1022988	1690483	2352028	2923388
	Day 3	613255	1074237	1628766	2172662	3108189
	Mean	496470	1065670	1678381	2206774	2934895
	Std deviation	106627	39109	44807	131558	167836
	% RSD	21.5	3.7	2.7	6.0	5.7
PCB- 18	Day 1	469177	1074204	1705822	2040758	2724682
	Day 2	386647	1004933	1677766	2279779	2811597
	Day 3	590058	1018388	1561347	2087201	2973351
	Mean	481961	1032508	1648312	2135913	2836543
	Std deviation	102306	36731	76609	126737	126197
	% RSD	21.2	3.6	4.6	5.9	4.4
PCB- 31	Day 1	387803	970081	1551339	1925853	2604141
	Day 2	323740	909695	1521855	2122031	2716349
	Day 3	534153	924904	1458425	2022956	2920057
	Mean	415232	934893.3	1510540	2023613	2746849
	Std deviation	107855	31408	47479	98091	160151
	% RSD	26.0	3.4	3.1	4.8	5.8

Table A2.2: Variation between replicates for PCB standard over 3 days

PCB Congeners	Mass / ng	Peak area				
		20	40	60	80	100
PCB-44	Day 1	381583	940754	1481820	1844389	2469457
	Day 2	308422	875001	1469034	2070073	2607609
	Day 3	498785	862594	1348695	1897631	2698526
	Mean	396263	892783	1433183	1937364	2591864
	Std deviation	96027	42005	73448	117972	115343
	% RSD	24.2	4.7	5.1	6.1	4.4
PCB-52	Day 1	367418	905627	1480752	1828430	2465037
	Day 2	293677	856341	1457813	2061292	2541912
	Day 3	480561	831208	1349884	1861160	2698526
	Mean	380552	864392	1429483	1916961	2568492
	Std deviation	94132	37857	69882	126061	118992
	% RSD	24.7	4.4	4.9	6.6	4.6
PCB- 66	Day 1	284203	767374	1280579	1657768	2270838
	Day 2	210172	694286	1255994	1821503	2291847
	Day 3	395827	687312	1132517	1661701	2437545
	Mean	296734	716324	1223030	1713657	2333410
	Std deviation	93460	44348	79345	93418	90793
	% RSD	31.5	6.2	6.5	5.5	3.9
PCB- 87	Day 1	261422	710775	1172676	1521046	2076591
	Day 2	193543	644229	1161522	1715555	2109060
	Day 3	359706	614412	1053142	1552123	2299857
	Mean	271557	656472	1129113	1596241	2161836
	Std deviation	83544	49334	66029	104490	120627
	% RSD	30.8	7.5	5.8	6.5	5.6

Table A2.3: Variation between replicates for PCB standard over 3 days

PCB Congeners	Peak area					
	Mass / ng	20	40	60	80	100
PCB-101	Day 1	247778	664838	1129962	1469170	1991857
	Day 2	185548	599586	1111855	1666551	2056776
	Day 3	349221	580650	1024032	1530694	2254155
	Mean	260849	615024.7	1088616	1555472	2100929
	Std deviation	82616	44166	56660	100996	136610
	% RSD	31.7	7.2	5.2	6.5	6.5
PCB-110	Day 1	257675	692540	1134054	1496889	2083785
	Day 2	197114	634078	1134857	1658494	2073565
	Day 3	342432	588803	1038427	1533067	2250839
	Mean	265740	638474	1102446	1562817	2136063
	Std deviation	72994	52008	55444	84811	99530
	% RSD	27.5	8.1	5.0	5.4	4.7
PCB- 151	Day 1	221903	619054	1017451	1357426	1867852
	Day 2	160866	552067	992015	1484456	1872397
	Day 3	307432	519991	911656	1346737	2001831
	Mean	230067	563704	973707	1396206	1914027
	Std deviation	73623	50546	55222	76613	76075
	% RSD	32.0	9.0	5.7	5.5	4.0
PCB- 153	Day 1	201405	571350	977443	1296650	1815966
	Day 2	145622	495755	943035	1426067	1816754
	Day 3	292203	483786	840028	1297648	1938781
	Mean	213077	516964	920169	1340122	1857167
	Std deviation	73984	47479	71504	74433	70681
	% RSD	34.7	9.2	7.8	5.6	3.8

Table A2.4: Variation between replicates for PCB standard over 3 days

PCB Congeners	Mass / ng	Peak area				
		20	**40**	**60**	**80**	**100**
PCB-138	Day 1	217070	619153	1011173	1363242	1931697
	Day 2	149263	496838	949306	1414655	1768552
	Day 3	280812	551728	962697	1466506	2227005
	Mean	215715	555906	974392	1414801	1975751
	Std deviation	65785	61264	32549	51632	232380
	% RSD	30.5	11.0	3.3	3.6	11.8
PCB-141	Day 1	187496	554602	915168	1244477	1740448
	Day 2	127511	465802	908414	1345231	1687595
	Day 3	264496	459699	807883	1250768	1867254
	Mean	193168	493368	877155	1280159	1765099
	Std deviation	68668	53118	60086	56442	92331
	% RSD	35.5	10.8	6.9	4.4	5.2
PCB-180	Day 1	114229	397636	679940	924637	1369237
	Day 2	73305	313343	657473	1007067	1313638
	Day 3	187957	297825	583347	913563	1458315
	Mean	125164	336268	640253	948422	1380397
	Std deviation	58103	53710	50546	51089	72981
	% RSD	46.4	16.0	7.9	5.4	5.3
PCB-170	Day 1	103130	355706	649527	875370	1305850
	Day 2	61096	278757	611599	955244	1222752
	Day 3	181705	258240	535558	891281	1411554
	Mean	115310	297568	598895	907298	1313385
	Std deviation	61220	51384	58037	42277	94626
	% RSD	53.1	17.3	9.7	4.7	7.2

Table A2.5: Variation between replicates for PCB standard over 3 days

Compound	Mass / ng	Peak area				
		20	**40**	**60**	**80**	**100**
PCB-206	**Day 1**	45330	160540	282361	383872	644721
	Day 2	15158	86491	240869	453104	551116
	Day 3	72770	95358	191413	370204	683356
	Mean	44419	114130	238214	402393	626398
	Std dev	28817	40436	45532	44445	67998
	% RSD	64.9	35.4	19.1	11.0	10.9

Appendix 3
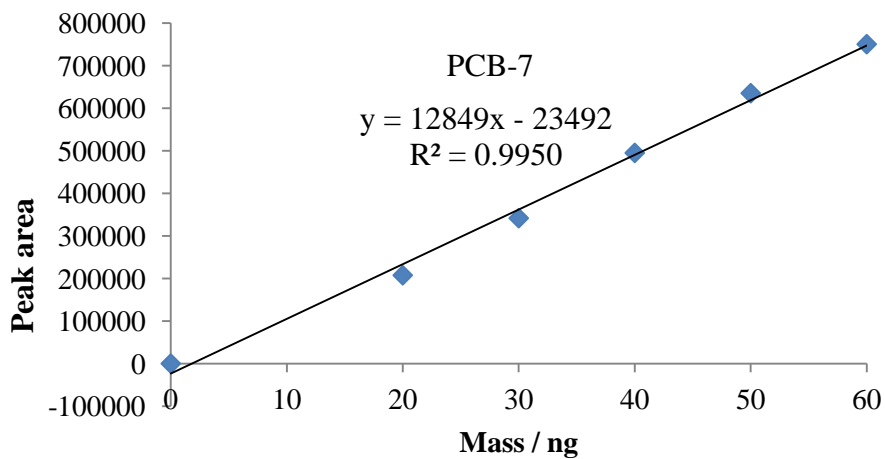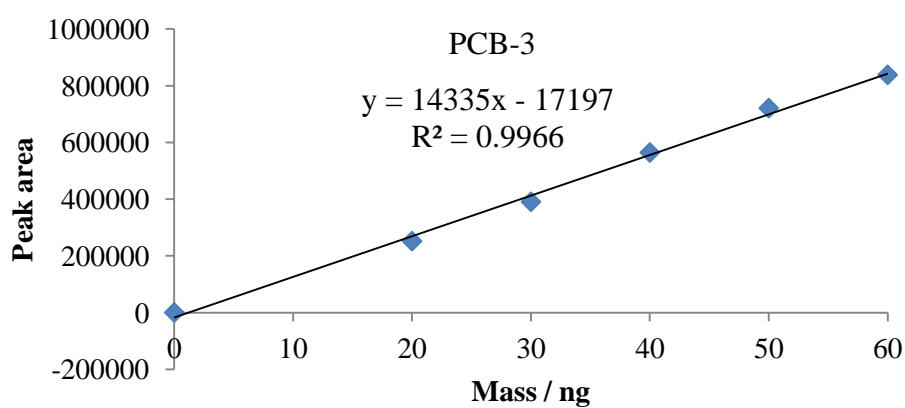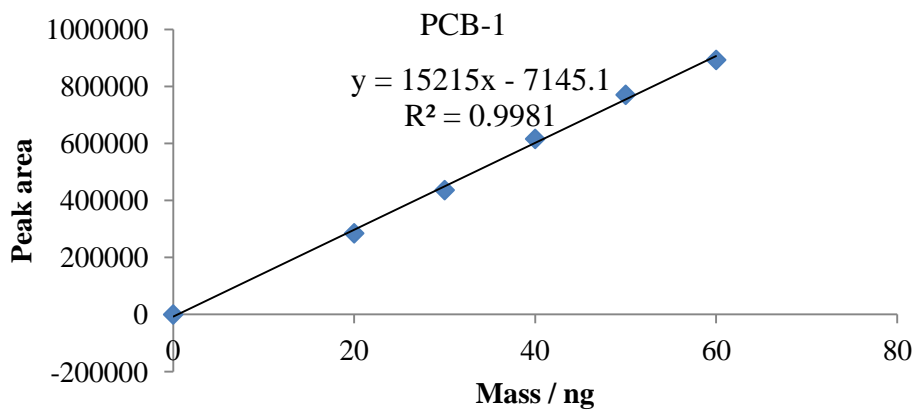
Appendix 3.1: Calibration curves for PCB – 1, 3 and 7

PCB-14

$y = 15277x - 27729$

$R^2 = 0.9956$

PCB-12

$y = 12332x - 29892$

$R^2 = 0.9921$
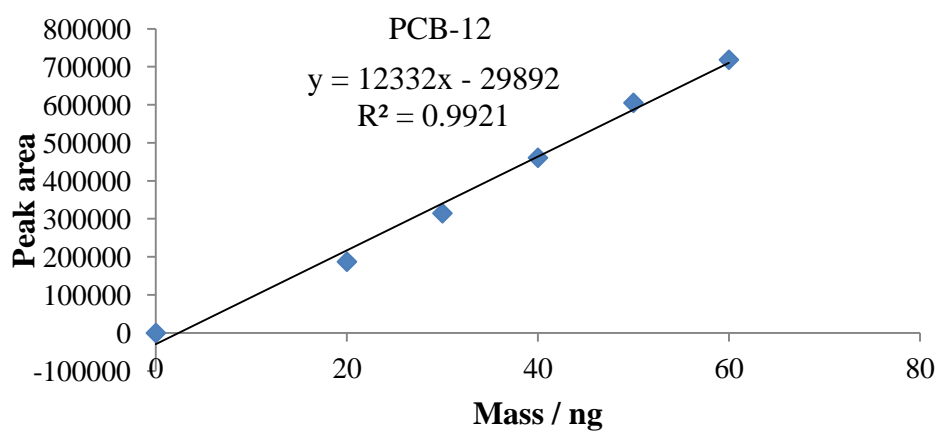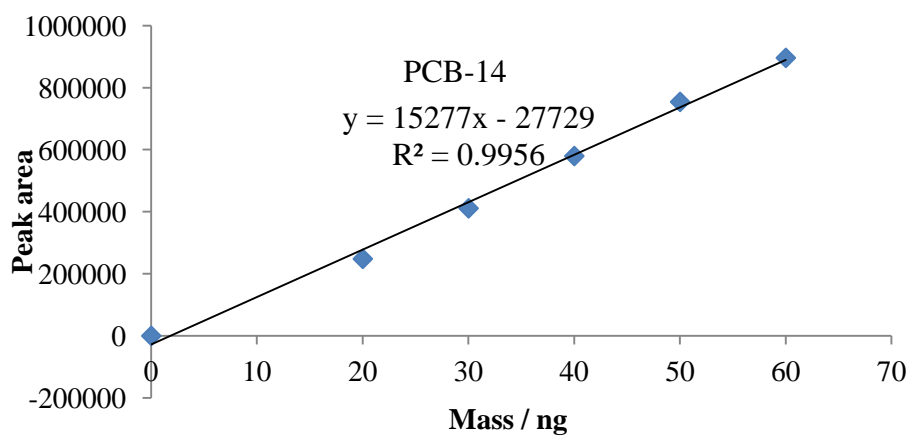
Appendix 3.2 Calibration curve for PCB – 14 and 12